EFFECTS OF MONOMER STRUCTURE AND TYPE OF METAL OXIDE NANOPARTICLES ON COLORIMETRIC RESPONSE OF POLYDIACETYLENE/METAL OXIDE NANOCOMPOSITES

Mr. Amornsak Chanakul

A Dissertation Submitted in Partial Fulfillment of the Requirements
for the Degree of Doctor of Philosophy Program in Materials Science
Department of Materials Science
Faculty of Science
Chulalongkorn University
Academic Year 2013

ผลของโครงสร้างมอนอเมอร์และชนิดอนุภาคโลหะออกไซด์ระดับนาโนเมตรต่อการตอบสนองโดยการเปลี่ยนสีของวัสดุเชิงประกอบระดับนาโนเมตรพอลิไดแอเซทิลีน/โลหะออกไซด์

นายอมรศักดิ์ ชนะกุล

วิทยานิพนธ์นี้เป็นส่วนหนึ่งของการศึกษาตามหลักสูตรปริญญาวิทยาศาสตรดุษฎีบัณฑิต
สาขาวิชาวัสดุศาสตร์ ภาควิชาวัสดุศาสตร์
คณะวิทยาศาสตร์ จุฬาลงกรณ์มหาวิทยาลัย
ปีการศึกษา 2556

Thesis Title	EFFECTS OF MONOMER STRUCTURE AND TYPE OF METAL OXIDE NANOPARTICLES ON COLORIMETRIC RESPONSE OF POLYDIACETYLENE/METAL OXIDE NANOCOMPOSITES
By	Mr. Amornsak Chanakul
Field of Study	Materials Science
Thesis Advisor	Assistant Professor Nisanart Traiphol, Ph.D.
Thesis Co-advisor	Assistant Professor Rakchart Traiphol, Ph.D.

Accepted by the Faculty of Science, Chulalongkorn University in Partial Fulfillment of the Requirements for the Doctoral Degree

.....Dean of the Faculty of Science
(Professor Supot Hannongbua, Dr. rer. nat.)

THESIS COMMITTEE

.....Chairman
(Assistant Professor Sirithan Jiemsirilers, Ph.D.)

.....Thesis Advisor
(Assistant Professor Nisanart Traiphol, Ph.D.)

.....Thesis Co-advisor
(Assistant Professor Rakchart Traiphol, Ph.D.)

.....Examiner
(Assistant Professor Kanoktip Boonkerd, Ph.D.)

.....Examiner
(Karn Serivalsatit, Ph.D.)

.....External Examiner
(Assistant Professor Toemsak Srikhirin, Ph.D.)

อมรศักดิ์ ชนะกุล : ผลของโครงสร้างมอนอเมอร์และชนิดอนุภาคโลหะออกไซด์ระดับนาโนเมตรต่อการตอบสนองโดยการเปลี่ยนสีของวัสดุเชิงประกอบระดับนาโนเมตรพอลิไดแอเซทิลีน/โลหะออกไซด์. (EFFECTS OF MONOMER STRUCTURE AND TYPE OF METAL OXIDE NANOPARTICLES ON COLORIMETRIC RESPONSE OF POLYDIACETYLENE/METAL OXIDE NANOCOMPOSITES) อ.ที่ปรึกษาวิทยานิพนธ์หลัก : ผศ.ดร.นิศานาถ ไตรผล, อ.ที่ปรึกษาวิทยานิพนธ์ร่วม : ผศ.ดร.รักชาติ ไตรผล, 163 หน้า.

งานวิจัยนี้ได้นำเสนอวิธีการอย่างง่ายในการควบคุมพฤติกรรมการเปลี่ยนสีของวัสดุเชิงประกอบระดับนาโนเมตรพอลิไดแอเซทิลีนเวสิเคิล/ซิงก์ออกไซด์โดยการปรับเปลี่ยนโครงสร้างของมอนอเมอร์และระยะเวลาพอลิเมอไรเซชัน มอนอเมอร์ที่ใช้ในการเตรียมวัสดุเชิงประกอบระดับนาโนเมตรมีความยาวสายโซ่แอลคิลต่างกัน ได้แก่ 10,12-เพนตะโคซะไดอายน์โนอิกแอซิด 10,12-ไตรโคซะไดอายน์โนอิกแอซิด และ 5,7-เฮกซะเดกคะไดอายน์โนอิกแอซิด จากการทดลองพบว่าการเปลี่ยนสีเมื่อได้รับการกระตุ้นด้วยอุณหภูมิของวัสดุเชิงประกอบระดับนาโนเมตรพอลิไดแอเซทิลีนเวสิเคิล/ซิงก์ออกไซด์มีความแตกต่างไปจากพอลิไดแอเซทิลีนบริสุทธิ์ที่เตรียมจากมอนอเมอร์ชนิดเดียวกัน โดยวัสดุเชิงประกอบระดับนาโนเมตรทั้งหมดเกิดการเปลี่ยนสีแบบผันกลับได้ระหว่างสีน้ำเงินและสีม่วงในหลายรอบของการเพิ่ม/ลด อุณหภูมิ และพบว่าวัสดุเชิงประกอบที่เตรียมจากมอนอเมอร์ที่มีสายโซ่แอลคิลที่สั้นกว่าจะเกิดการเปลี่ยนสีขึ้นที่อุณหภูมิต่ำกว่า สำหรับการตอบสนองโดยการเปลี่ยนสีต่อสภาวะกรด-เบส พบว่าวัสดุเชิงประกอบระดับนาโนเมตรทั้งหมดมีความไวในการตอบสนองต่อสภาวะกรดได้อย่างน่าสนใจ อย่างไรก็ตาม ในสภาวะเบสการเปลี่ยนสีจะเกิดขึ้นที่พีเอชสูงกว่าพอลิไดแอเซทิลีนบริสุทธิ์ที่เตรียมได้จากมอนอเมอร์ชนิดเดียวกัน และวัสดุเชิงประกอบที่เตรียมจากมอนอเมอร์ที่มีสายโซ่แอลคิลสั้นกว่าจะมีความไวมากกว่าในการตอบสนองต่อสภาวะกรด-เบส และแอลกอฮอล์ นอกจากนี้ยังพบว่าระยะเวลาพอลิเมอไรเซชันโดยการฉายรังสียูวีส่งผลต่อพฤติกรรมการเปลี่ยนสีของวัสดุเชิงประกอบระดับนาโนเมตรพอลิไดแอเซทิลีนเวสิเคิล/ซิงก์ออกไซด์ โดยการฉายรังสีเป็นเวลานานจะทำให้อุณหภูมิที่เกิดการเปลี่ยนสีของวัสดุเชิงประกอบลดต่ำลง การเปลี่ยนสีแบบผันกลับได้โดยสมบูรณ์สามารถพบได้ในวัสดุเชิงประกอบที่เตรียมจาก 10,12-ไตรโคซะไดอายน์โนอิกแอซิด โดยฉายรังสีเป็นเวลา 4 และ 60 นาที และวัสดุเชิงประกอบที่เตรียมจาก5,7-เฮกซะเดกคะไดอายน์โนอิกแอซิดที่ฉายรังสีเป็นเวลา 30 นาที การเพิ่มระยะเวลาพอลิเมอไรเซชันยังส่งผลให้ระดับการเปลี่ยนสีลดลงเมื่อสภาวะกรด-เบสเปลี่ยนแปลงไปหรือมีการเติมแอลกอฮอล์ นอกจากนี้อนุภาคโลหะออกไซด์ระดับนาโนเมตรชนิดอื่นเช่น ซิลิกอนไดออกไซด์ ไทเทเนียมไดออกไซด์ และอะลูมินาออกไซด์ ได้ถูกนำมาใช้ในการเตรียมวัสดุเชิงประกอบระดับนาโนเมตรพอลิไดแอเซทิลีน/โลหะออกไซด์ และพบว่าพฤติกรรมการเปลี่ยนสีของวัสดุเชิงประกอบมีความใกล้เคียงกันกับของพอลิไดแอเซทิลีนบริสุทธิ์

ภาควิชา วัสดุศาสตร์ ลายมือชื่อนิสิต .....

สาขาวิชา วัสดุศาสตร์ ลายมือชื่อ อ.ที่ปรึกษาวิทยานิพนธ์หลัก .....

ปีการศึกษา 2556 ลายมือชื่อ อ.ที่ปรึกษาวิทยานิพนธ์ร่วม .....

5273930223 : MAJOR MATERIALS SCIENCE

KEYWORDS : POLYDIACETYLENE / CONJUGATED POLYMER / COLOR TRANSITION / OPTICAL SENSOR/ INTERFACIAL INTERACTION

AMORNSAK CHANAKUL : EFFECTS OF MONOMER STRUCTURE AND TYPE OF METAL OXIDE NANOPARTICLES ON COLORIMETRIC RESPONSE OF POLYDIACETYLENE/METAL OXIDE NANOCOMPOSITES. ADVISOR : ASST. PROF. NISANART TRAIPHOL, Ph.D., CO-ADVISOR : ASST. PROF. RAKCHART TRAIPHOL, Ph.D., 163 pp.

In this study, a simple route for controlling the colorimetric behaviors of PDA/ZnO nanocomposites is presented by varying monomer structures and polymerization time. Three types of monomers with different alkyl chain length 5,7-hexadecadiynoic acid (HDDA), 10,12-tricosadiynoic acid (TCDA), and 10,12-pentacosadiynoic acid (PCDA) were used for preparing the nanocomposites. All PDA/ZnO nanocomposites exhibit rather different thermochromic behaviors compared to their pure PDA counterparts. All nanocomposites show reversible blue/purple color transition upon multiple heating/cooling cycles. The shortening of alkyl chain length leads to the decrease in color-transition temperature. For the colorimetric response to pH, it is found that all nanocomposites are interestingly sensitive to acidic conditions. However, in basic condition, the color transition takes place at much higher pH compared to that of the pure PDAs. The nanocomposites with shorter alkyl length are found to be more sensitive to pH and alcohols. Moreover,the polymerization time by UV irradiation is also found to affect the colorimetric behaviors of the PDA/ZnO nanocomposites. Long period of irradiation reduces color- transition temperature of the nanocomposites. The complete color reversibility was detected in poly(TCDA)/ZnO irradiated for 60 min and poly(HDDA)/ZnO irradiated for 30 min. Increasing in polymerization time also reduces the magnitude of color changing upon variation of pH or addition of alcohols. In addition, other metal oxide nanoparticles such as SiO_2, TiO_2 and Al_2O_3 are used to prepare the PDA/metal oxide nanocomposites. It is found that their colorimetric behaviors are similar to the pure PDAs.

Department: .....Materials Science ……...Student's Signature……..…

Field of Study: .....Materials Science ……...Advisor's Signature.....

Academic year .....2013……Co-advisor's Signature……..…

ACKNOWLEDGEMENTS

Firstly, I would like to express my sincere appreciation to my advisor, Asst. Prof. Dr. Nisanart Traiphol and my co-advisor, Asst. Prof. Dr. Rakchart Traiphol, for invaluable support, including their kindnessand guidance. Their comments and suggestions not only provide valuable knowledge but also broaden perspective in practical applications.

I would like to thank the chairman, Asst. Prof. Dr. Sirithan Jiemsirilers and other committee members, Asst. Prof. Dr. Kanoktip Boonkerd, Dr. Karn Serivalsatit and Asst. Prof. Dr. Toemsak Srikhirin for many valuable comments and their perceptive suggestions.

I would like to gratefully acknowledge Center of Excellence on Petrochemical and Materials Technology, Ratchadaphiseksomphot Endowment Fund (Contract No. CU's SRP_04_54_23_2) and 90th Year Chulalongkorn Scholarship for my scholarship.

I would like to thank my colleagues at Laboratory of Advanced Polymers and Nanomaterials, Department of Chemistry and Center for Innovation in Chemistry, Faculty of Science, Naresuan University for facilitating in the experiment of thermochromism.

I would like to thanks all my colleagues and staff members in Department of Materials Science, Faculty of Science, Chulalongkorn University for their friendship and encouragement.

Finally, I am eternally grateful to my beloved family for their forever support, love and encouragement throughout my life.

CONTENTS

Page

Page

Page

Page

Page

LIST OF TABLES

Page

LIST OF FIGURES

Page

Page

Page

Page

Page

Page

Page

Page

Page

Page

Page

Page

Page

CHAPTER I

INTRODUCTION

Nowadays, the development of sensing materials based on colorimetric response has become considerably attractive. This is due to color transition property, which can be observed by naked eyes and do not require any expensive equipments. Polydiacetylene (PDA), one of the conjugated polymers with interesting chromic properties, has received much attention from many researchers over the past decades. It has been observed that PDA vesicles exhibit blue to red color transition when subjected to various external stimuli such as solvents (solvatochromism)[1-9], temperature (thermochromism)[10-21], pH[22-28], ions[29-33], biomolecules[34-42] and other chemicals[43-44].

PDA vesicles can be easily prepared by dispersing diacetylene (DA) monomer in water. DA monomer is an amphiphilic molecule constituting polar head and long alkyl tail which can assemble into a stable vesicular structure in aqueous medium at suitable conditions. The topopolymerization of DA monomers is initiated by UV irradiation without the need of chemical initiators or catalysts. PDA vesicles in aqueous solution typically exhibit a deep blue color with a λ_{max} ~640 nm and vibronic shoulder at ~590 nm. Mechanism of a blue-to-red color transition of this polymer has been widely investigated by many research groups[10,45-49]. The external stimuli such as heat, pH or organic solvents can generally disturb the side chain packing by breaking hydrogen bonds between the head groups and weakening the dispersion interactions between alkyl side chains. This causes an increasing of side chain dynamics, which affects the electronic absorption of the conjugated backbone of PDA, resulting in its color transition from either blue to red or red to yellow. In general, the color transition of PDA vesicles exhibits in an irreversible fashion. Accordingly, the blue-to-red color change that occurs when applying external stimuli is not reversed when those external stimuli are removed. Many researchers have attempted to increase the attractive interactions of side chains or head groups by using chemical modification and achieved the PDAs with thermochromic

reversibility[10,14,18,43,50]. However, this synthetic procedure generally requires expensive chemicals and a time consuming purification process. In our recent studies[21], we presented a simple method for preparing PDA/ZnO nanocomposites, which exhibit interesting colorimetric behaviors. We believe that the strong attractive interactions between Zn-OH, Zn-OH_2^+ and carboxylic, carboxylate headgroups of PDAs can restrict the side chains upon increasing temperature. The color transition temperature of the nanocomposites takes place at higher temperature compared to that of pure PDA and interestingly exhibits color reversibility after cooling to room temperature.

In this research, we look further into factors for controlling colorimetric responses of the nanocomposites, including alkyl side chain length, types of metal oxide nanoparticles and polymerization time. Variations in alkyl chain length are expected to affect the chain rigidity and the overall inter- and intrachain interactions, which alter colorimetric response of the nanocomposites to external stimuli. Metal oxide nanoparticles with different surface properties are expected to influence the interfacial interactions between head groups of diacetylene monomer and nanoparticles, which, in turn, affect the color transition behaviors. Finally, effects of photopolymerization time are investigated in this research. This is an interesting parameter, which is expected to affect the colorimetric responses of PDA vesicles and their nanocomposites and has not been studied in the system.

Objectives

1. To study the effects of alkyl side chain length on colorimetric responses of polydiacetylene/ZnO nanocomposites

2. To study the effects of type of metal oxide nanoparticles on colorimetric responses of the nanocomposites

3. To study the effect of UV irradiation time on colorimetric responses of polydiacetylene/ZnO nanocomposites

Expected beneficial outcome(s) from the dissertation

1. Mechanism of colorimetric responses of PDA vesicles and PDA/metal oxide nanocomposites can be proposed.

2. Colorimetric responses of PDA vesicles and PDA/metal oxide nanocomposites can be controlled and utilized in sensing applications.

CHAPTER II

THEORIES AND LITERATURE REVIEWS

2.1. Micelles[51]

An amphiphilic molecule can arrange itself at the surface of the water. The hydrophilic part (head group) contacts with the water while the hydrophobic part (tail group) is held above the surface. When the concentration of surfactant is greater than the critical micelle concentration (CMC), these molecules will be forced to enter into the water phase. A new molecular aggregation called micelles is arranged in the water phase in order to minimize their surface free energy.. For typical micelle, the hydrophobic tail regions are oriented in the micelle center, and the hydrophilic head regions contact with the water phase. In general, spherical micelles are formed to achieve the lowest interfacial area (see Fig. 2.1). However, other types of geometric morphologies can also be formed, such as cylindrical (rod-like) micelle, bilayers and vesicles.

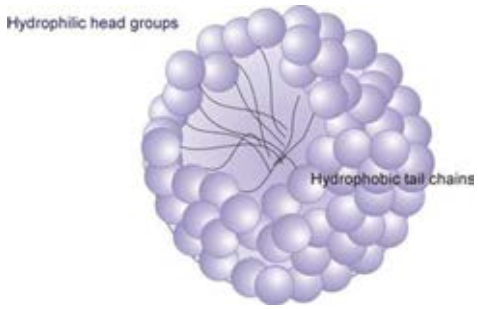

Fig. 2.1 Spherical micelle[52]

The shapes and size of micelles can be controlled by the molecular architecture of the surfactant as well as by varying the pH, charge, ionic strength, temperature and hydrocarbon tail length. The shapes of micelles can be explained through packing considerations based on simple geometrical features of the surfactant as shown in Fig. 2.2 There are three effective geometric parameters of a surfactant:

1. The optimal head-group area, A_h, depending on the hydrophilic, steric and ionic repulsions between adjacent head-groups.

2. The tail volume, V_t, which is the volume of hydrocarbon liquid per hydrocarbon molecule. V_t is a uniform conic volume per surfactant from a spherical micelle. However, if it is not a spherical micelle, V_t is not a uniform cone. It exhibits other shapes such as a truncated cone (a cylinder to form a bilayer micelle) to produce a cylindrical micelle, vesicle or liposome, or an inverted cone to form an inverted micelle.

3. The height of the cone, L_c, which is slightly less than the radius of the micelle and depends on the effective chain length of the hydrocarbon tail.

If we have the estimated values of A_h, V_t, and L_c, then it is possible to define a surfactant packing parameter as followed

$$\lambda_p = V_t/(L_c A_h)$$

This equation can be used to predict the morphology of micelles. For example, if $\lambda_p < 0.33$ spherical micelles is predicted to be formed. The increase in the value of λ_p decreases the curvature of the micelles. For a cone, $\lambda_p = L_c A_h/3(L_c A_h) = 0.33$; for a wedge having a square or rectangular base, $\lambda_p = L_c A_h/2(L_c A_h) = 0.5$; for a cylinder, $\lambda_p = L_c A_h/(L_c A_h) = 1$, and for a truncated cone, $\lambda_p > 0.33$.

In general, surfactants which have single chains with large head-groups can form spherical micelles. Most ionic surfactants also form spherical micelles at low salt concentrations because the electrostatic repulsion in these conditions leads to large head-group areas. However, if the salt concentration in the solution increases, the value of A_h decreases. Correspondingly, λ_p increases to give different micelle shapes. Cylindrical micelles are formed when the surfactant has a packing parameter of $\lambda_p \approx 0.50$.

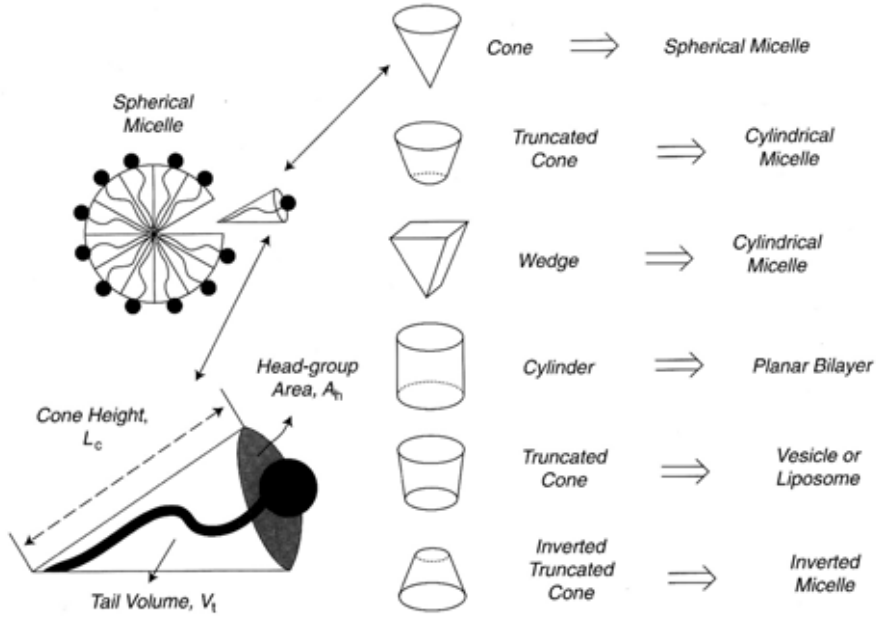

Fig. 2.2 Dependence of the shape and structure of micelles on the molecular architecture of the basic surfactant units[51]

2.2. Bilayers and vesicles[51]

If the head-group and tail cross- sectional areas of a surfactant are nearly equal, giving an exactly cylindrical shape, the packing parameter is around 1.0. Then, bilayer micelle is formed with a tail-to-tail configuration as shown in Fig. 2.3a. The thickness of bilayer micelles is 3-10 nm. Bilayer micelles can be used in the design of supported membrane biosensors for medical and pharmaceutical applications.

Vesicles are a different kind of bilayer micelle (see Fig. 2.3b). If the head-tail shape of a surfactant is a truncated cone, and the packing parameter is >0.33 but <1.0, there is curvature on the micellar structure. Then, a vesicle is formed. Both double-tail and single-tail surfactants such as single-chain fatty acids can be used for preparing vesicles. Diameter of vesicles may be in a range of 100 nm - 10 μm depending on the preparation condition.

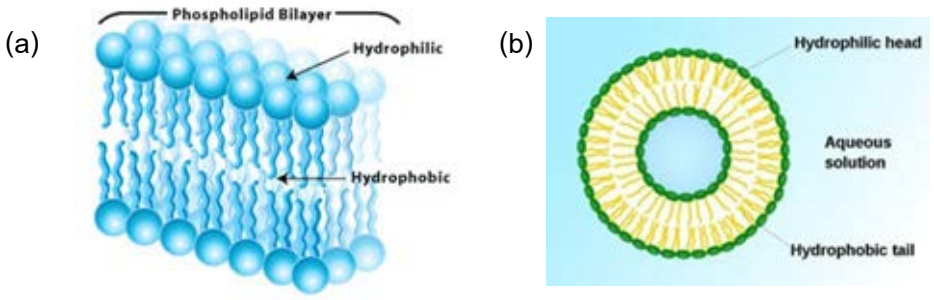

Fig. 2.3 (a) Bilayer micelles[53] and (b) vesicles[54]

2.3. Polydiacetylene

Diacetylene (DA) monomer (Fig. 2.4) is an amphiphilic molecule with carboxylic head group and long alkyl tail, which can arrange into stable vesicular structure in aqueous medium at suitable conditions. The size and morphology of vesicles depend on the structure of monomers such as the length of alkyl chain. The assembled DA monomers can undergo polymerization by 1,4-addition reaction to form polymer backbone upon UV irradiation[55] (Fig. 2.5). The conjugated backbone of PDA constitutes of alternating double and triple bonds (ene-yne). In general, the unperturbed PDA vesicles, which have well-organized arrangement of the side chains, posses long conjugation length and exhibit a deep blue color with a λ_{max} ~640 nm. This conjugated polymer has received much attention from many researchers due to its chromic property. PDA vesicles interestingly exhibit blue to red-color transition when subjected to various stimuli such as temperature, pH and solvents. The color transition can be easily detected by the naked eyes (Fig. 2.6).

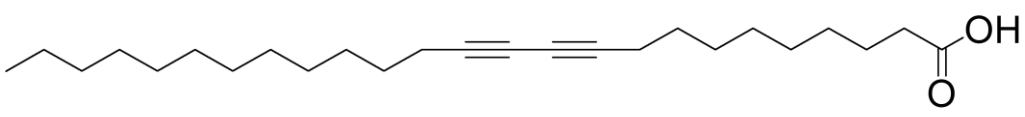

Fig. 2.4 Diacetylene monomer

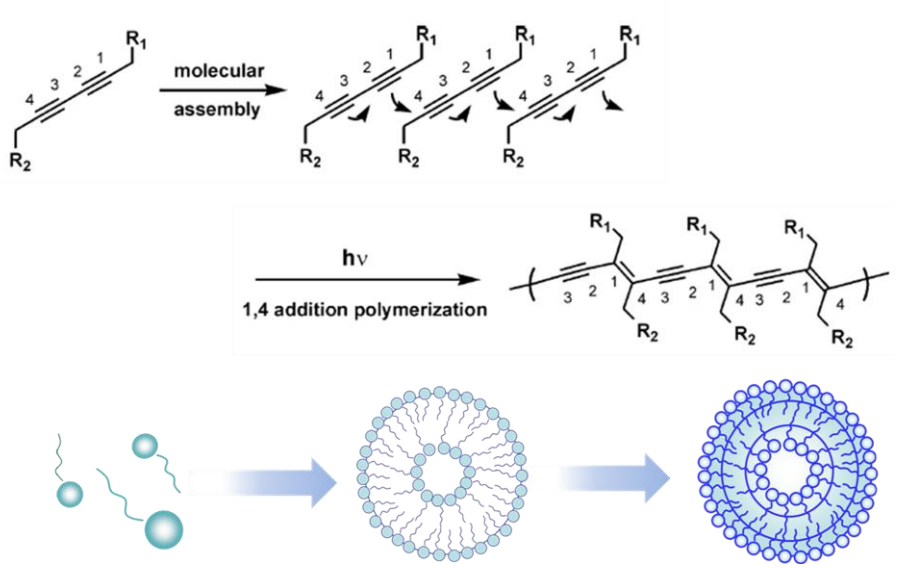

Fig. 2.5 Preparation of polydiacetylene[55]

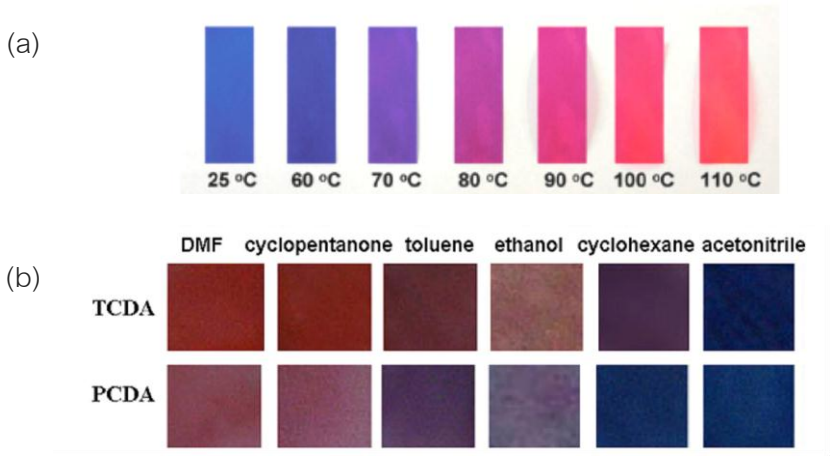

Fig. 2.6 Color transition of polydiacetylene upon (a) increasing temperature[11] and (b) addition of solvents[56]

A quantitative value for the magnitude of blue-red color transition is determined by the colorimetric response (CR), which can be calculated by the the following equation;

$$CR\ (\%) = [(PB_0 - PB)/PB_0] \times 100$$

where $PB = A_{blue}/(A_{blue}+A_{red})$, A_{blue} and A_{red} are the absorbance at the blue component (≈650 nm and the red component (≈540 nm)) in the UV-Vis spectrum, respectively. PB_0 is the initial percent blue of the vesicle solution, and PB is the final percent blue after addition of external stimuli. For a completely converted vesicle solution, PB = 0 and the CR = 100%.

2.4. Mechanism of color transition

The mechanism of the blue to red color transition of PDA vesicles has been deeply investigated in the past few years. It has been generally accepted that the molecular conformation changes such as side chain packing, ordering and orientation affect the electronic states of the polymer, corresponding to the change of optical absorption. Numerous investigations have been performed to understand the exact thermochromism of PDA but it is still not fully understood. However, it can be strongly accepted that with increasing temperature, side chains of PDA normally have higher mobility, which eventually break the hydrogen bonds at the surface of PDA vesicles. This can reduce the planarity of **π**-orbital arrangement along the conjugated backbone, resulting in the decrease of conjugation length. This perturbed PDA absorbs relatively higher energy and exhibits red or purple color. D.J. Ahn and co-workers[10] proposed the mechanism of chromic transition upon increasing temperature of irreversible PDAs as illustrated in Fig. 2.7. They explained that head group interactions (hydrogen bonding, aromatic interactions, etc.) controlled the molecular orientation and caused strain in the alkyl chains of PDAs. Increasing temperature broke head group interactions, resulting in the release of mechanical strain and distortion of the conjugated backbone. Once the head group interactions were broken, the original molecular conformation cannot be restored after cooling to room temperature.

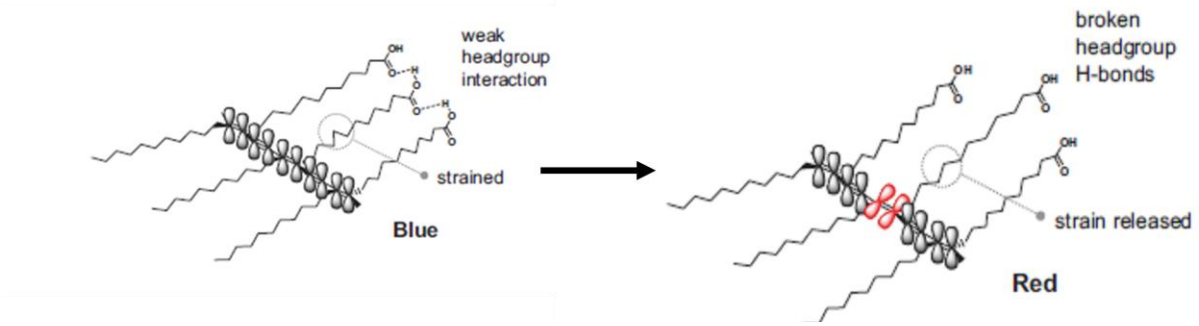

Fig.2.7 A mechanism of chromic responses upon increasing temperature[10]

The perturbation of PDA vesicles upon variation of pH has been deeply investigated by many scientists[7,24]. It is believed that the addition of OH^- ions can remove acidic protons from the carboxylic heads, which leads to the breaking of hydrogen bonds at surface of the vesicles. This acid-base reaction can transform carboxylic group to the carboxylate one withthe negative charge. Therefore, the ionic repulsion between the head groups takes place, which results in the rearrangement of PDA segments.

Kew and Hall[24] intensively studied the colorimetric response to pH of carboxy-terminated polydiacetylene vesicles. Polydiacetylene used in this study was prepared from 10,12-tricosadiynoic acid (TRCDA). Irreversible blue-red transition of this PDA took place when pH increased. However, acidification to pH < 4 exhibited no effects on color of the vesicles. Moreover, the vesicles began to precipitate after incubation for a few hours. They demonstrated that the chromic response to NaOH resulted from two steps (see Fig. 2.8). The first was the deprotonation of the carboxylic acid head groups upon addition of OH^- ions. The second was specific sodium cation binding to the carboxylate groups, which then causes the blue-red transition.

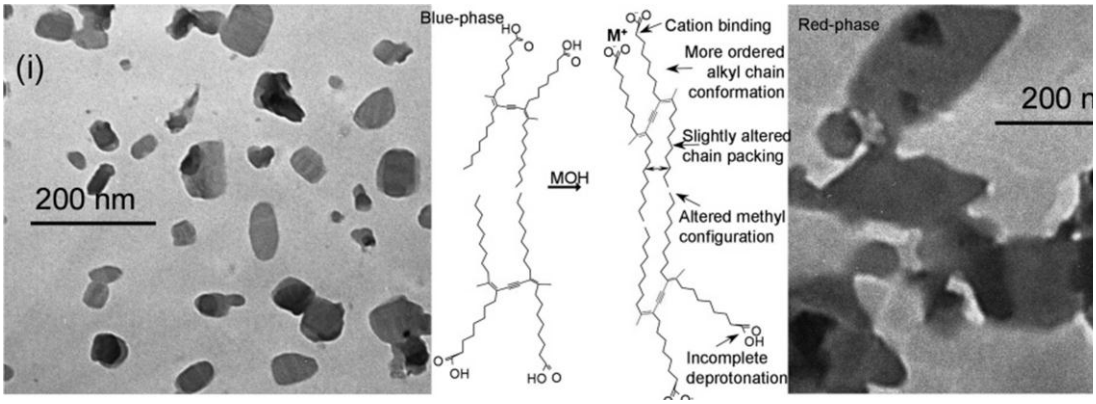

Fig. 2.8 Transmission electron microscopy of dehydrated 0.50 mM TRCDA blue-phase vesicles before (i) and after (ii) basification to form the red-phase by the addition of 1 molar equivalent of 0.1 N NaOH. Schematic shows the proposed structural transition that accompanies the blue-red colorimetric process[24].

In addition, the morphology of this PDA upon increasing pH was also examined in this study. The TEM images of TRCDA vesicles were shown in Fig. 2.8. At normal condition (before basification (i)), mainly well-defined assemblies of blue-phase TRCDA was observed, whereas the red-phase after basification (ii) showed polymer aggregations. Moreover, the particles were not globular but faceted. This structural transition in the red phase can explain irreversible chromatic transition upon increasing pH.

The perturbation of PDA vesicles by addition of alcohol affects the organization of head groups and alkyl side chains near surface region as shown in Fig. 2.9. The hydrophobic alkyl tails of alcohols are expected to penetrate into the hydrocarbon layer of PDA to minimize their contact with the polar medium. The –OH group preferably interacts with carboxylic head group of PDA by hydrogen bonding and/or dipole-dipole interaction. This process breaks hydrogen bonds between the head groups and weakens the dispersion interactions between alkyl side chains. This causes the rearrangement of PDA segments[7,57].

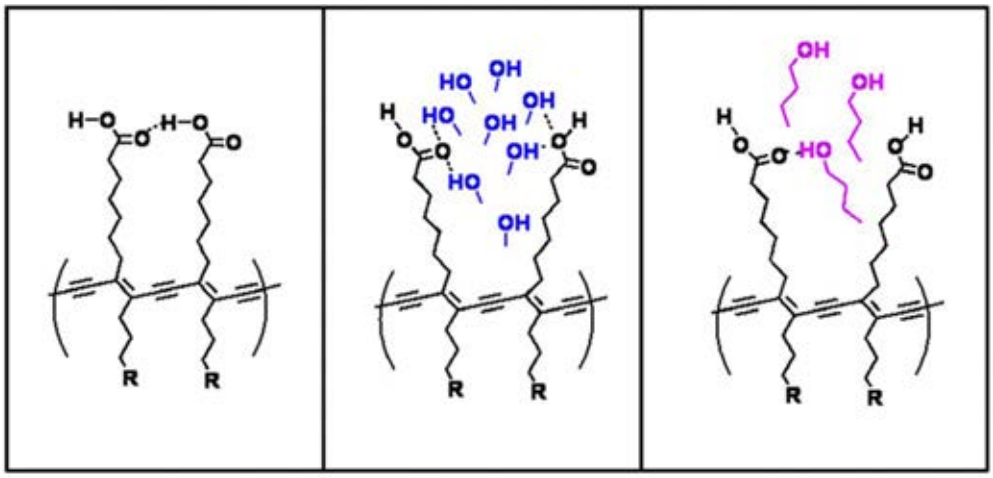

Fig. 2.9 Schematic drawings of penetration of ethanol into the layer of PDA[7]

Effect of amphiphilic molecules upon the color transition of polydiacetylene vesicles was reported by Y-L. Su et al[44]. In this study, they demonstrated that the color transitions of polymerized 10,12-pentacosadiynoic acid (PCDA) vesicles upon addition of sodium dodecyl sulfate (SDS) and Triton X-100 were lower than that of cetyltrimethylammonium bromide (CTAB) as illustrated in Fig 2.10a. This was due to the positive-charge head groups of CTAB, which favorably approached negative-charge carboxylate groups at the vesicle surface. The alkyl chain of CTAB thoroughly inserted in the hydrophobic layer of the vesicles and perturbed the conformation of the polymer backbone, leading to color change of polydiacetylene vesicles (see Fig 2.10b).

In the case of non-ionic Triton X-100, there is no ionic attraction between the head groups of the surfactant and polydiacetylene vesicles. However, molecules of Triton X-100 can be adsorbed onto the surface of the vesicles due to van de Waals force, hydrophobic interaction and etc. Therefore, this molecule can moderately perturb the conformation of polymer backbone. In the system of SDS, the color transition was not observed. The same negatively charged head groups of anionic surfactant SDS and the polymer caused ionic repulsion, which hindered the approach of SDS molecules to the polydiacetylene vesicles.

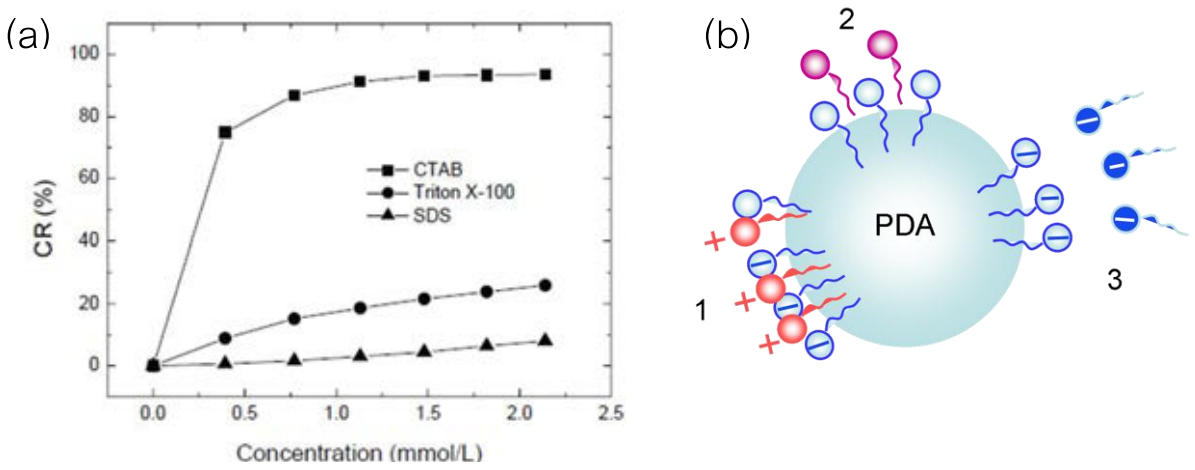

Fig. 2.10 (a) Colorimetric response of polydiacetylene vesicles in aqueous solutions as a function of the concentration of sodium dodecyl sulfate (SDS), Triton X-100, and cetyltrimethylammonium bromide (CTAB)[44], (b) Schematic shows perturbation of surfactant molecules in the polymer vesicles (1) CTAB, (2) Triton X-100 and (3) SDS

2.5. Improving chromic properties of polydiacetylene

The chromic properties of polydiacetylene depend on the molecular structure of this polymer. In general, the colorimetric behavior in the system of PDAs with carboxylic head group is an irreversible process because of the weak interaction of hydrogen bonding between head groups. Several researches challenge in tuning colorimetric response of PDAs for using in wider sensing applications.

2.5.1. Chemical Modification process

A number of works have studied in the increase of the attractive interactions of side chains or head groups by using chemical modification[10,14,15,50,58]. Most of these works mainly focus on the colorimetric response to temperature. X. Chen and co-worker[58] successfully synthesized a new conjugated polymer based on diacetylene by modifying the head group of polydiacetylene with phenyl acetamide group as shown in Fig. 2.11.

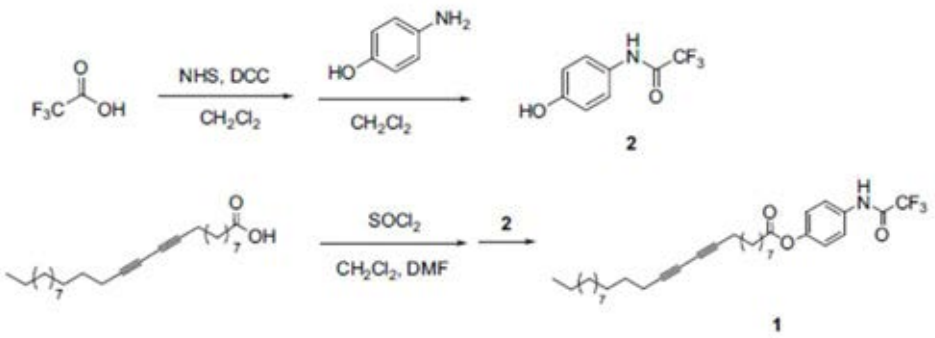

Fig. 2.11 Synthesis of monomer[58]

This PDA solution exhibited a color change from blue to red when the temperature initially increased to 70 °C. The absorption spectra measured during heating and cooling are shown in Fig. 2.12a and b, respectively. When the temperature increased to 70 °C, the absorbance at 625 nm significantly dropped while the peak at 535 nm increased. When the sample was cooled to 30 °C, the absorbance at 625 nm was recovered and the color of PDA solution reverted to purple as illustrated in Fig. 2.12c.

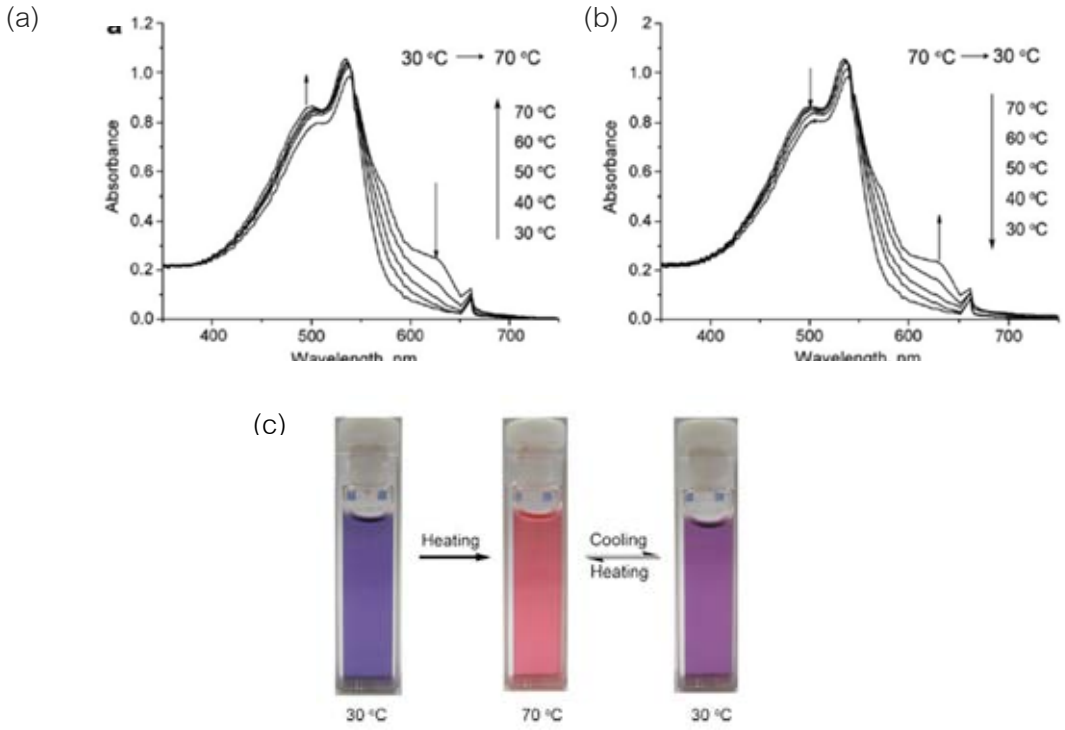

Fig. 2.12 Absorption spectra of PDA solution during (a) heating and (b) cooling, (c) photographs of different color stages at 30 °C and 70 °C[58]

They explained that the reversible thermochromic behavior of this PDA resulted from the strong head group interactions. The introduction of phenylacetamide head into PDA derivative can increase intermolecular interaction (such as **π-π** stacking from phenyl groups and hydrogen bonding from amide groups) between side chains. Therefore, the molecular structure of this PDA can recover to their initial state, resulting in the reversible thermochromic properties and enhanced thermal stability.

J-M. Kim and co-worker[50] demonstrated that polydiacetylene prepared from PCDA-mBzA1, bearing terminal *m*-carboxyphenylamido groups, displayed complete thermochromic reversibility. They also studied the effects of (1) amide hydrogen bonding, (2) aromatic interactions, (3) alkyl chain lengths, and (4) carboxylic groups on the reversibility thermochromism. Various diacetylene monomers were prepared for these purposes as shown in Fig. 2.13. The results of thermochromic behaviors of PDA derivatives liposome investigated by visible spectroscopic are illustrated in Fig. 2.14. Strong, integrated double hydrogen-bonding networks and aromatic interactions in head groups provided supramolecular assemblies (vesicles and films), which can be recovering to their initial molecular structures and average **π**-electron conjugation length following external stimulation.

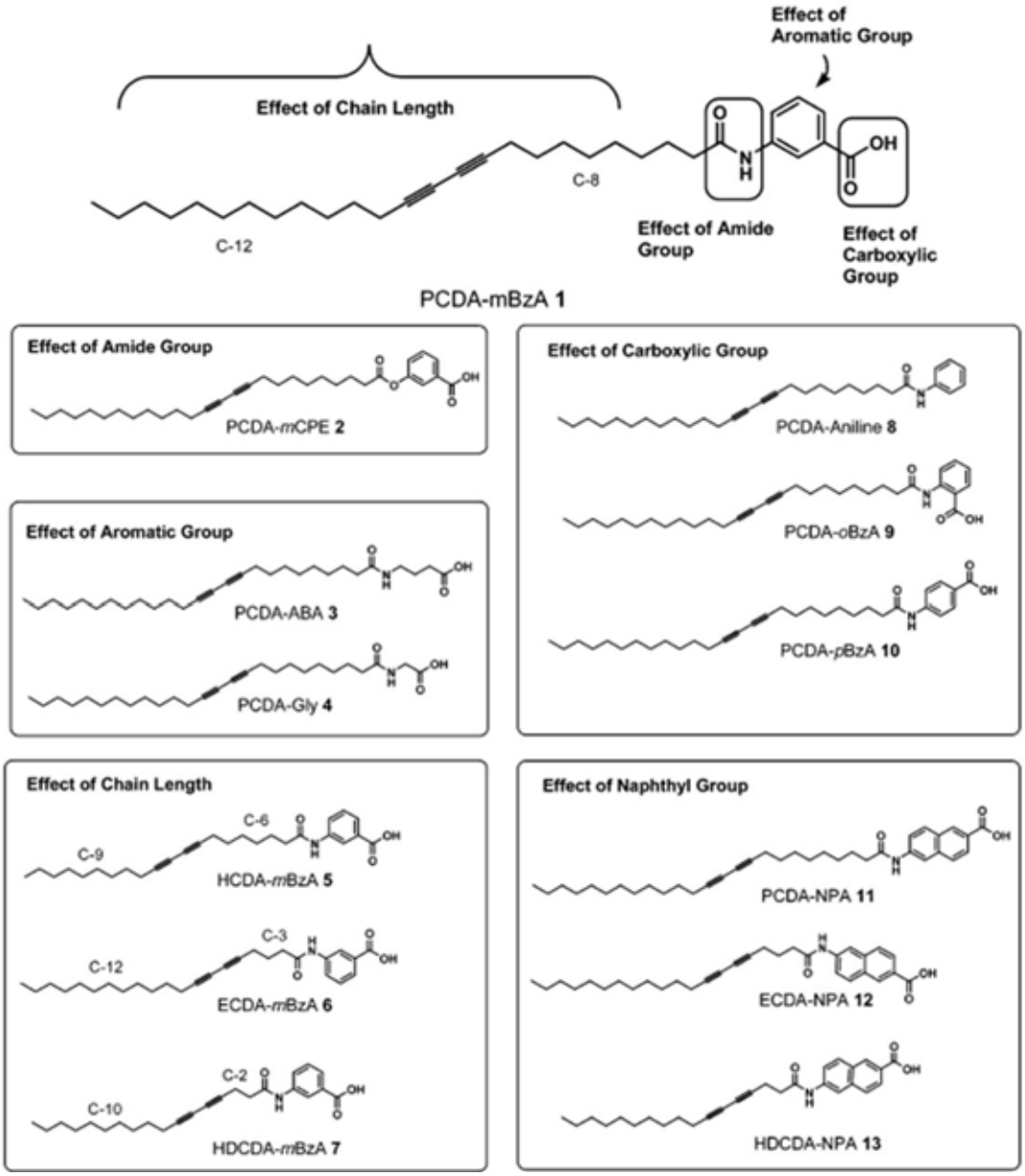

Fig. 2.13 Structures of diacetylene monomers investigated for thermochromism[50]

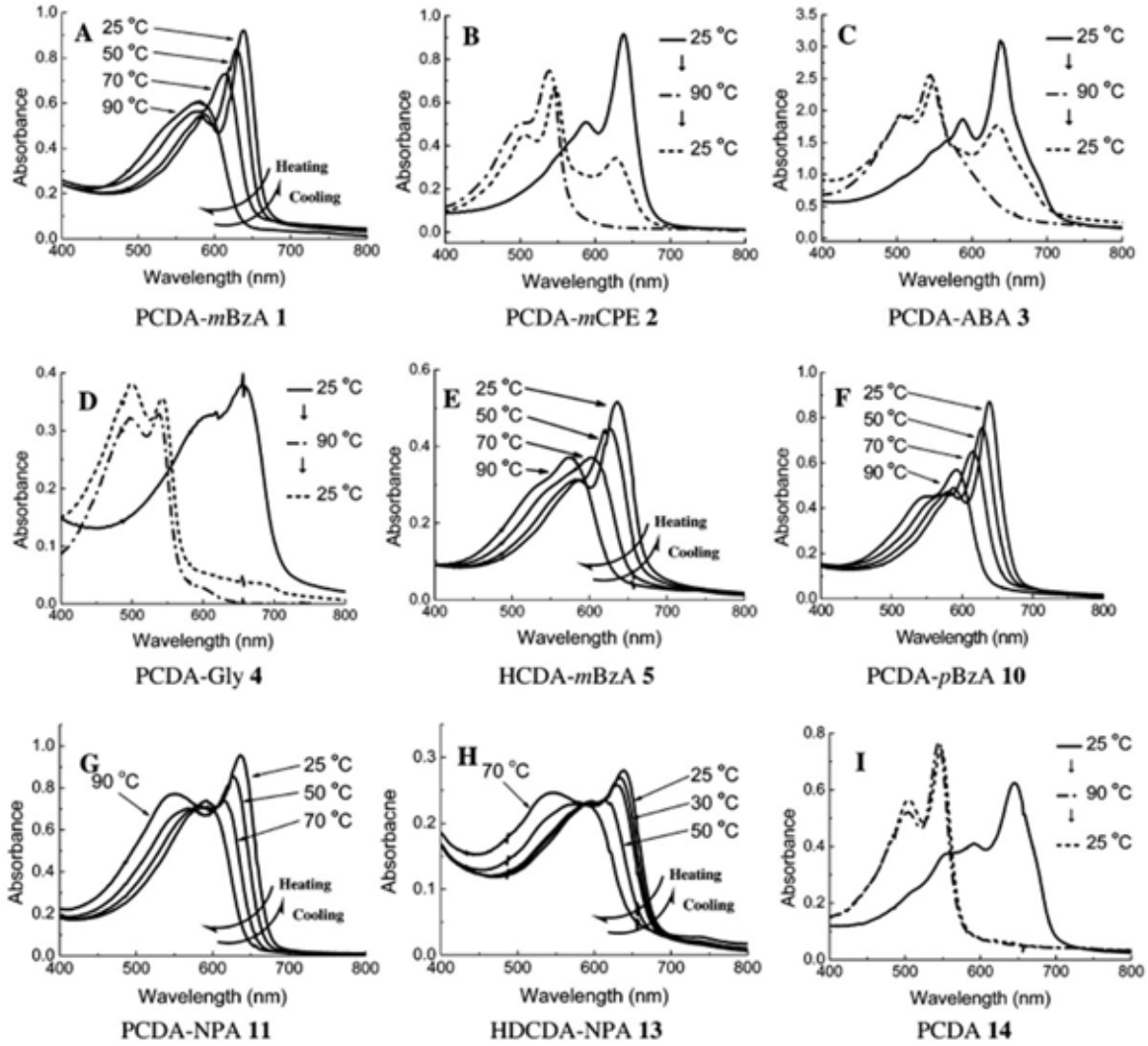

Fig. 2.14 Colorimetric behaviors of PDA derivatives liposome solution upon heating and cooling process[50]

In 2010, S. Wacharasindhu and co-workers[14] modified the head group of polydiacetylene with mono- and diamides derivatives as shown in Fig. 2.15a. In this work, the color transition temperature and thermochromic reversibility of polydiacetylenes could be tuned by the variation of the number of internal amide functional groups in the monomers and the structures of the linkers between the amide groups (see Fig. 2.15b).

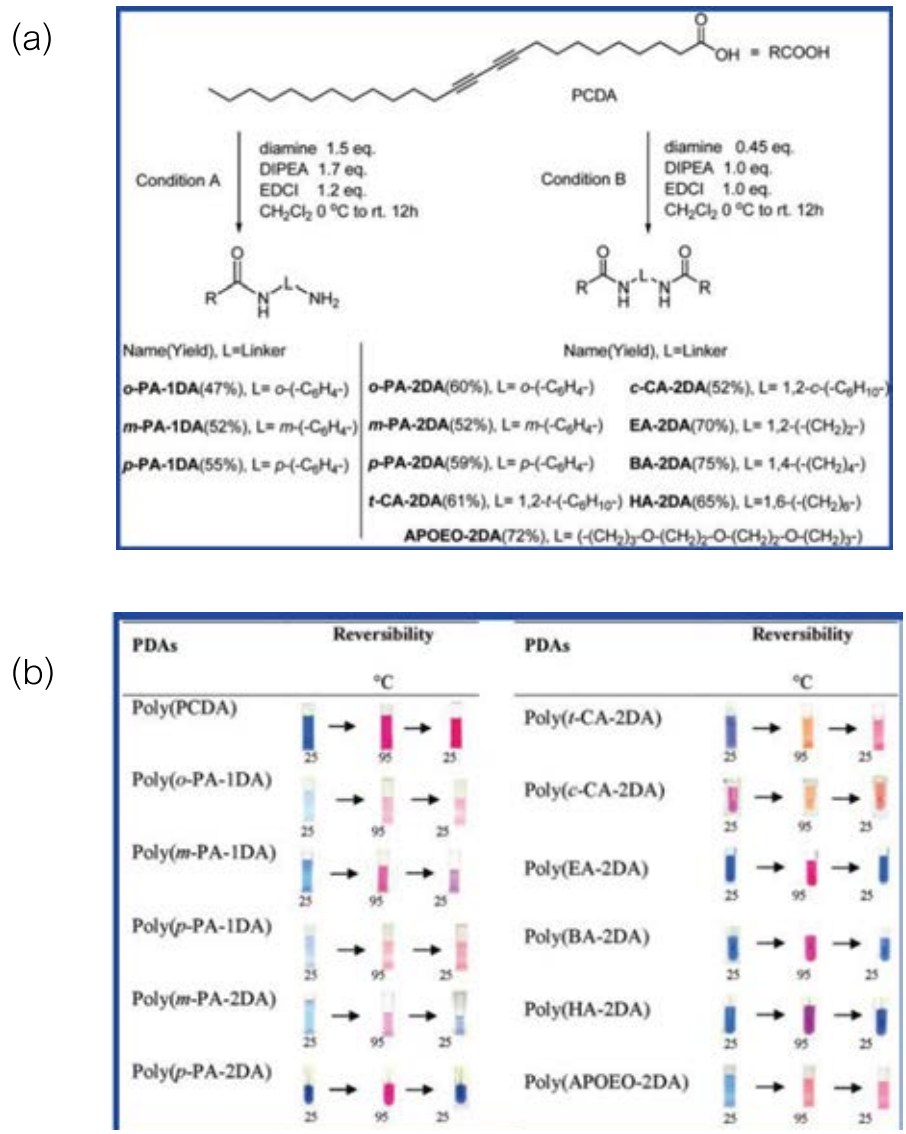

Fig. 2.15 Synthesis of (a) diacetylene lipid monomers and (b) thermochromic reversibility of polydiacetylene with mono- and diamides derivatives[14]

Chemical modification of PDA head groups also affects the colorimetric behaviors upon variation of pH. N. Charoenthai and research group[7] prepared polydiacetylene by using N-(2-aminoethyl) pentacosa-10,12-diynamide (AEPCDA) as a monomer. The head groups of poly(AEPCDA) changed from carboxylic group to amine and amide groups, which affected the strength of hydrogen bonding at the surface of vesicles. The addition of hydroxide ions did not induce chromatic transition of this PDA vesicle because the OH^- could not abstract protons of the amine group. In contrast, the color transition was

observed when the pH decreased. Fig. 2.16a presents systematic change of poly(AEPCDA) absorption spectra, indicating blue-red transition upon the addition of HCl solution. The addition of H^+ ions protonated N atom in the amine groups. Therefore, the head groups possessed positive charges, causing repulsive-ionic interaction between them. This affected the conformation of the polymer backbone, which caused slight color-transition.

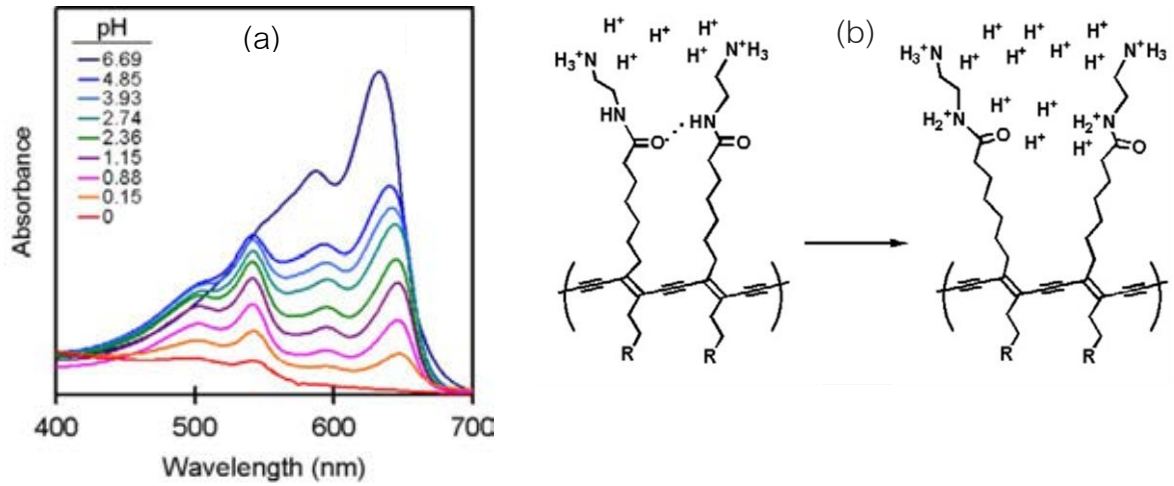

Fig. 2.16 (a) Absorption spectra of poly(AEPCDA) and (b) possible mechanism of color-transition of this PDA upon addition of H^+ ions[7]

In 1999, Jonas and co-workers[59] successfully synthesized liposomes with hydrazine head groups (see Fig. 2.17). They demonstrated that this liposome cannot be polymerized in the neutral condition. However, after adding HCl, the terminal amines were protonated. Instead of disrupting the assembly by repulsion of the charged head groups, this new assembly was organized properly for photopolymerization and blue form of the PDA backbone was obtained.

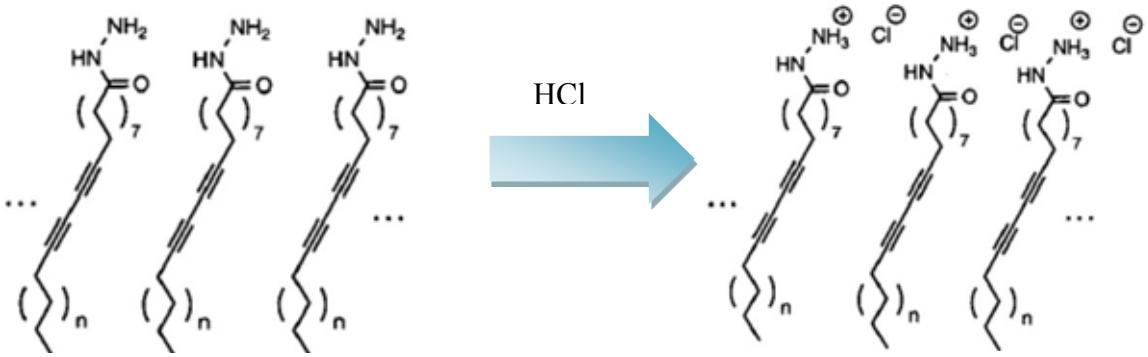

Fig. 2.17 Diacetylene hydrazides and diacetyline hydrazides after addition of HCl[59]

Yuan and Hanks[60] studied the colorimetric behaviors upon variation of pH of this PDA. The absorption spectra of the vesicle solution under various conditions are shown in Fig. 2.18. The as-formed liposome (Fig. 2.18a) showed absorptions at 530 and 567 nm due to BO558, the lipid fluorophore. This solution could not be efficiently polymerized by irradiating with UV light. After treatment with dilute HCl, the absorption spectrum did not significantly change (Fig. 2.18b), but this vesicles could be polymerized within 1 min by UV light (λ = 254nm). The typical PDA absorption spectrum with λ_{max} at 640 nm and a shoulder at 575 nm was obtained as shown in Fig. 2.18c.

Addition of NaOH to neutralize the blue liposomes caused rapid color transition. The red form of this PDA was observed with absorption maximum at 544 nm (Fig. 2.18d). This resulted from the elimination of the hydrogen bond network from the terminal amines after adding OH^- ions. Acidification with HCl again returned the color of the liposome solution to blue (Fig. 2.18e) and then reversed to red after adding NaOH (Fig. 2.18f). The decrease of overall intensity with each cycle resulted from the dilution of the solution upon the addition of the aqueous acid and base, and the aggregation and precipitation of the liposomes during the acidification. This was evidenced by the increase of the baseline at 450 nm, which was due to scattering from the aggregated liposomes.

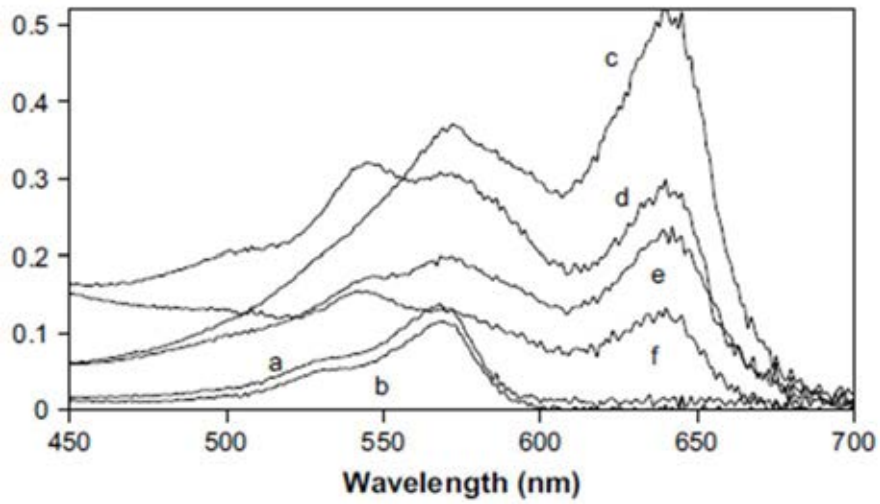

Fig. 2.18 UV–visible absorption spectra of liposomes with hydrazine head groups and BO558: (a) as prepared; (b) solution 'a' treated with 0.02 ml 1 M HCl; (c) solution 'b' irradiated at 254 nm for 1 min; (d) solution 'c' treated with 0.02 ml 1 M NaOH; (e) solution 'd' treated with 0.02 ml 1 M HCl; (f) solution 'e' treated with 0.02 ml 1 M NaOH[60]

From many previous literatures, we can conclude that the chemical modification technique is very effective in improving colorimetric behaviors of PDAs upon addition of external stimuli. However, it requires complicate synthetic procedure, expensive chemicals or catalysts and a time consuming purification process, which are the main problems for applying in industrial scale.

2.5.2. Addition of nanoparticles

Another approach to control colorimetric response of PDA based materials is to incorporate nanoparticles to the system. Only a few previous researches on this subject are presented. T. Yokoyama and his co-workers[61] successfully developed the fabrication process for Ag/polydiacetylene (core/shell) hybridized nanocrystals by using co-reprecipitation/microwave irradiation method. In this work, Ag nanoparticles were synthesized by the reaction between $AgNO_3$ and trisodium citrate at boiling temperature. PPCDA was prepared by using 10,12-heptacosadiynoic acid (14,8-ADA) as a monomer. TEM images of Ag/polydiacetylene hybridized nanocrystals are shown in Fig. 2.19. It

was found that Ag core was evidently coated with poly(14,8-ADA) shell of ~ 5 nm in thickness.

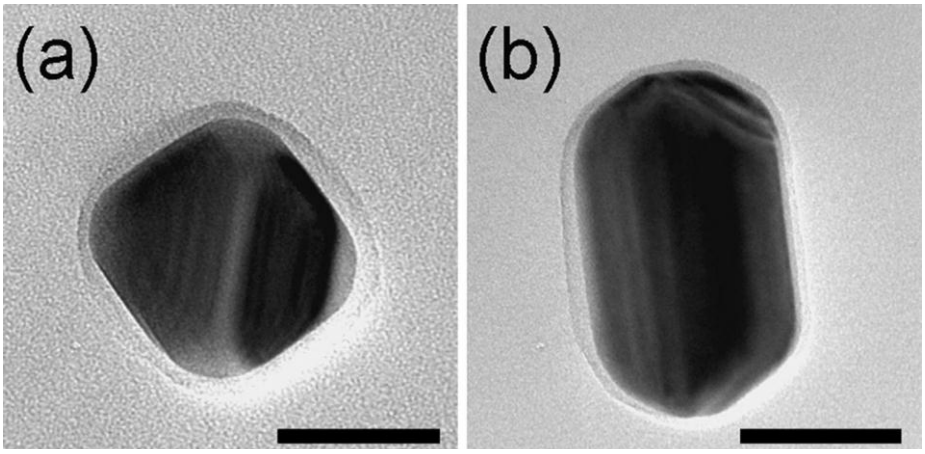

Fig. 2.19 TEM images of core/shell hybridized nanocrystals composed of Ag nanoparticle core and poly(14,8-ADA) shell. The scale bar corresponds to 50 nm[61].

UV–vis spectra of the hybridized nanocrystals aqueous dispersion before and after UV irradiation are exhibited in Fig. 2.20. The broad and large peak at 460 nm attributed to localized surface plasmon resonance from Ag nanoparticles. After UV irradiation, very weak absorption peak appeared at 540 nm as a shoulder. The inset in Fig. 2.20(a) shows the new spectrum at around 500–600 nm after UV irradiation. The absorption spectra of pure poly(14,8-ADA) suspension are shown in Fig. 2.20(b). The excitonic absorption peak in the blue phase appeared in the range from 580 to 650 nm. In contrast, the red phase appeared in more blue-shifted range, from 500 to 550 nm. The results suggested that poly(14,8-ADA) shell as shown in Fig. 2.20(a) was in the red phase in which the π-conjugated backbone of poly(14,8-ADA) was distorted due to anchoring effect and curved surface of Ag nanoparticles core.

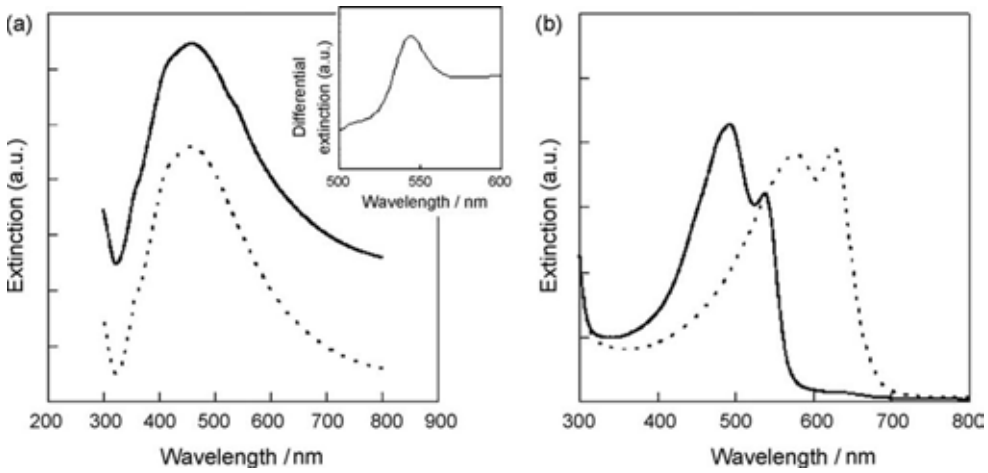

Fig. 2.20 (a) UV–vis spectra of the hybridized nanocrystals aqueous dispersion before (dotted line) and after (solid line) UV irradiation. The inset indicates the differential spectrum before and after UV irradiation. (b) UV–vis spectra of poly(14,8-ADA) nanocrystals aqueous dispersion in the blue phase (dotted line) and the red phase (solid line)[61]

In 2006, Yan-lei Su[62] successfully prepared polydiacetylene/silica nanocomposites for use as a chemosensor. Silica nanoparticles with average size around 46 nm were synthesized by hydrolysis of TEOS in ethanol in the presence of aqueous ammonia. PDA/SiO_2 nanocomposites were prepared by mixing 10,12-pentacosadiynoic acid (PCDA) dissolved in ethanol and aqueous silica nanoparticle solution and then stirring at 20 ^{o}C for 4 hr. Finally, the solution was irradiated with UV light. In this work, PCDA aggregates in aqueous solution without silica nanoparticles could not be polymerized after irradiating with UV light. With SiO_2 nanoparticles, PCDA aggregates absorbed on the surfaces of these nanoparticles. The disordered PCDA molecules in aggregates were orderly arranged on the surface of SiO_2 nanoparticle as illustrated in Fig. 2.21. When this nanocomposite suspension was irradiated with UV light, the color of the suspension turned into blue.

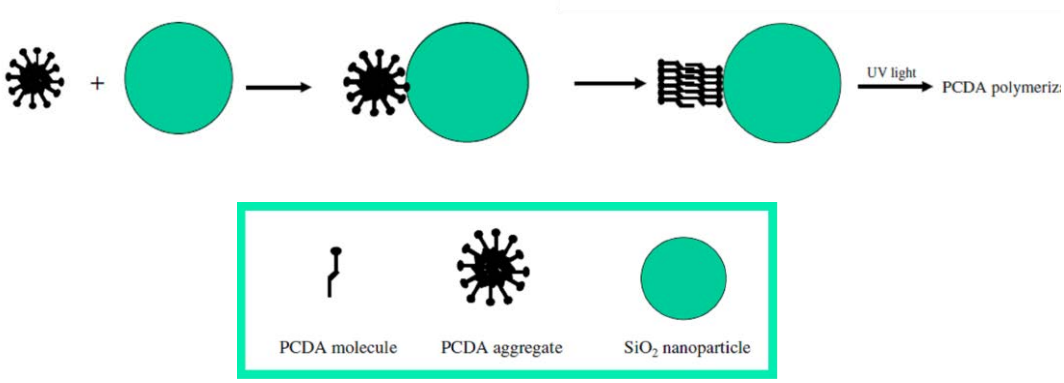

Fig. 2.21 Schematic illustration of the adsorption of PCDA aggregates on the surface of SiO_2 nanoparticles, and the formation of ordered PCDA arrangement on the surface of SiO_2 nanoparticles[62]

PDA/SiO_2 nanocomposite prepared in this work could be used for thermosensor as illustrated in Fig. 2.22a. The color transition from blue to red was observed when increasing temperature from 20 to 70 ^{o}C. Moreover, chromatic transitions of the nanocomposites upon the addition of surfactants were also examined (Fig. 2.22b). The addition of Triton X-100 or CTAB caused a colorimetric change of the PDA/SiO_2 nanocomposites from blue to red phase.

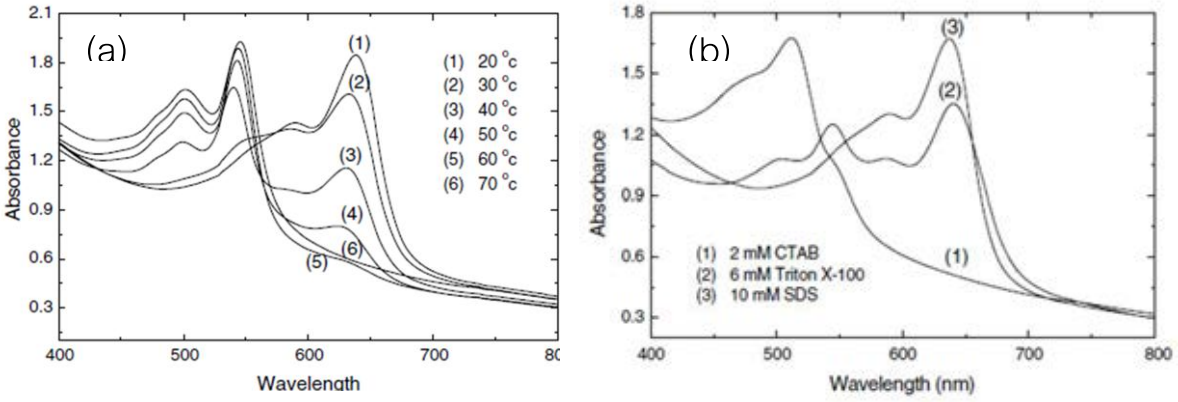

Fig. 2.22 UV–visible absorption spectra of polydiacetylene/SiO_2 nanocomposites subjected to (a) an increasing temperature and (b) an addition of surfactants[62]

In 2011, X. Chen and co-workers[63] successfully prepared PDA/Fe_3O_4 nanocomposite. Fig. 2.23a illustrates the synthesis of the magnetochromatic polydiacetylene by incorporation of Fe_3O_4 nanoparticles. Fe_3O_4 nanoparticles with diameters from 4 to 13 nm were synthesized by co-precipitation technique (see Fig. 2.23b). The Fe_3O_4 nanoparticles constituted of hydroxide groups on their outer surfaces. Therefore, diacetylene monomers attached on the Fe_3O_4 nanoparticles by hydrogen bonding between carboxy and hydroxide groups. Diacetylene monomers coated on the surface of Fe_3O_4 nanoparticles were also confirmed by high-resolution TEM analysis as shown in Fig. 2.23c. Thin layer of the monomer on the surface of the nanoparticle was observed with relatively lighter contrast. After evaporation of solvent, this nanocomposite film was polymerized under UV irradiation and blue color was obtained.

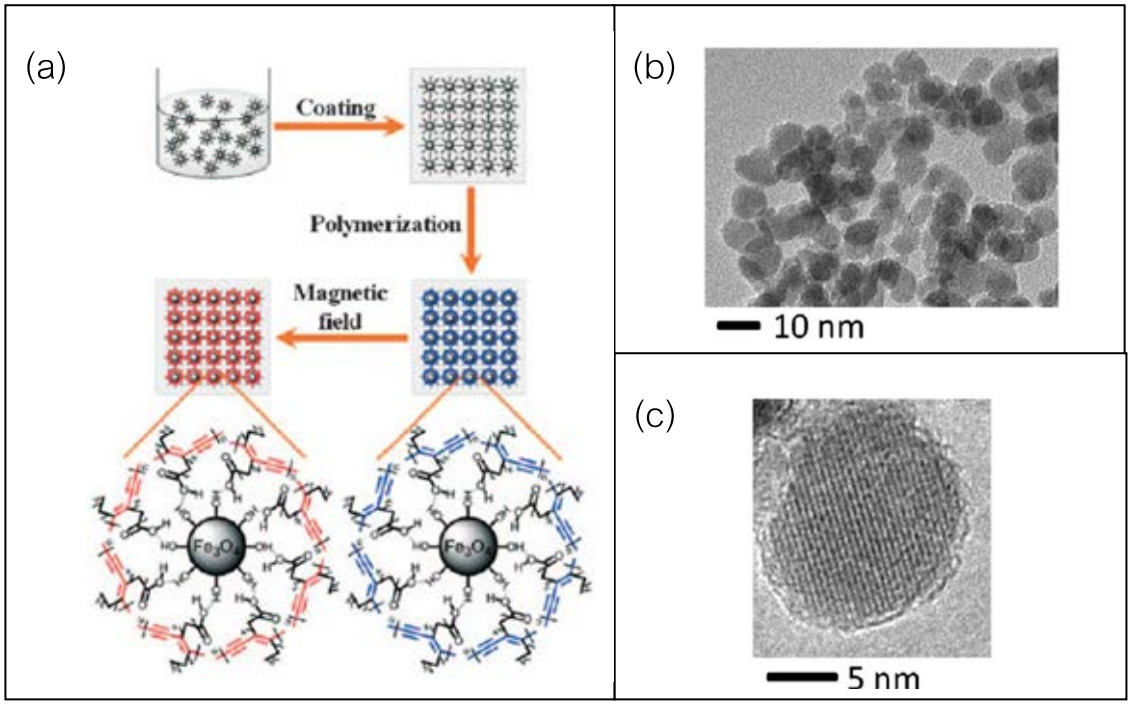

Fig. 2.23 (a) Schematic shows synthesis of the magnetochromatic polydiacetylene by incorporation of Fe_3O_4 nanoparticles, (b) TEM images of Fe_3O_4 nanoparticles and (c) a Fe_3O_4 composite nanoparticle derived from $CH_3(CH_2)_9CCCC(CH_2)_3COOH$[63]

The resulting composite films was uniform and showed a crystalline-like structure (Fig. 2.24a,b). The SEM image at higher magnification in Fig. 2.24c indicated that Fe_3O_4 particles were uniformly dispersed in the PDA matrices. Upon exposure to an AC magnetic field, the derived PDA/Fe_3O_4 film exhibited blue-to-red color transition, which also easily observed by the naked eye. Fig. 2.24d shows photographs of the composite film in blue and red phases, respectively.

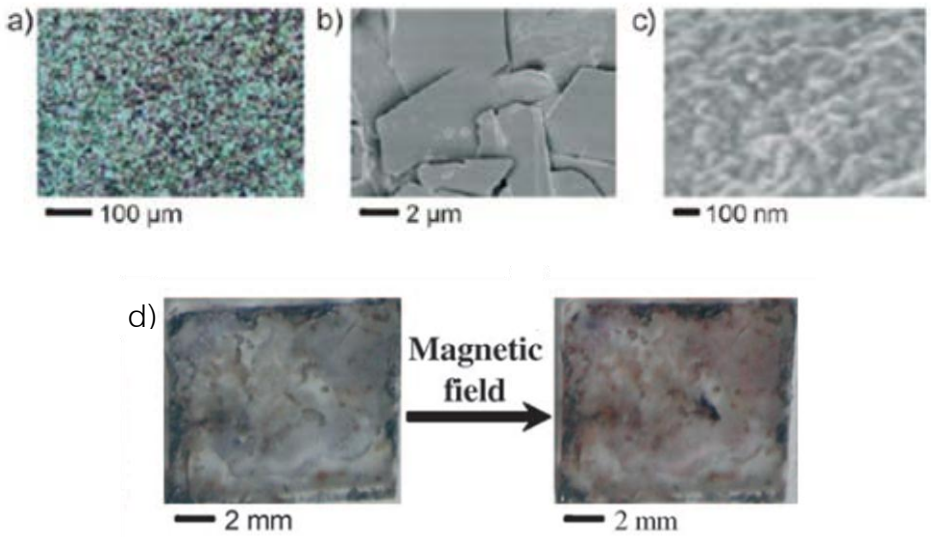

Fig. 2.24 (a) Optical microscopy image, (b) SEM image and (c) SEM image at higher magnification of the nanocomposite film. (d) Photographs of the PDA/Fe_3O_4 composite film before and after color changes upon exposure to an AC[63]

2.5.3. Polymerization time

In preparation of PDA based nanocomposites, polymerization by UV irradiation is involved. However, effects of photopolymerization time on the colorimetric behaviors of polydiacetylene are rarely reported. In general, continuous irradiation tends to induce a blue shift of the absorption maximum and causes a blue-to-red color transition. J. Yoon

and co-workers[64] studied the effect of UV irradiation time on the colorimetric behaviors of polydiacetylene derived from 10,12-pentacosadiynoic acid (PCDA) and aminobutyric acid (ABA). A short period of UV irradiation of this dispersion resulted in the formation of intermediate 640 nm absorbing PDAs, which were transformed to 686 nm-absorbing polymers upon further irradiation (see Fig. 2.25). The absorption spectra upon heating-cooling cycle shown in Fig. 2.26 exhibited that PDAs obtained by a short period of irradiation displayed better colorimetric reversibility during heating-cooling cycles. This result showed that PDAs obtained after a short irradiation time possessed stronger head group interactions than those derived by using long irradiation times.

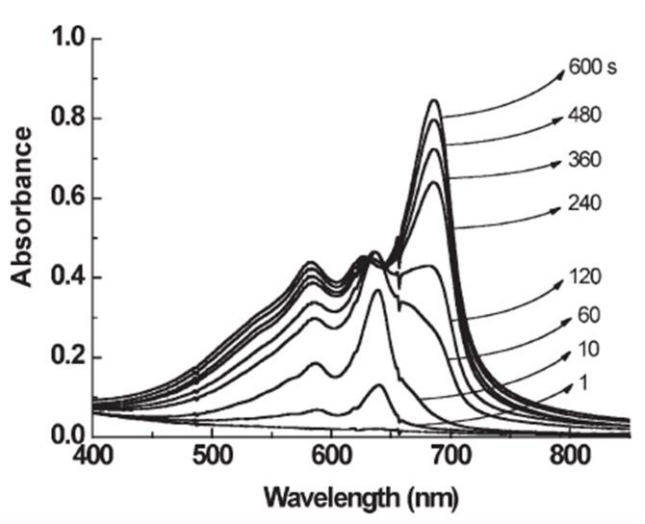

Fig. 2.25 Visible absorption spectra of a PDA vesicle dispersion derived from PCDA-ABA as a function of 254 nm UV irradiation time[64]

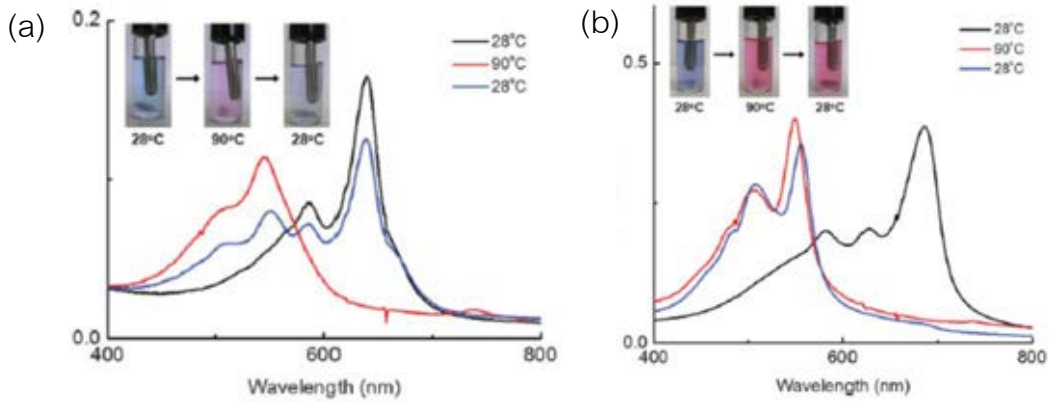

Fig. 2.26 Visible spectroscopic monitoring of PDA dispersions, obtained from (a) short (10 s) and (b) long (600 s) irradiation times when subjected to heating and cooling. The inserts are photographs of the PDA dispersions during the thermal cycles[64]

Q.Huo and co-workers[65] prepared monolayer films of polydiacetylene and polydiacetylene with triaminotriazine (PDATAZ) on different subphases (water, barbituric acid (BA) and cyanuric acid (CA)). They studied the effect of photopolymerization time of these films and found that PDA on pure water subphase completely exhibited red phase when irradiating with UV for 400 s, while PDATAZ on CA and BA subphases exhibited in blue form even after 1200 s irradiation. In discussion, they demonstrated that the change to red phase of PDA upon long period of irradiation did not result from the side chain disorder. They proposed that the length of polymer chain continuously increased with increasing UV irradiation time, and then the polymer backbone started to self-fold to a zigzag structure due to the free rotation of single bonds within the polymer chain, leading to a chromatic transition of PDA (see Fig. 2.27). In the system of PDATAZ on CA and BA subphases, with strong intermolecular interactions existing between the polar groups of the side chains, the side chain dynamic was restricted. Therefore the backbone of polymer was able to maintain its extended chainlike conformation, the blue phase was only observed.

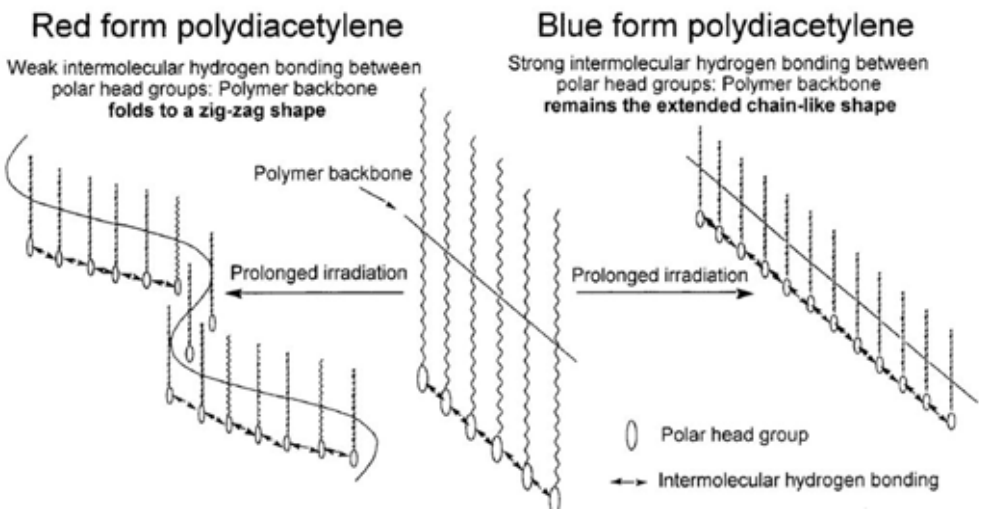

Fig. 2.27 "Self-folding" model of the polymer backbone to explain the chromatic properties of polydiacetylene films upon prolonged UV irradiation[65]

2.6. Polydiacetylene/ZnO nanocomposite

From previous researches mentioned above, polydiacetylene constituting of SiO_2 exhibited weaker colorimetric responses compared to pure polydiacetylene. Ag/polydiacetylene hybridized nanocrystals exhibited only red phase, which could not be used as sensing materials. Polydiacetylene/Fe_3O_4 nanocomposite interestingly exhibited the color transition upon exposure to an AC magnetic field, however, the colorimetric response to other stimuli is not observed. In 2011, N. Traiphol and co-workers[22] presented a simple method for preparation of new class of poly(PCDA)-based materials constituting of ZnO nanoparticles, which exhibited a drastic change in thermochromic behaviors. Carboxylate groups of 10,12-pentacosadiynoic acid (PCDA) monomers in suspension of ZnO nanoparticles were expected to assemble onto the ZnO surface by ionic interaction and/or hydrogen bonding. The interactions between the head groups of the polymer and Zn–OH and Zn-OH_2^+ groups at the surface of ZnO nanoparticles are illustrated in Fig. 2.27. With these strong interfacial interactions, the side chain can be restricted upon increasing temperature. The absorption spectra of the nanocomposites significantly exhibited color transition at higher temperature region

compared to that of pure PDA as shown in Fig. 2.28. In addition, this nanocomposite interestingly displayed thermochromic reversibility. The color of the suspension turned back to blue after cooling to room temperature. The reversibility can be repeated for more than 10 heating and cooling cycles (Fig. 2.29), indicating high thermal stability of the nanocomposites.

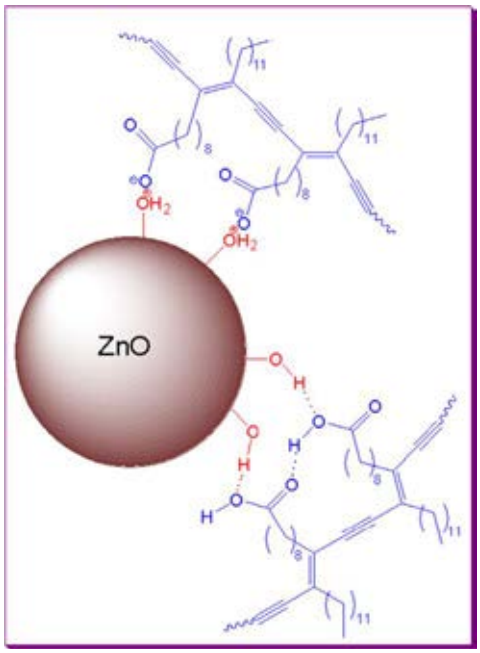

Fig. 2.28 Illustration of hydrogen bonding and ionic interaction between –COOH and –COO^- groups of PDA and Zn–OH and Zn—OH_2^+ groups at the surface of ZnO nanoparticles[22]

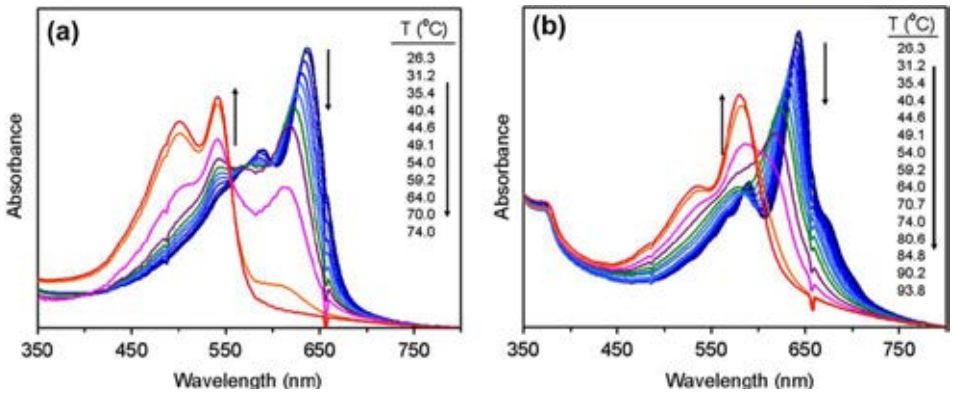

Fig. 2.29 Absorption spectra of (a) pure poly(PCDA) vesicle and (b) poly(PCDA)/ZnO nanocomposites in aqueous suspension upon increasing temperature[22]

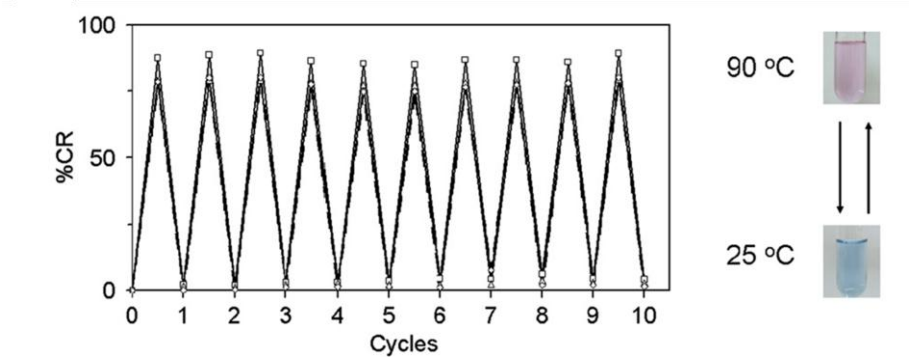

Fig. 2.30 Change of %CR during heating–cooling cycles between 25 °C and 90 °C[22]

The strong interactions at the surface of ZnO between Zn—OH_2^+ groups and carboxylic head groups of poly(PCDA) drastically affected the colorimetric behaviors of the nanocomposites when subjected to other external stimuli such as pH and ethanol. N. Rungruangviriya and N. Traiphol[66] demonstrated that the colorimetric response to pH of poly(PCDA)/ZnO nanocomposite was significantly different from pure poly(PCDA) vesicles. The nanocomposite exhibited higher color stability upon addition of OH^- ions. The spectra represented the color transition upon increasing pH in Fig. 2.30 clearly exhibited that the nanocomposites changed color from blue to purple upon increasing pH to ~12.6 while the color transition from blue to red of poly(PCDA) occurred at pH~8. Moreover, it was shown from the absorption spectra measured upon addition of ethanol in Fig. 2.31 that the addition of ethanol did not induce the color transition of this nanocomposite. The pattern of the spectra did not change although the concentration of ethanol increased to more than 90%v/v. The decrease of the intensity was due to the dilution of the solution after adding ethanol. This was different from the system of pure poly(PCDA) vesicles, which showed the complete blue-red color transition after adding ~50%v/v of ethanol.

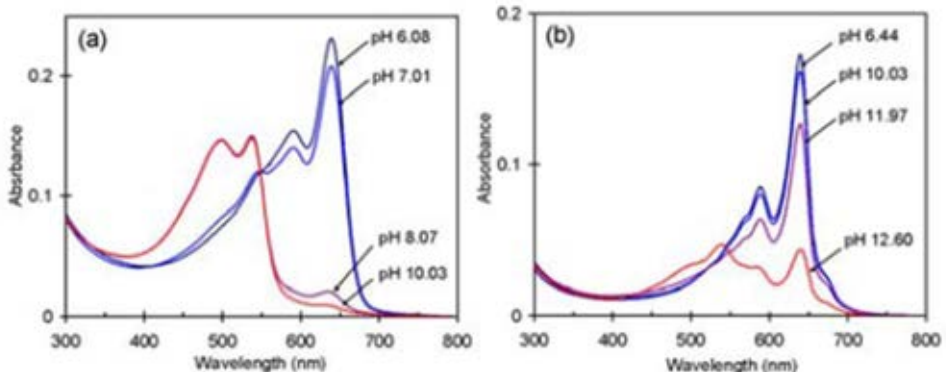

Fig. 2.31 Absorption spectra of (a) pure poly(PCDA) vesicles and (b) poly(PCDA)/ZnO nanocomposites in aqueous suspensions measured at different pH[66]

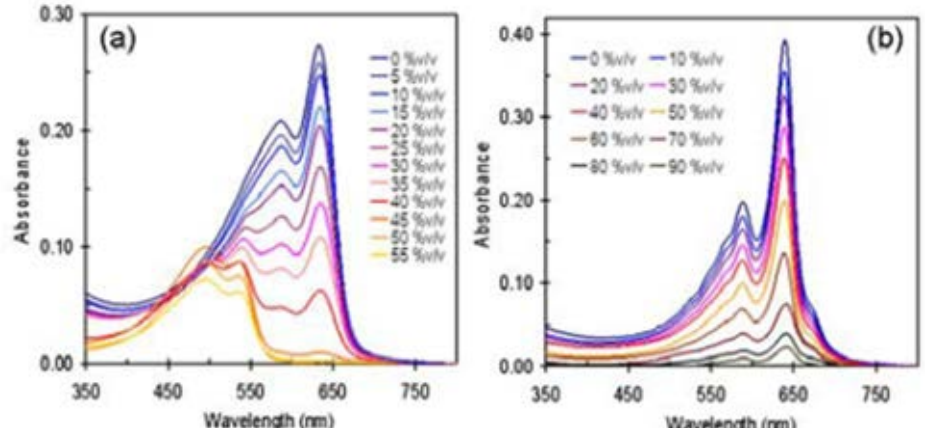

Fig. 2.32 Absorption spectra of (a) pure poly(PCDA) vesicles and (b) poly(PCDA)/ZnO nanocomposites in aqueous suspensions measured upon addition of ethanol[66]

In our group, effects of polymerization time on colorimetric behaviors of polydiacetylene/ZnO nanocomposite were investigated by K. Faisadcha[67]. The 10, 12-pentacosadiynoic acid (PCDA) was used as the monomer and polymerization times were varied from 10 sec to 120 min. The results of chromatic transition upon increasing temperature demonstrated that the increasing of polymerization time caused the color changing of nanocomposite suspension to take place at lower temperature (see Fig. 2.32). Moreover, the nanocomposites polymerized for less than 60 min exhibited complete thermochromic reversibility while nanocomposites polymerized for 60 min and longer exhibited the decrease of reversibility.

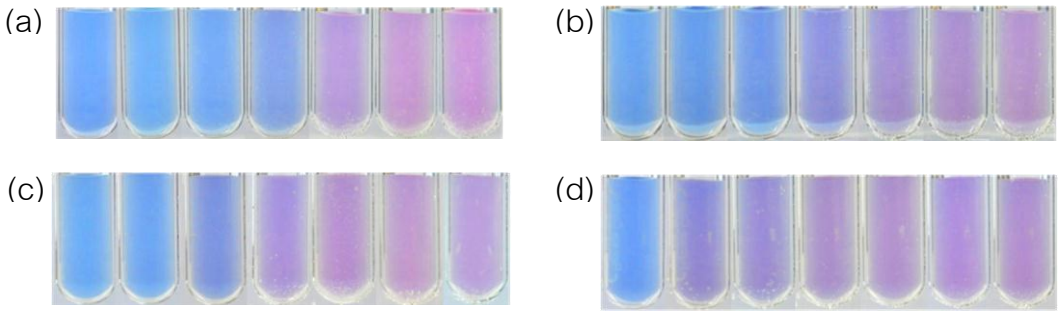

Fig. 2.33 Color photograph of poly(PCDA)/ZnO nanocomposites with variation of polymerization times upon increasing tempertature (a) 5 min, (b) 30 min, (c) 60 min and (d) 120 min[67]

The colorimetric behaviors of the nanocomposites upon variation of pH showed that the nanocomposites polymerized for less than 5 min were more sensitive to acidic condition and exhibited higher degree of color change than the nanocomposites polymerized for 60 min (Fig. 2.33a). In contrast, all of the nanocomposites exhibited high color stability in basic condition (see Fig. 2.33b). Their colors slightly changed at pH more than 13. In addition, the colorimetric response to solvents including propanol, THF and chloroform was also studied. However, the blue-to-red color transition of all nanocomposites was not observed.

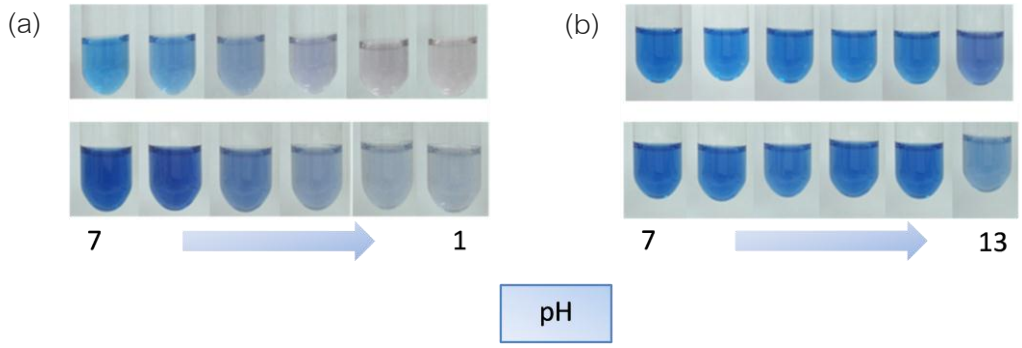

Fig. 2.34 Color photograph of poly(PCDA)/ZnO nanocomposites with polymerization time of 5 min and 60 min taken upon variation of pH[67]

2.7. Types of nanoparticles

Nanoparticles are microscopic particles with at least one dimension less than 100 nm, which are currently an area of intense scientific interest. This is due to specific properties which cannot be observed from bulk materials. In this work, we used many types of inorganic-oxide nanoparticles as follows;

ZnO nanoparticles

Zinc oxide is an inorganic compound, which is in the II-VI semiconductor group. ZnO has a wide band gap of ~3.3 eV at room temperature. ZnO has two main crystal structures. At ambient pressure and temperature, the structure of hexagonal wurtzite is formed. Zincblende ZnO is stable only by growth on cubic structures. In addition, ZnO can be formed as rocksalt structure at very high pressure (~10GPa). ZnO nanoparticles have received much attention within scientific community due to their unique properties (e.g. photocatalytic activity, optical property, antibacterial activity, high thermal conductivity, etc.), which can be used in many industrial applications such as gas sensor, cosmetics, photocatalyst, paints, solar cell, etc.

TiO_2 nanoparticles

Titanium dioxide is one of inorganic compounds extensively synthesized in nanoscale materials. TiO_2 exists in three main structures; anatase, rutile, which are in tetragonal form and brookite, which has orthorhombic form. TiO_2 nanoparticles can be used for a variety of potential applications such as a photocatalyst for decomposing organic pollutants, a pigment in sunscreen and cosmetic products, producing hydrogen by water splitting, a smart material with self-cleaning due to super-hydrophilic properties, dye-sensitized solar cells, etc.

SiO_2 nanoparticles

Silicon dioxide, also known as silica is most commonly found as sand or quartz in nature. SiO_2 has many different crystalline forms (polymorphs) in addition to amorphous

forms, which relate to different arrangements of tetrahedral SiO_4 units, such as quartz, tridymite, cristobalite etc. The technique that widely uses for synthesizing SiO_2 nanoparticle is sol-gel process by hydrolysis of TEOS (Tetraethyl orthosilicate). This nanomaterial can be used for various industrial applications such as catalyst, cosmetic, pigments, fillers, etc.

Al_2O_3 nanoparticles

Aluminium oxide or alumina has many interesting properties, for example high hardness, high stability, high insulation, and transparency. The most general form of crystalline aluminium oxide is known as corundum. There are many crystalline forms of Al_2O_3 such as gamma, delta, theta, and alpha. However, the alpha alumina phase (e.g. corundum/sapphire) is the most stable phase. Al_2O_3 nanoparticles can be prepared by many techniques including sol-gel, pyrolysis, sputtering, microemulsion, hydrothermal, and laser ablation. Al_2O_3 nanoparticles is widely used for additive in polymer to increase wear resistance, improving ceramic properties, cosmetic filler, catalyst, fluorescent materials, etc.

CaO nanoparticles

Calcium oxide, commonly known as quicklime or burnt lime is a widely used chemical compound because it is inexpensive, has a high basicity, and is non-corrosive, easy to handle compared to homogeneous base catalysts and can also be recycled. CaO nanoparticles can be synthesized by sol-gel process, thermal decomposition and microwave–assisted synthesis. Recently, calcium oxide nanoparticles can be utilized for as catalyst in many chemical transformations.

MgO nanoparticles

Magnesium oxide or magnesia is an important inorganic oxide which can be used in many applications such as catalyst supports, waste remediation, refractory materials and pharmaceutical. MgO generally has rocksalt structure. In commercial, MgO particles are produced by thermal decomposition of magnesium salts or magnesium

hydroxide. MgO nanocrystals can be prepared by several techniques including sol-gel, hydrothermal, microwave-induced combustion, laservaporization, etc. MgO nanosized particless can be applied in the filling subjects (in painting, paper, cosmetic, plastic), catalysis and the co-assistant materials of some electric materials.

In this study, we focus on the nanocomposites based on PDAs, which were found to show remarkable colorimetric behaviors. Factors controlling their colorimetric responses are systematically investigated. Influences of alkyl side chain length on colorimetric responses are studied by preparing nanocomposites with various types of diacetylene monomers including 5,7-hexadecadiynoic acid (HDDA), 10,12-tricosadiynoic acid (TCDA), and 10,12-pentacosadiynoic acid (PCDA). The variation in alkyl chain length is expected to affect the chain rigidity and the overall inter- and intrachain interactions, which causes the change of their colorimetric responses to external stimuli. Effects of types of metal oxide nanoparticles are also investigated. Metal oxides, such as SiO_2, TiO_2, Al_2O_3, CaO and MgO with sizes between 20-50 nm are purchased from commercial suppliers. Interfacial interactions between the head groups of diacetylene monomer and nanoparticles are expected to be affected by surface charge of nanoparticles, which, in turn, altered dynamics of the side chains upon subjecting to external stimuli. Finally, effects of photopolymerization time are studied in this research. Periods of UV irradiation could strongly affect the colorimetric behaviors of the PDAs and there have not been studied in the nanocomposite system.

CHAPTER III

EXPERIMENTAL PROCEDURE

3.1. Materials

The DA monomers used in this study, 5,7-hexadecadiynoic acid (HDDA), 10,12-tricosadiynoic acid (TCDA), and 10,12-pentacosadiynoic acid (PCDA), were commercially available at Fluka. The ZnO nanoparticles with a size < 20 nm (from the label) were purchased from Nano Materials Technology (Thailand). TiO_2 nanoparticles (< 25 nm), SiO_2 nanoparticles (10-20 nm), Al_2O_3 nanoparticles (< 50 nm), MgO nanoparticles (< 50 nm) and CaO nanoparticles (< 160 nm) were purchased from Sigma-Aldrich.

3.2. Preparation of PDA vesicles and PDA/ZnO nanocomposites

PDA vesicles and PDA/ZnO nanocomposites were prepared from three types of diacetylene monomers including 5,7-hexadecadiynoic acid (HDDA), 10,12-tricosadiynoic acid (TCDA) and 10,12-pentacosadiynoic acid (PCDA),

To prepare PDA/ZnO nanocomposites diacetylene monomers were purified by dissolving them in chloroform. The suspensions were filtered through 0.45 μm pore size nylon membrane to remove polymerized materials and then heated to completely evaporate chloroform. ZnO nanoparticles were dispersed in deionized water by using probe sonication for 10 min and then added into the purified diacetylene monomers. The concentration of DA monomers was 1 mM, while the ratio of ZnO/DA was kept at 10 wt% in all experiments. The suspensions were sonicated at about 80 ^{o}C for 60 min to co-disperse the DA monomers and ZnO nanoparticles into aqueous medium. Then the suspension was kept at ~4 ^{o}C for ~24 h to allow assemble of monomers onto particle surface. Topopolymerization of the assembled DA monomers was initiated by irradiating with ordinary UV light (λ~254 nm, 10 W). Schematic of preparation of PDA/ZnO

nanocomposites is illustrated in Fig. 4.1. For the PDA vesicles, the pure PDA assemblies were prepared by using the same procedure but without adding the ZnO nanoparticles.

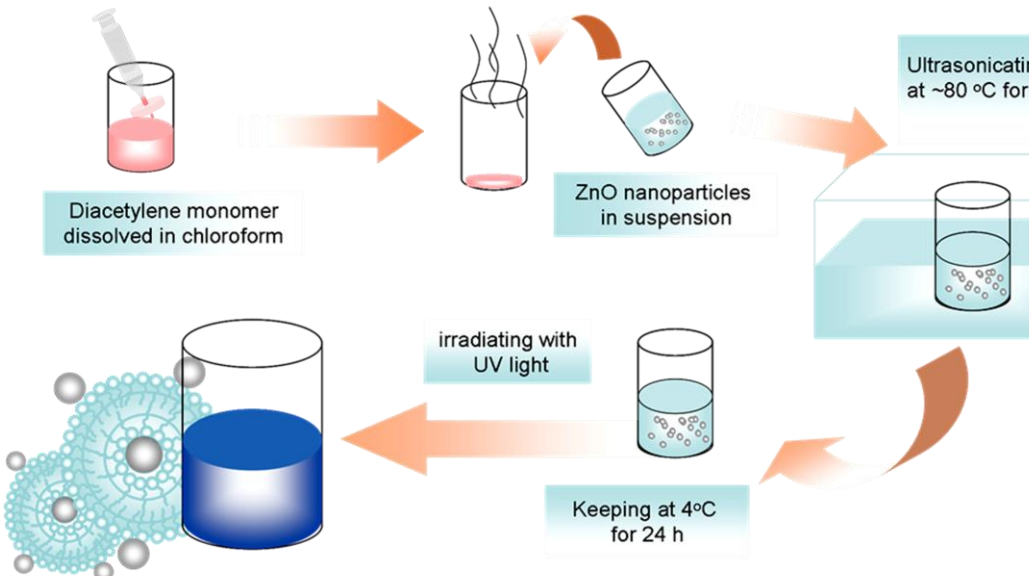

Fig. 3.1 Preparation of PDA/ZnO nanocomposites

3.3. Preparation of nanocomposites using various metal oxides

In this study, PDA/metal oxide nanocomposites were prepared by using 10,12-pentacosadiynoic acid (PCDA) as a monomer. The preparation was the same as described in 4.2, but other types of metal oxide nanoparticles including SiO_2, TiO_2, Al_2O_3, CaO and MgO were used instead of ZnO.

3.4. Preparation of PDA/ZnO nanocomposites by varying UV irradiation times

To study effects of polymerization period, PDA/ZnO nanocomposites were prepared as described in 4.2 by using 5,7-hexadecadiynoic acid and 10,12-tricosadiynoic acid as monomers However, UV irradiation time was varied in the ranges of 15s-120 min.

3.5. Characterizations

3.5.1. Colorimetric behaviors

Thermochromic behaviors were investigated by using UV–Vis spectrometer (Analytik Jena Specord S100) equipped with water-circulating variable temperature unit. Temperature of the samples was measured by placing a thermocouple directly into the aqueous suspension. The samples were heated to temperature ranged from 30-90 ^{o}C. Colorimetric responses to alcohols were examined by adding ethanol or isopropanol into the aqueous suspension and then obtaining the absorption spectra. The responses to pH of PDA vesicles and nanocomposites were examined by adding NaOH or HCl solutions into the aqueous suspensions to adjust pH in the ranges of 0.5-13.5. The colorimetric response (CR) was calculated by the following equation to quantify the magnitude of blue-red transition of the PDA vesicles and the nanocomposites.

$$CR\ (\%) = [(PB_0 - PB)/PB_0] \times 100$$

$$PB = A_{blue}/(A_{blue}+A_{red})$$

A_{blue} and A_{red} were the absorbance of the blue phase (~645 nm) and the red phase (~540 nm), respectively. PB_0 was the initial value before exposure to each stimulus. For the poly(PCDA)/ZnO and poly(TCDA)/ZnO nanocomposites, the color changed from blue to purple with absorbance at 580 nm. Therefore, the calculation of PB values used A_{580}(purple) instead of A_{540}. For poly(HDDA)/ZnO nanocomposite, absorption peaks of blue and purple phases were detected at 660 nm and 600 nm, respectively. Therefore, we used the absorbance at 660 nm (A_{660}(blue)) and 600 nm (A_{600}(purple)) for the calculation of CR values.

3.5.2. Size and Morphology

Morphologies of PDA vesicles and the PDA/ZnO nanocomposites were investigated by scanning electron microscopy SEM (JEOL, JSM-6400). Samples for SEM measurements were prepared by drop casting from aqueous suspensions onto a glass

slide and coating with gold. Their size distributions were measured by utilizing dynamic light scattering (Brookhaven, ZetaPaLs). The concentrations of PDA vesicles and the nanocomposite suspensions were diluted until suitable for the measurements.

3.5.3. Zeta potential

Surface charges of PDA vesicles and the nanocomposites upon variation of pH were measured using electrophoresis technique (Brookhaven, ZetaPaLs). The sample suspensions were diluted and then added about 1.5 ml into the cuvette. The cuvette was equipped with electrodes and connected to the instrument.

3.5.4 The functional groups

The functional groups of pure PDA assemblies and PDA/ZnO nanocomposites were investigated by FT-IR (Perkin Elmer Spectrum GX spectrometer) in transmittance mode to study interactions between side chains and interfacial interaction between ZnO nanoparticles and head groups. The samples were prepared by mixing dried PDAs assemblies or PDA/ZnO nanocomposites with KBr powder and pressed into pellets.

3.6. Experimental diagram

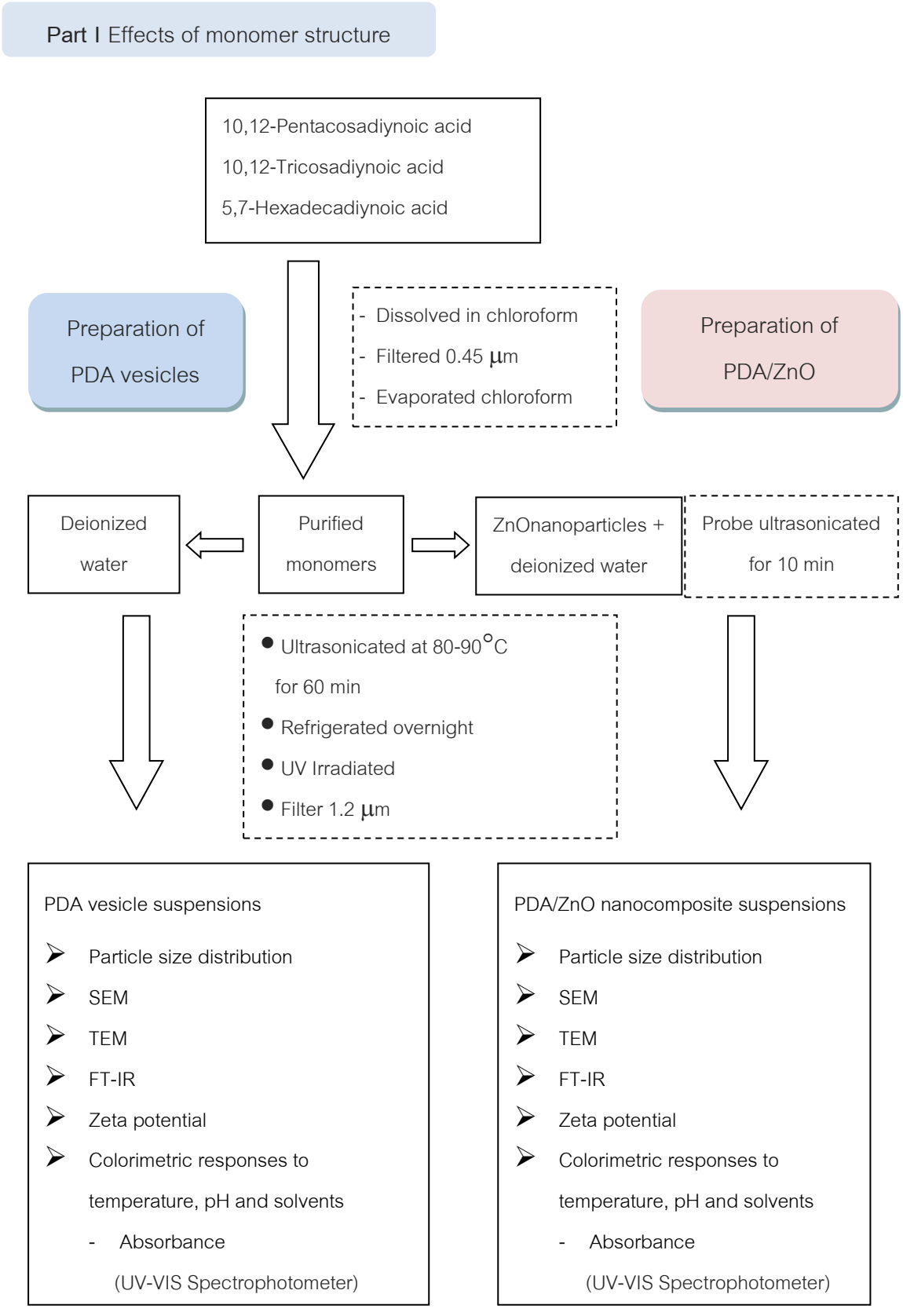

Part II Effects of polymerization time

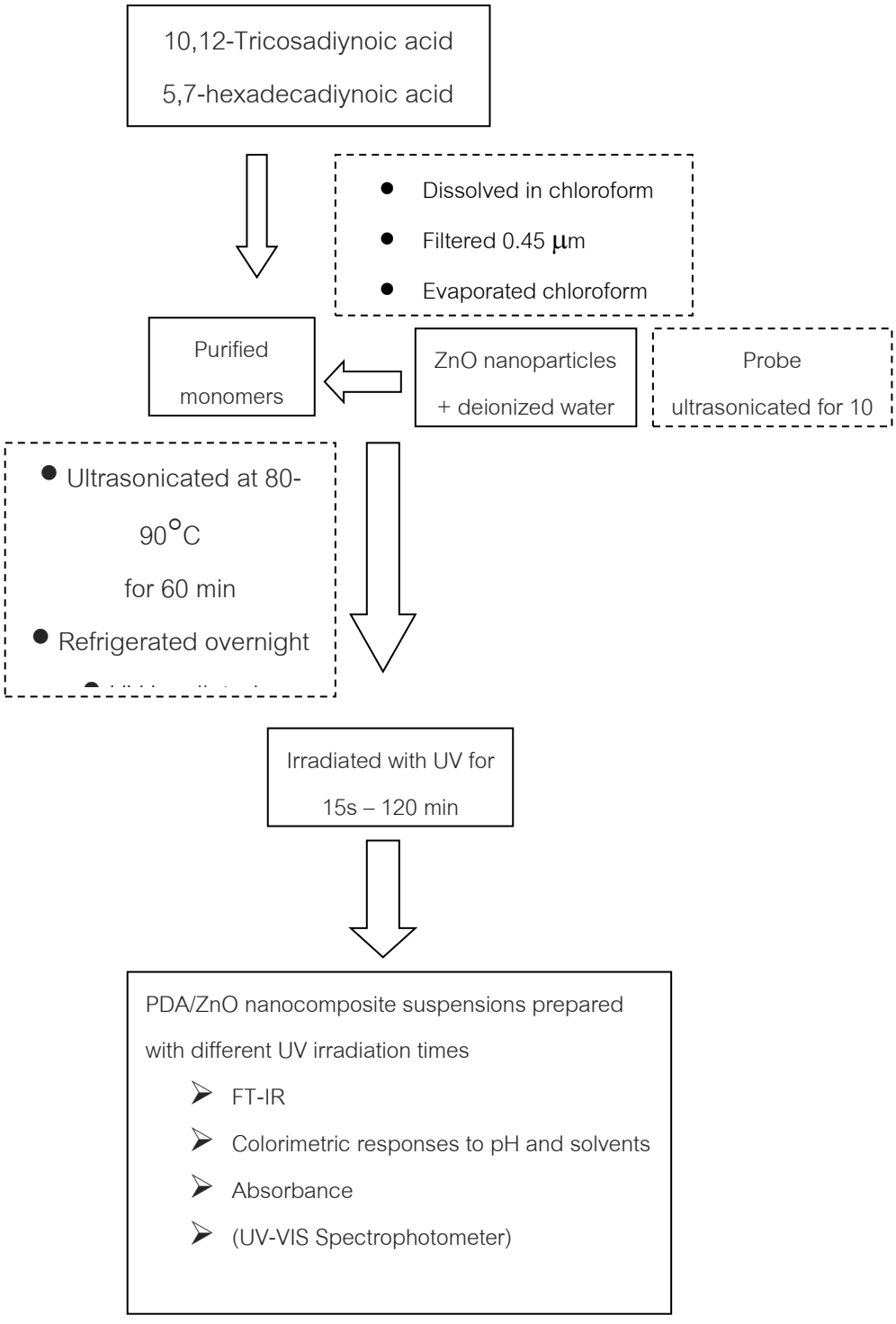

Part III Effects of metal oxide nanoparticles

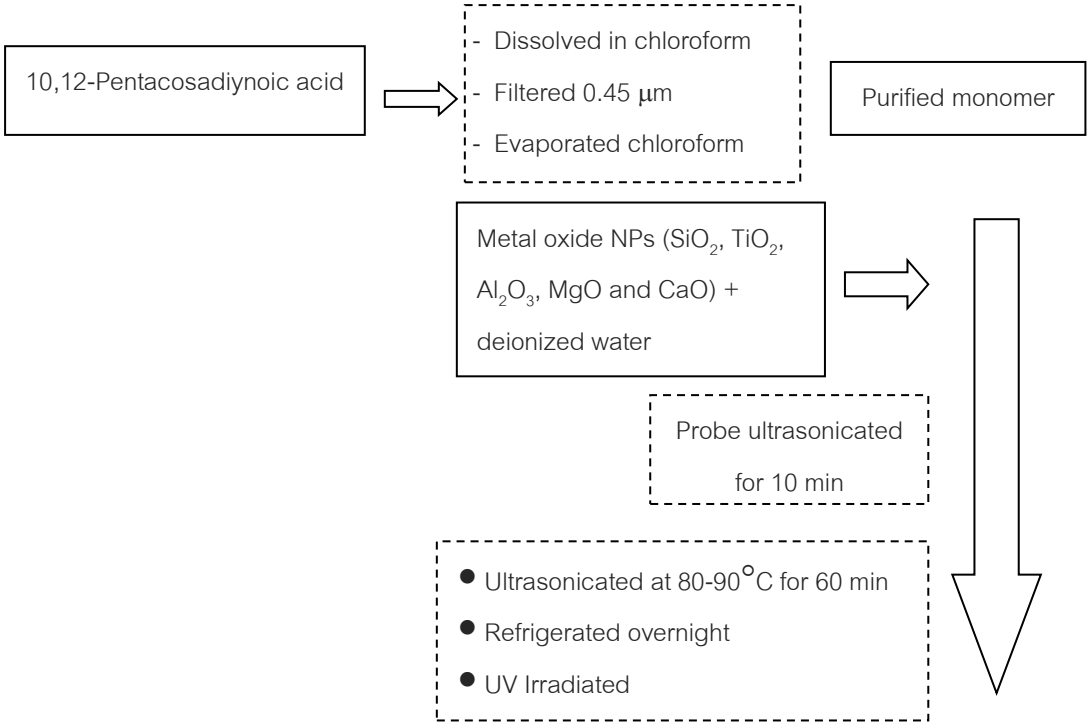

PDA/Metal Oxide nanocomposite suspensions

- Particle size distribution
- TEM
- FT-IR
- Colorimetric responses to temperature, pH and solvents
  - Absorbance (UV-VIS Spectrophotometer)

CHAPTER IV

METHODOLOGY

4.1. Scanning Electron Microscopy

The scanning electron microscope (SEM) is the technique for typically investigating size and morphology of samples. In addition, SEM is useful for determining chemical composition, element and crystalline structure. Fig. 4.1 illustrates the schematic of SEM. In the column of this equipment has electron gun which is the source of primary electrons. The electron beam which typically has an energy ranging from 0.2 keV to 30 keV, is controlled under high voltage condition. The electron beam is focused by electromagnetic lens. When electrons interact with atom at or near surface of sample, it produces various types of signal that can be detected (see Fig. 4.2). The main signals generated by this interaction which can be generally utilized in SEM are secondary electrons, backscattered electrons and X-rays.

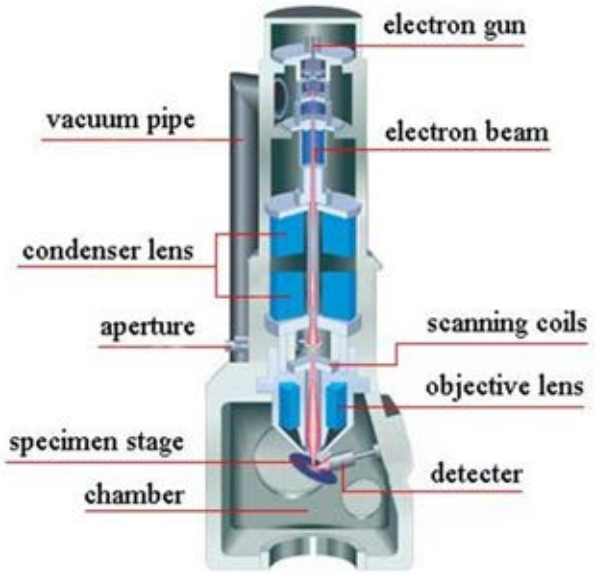

Fig. 4.1 Schematic of Scanning electron microscope[68]

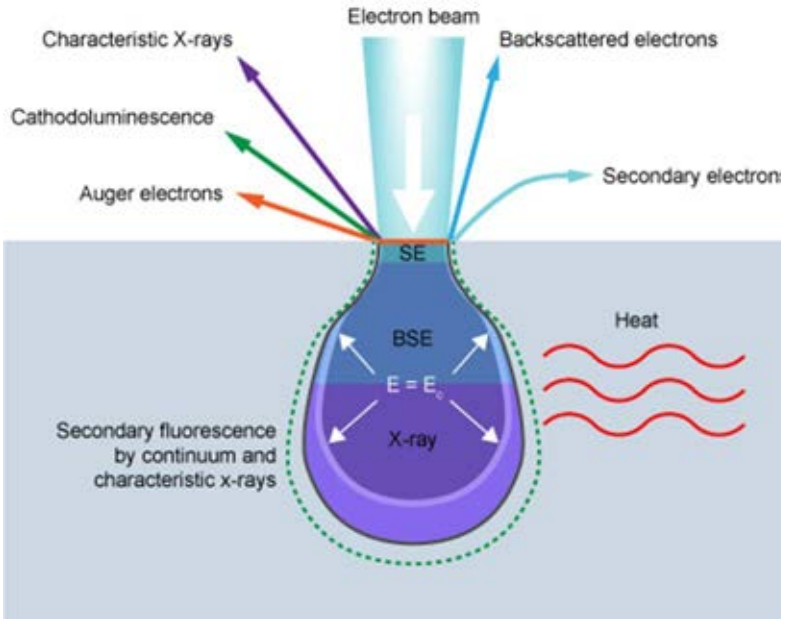

Fig. 4.2 The interaction volume when the primary electron beam interacts with the sample[69]

Secondary electrons or SE are electrons released from a small layer on the surface of the sample. Secondary electron image is the most standard detection mode. It can produce images with very high resolution of morphology and surface of samples, revealing details less than 1 nm in size. In addition, due to the very narrow electron beam, SEM micrographs have a large depth of field yielding a characteristic three-dimensional appearance. The backscattered electrons (BSE) are electrons reflected from the sample by elastic scattering. The BSE come from the deeper region of the sample. They are useful for determining composition of multiphase samples because the intensity of BSE signal related to the atomic number of the specimen. X-rays, which result from ionization processes of inner shells of the atom leading to electromagnetic radiation, are used for determining the chemical composition of the material.

4.2. Dynamic (quasi-elastic) light scattering[70,71]

Dynamic Light Scattering (sometimes referred to as Photon Correlation Spectroscopy or Quasi-Elastic Light Scattering) is a technique used for measuring the size of particles. DLS measures the fluctuation in scattering intensity, and then diffusion coefficient is calculated and used to determine the size of particles within the sample by the Stokes-Einstein equation. The light scattering technique has many advantages such as speed, versatility, small sample size, non-destructive, and measurement time independent of particle density.

When the light hits the particle, the light will be scattered in all directions. Considering in the case of thousands of stationary particles, if a screen is held close to these particles, it will show the bright and dark areas of the scattered light as illustrated in Fig. 4.3a. The bright areas result from the scattered light arriving at the screen with the same phase which can interfere constructively to form a bright patch (see Fig. 4.3b). The dark patches arise from the phase additions which are destructive and cancel each other out.

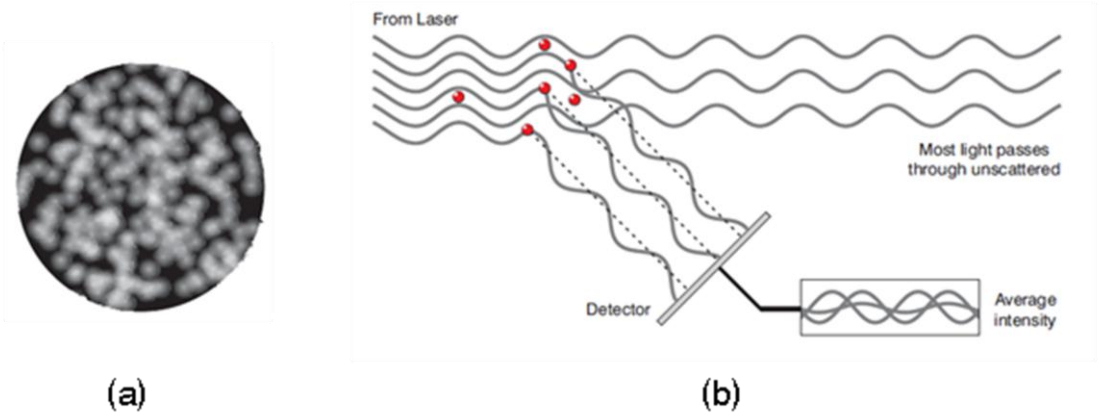

Fig. 4.3 (a) The speckle pattern and (b) The scattered light falling on the detector[70]

In practice, the particles suspended in solvent are not stationary but they constantly move due to Brownian motion, which is the random movement of particles due to the collision by the surrounding solvent molecules. Therefore, the intensities of the

constructive and destructive phases are fluctuating. DLS measures the rate of the intensity fluctuation and then calculates the size of the particles.

From light scattering theories, Rayleigh theory is applicable for small particles and molecules whose diameters are less than $\lambda/10$ or about 60 nm for a He-Ne laser. It defines that $I \alpha d^6$ and also that $I \alpha 1/\lambda^4$, where I is intensity of scattered light, d is particle diameter and λ is laser wavelength. From this relation, if the size of particles is 50 nm, the intensity of scattered light is much greater (one million times) than that of 5 nm particles. The light from the larger particles will swamp the scattered light from the smaller ones. This behavior causes a problem in size analysis when the suspension consists of particles with much different in sizes, e.g. 10 and 1000 nm. Mie theory, however, is suitable for the particle whose diameter is roughly equivalent or slightly larger than λ of laser. This theory explains correctly the maxima and minima in the plot of intensity with angle and gives the correct answer over all wavelengths, sizes and angles. Thus, Mie theory is used in DLS software to converse the intensity distribution into volume.

As mentioned above, the fluctuation in scattering intensity is measured. The fluctuating signal is processed by forming the autocorrelation function and then diffusion coefficient (D) is calculated. This parameter is used to calculate the particle size by the Stokes-Einstein equation.

$$d(H) = kT/3\pi\eta D$$

where:

d(H) = hydrodynamic diameter

D = translational diffusion coefficient

k = Boltzmann's constant

T = absolute temperature

η = viscosity

At first, the result of particle size distribution derived from this technique is an intensity distribution. However, it can be converted to volume distribution by using Mie

theory. The volume distribution can be further converted to a number distribution. The difference between these distributions can be easily explained as follows. Considering the suspension which has two different sizes of particles (e.g. 5 nm and 50 nm) but equal numbers of each size, the resulting number distribution exhibits two peak with a same size as there equal numbers of particles (see Fig. 4.4). For volume distribution, the area of the peak for 50 nm particles is 1000 times larger than that of the peak for 5 nm. This is because the volume of 50 nm particle is 1000 times larger than the volume of 5 nm particle ($V_{sphere} \alpha r^3$). For intensity distribution, because the intensity of scattered light is proportional to the sixth power of its diameter, the peak area of 50 nm particle is 1000000 times larger than that of 5 nm particle.

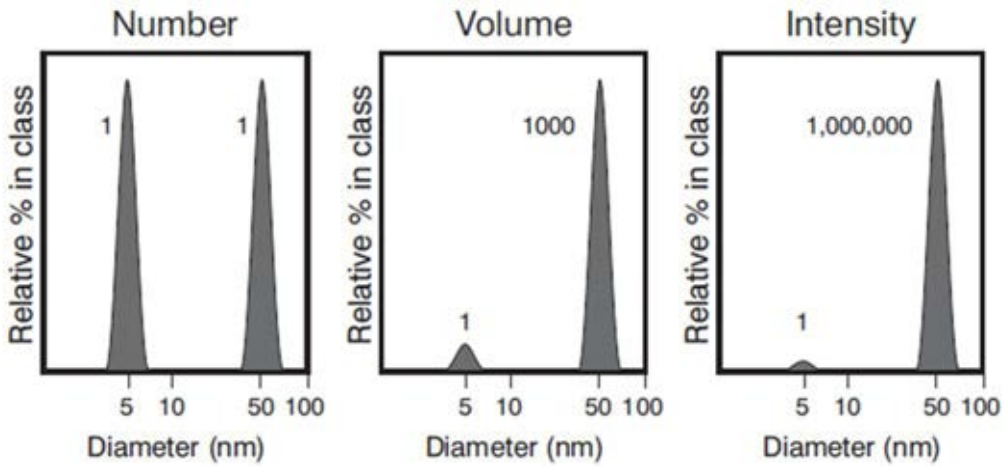

Fig. 4.4 Three types of size distribution obtained from DLS[70]

4.3. Zeta Potential[70,72,73]

Zeta potential is an important and useful indicator which can be used to predict and control the stability of colloidal suspensions or emulsions. When almost all particles contact with a polar medium such as water, they show an electronic charge on their surfaces. These charges affect the arrangement of neighboring ions of the polar medium. For example, if the charge on particle surface is negative, the positive ions

strongly attach to that negative surface while ions with the same charge type are repulsed from the surface. Then, an electrical double layer is formed as shown in Fig. 4.5.

When the particle surface is negatively charge, the double layer consists of two parts; the inner region of positive charges tightly bound to the surface called the Stern layer. Another is the outer region of diffuse layer, in which the ions are less firmly associated. At the boundary of the outer region, there is a special plane called shear plane or slipping plane. Inside this plane, the liquid and ions also move with the particle because they are strongly attached to the surface whereas ions beyond this plane do not move with the colloidal particle. The potential at this boundary is known as the zeta potential. The zeta potential depends on solution conditions such as pH in water and electrolyte concentration.

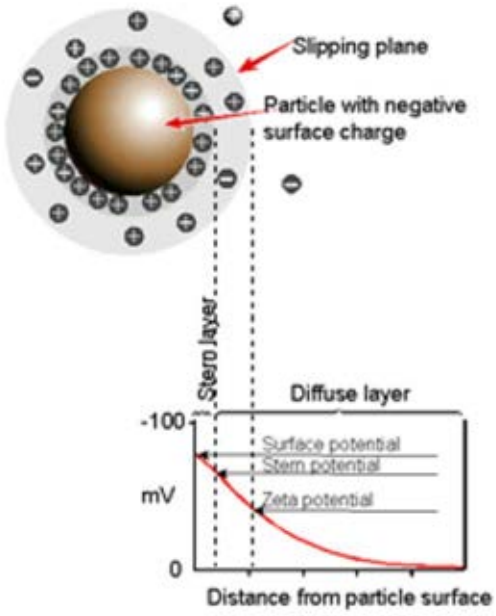

Fig. 4.5 Diagram showing the ionic concentration and potential difference as a function of distance from the charged surface of a particle suspended in a dispersion medium[72]

The pH of the sample is one of the most important factors that affect the value of zeta potential. If a particle in suspension has a negative zeta potential, when more alkali is

added into this suspension, the particles tend to exhibit more negative charge. In contrast, if acid is added, then the negative charge decreases until the charge is neutralized. Further addition of acid causes the increase of positive charge. Therefore, a zeta potential versus pH curve is positive at low pH and negative at high pH. A point where the plot passes through zero zeta potential is called the isoelectric point (IEP) (see Fig. 4.6). At this point, the colloidal system is the least stable.

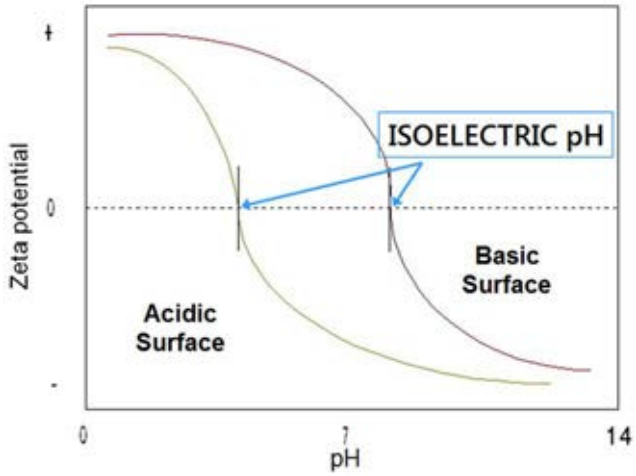

Fig. 4.6 A typical plot of zeta potential versus pH[73]

The zeta potential is determined by measuring the electrophoretic mobility of the particles in an electric field. When an electric field is applied in the colloidal suspension, the charged particles will move to either the negative or the positive pole. The moving direction indicates the sign of the particle charge and the velocity is proportional to the magnitude of the charge. The particle velocity also depends on the strength of electric field, dielectric constant and viscosity of the medium. Therefore, if the direction and velocity of charged particles are measured, the electrophoretic mobility and zeta potential can be calculated from the equation;

$$V_s = U_e E$$

where V_s = average drift velocity of charged particle

U_e = the electrophoretic mobility

E = electric field

and zeta potential is related to the electrophoretic mobility by the Henry equation

$$U_e = (2 \varepsilon z f(\kappa a))/ 3\eta$$

where z = zeta potential (mV), ε = dielectric constant of medium

η = viscosity, f(κa) = Henry's function

As mentioned above, the value of zeta potential is related to the stability in colloidal suspension. This value indicates the degree of repulsion between particles. If the value is high enough, the repulsion of particles occurs and prevents the agglomerations in the suspension. In general, if the value of zeta potential is greater than -30 mV or +30 mV, the dispersion is likely to be stable.

4.4. UV-Visible Spectroscopy[74]

UV-Visible Spectroscopy is the technique used for measuring an intensity of ultraviolet (180 nm - 400 nm) and visible light (400 nm - 800 nm) passing through a sample. Samples for UV/Vis spectrophotometry are most often liquids, although the absorbance of gases and even of solids can also be measured. This technique can be used to analyze both quantitative and qualitative data.

When radiation interacts with objects, many processes can take place, including reflection, scattering, absorbance, fluorescence/phosphorescence (absorption and reemission), and photochemical reaction (absorbance and bond breaking). For measuring UV-vis spectra, it is generally focuses on absorbance of a sample. The total potential energy of molecule of any substance can be considered as a sum of its electronic, vibrational and rotational energy. The amount of energy in each form is not continuous but separated. The differences in energy between the stages are in order;

$$E_{electronic} > E_{vibrational} > E_{rotational}$$

The electronic energy level in simple molecules is widely separated; therefore it requires high energy of light such as UV or visible light to move electrons from a lower energy level to a higher energy level. Fig. 4.7 illustrates the wavelength of light that causes electronic transitions in formaldehyde. The vibrational energy states are much

closer than the electronic energy levels. Therefore, light with lower energy such as infrared are sufficient to bring about vibrational changes. For the rotational energy states, energy levels are so narrow, light in a range of the far infrared and microwave has enough energy to cause the stage changes.

‘

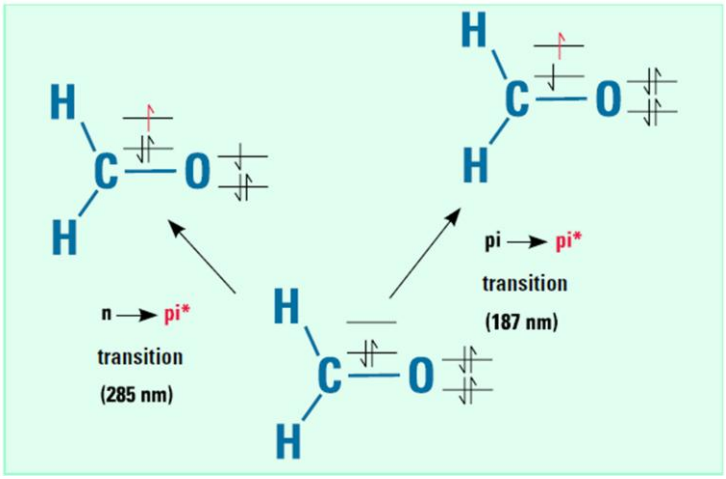

Fig. 4.7 Electronic transitions in formaldehyde[74]

If energy of the incident photon exactly equal to the energy of the electronic gap, which causes the electronic transition, the plot of the absorbance against wavelength results in a very sharp line as shown in Fig. 4.8. However, in practice, vibrational and rotational energy levels of molecules are superimposed on the electronic energy levels. Combination of these transitions with different energies results in the broaden bands as illustrated in Fig. 4.9.

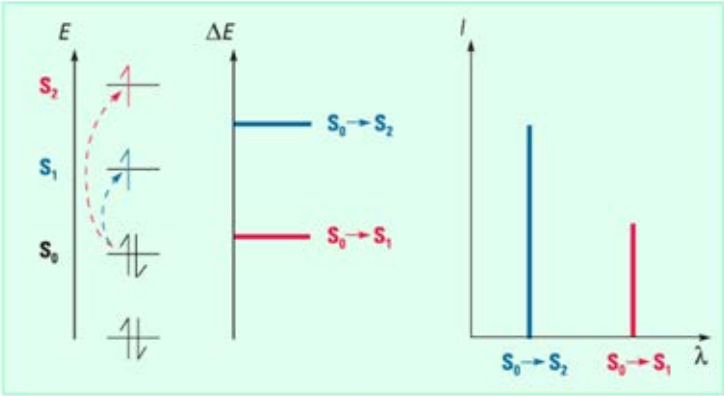

Fig. 4.8 Electronic transitions and absorption spectra of atoms[74]

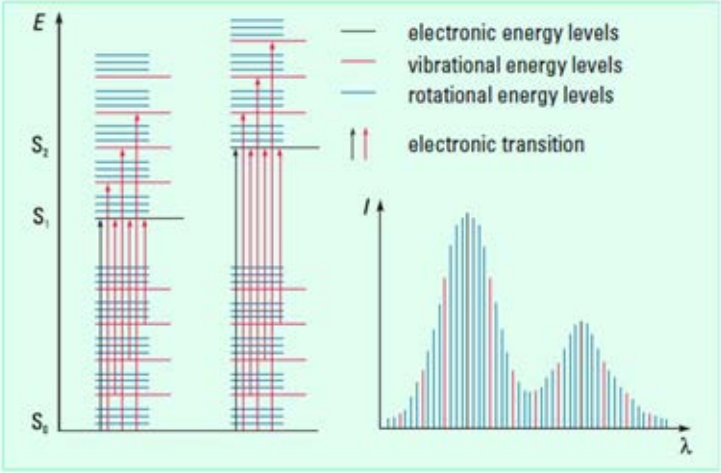

Fig. 4.9 Electronic transition and UV-vis spectra of molecules[74]

UV-visible spectra generally exhibit only a few broad absorbance peaks. Therefore, it provides a limited amount of qualitative information. In general, spectra of organic compounds are resulted from the presence of π (unsaturated) bonds and can be detected at the wavelength ranging from 185 to 1000 nm. For transition metal ions, electronic energy levels cause absorption in the range of 400–700 nm, which is the visible region.

In quantitative analysis, UV-vis spectroscopy can be used to determine concentration of substances. Considering when light passes through or reflects from sample, the difference between the intensity of incident light (I_o) and the intensity of light passing

though the sample (I) is the amount of absorbed light. Transmittance (T) and absorbance (A) is defined as follows:

$$T = I/I_o \quad \text{or} \quad \%T = (I/I_o) \times 100$$

$$A = -\log(T)$$

From the Beer-Lambert law; the absorbed light is proportional to the path length and the concentration of the sample. The mathematical expression is:

$$T = I/I_o = e^{-kbc}$$

where c is the concentration of the sample and b is a path length.

This equation can be transformed into a linear expression by taking the logarithm:

$$A = -\log(I/I_o) = \log(I_o/I) = \log(100/T) = 2\text{-}\log(T) = \varepsilon bc$$

where ε is the molar absorption or extinction coefficient.

From these equations, when the concentration is doubled, the absorbance is two times increased. Therefore, it is more convenient to work in absorbance than transmittance for the purposes of quantitative analysis. In addition, the extinction coefficient is a constant, which is dependent only on the nature of the molecule and the wavelength of the radiation, thus, it can be utilized for identifying sample.

4.5. Fourier transform infrared spectroscopy[75,76]

Fourier transform infrared spectroscopy (FT-IR) is the technique for investigating types of chemical bonds in a molecule. The information from FT-IR can be used to identify unknown materials and determine the amount of components in a mixture. Unlike UV-vis spectroscopy, FT-IR produces many narrow peaks, which can give more qualitative information.

As mentioned above, light in infrared region has sufficient energy to bring about vibrational and rotational changes. An infrared spectrum utilized for chemical analysis is middle infrared (4000-200 cm^{-1}). When subjected to infrared, molecules can absorb only the spectrum which has the frequency corresponding to the frequencies of vibrations between the bonds of the atoms. Moreover, IR peaks are only observed when the

vibrations or rotations within a molecule cause a change in the dipole moment of the molecule. For example, the vibration of C=C in RCH=CHR cannot be observed the IR peak but the vibration of C=O can be detected. In addition, molecules with permanent dipole moment such as HCl, H_2O, NO, etc. are IR active. There are two major types of molecular vibrations: stretching and bending vibrations. Some types of molecular vibration are shown in Fig. 4.10.

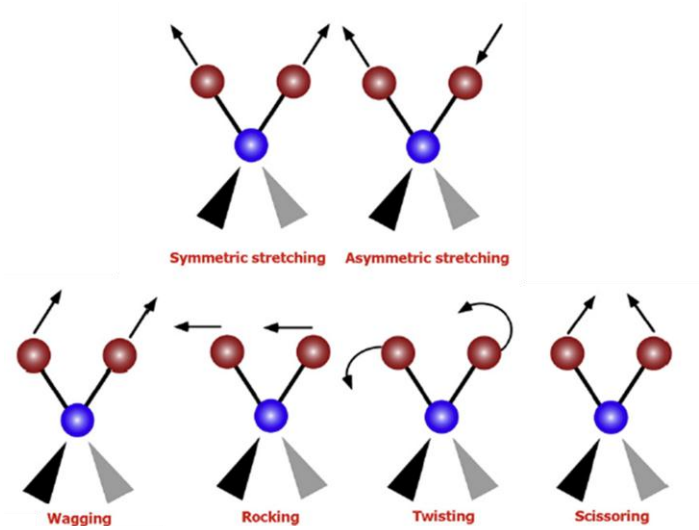

Fig. 4.10 Six different types of molecular vibration of ethylene[77]

Since each material is a unique combination of atoms, there are no compounds to produce the same infrared spectrum. Therefore, infrared spectroscopy can be used for identifying (qualitative analysis) every different kind of materials. In addition, the size of the peaks in the spectrum is a direct indication of the amount of material presented.

CHAPTER V

RESULTS AND DISCUSSION

5.1 Effect of monomer structure on colorimetric behaviors of PDA/ZnO Nanocomposites

In this study, three types of DA monomers, 5,7-hexadecadiynoic acid (HDDA), 10,12-tricosadiynoic acid (TCDA) and 10,12-pentacosadiynoic acid (PCDA) (see Fig. 5.1a) are used for preparing the PDA/ZnO nanocomposites. The illustration in Fig. 5.1b shows the ionic interaction between $-COO^-$ group of these three PDAs and $Zn\text{-}OH_2^+$ groups at the surface of ZnO nanoparticle. The variation of their alkyl chain length is expected to influence the chain rigidity and the overall inter- and intrachain interactions, which in turn causes the change of their color-transition behaviors.

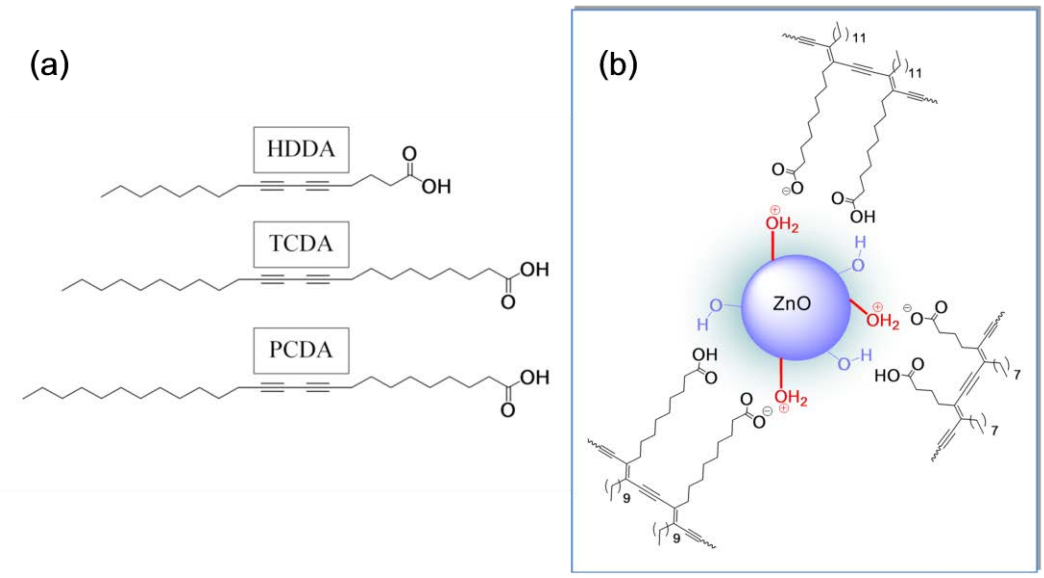

Fig. 5.1 (a) Monomer structures used in this work and (b) the ionic interaction between $-COO^-$ group of these three PDAs and $Zn\text{-}OH_2^+$ groups at the surface of ZnO nanoparticle

5.1.1. Morphologies and size distribution

Morphologies of pure PDA assemblies and PDA/ZnO nanocomposites are illustrated in Fig. 5.2. The SEM images show that poly(PCDA) assemblies exhibit spherical and ellipsoid shapes with diameter ranging from about 30 nm to 200 nm. The poly(TCDA) assemblies exhibit similar shape, however the size increases significantly ranging from around 80 nm to 350 nm. For poly(HDDA) system, most of the assemblies exhibit irregular shape and their size further increases up to about 600 nm.

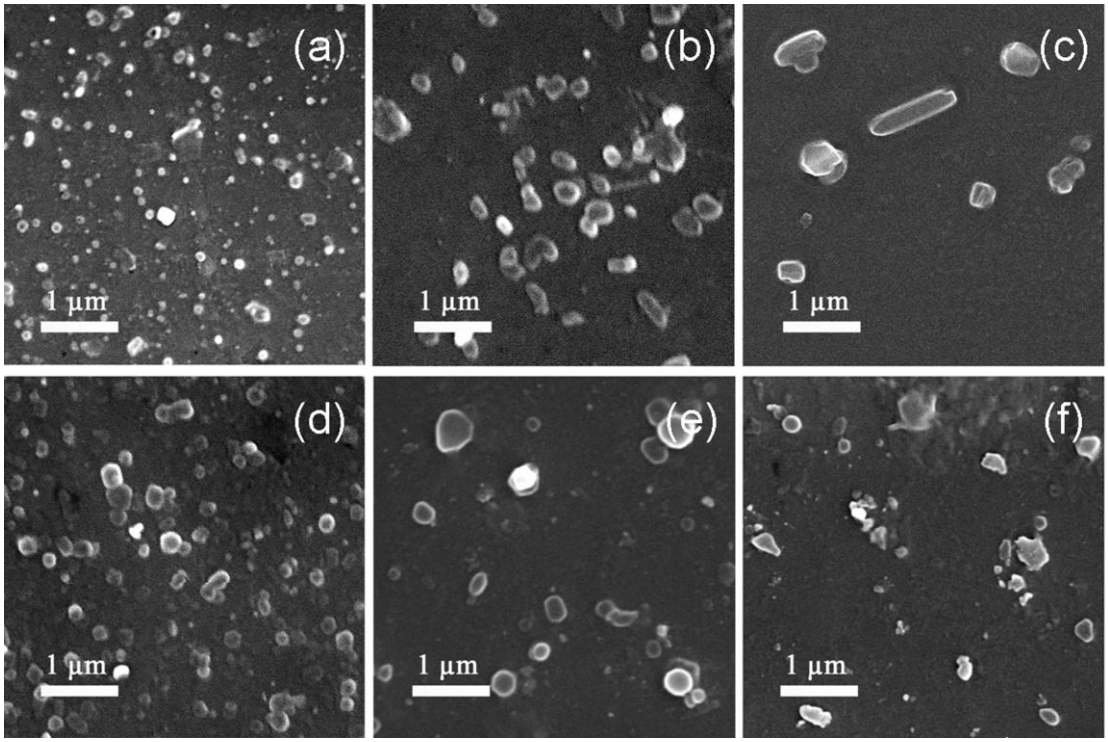

Fig. 5.2 SEM images of pure PDA assemblies, (a) poly(PCDA), (b) poly(TCDA), (c) poly(HDDA) and the nanocomposites, (d) poly(PCDA)/ZnO, (e) poly(TCDA)/ZnO, (f) poly(HDDA)/ZnO

The measurements of their size distribution provide consistent results as shown in Fig. 5.3a. The average sizes are about 85, 160 and 200 nm for poly(PCDA), poly(TCDA) and poly(HDDA), respectively. The variation in shape and the increase in size of the PDA assemblies are attributed to the shortening of hydrophobic DA tails. It is known that

the structures of assemblies are dictated by molecular architecture of the constituent amphiphilic molecules[51]. A packing parameter, based on geometrical features of the surfactant, can be used to predict shape of the formed assemblies. R. Nagarajan[78] showed that the length of hydrophobic tail affected the equilibrium head group area and thereby the packing parameter. In their work, the numerical calculations revealed that the packing parameter slightly increased with decreasing the length of hydrophobic tail. This suggests that the decrease of surfactant tail can lead to the formation of larger spherical or cylindrical assemblies.

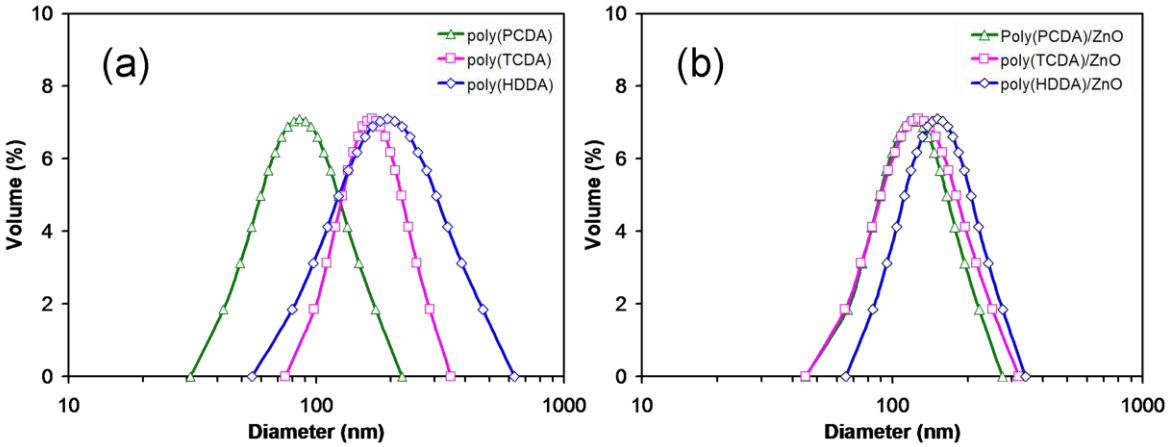

Fig. 5.3 Particle size distribution of pure PDA assemblies and PDAs/ZnO nanocomposites in aqueous suspension

The decrease of alkyl chain length has slight effect on morphologies of the nanocomposites. The SEM images in Fig. 5.2(d-f) show that all nanocomposites exhibit similar shapes. Their size distributions are also comparable (see Fig. 5.3b). The average sizes of poly(PCDA)/ZnO, poly(TCDA)/ZnO and poly(HDDA)/ZnO nanocomposites are about 120, 130 and 150 nm, respectively. These results demonstrate that the presence of ZnO nanoparticles influences the self-assembling behaviors of the DA monomers. In this system, the ZnO nanoparticle behaves as a nanosubstrate for the DA monomers. Strong ionic and dipolar interactions between the DA head groups and ZnO surface facilitate the molecular organization. Therefore, the nanocomposites consist of ZnO core

and PDA shell as illustrated in Fig. 5.1b. The result obtained from transmission electron microscopy clearly shows the coating of PDA around the ZnO nanoparticles[21]. Since the same synthetic batch of ZnO nanoparticles are used in all systems, the nanocomposites exhibit comparable size distributions. Fig. 5.3b still shows slight increase of the nanocomposite size upon decreasing the alkyl chain length. This probably results from the increase of PDA thicknesses in the systems arising from the difference of DA structure.

5.1.2. Optical properties and interfacial interactions

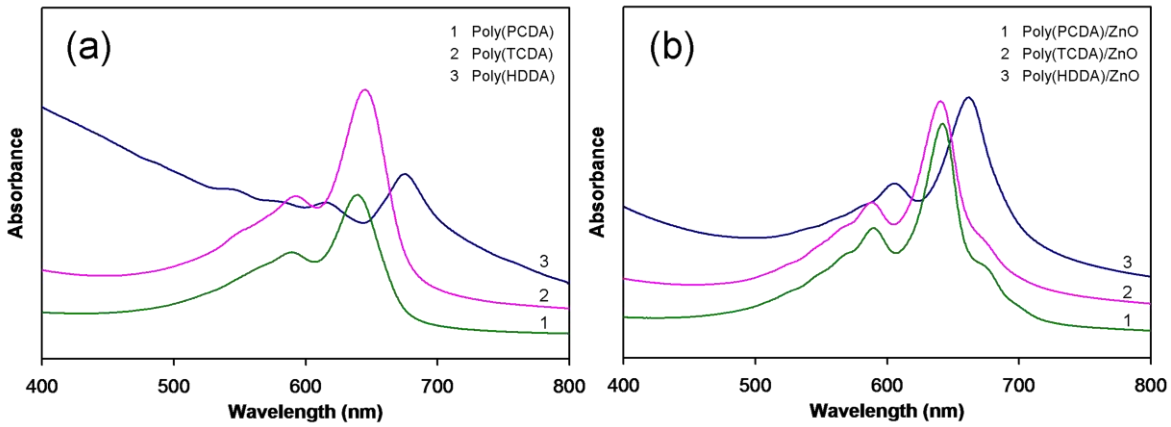

Fig. 5.4 Absorption spectra of initial blue phase of (a) pure PDA assemblies and (b) PDAs/ZnO nanocomposites in aqueous solutions

Firstly, absorption spectra of aqueous suspensions of pure PDA assemblies in blue phase are observed as illustrated in Fig. 5.4a. The spectrum of poly(PCDA) assemblies exhibit a typical peak at 640 nm with broad shoulder at 590 nm. The λ_{max} of poly(TCDA) assemblies slightly red shifts to 645 nm. The red shift of spectrum is much larger in the poly(HDDA) system where the λ_{max} is detected at ~675 nm. This result indicates the increase of conjugation length of PDA backbone when their alkyl chain lengths decrease. The shortening of alkyl chain length leads to the increase of PDA chain rigidity, which in turn promotes the molecular packing. Therefore, the more rigid and

well-organized poly(HDDA) backbones allow longer distance of π electron delocalization within the system. The effect of local curvature may also play an important role. The relatively small size of poly(PCDA) assemblies can cause local distortion of their conjugated backbone, leading to the decrease of conjugation length. The spectra of poly(TCDA)/ZnO and poly(PCDA)/ZnO nanocomposites shown in Fig. 5.4b exhibit comparable λ_{max} values but much sharper patterns compared to those of the pure PDAs. This observation suggests that the molecular ordering of PDA chains increases, resulting from the increase of interfacial interactions[21]. A weak low-energy band at about 675 nm is also observed, indicating the existence of PDA chains with relatively long conjugation length. The spectrum of poly(HDDA)/ZnO nanocomposite exhibits a λ_{max} at ~663 nm which is about 10 nm lower than that of its pure PDA. In this system, the smaller size of the nanocomposite probably causes higher extent of backbone distortion, resulting in the decrease of conjugation length of poly(HDDA).

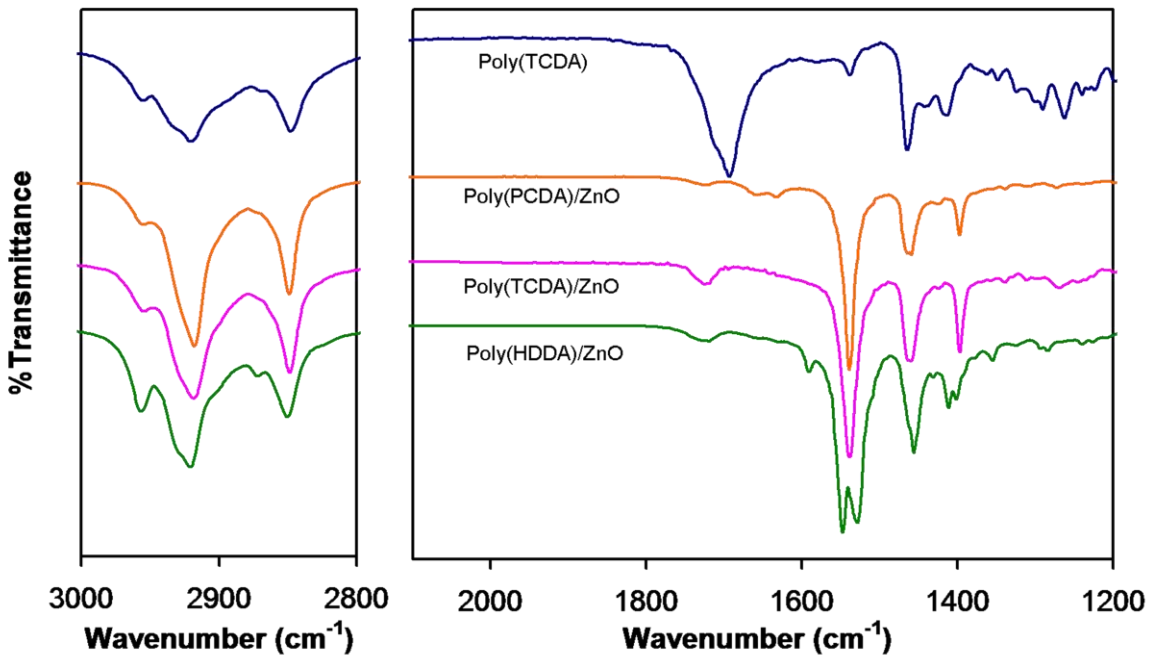

Fig. 5.5 FT-IR spectra of pure poly(TCDA) and PDA/ZnO nanocomposites embedded in KBr pellets. The samples are in blue phase.

The interactions between PDA head groups and surface of ZnO nanoparticle are investigated by utilizing infrared (IR) spectroscopy. Fig. 5.5 compares the IR spectra of pure PDAs and PDA/ZnO nanocomposites. The spectra of all pure PDAs exhibit similar patterns. The peaks at 2848, 2918 and 2954 cm^{-1} correspond to $\nu_s(CH_2)$, $\nu_{as}(CH_2)$ and $\nu_{as}(CH_3)$, respectively. A broad peak near 1690 cm^{-1} is due to hydrogen-bonded carbonyl stretching of –COOH head group while the peaks around 1470-1420 cm^{-1} are assigned to methylene scissoring, $\delta(CH_2)$, of the alkyl side chain[23,79,80]. The IR spectra of PDA/ZnO nanocomposites show quite different patterns. In the systems of poly(PCDA)/ZnO and poly(TCDA)/ZnO nanocomposites, new peaks at 1540 and 1398 cm^{-1} are clearly observed, corresponding to the antisymmetric, $\nu_{as}(COO)$, and symmetric, $\nu_s(COO)$, stretching vibrations, respectively, of carboxylate anion[12,24,47]. These results are consistent with our previous study[21], confirming the presence of ionic interaction between the carboxylate head groups and Zn-OH_2^+ groups at the surface of ZnO nanoparticles. A weak peak at 1725 cm^{-1} is attributed to the vibration of –COOH groups that do not form hydrogen bonds with their neighboring groups.

The spectrum of poly(HDDA)/ZnO nanocomposite shows a rather interesting pattern. The absorption bands corresponding to the stretching vibrations, $\nu_{as}(COO)$ and $\nu_s(COO)$, of carboxylate anion split into multiple peaks. The $\nu_{as}(COO)$ peaks are detected at 1590, 1548 and 1530 cm^{-1} while the peaks at 1412, 1403 and 1380 cm^{-1} are assigned to $\nu_s(COO)$ vibration. It was observed that the location of $\nu_{as}(COO)$ and $\nu_s(COO)$ of the PDA carboxylate head group depended significantly on the type of specific interactions with cations[47]. Therefore, our observation suggests that the strength of interactions between poly(HDDA) carboxylate heads and Zn-OH_2^+ groups at ZnO surface is not homogeneous. The detection of multiple $\nu_{as}(COO)$ and $\nu_s(COO)$ bands indicates the variation of their vibrational spring constant. This probably stems from the relatively short alkyl side chain and the high rigidity of conjugated poly(HDDA) backbone. The anchoring of head groups on ZnO surface forces the PDA chains to curve around the round-shape substrate. The stress within rigid PDA backbone is expected to increase upon decreasing the dimension of ZnO nanoparticles (i.e.

increasing of local curvature). Since the ZnO nanoparticles used in this study exhibit relatively large size distribution, ranging from about 20 to 200 nm, the interfacial interaction must vary with their size in order to compromise the stress of PDA backbone. To verify this hypothesis, however, one requires monodisperse ZnO nanoparticles in the preparation of nanocomposites. In the poly(PCDA)/ZnO and poly(TCDA)/ZnO systems, the relatively long alkyl side chain provides the flexibility to relieve stress in the rigid PDA backbone. Therefore, only one type of interfacial interaction is observed.

5.1.3. Thermochromisms

It is known that PDA assemblies exhibit color transition when subjected to thermal stimulus. By increasing temperature, the dynamics of all PDA segments including alkyl tail, polar head and conjugated backbone are promoted. When the inter- and intrachain interactions within PDA assemblies are sufficiently weaken, the rearrangement of molecular segments occurs, which in turn alters the electronic state of conjugated backbone[10,26,45-49]. The HOMO-LUMO energy gap of perturbed PDA is widen, resulting in the color transition from blue to purple, red or orange. The color of perturbed PDA depends on the extent of local perturbation. The effect of alkyl chain length on thermochromism of PDA assemblies was previously investigated. In the system of PDAs bearing terminal m-carboxyphenylamido groups, the change of alkyl chain length hardly affects their thermochromic behaviors[50]. The study of urethaned-subsituted PDAs observed an even-odd effect of the alkyl chain length on their thermochromic transition and colorimetric reversibility[81]. In recent study by one of the author, the decrease of alkyl chain length in system of PDAs with carboxylic head group led to the decrease of color-transition temperature[7]. Therefore, we attempt to control color-transition temperature of PDA/ZnO nanocomposites by using similar approach.

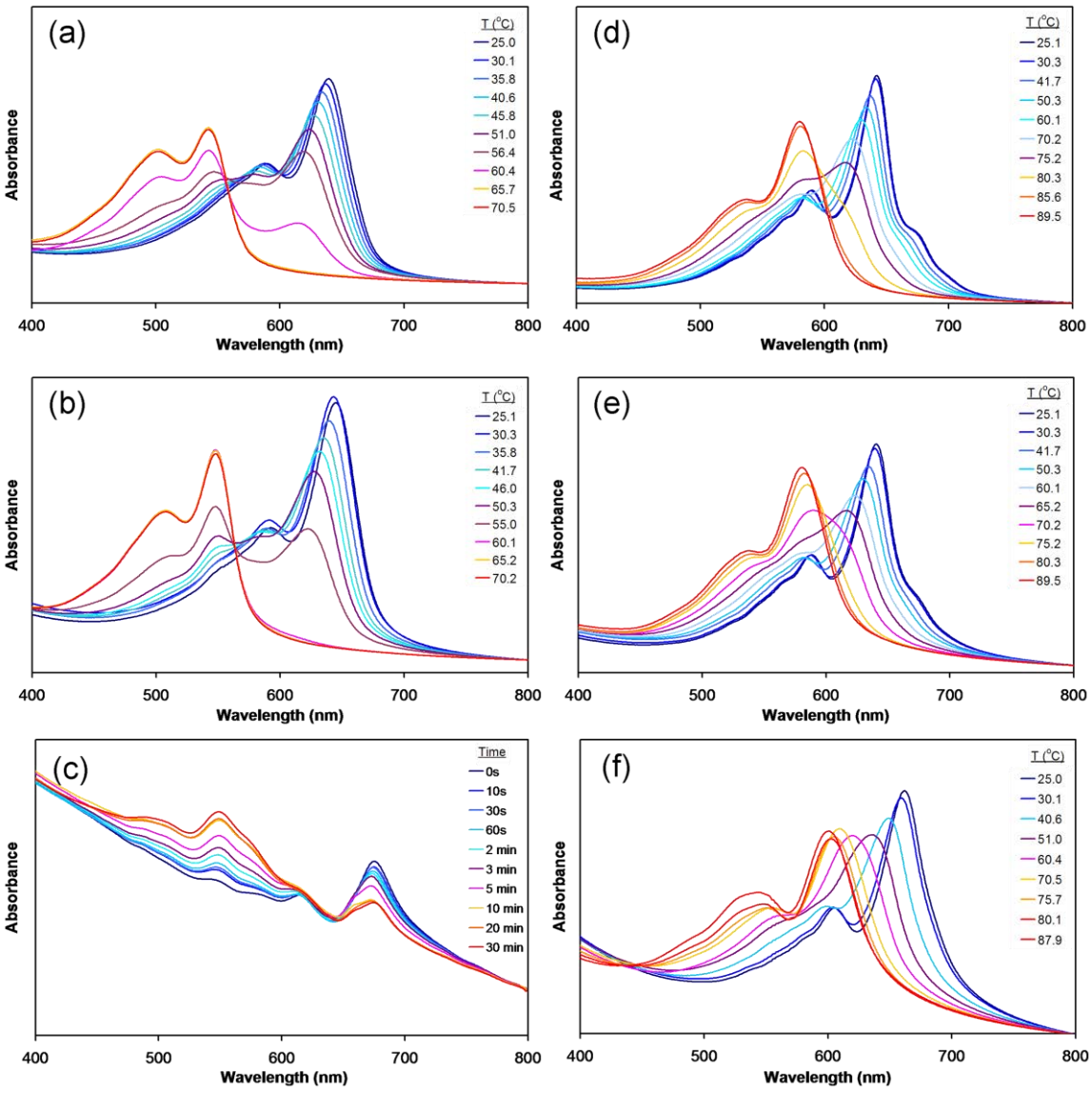

Fig. 5.6 Absorption spectra of (a) pure poly(TCDA), (b) pure poly(PCDA), (d) poly(PCDA)/ZnO, (e) poly(TCDA)/ZnO and (f) poly(HDDA)/ZnO nanocomposites measured upon heating. (c) Absorption spectra of pure poly(HDDA) changes with time at room temperature.

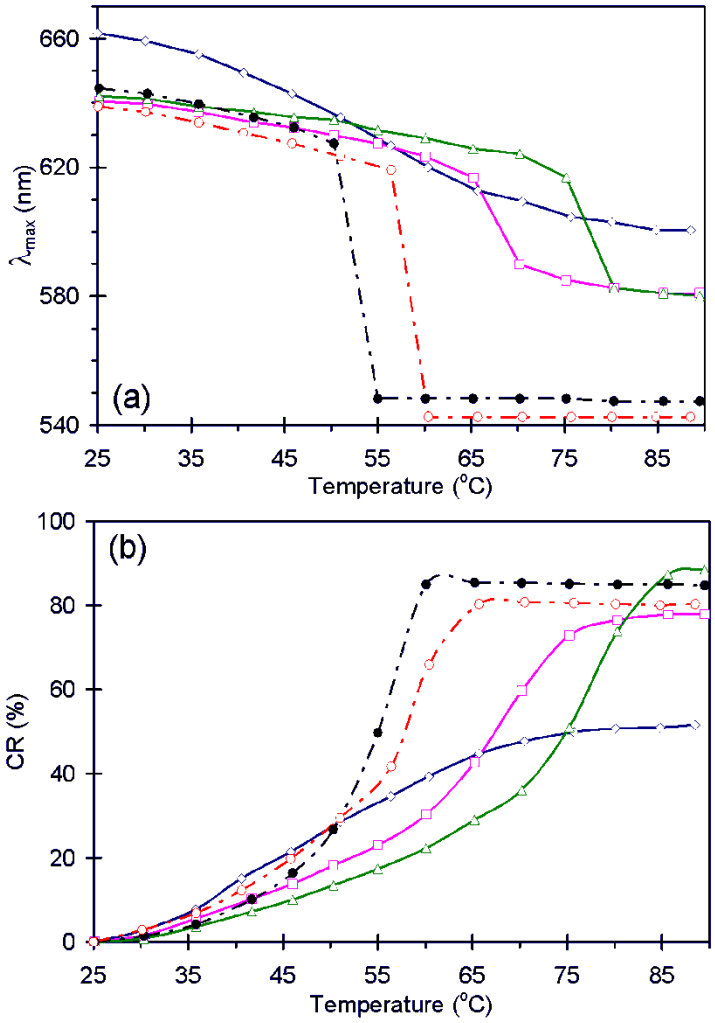

Fig. 5.7 (a) Plots of λ_{max} and (b) colorimetric response (CR) as a function of temperature. Symbols are for (○) poly(PCDA), (●) poly(TCDA), (Δ) poly(PCDA)/ZnO, (□) poly(TCDA)/ZnO and (◊) poly(HDDA)/ZnO nanocomposites.

In this work, three DA monomers with different alkyl chain length are used to prepare pure PDA assemblies and PDA/ZnO nanocomposites. Their thermochromic behaviors are systematically investigated and compared. The temperature-dependent absorption spectra of all samples are illustrated in Fig. 5.6. In low temperature range, the spectra gradually blue shift upon increasing temperature due to the increase of molecular dynamics. When the temperature is increased above 60 °C, an abrupt change of absorption pattern is detected in poly(PCDA) system. The λ_{max} value initially detected at

640 nm shifts to about 540 nm, corresponding to the color transition from blue to red. Similar behaviors are observed in poly(TCDA) system. However, the blue/red color transition takes place at lower temperature. The decrease of transition temperature is attributed to the reduction of dispersion interactions within the assemblies due to the shortening of alkyl chain[7]. In poly(HDDA) system where the alkyl chain is much shorter, the initial blue color is unstable at room temperature. The absorption spectra of poly(HDDA) assemblies measured as a function of time are illustrated in Fig. 5.6c. The blue-shift peak at about 540 nm continuously grows with time. The aqueous suspension of poly(HDDA) assemblies changes color from blue to reddish purple within 10 min. The inter- and intra-chain interactions within the poly(HDDA) assemblies are expected to be much weaker than those of poly(PCDA) and poly(TCDA) because of its relatively short alkyl chain. From this reason, the color-transition temperature of poly(HDDA) assemblies is probably lower than room temperature.

The thermochromic behavior of PDA/ZnO nanocomposites is rather different. All nanocomposites change colors at higher temperature compared to their pure constituent polymers. Absorption spectra measured upon heating of the nanocomposites are illustrated in Fig. 5.6(d-f). The significant change of the absorption pattern is detected at about 80, 70 and 60 ^{o}C in poly(PCDA)/ZnO, poly(TCDA)/ZnO and poly(HDDA)/ZnO systems, respectively. An isosbestic point is observed in all systems indicating the transition between two distinct electronic species. To compare the color-transition behaviors in more details, the λ_{max} and colorimetric response (CR) values are plotted as a function of temperature as shown in Fig. 5.7. In low temperature range, a gradual decrease of λ_{max} is observed in all systems. The drastic drop of λ_{max} is detected at 55 and 60 ^{o}C in the systems of pure poly(TCDA) and poly(PCDA), respectively, corresponding to the blue/red transition. The red phase of these PDAs exhibits λ_{max} at about 545 nm. In the nanocomposite systems, the drop of λ_{max} occurs at higher temperatures, i.e., 80 and 70 ^{o}C for poly(PCDA)/ZnO and poly(TCDA)/ZnO, respectively. At these temperatures, the nanocomposites exhibit a purple color with λ_{max} near 580 nm. Our result demonstrates that the transition temperature of the nanocomposites can be

controlled by varying length of alkyl tail of the constituent PDA. The shortening of two methylene units in alkyl tail (see Fig. 1) causes the lowering of transition temperature by about 10 ^{o}C. This is attributed to the decrease of dispersion interactions within the PDA layers.

The investigation of poly(HDDA)/ZnO nanocomposites provides rather interesting result. In this system, the alkyl tail of poly(HDDA) is two methylene unit shorter than that of poly(TCDA). The alkyl segment connecting the head group is also five methylene unit shorter (see Fig. 1), which causes significant drop of the dispersion interactions within its assemblies. As mentioned in our earlier discussion, the color-transition temperature of pure poly(HDDA) assemblies is below room temperature. The incorporation of ZnO nanoparticles into the assemblies leads to a significant increase of its color-transition temperature. The blue color of poly(HDDA)/ZnO nanocomposites is stable at room temperature. The blue/purple color transition takes place at about 60 ^{o}C, which is indicated by an inflection point of the plot between λ_{max} and temperature shown in Fig. 5.7a. The increase of transition temperature compared to that of the pure polymer is more than 35 ^{o}C. In the systems of poly(TCDA)/ZnO and poly(PCDA)/ZnO nanocomposites, the increase of transition temperatures compared to those of their pure polymers is about 15-20 ^{o}C. These results indicate that the ZnO nanoparticles have stronger effects on the color-transition temperature of poly(HDDA). The rationalization for this behavior is as follows. The increase of color-transition temperature of the nanocomposites is due to the presence of strong interfacial interactions between carboxylate head of PDAs and active groups at ZnO surface. The anchoring of head group on the solid substrate enhances the overall interactions within the system and also limits the dynamics of PDA segments[21]. In the system of poly(HDDA)/ZnO nanocomposite, the distance between anchoring sites and conjugated backbone is relatively short. Therefore, its local molecular dymanics are expected to be lesser than those of the poly(TCDA)/ZnO and poly(PCDA)/ZnO nanocomposites, which leads to the greater increase of the transition temperature. In other words, the confinement effect is stronger in the poly(HDDA)/ZnO nanocomposite. This hypothesis is parallel to the

studies of other polymers where the decrease of film thickness leads to the increase of glass transition temperature[82,83].

The color-transition behavior of poly(HDDA)/ZnO nanocomposite is also quite different. Fig. 5.7a shows that the change of λ_{max} upon increasing temperature is less obvious compared to poly(TCDA)/ZnO and poly(PCDA)/ZnO nanocomposites. The plot of λ_{max} as a function of temperature shows a continuous curve. This probably arises from the co-existence of nanocomposites that possess various types of interfacial interactions with ZnO substrate as revealed by the IR spectroscopy. The color-transition temperature of these nanocomposites may slightly vary, depending on the strength of interfacial interactions, which results in the continuous decrease of the λ_{max}. The shortening of alkyl chain length of poly(HDDA) also affects color of the nanocomposites. Their blue phase at 25 ^{o}C and purple phase at 85 ^{o}C exhibit λ_{max} at 662 and 600 nm, respectively, which are about 20 nm higher than those of the other nanocomposites. The increase of conjugation length of poly(HDDA) in both phases is attributed to the increase of backbone rigidity. The plots of CR values as a function of temperature shown in Fig. 5.7b illustrate the magnitude of color transition. The color-transition temperature, corresponding to a sharp increase in the plot, is consistent with the drop of λ_{max}. The magnitudes of color transition of poly(PCDA)/ZnO and poly(TCDA)/ZnO nanocomposites are comparable to their pure polymers while the color of poly(HDDA)/ZnO nanocomposite exhibits gradual changes.

5.1.3.1 Color reversibility and stability

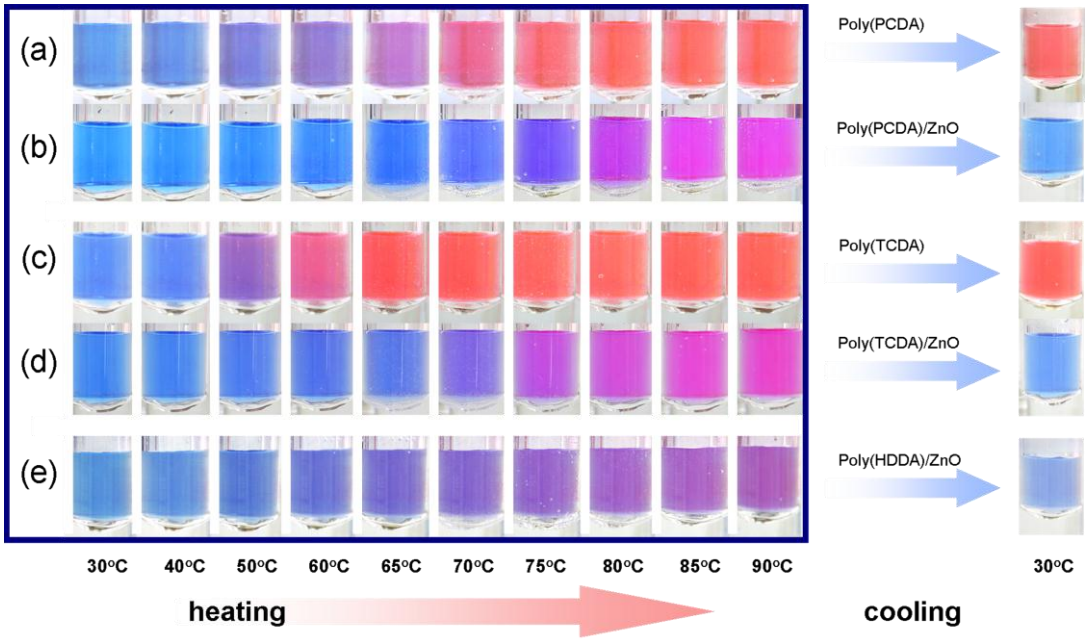

Fig. 5.8. Color photographs of the aqueous suspensions of (a) pure poly(PCDA), (b) poly(PCDA)/ZnO nanocomposite, (c) pure poly(TCDA), (d) poly(TCDA)/ZnO nanocomposite and (e) poly(HDDA)/ZnO nanocomposite taken upon increasing temperature from 30 to 90 $^{\circ}$C, followed by cooling to room temperature

It has been observed that PDAs with carboxylic head group normally exhibit an irreversible thermochromism[7,10,21,26]. To utilize PDAs in a wider range of applications, many research groups have attempted to achieve reversible thermochromism by structural modification of the head group. Various classes of PDAs exhibiting reversible thermochromism with different color-transition temperatures have been synthesized[10,14,18,43,50]. Although this approach is quite effective, it is rather difficult to predict the color-transition temperature of the modified PDAs. In this study, we demonstrate in the previous section that the color-transition temperature of PDA/ZnO nanocomposites can be systematic controlled by varying the alkyl chain length. Synthetic chemists can utilize our approach for preparing PDA/ZnO nanocomposites by using their existing DA monomers. New classes of DA monomers with systematic modification of alkyl chain length and/or head group could be synthesized, which will

provide PDA/ZnO nanocomposites with predictable color-transition temperatures. Furthermore, the reversible thermochromism can be achieved.

Color photographs of the aqueous suspensions of pure PDA assemblies and the PDA/ZnO nanocomposites taken during heating/cooling cycle are illustrated in Fig. 5.8. The color transition of all samples is visually observed. It is clear that color-transition temperatures of the PDA/ZnO nanocomposites are higher than those of pure PDA assemblies and vary with structure of the constituent polymers. The color reversibility is also affected. The pure poly(PCDA) and poly(TCDA) assemblies exhibit an irreversible thermochromism. On the other hand, the thermochromic transition of their nanocomposites is fully reversible. Strong interfacial interactions in these systems limit the segmental reorientation upon increasing temperature. Therefore, the original chain conformation can be restored upon cooling to room temperature. Detailed discussion of this issue is available in our previous report[21]. However, it can be observed that the color of poly(HDDA)/ZnO nanocomposites is slightly changed when the temperature is cooled to room temperature.

To further explore the color reversibility, absorption spectra of the nanocomposites upon heating and cooling are measured as shown in Fig. 5.9. In the system of poly(PCDA)/ZnO and poly(TCDA)/ZnO nanocomposites, the spectrum after cooling to room temperature exhibits similar pattern compared to that of the initial blue phase (see Fig. 5.9a and b). In addition, the plots of CR values obtained from the heating/cooling cycle illustrated in Fig. 5.10 are almost the same in the systems of poly(PCDA)/ZnO and poly(TCDA)/ZnO nanocomposites, indicating to complete themochromic reversibility.

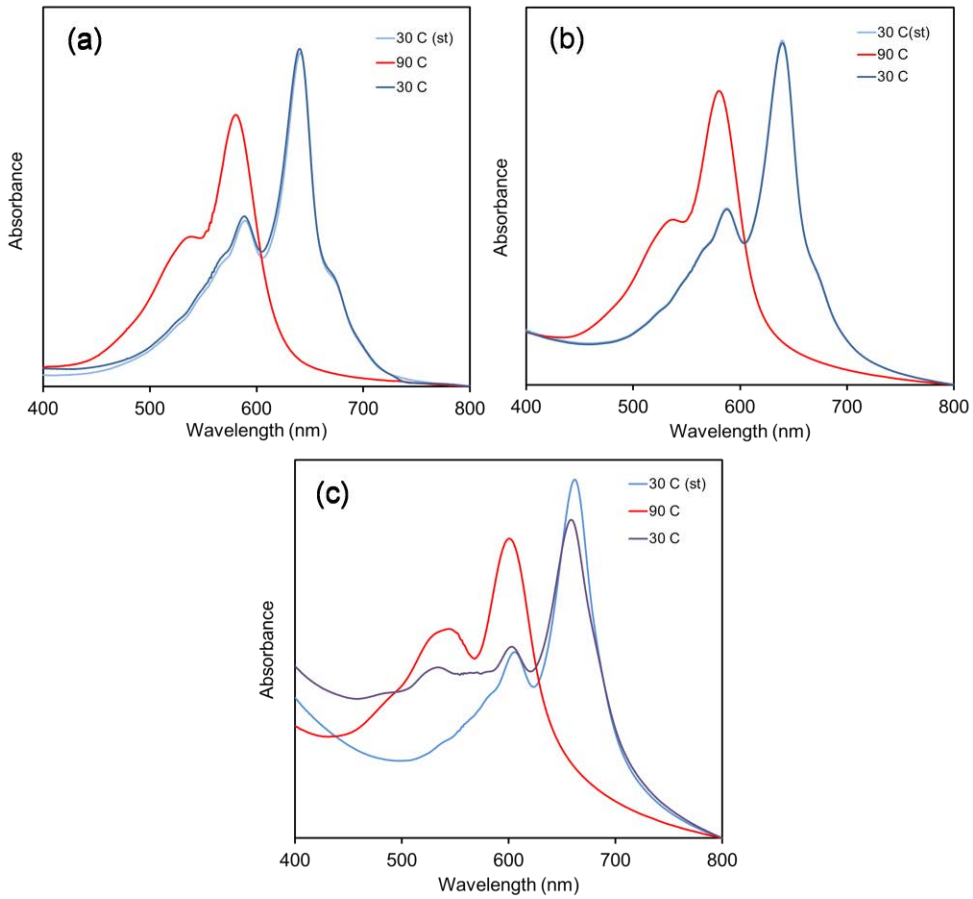

Fig. 5.9 Absorption spectra of (a) poly(PCDA)/ZnO, (b) poly(TCDA)/ZnO and (c) poly(HDDA)/ZnO nanocomposites when subjected to heating and cooling

In contrast, the spectrum of poly(HDDA)/ZnO nanocomposite after cooling to room temperature shows the growth of new peak at about 540 nm (see Fig. 5.9c), corresponding to the formation of a small fraction of red phase. A slight increase of CR values is detected in the system of poly(HDDA)/ZnO nanocomposites when the temperature is decreased below 40 ^{o}C (see Fig.5.10c). We suggest that the partial color-irreversibility arises from the heterogeneity of interfacial interactions within the system. Some of poly(HDDA)/ZnO nanocomposites that possess relatively weak interfacial interactions probably exhibit an irreversible thermochromism. The formation of red phase cannot be attributed to the presence of pure poly(HDDA) assemblies. As mentioned in the earlier discussion, the pure poly(HDDA) assemblies have no color

stability at room temperature. On the other hand, the color of poly(HDDA)/ZnO nanocomposite is stable over a long period of time.

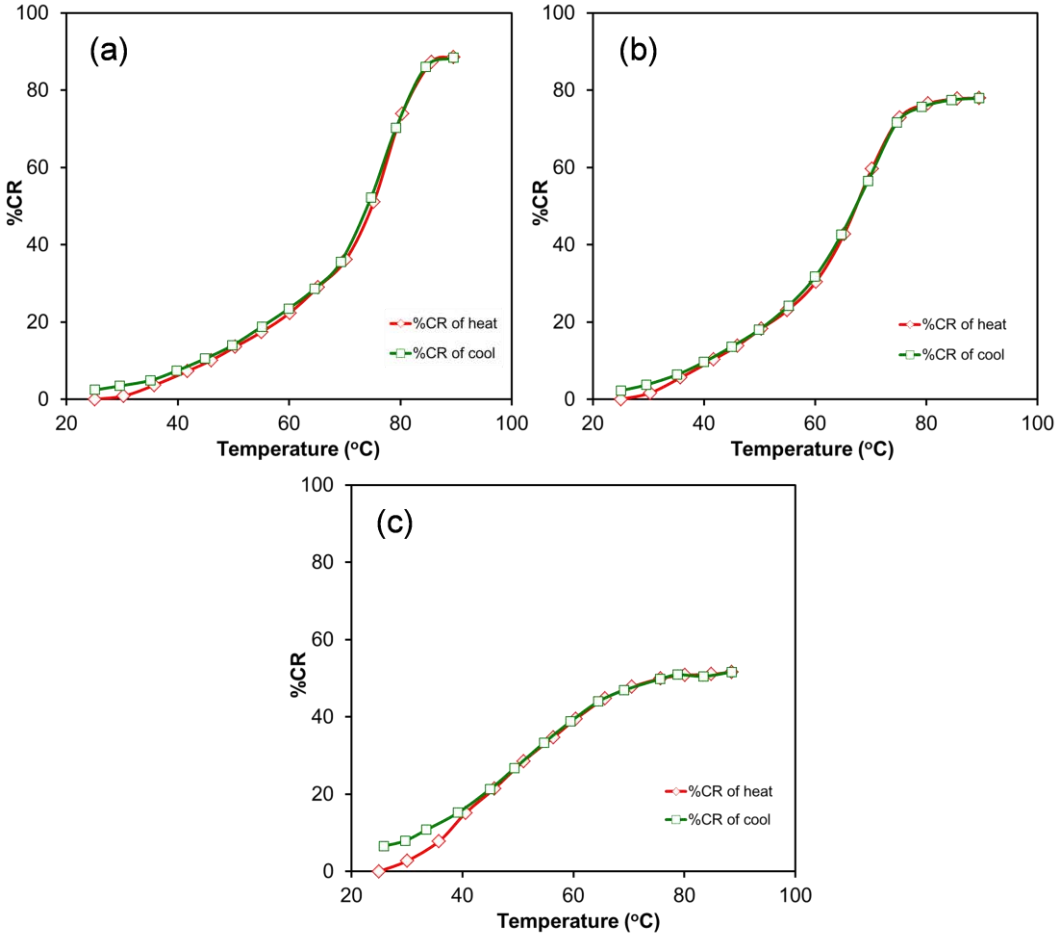

Fig. 5.10 The CR of (a) poly(PCDA)/ZnO, (b) poly(TCDA)/ZnO and (c) poly(HDDA)/ZnO nanocomposites measured during heating and cooling cycle

Thermal stability of the nanocomposites is also investigated. Their aqueous suspensions are subjected to multiple heating/cooling cycles, switching between 25 and 90 °C. The purple color of poly(PCDA)/ZnO and poly(TCDA)/ZnO nanocomposites at elevated temperature fully reverses to the original blue color upon cooling. The color switching occurs within a few seconds. The color reversibility can be repeated for more than 10 heating/cooling cycles as illustrated in the plot of CR value (see Fig. 5.11a,b). These results show that the poly(PCDA)/ZnO and poly(TCDA)/ZnO nanocomposites

exhibit high thermal stability. In the system of poly(HDDA)/ZnO nanocomposite, its color does not return to the original one after the first heating/cooling cycle. The light blue color is obtained. However, this color is stable over the next 9 heating/cooling cycles as shown by the plot of CR values in Fig. 5.11c. The inspection of absorption spectra reveals that the red phase forms in the first heating/cooling cycle. The amount of red phase slightly increases in the next 5 cycles and then becomes stable. Therefore, large fraction of the nanocomposite is thermally stable. From the drop of absorbance of the blue phase (λ = 662 nm), fraction of the thermo-reversible nanocomposite is estimated to be about 65%. Since the color transition is still clearly observed after the consecutive heating/cooling cycles, we can also utilize poly(HDDA)/ZnO nanocomposite as a reversible thermochromic material.

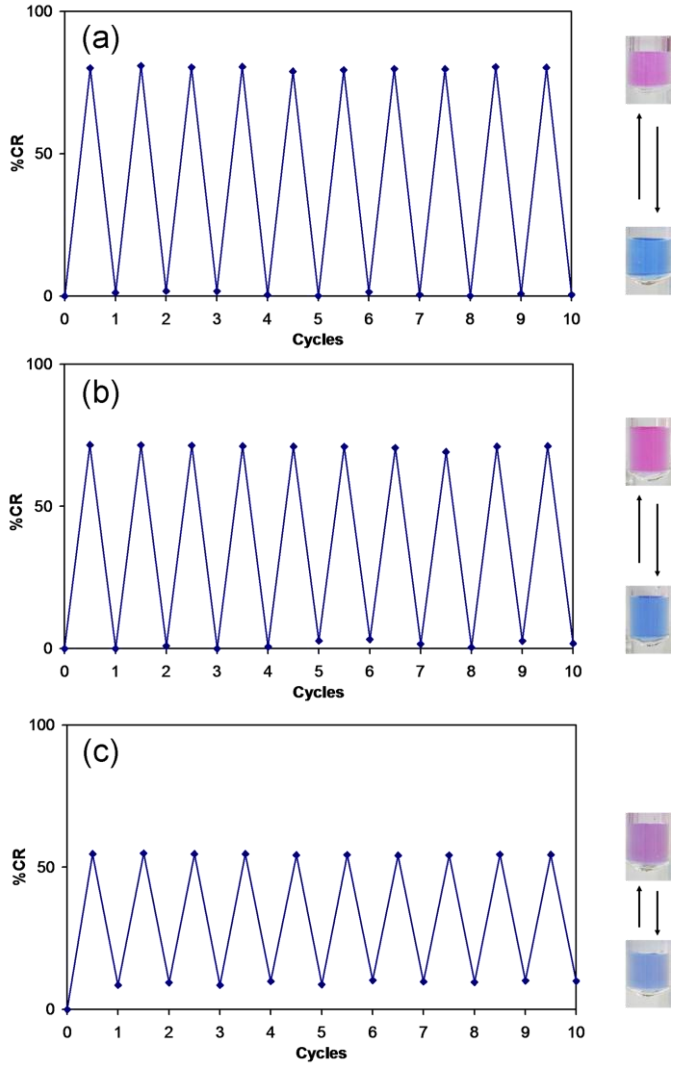

Fig. 5.11 Change of CR during 10 heating/cooling cycles switching between 25 °C and 90 °C of (a) poly(PCDA)/ZnO, (b) poly(TCDA)/ZnO and (c) poly(HDDA)/ZnO nanocomposites

5.1.4. Temperature dependences of PDA/ZnO nanocomposite drop-cast films

Because the thermochromic transition of the nanocomposite solution cannot be observed at temperature above 100 ^{o}C, the drop-cast films are prepared to investigate the thermochromic behaviors when temperature is higher than 100 ^{o}C. The films are annealed at different temperatures for 5 min before measuring the absorption. In general, the color transition of PDA film takes place at higher temperature compared to PDA in solution form. This is due to the retarded mobility of PDA molecules in the film[84]. Fig. 5.12a shows absorption spectra of drop-cast film of poly(PCDA)/ZnO nanocomposite upon heating. The significant decrease of λ_{max} to ~ 580 nm when temperature is increased to around 110 ^{o}C is observed. The sample turns from blue to purple color. In addition, the peak at ~ 540 nm continuously grows while the peak at 580 significantly drop after increasing temperature from 110 to 170 ^{o}C. At 180 ^{o}C, the peak at ~ 580 nm is nearly disappeared and the color of the film changes to red.

To explore thermal reversibility of drop-cast film of this nanocomposite, the film was cooled to room temperature. Absorption spectra measured after cooling to room temperature are illustrated in Fig. 5.12b. The complete thermochromic reversibility is still observed when the film was cooled from 130 ^{o}C to 30 ^{o}C. At temperature above 130 ^{o}C, partial color reversibility of the film is observed. The completely irreversible color transition of this nanocomposite film takes place at ~180 ^{o}C

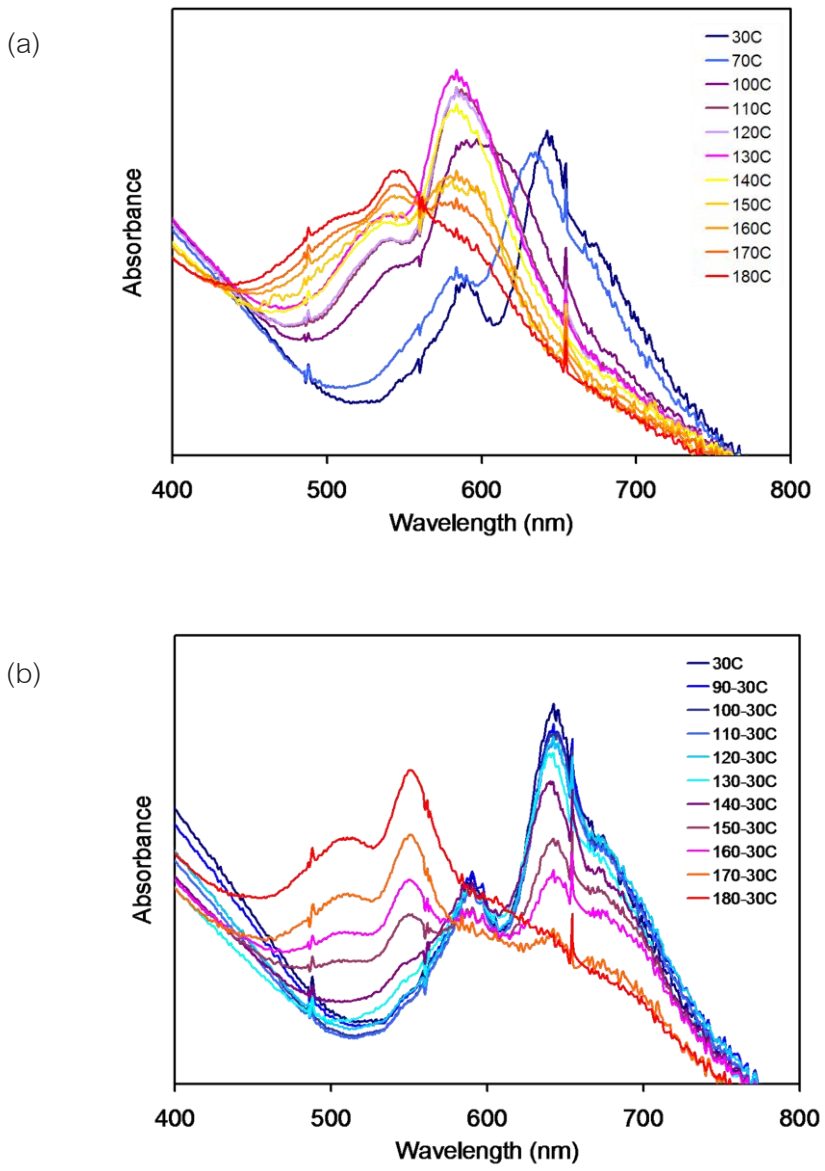

Fig. 5.12 Absorption spectra of drop-cast films (a) poly(PCDA)/ZnO nanocomposite at different annealing temperatures and (b) after cooling from designate temperatures to room temperature

In the system of poly(TCDA)/ZnO nanocomposite, the color transition of the drop-cast film takes place at slightly lower temperature compared to that of poly(PCDA)/ZnO nanocomposite. From absorption spectra shown in Fig 5.13a, the significant decrease of λ_{max} is observed at about 90 ^{o}C. The color of the film completely changes to purple after

increasing temperature to around 120 °C, which is about 40 °C higher than that of aqueous suspension. Further increasing temperature from 120 to 170 °C causes continuous growth of a peak at around 545 nm while the band at 585 nm simultaneously drops. The complete red phase of the film takes place at 180 °C, where the peak at 585 nm disappears.

(a)

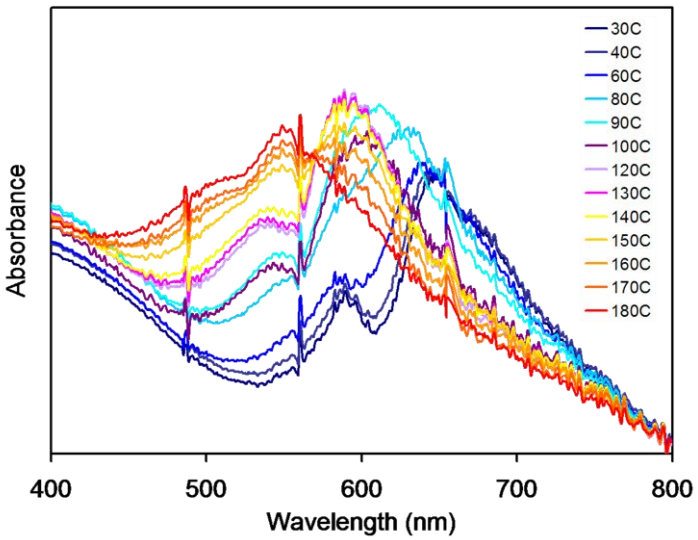

(b)

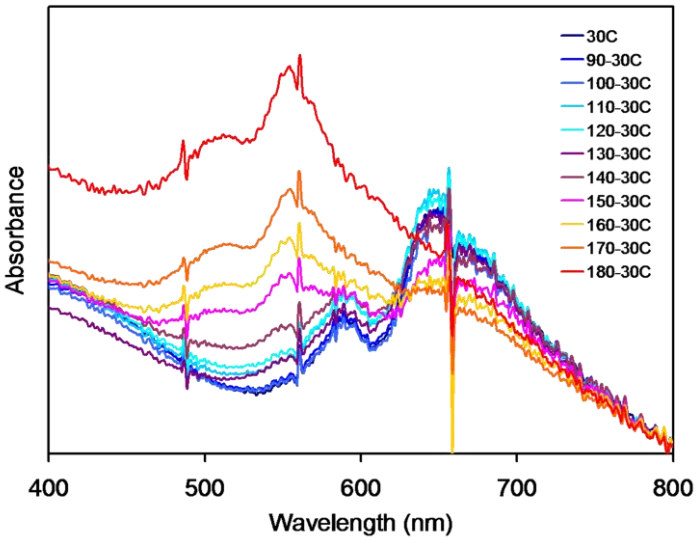

Fig. 5.13 Absorption spectra of (a) drop-cast film of poly(TCDA)/ZnO nanocomposite at different annealing temperatures and (b) after cooling from designate temperature to room temperature

Absorption spectra illustrated in Fig. 5.13b exhibit that the thermochromic reversibility of poly(TCDA)/ZnO nanocomposite film is not significantly different from poly(PCDA)/ZnO nanocomposite. The color of the film completely returns to the initial blue when it is cooled from 130 °C. However, partial color reversibility is observed when cooling form above 130 °C. The color reversibility decreases at higher degree compared to the system of poly(PCDA)/ZnO nanocomposite. The completely irreversible color transition of the film also takes place when it is annealed at ~180 °C.

Absorption spectra measured upon heating of poly(HDDA)/ZnO nanocomposite film are illustrated in Fig. 5.14a. With relatively short alkyl chain, the color transition of poly(HDDA)/ZnO nanocomposite film is observed at lower temperature than that of poly(PCDA)/ZnO and poly(TCDA)/ZnO nanocomposites. The blue-purple transition takes place at about 80 °C, in which the decrease of λ_{max} to ~620 nm occurred. When temperature is increased from 80 to 130 °C, the λ_{max} slightly shifts to high-energy region (about 600 nm). Further increasing in temperature to 180 °C does not significantly affect the spectrum of the film. This observation indicates that the complete color transition of this nanocomposite film takes place at about 130 °C.

Absorption spectra at room temperature of annealed poly(HDDA)/ZnO nanocomposite film are illustrated in Fig 5.14b. Interestingly, the complete reversibility of this nanocomposite film can be observed. The color of the film annealed below 90 °C turns to the initial blue after cooling to room temperature. This possibly results from the limitation of segmental dynamics in solid state. At annealing temperature above 90 °C, the degree of color reversibility decreases. The irreversible color transition of this nanocomposite film completely takes place at ~160 °C.

(a)

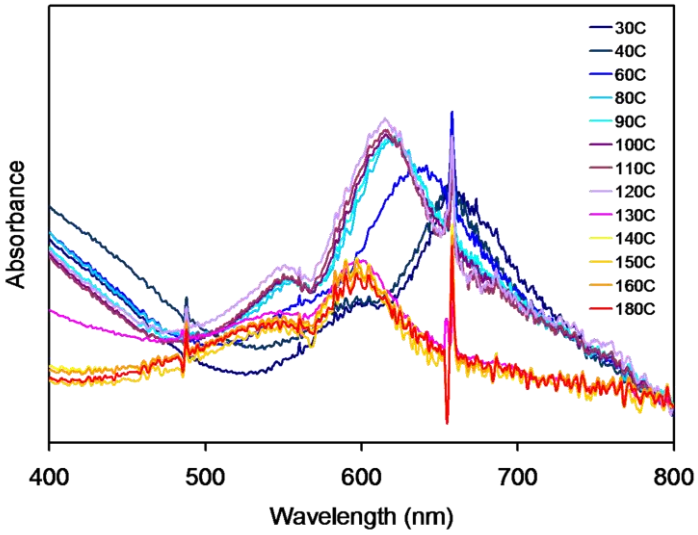

(b)

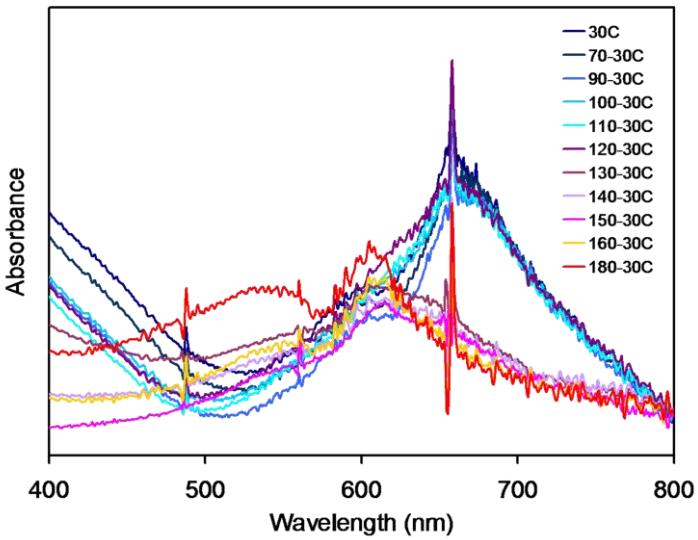

Fig. 5.14 Absorption spectra of (a) drop-cast film of poly(HDDA)/ZnO nanocomposite at different annealing temperatures and (b) after cooling from designate temperature to room temperature

Color photographs of drop-cast films of the PDA/ZnO nanocomposites taken upon increasing temperature are illustrated in Fig. 5.15. The chromic transition of the films is visually observed. It is clear that color-transition temperatures of the PDA/ZnO nanocomposite films vary with structure of the constituent polymers. The shortening of alkyl chain length leads to the decrease in color-transition temperature. In addition, we

can observed that the degree of color change in poly(HDDA)/ZnO nanocomposite film is less than that of poly(TCDA)/ZnO and poly(PCDA)/ZnO nanocomposites,. This result is similar to the nanocomposite in the form of aqueous suspension. The result is due to relatively short distance between anchoring sites and conjugated backbone of poly(HDDA/ZnO nanocomposite, which decreases its local molecular dynamics upon heating. Fig. 5.16 shows color photographs of the nanocomposite films demonstrated thermochromic reversibility, which is in agreement with the absorption spectra.

Fig. 5.15 Photographs of drop-cast film of polydiacetylene/ZnO nanocomposite taken at different temperatures (30-180 °C)

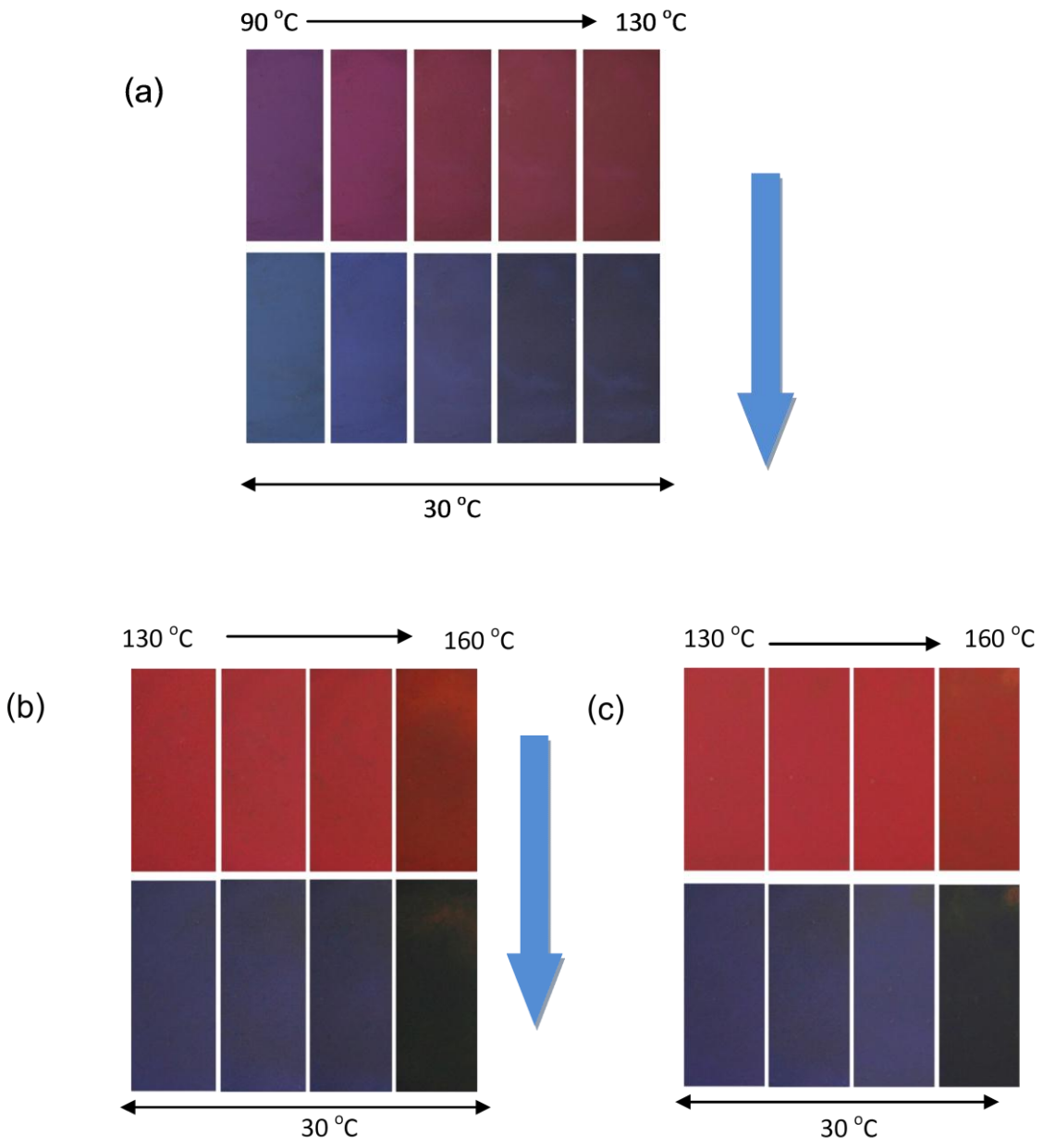

Fig. 5.16 Color photographs of the films annealed at various temperatures (top) and after cooling to 30 °C (bottom); (a) poly(HDDA)/ZnO (b) poly(TCDA)/ZnO and (c) poly(PCDA)/ZnO nanocomposites

5.1.5. Colorimetric response to pH

In previous studies, the color-transition behaviors of pure poly(PCDA) and poly(TCDA) vesicles are normally investigated in high pH region[7,24,85]. For comparison purpose in this study, we explore the system of pure poly(TCDA) vesicles in both low and high pH regions. Absorption spectra of aqueous suspension of poly(TCDA) vesicles measured upon decreasing and increasing pH are shown in Fig. 5.17. In low pH region, the addition of H^+ ions hardly affects the color of vesicles. The absorption pattern remains roughly the same at pH ~2.5. The further decrease of pH causes a growth of small shoulder at ~550 nm, corresponding to slight change of the suspension color. An incubation of the vesicles at this pH region causes precipitation. Previous study observed the aggregation at pH value lower than 4 when the vesicles were incubated for a few hour[24,85]. In our study, the poly(TCDA) suspension was continuously stirred for a few minutes prior to the measurement. Therefore, the aggregation of vesicles was minimal, indicated by relatively strong absorbance.

In the basic condition, an irreversible blue to red color transition of poly(TCDA) vesicles occurs upon increasing the pH. A peak of red phase at ~546 nm grows significantly when the pH is above 8. At this stage, the added OH- ions abstract carboxylic protons of the head groups causing a systematic increase of the negatively charged carboxylate. When strong ionic-repulsive force between the carboxylate groups overcomes the dispersion interaction between the alkyl tails, the rearrangement of poly(TCDA) segments occurs. The color transition completes at pH ~10 where absorption spectra constitute peak and shoulder at ~546 nm and ~505 nm, respectively. The pure poly(PCDA) vesicles exhibit similar color-transition behavior. However, the color transition takes place at slightly higher pH compared to that of the poly(TCDA) due to the stronger attractive dispersion interaction between the alkyl tails[7].

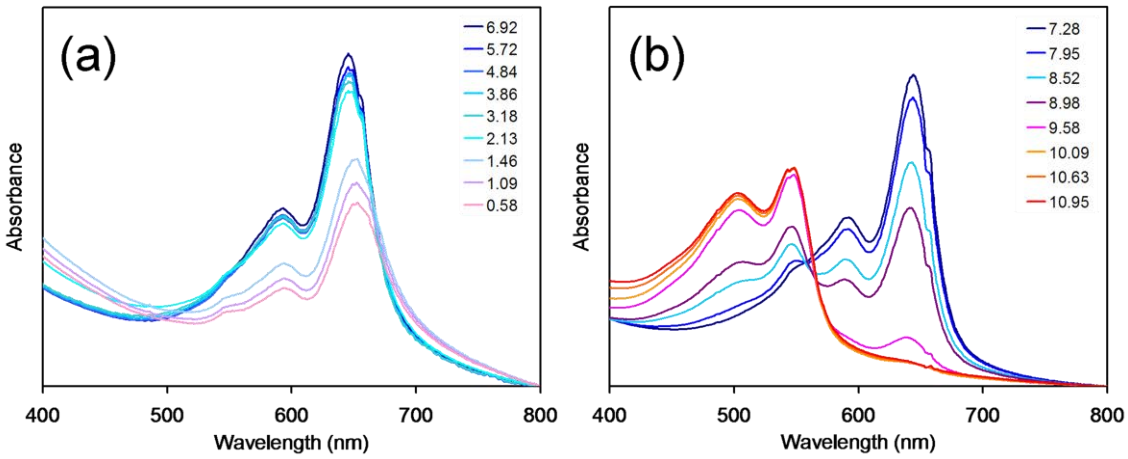

Fig. 5.17 Absorption spectra of poly(TCDA) vesicles measured upon variation of pH; (a) at low pH and (b) at high pH

The PDA/ZnO nanocomposites show rather different color-transition behaviors when exposed to acid and base. The absorption spectra of poly(PCDA)/ZnO nanocomposite measured upon decreasing pH are illustrated in Fig. 5.18a. Interestingly, color of the poly(PCDA)/ZnO nanocomposite is sensitive to acid. New peak at ~552 nm grows significantly when the pH is decreased below 2. At pH ~0.7, this peak dominates the entire spectrum, indicating the presence of large fraction of the red phase. The suspension changes to reddish purple at this condition. This result shows that the incorporation of ZnO nanoparticles promotes the colorimetric response of poly(PCDA) to acid. Moreover, the strong ionic interaction between carboxylate heads of poly(PCDA) and ZnO surface drastically alter the color-transition behavior at high pH region. Fig. 5.18b shows that the color transition of poly(PCDA)/ZnO nanocomposite also occurs upon increasing pH. However, it requires much higher concentration of OH^- to induce the color transition compared to the system of pure poly(PCDA) vesicle. The increase of pH to 12 hardly affects the absorption pattern. A small amount of red phase forms at pH ~13 as indicated by a growth of peak at ~540 nm. The suspension of nanocomposite exhibits light purple color at this pH. The increase of pH to ~9 causes comparable color transition in the pure poly(PCDA) system[7]. This comparison suggests that the color transition of the nanocomposite is likely to occur via different mechanism, requiring

much higher [OH^-] (i.e. about 10^4 times). Complete color transition of pure poly(PCDA) occurs at pH ~10 where the carboxylic head groups are mostly converted to the carboxylate one. However, the repulsive interaction between carboxylate heads is not sufficient to induce segmental rearrangement of poly(PCDA) within the nanocomposite. This is attributed to strong interfacial interaction within the system. The mechanism responsible for the color transition of the nanocomposite will be discussed in the following section.

The increase of pH causes similar color-transition behavior in the system of poly(TCDA)/ZnO nanocomposite (see Fig. 5.18d). The growth of red phase peak at ~540 nm is detected at pH ~13, corresponding to slight change of the suspension color. We observe rather different behavior in the low pH region. The color transition of poly(TCDA)/ZnO nanocomposite occurs at much lower concentration of H^+ ions (i.e. higher pH) compared to the system of poly(PCDA)/ZnO nanocomposite. Fig. 5.18c shows systematic change of absorption spectra upon decreasing pH. The color transition of poly(TCDA)/ZnO nanocomposite starts at pH~3.7 while the system of poly(PCDA)/ZnO nanocomposite is not affected at this condition. To compare the color-transition behaviors in more details, the colorimetric response (CR) of each system is plotted as a function of pH as shown in Fig. 5.19. The sharp increase of CR value indicates color-transition region. The plots clearly show that the shortening of PDA alkyl tail enhances the colorimetric response to acid. The color-transition behavior in basic condition, however, is hardly affected.

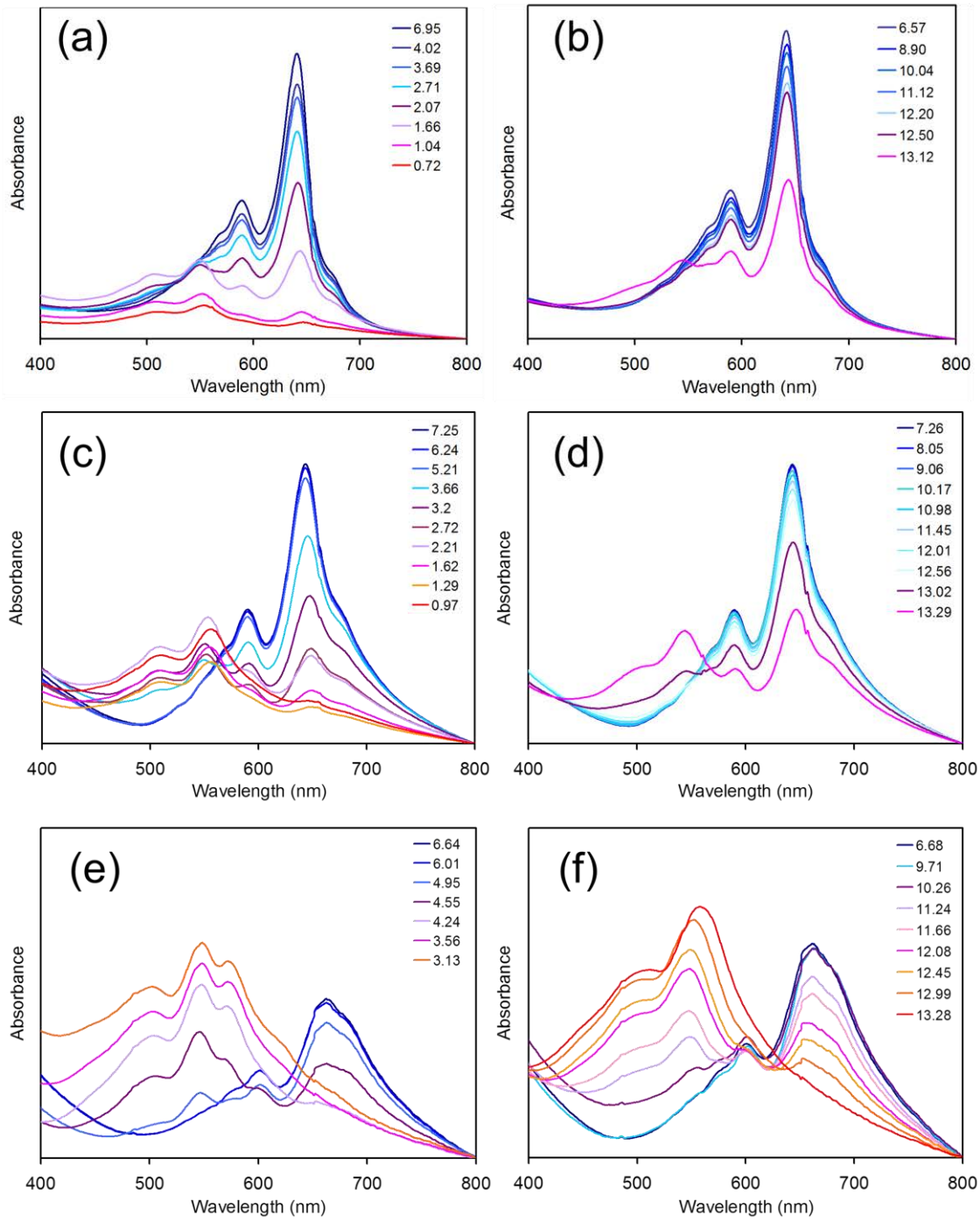

Fig. 5.18 Absorption spectra of (a), (b) poly(PCDA)/ZnO, (c), (d) poly(TCDA)/ZnO and (e), (f) poly(HDDA)/ZnO nanocomposites measured upon variation of pH

The investigation of poly(HDDA)/ZnO nanocomposite provides rather interesting results. The alkyl tail of poly(HDDA) is 4 methylene units shorter than that of the poly(PCDA). The alkyl segment connecting with carboxylic head group is also 5 methylene units shorter. These differences result in significant decrease of dispersive interactions within the poly(HDDA) vesicle, which in turn affects the color transition behavior. Our previous study observe that the blue color of pure poly(HDDA) vesicle is unstable at room temperature (see topic 5.1.3.). The color-transition temperature of poly(HDDA)/ZnO nanocomposite is also lower than that of the poly(PCDA)/ZnO system. In this study, it is easier to induce the color transition of poly(HDDA)/ZnO nanocomposite by addition of acid or base. Fig. 5.18e,f shows that the color transition occurs at pH ~5 and pH ~10.2 in acidic and basic conditions, respectively. The plots of CR value in Fig. 5.19 clearly illustrate the differences in colorimetric response of each system. Our major finding is summarized in Fig. 5.20, which compares the color photographs of pure poly(TCDA) vesicle and the three PDA/ZnO nanocomposites taken at pH ranging from 1 to 13. The pure poly(TCDA) vesicle only responses to the increase of pH. When the ZnO nanoparticles are incorporated into the PDA system, their color-transition behaviors change drastically. These PDA/ZnO nanocomposites exhibit dual colorimetric response to both acid and base. The color transition also occurs at different pH depending on the length of PDA alkyl segments. The shortening of PDA alkyl segment results in easier colorimetric response to acid and base. Therefore, this class of material can be utilized for sensing different concentrations of acid and base. It should be noted that the suspensions appear clear to naked eyes in all conditions. The precipitation tends to occur at pH below 2.

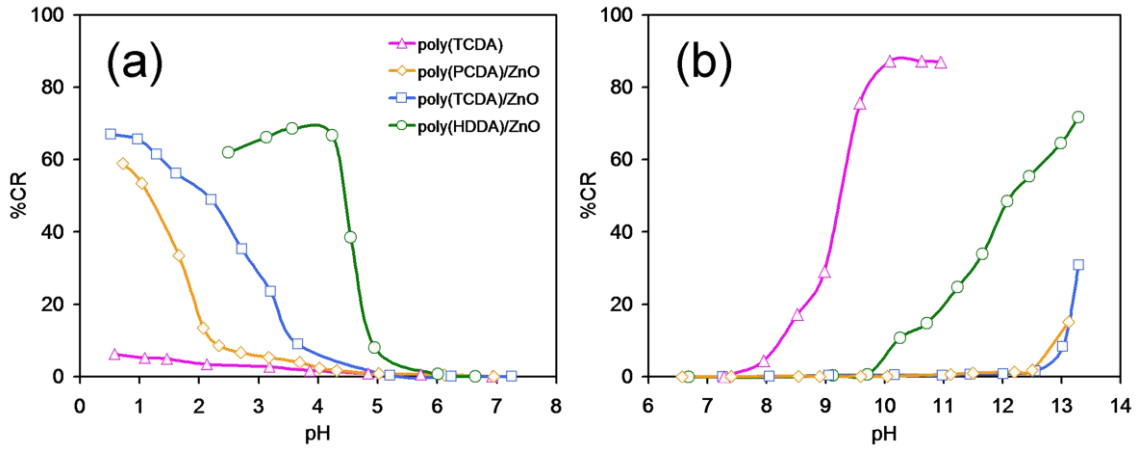

Fig. 5.19 The colorimetric response (%CR) of poly(TCDA) and PDA/ZnO nanocomposites plotted as a function of pH, symbols are for (Δ) poly(TCDA), (◊) poly(PCDA)/ZnO, (□)poly(TCDA)/ZnO and (o) poly(HDDA)/ZnO nanocomposites.

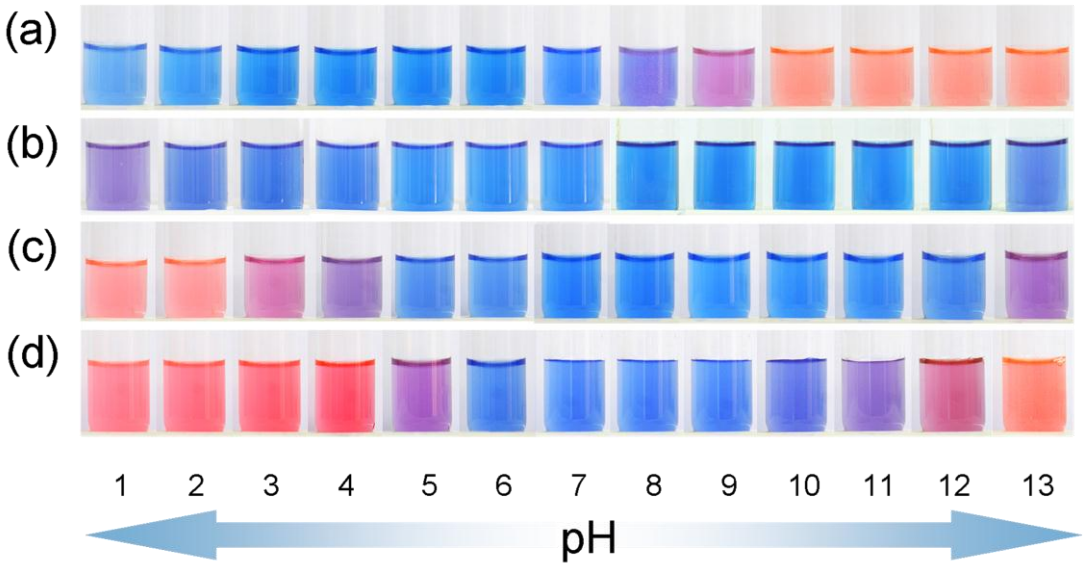

Fig. 5.20 Color photographs of aqueous suspensions of (a) poly(TCDA), (b) poly(PCDA)/ZnO (c) poly(TCDA)/ZnO and (d) poly(HDDA)/ZnO nanocomposites taken upon variation of pH

5.1.5.1. Interfacial interactions

The interfacial interactions between PDA head groups and ZnO nanoparticles upon variation of pH are investigated by utilizing infrared (IR) spectroscopy. The poly(HDDA)/ZnO nanocomposite is used for this investigation because its color transition is the most obvious in both low and high pH region. Fig. 5.21 compares the IR spectra of poly(HDDA)/ZnO nanocomposites measured from the original blue phase and the red phase obtained by increasing or decreasing pH. IR spectrum of the blue phase shows peaks at 2848, 2918, and 2954 cm^{-1} corresponding to $\nu_s(CH_2)$, $\nu_{as}(CH_2)$, and $\nu_{as}(CH_3)$, respectively. The peaks arising from the asymmetric and symmetric stretching vibrations, $\nu_{as}(COO)$ and $\nu_s(COO)$, of carboxylate anion appears at different wavenumbers. The $\nu_{as}(COO)$ peaks are detected at 1590, 1548, and 1530 cm^{-1} while the peaks at 1412, 1403, and 1380 cm^{-1} are assigned to $\nu_s(COO)$ vibration. This observation indicates that the strength of interfacial interactions between poly(HDDA) carboxylate heads and ZnO nanoparticles is not homogeneous. This topic is discussed in our previous report (see topic 5.1.2.). The $\nu_s(CH_2)$, $\nu_{as}(CH_2)$, and $\nu_{as}(CH_3)$ peaks of the red phase remain at the same position indicating that the alkyl side chains keep their conformation during the color transition. However, the band representing asymmetric $\nu_{as}(COO)$ of carboxylate head decreases significantly in the acidic region (pH~3.1) while a new band at ~1690 cm^{-1} grows simultaneously. The appearance of this new band indicates the presence of hydrogen-bonded –COOH head group in the system. Therefore, the decrease of pH transforms the carboxylate head of poly(HDDA) into the carboxylic one, which in turn destroys the ionic interfacial interaction with ZnO nanoparticles. The decrease of interfacial interaction allows segmental rearrangement of the poly(HDDA) resulting in the color transition.

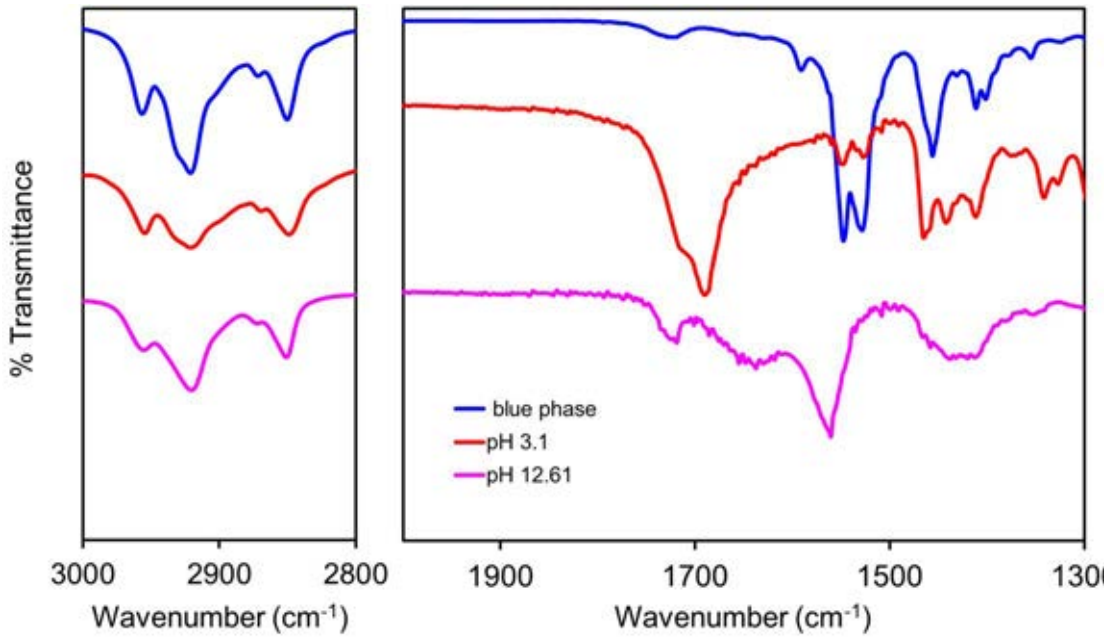

Fig. 5.21 FT-IR spectra of blue-phase poly(HDDA)/ZnO and red-phase poly(HDDA)/ZnO nanocomosites obtained at pH = 3.12 and pH = 12.61

The IR analysis of pure poly(TCDA) vesicles upon increasing pH was previously reported by Kew and Hall[24]. The blue phase of poly(TCDA) showed a strong peak at ~1690 cm^{-1} corresponding to hydrogen-bonded carbonyl stretching of –COOH head group. When the NaOH solution was added, a new peak at 1565 cm^{-1} emerged in the spectrum of red phase. This related to the presence of a bridging bidentate coordination of carboxylate head groups with the sodium cation. In the system of poly(HDDA)/ZnO nanocomposites, an increase of pH causes the shift of ν_{as}(COO) band to higher wavenumber. The IR spectrum of red phase constitutes a peak at ~1560 cm^{-1} accompanied with broad shoulder at ~1640 cm^{-1}. Previous study by Huang et.al[47] demonstrates that strength of interactions between carboxylate head and various cations dictates the vibrational energy levels of carbonyl group. The blue shift of ν_{as}(COO) band detected in this study corresponds to the weakening of interfacial interaction between carboxylate heads and ZnO nanoparticles, responsible for the color transition. The new peak at ~1560 cm^{-1} is very close to that of the red phase

poly(TCDA). Therefore, the carboxylate head groups are likely to coordinate with Na^+ ions at the high pH region.

5.1.5.2. Surface charges at different pH

The zeta potential is an important parameter for monitoring the variation of surface charge at different conditions. In our system, the measurement of zeta potential as a function of pH can shed more light on the mechanism responsible for the color transition of the nanocomposites. The suspension pH is adjusted by adding HCl or NaOH solutions and then incubated for 5 min. The results obtained from the systems of pure poly(TCDA), poly(TCDA)/ZnO and poly(HDDA)/ZnO nanocomposites are illustrated in Fig. 5.22. The zeta potential of original blue poly(TCDA) vesicles at pH~6.7 is -54 mV while surfaces of the nanocomposites exhibit slightly lower negative charge. The negative value of zeta potential indicates the presence of carboxylate anions at outer surface of the samples. Our previous study also observes that the zeta potential of PDA vesicles becomes positive when the carboxylic heads are replaced by the amine and amide groups[56]. In the system of poly(TCDA), the decrease of pH to ~4 causes slight decrease of the negative zeta potential. This is attributed to partial protonation of some carboxylate head groups, reducing the overall negative surface charge. At pH~1, the negative zeta potential drastically drops to about -5 mV. The relatively low surface charge at this condition leads the coagulation of the samples. The systems of poly(TCDA)/ZnO and poly(HDDA)/ZnO nanocomposites show similar behavior. The drastic change of zeta potential occurs at pH~1 and pH~2, respectively. The sharp decrease of negative charge is detected at higher pH value in the system of poly(HDDA)/ZnO nanocomposite. This is attributed to nature of the constituent polymer. The color transition of poly(TCDA)/ZnO and poly(HDDA)/ZnO nanocomposites takes place at pH ~5 and pH ~4, respectively (see Fig. 5.19,5.20). However, their surface charges are not affected at these conditions. This observation suggests that the structural change responsible for the color transition is likely to occur at the inner region

of the nanocomposites (see below). It is important to note that the high surface charge value of all samples at pH above 2.5 indicates good stability of the suspension.

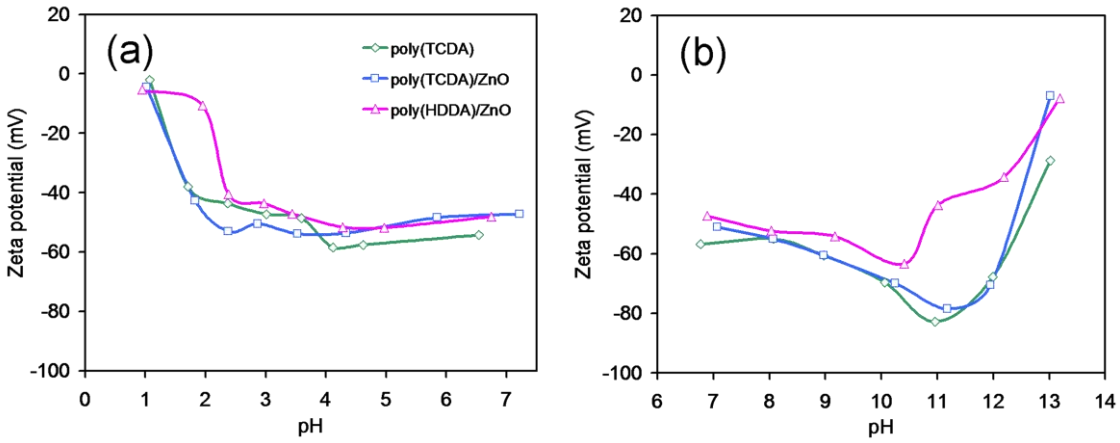

Fig. 5.22 Zeta potential of poly(TCDA) vesicles , poly(TCDA)/ZnO nanocomposite and poly(HDDA)/ZnO nanocomposite measured as a function of pH as shown in the plots

The zeta potentials measured in high pH region are shown in Fig. 5.22b. The variation of surface charges upon increasing pH of poly(TCDA) vesicles and the nanocomposites are quite similar. In the systems of poly(TCDA) vesicles and poly(TCDA)/ZnO nanocomposite, the negative surface charge systematically increases upon increasing pH to ~11. At this pH range, the added OH- ions abstract acidic protons of carboxylic head groups, transforming them into caboxylate anions. The zeta potential reaches highest negative value at pH~11 where most of the surface is populated by the carboxylate anions. The color transition of poly(TCDA) vesicles takes place at pH ~8.5, where the slight increase of negative surface charge is sufficient to induce segmental rearrangement of the poly(TCDA). In the system of poly(TCDA)/ZnO nanocomposite, however, the significant increase of negative surface charge at pH~11 still does not cause the color transition. This result indicates that the repulsive force between carboxylate head groups is not strong enough to overcome the strong attractive interfacial interaction at the surface of ZnO nanoparticles and dispersive interaction between alkyl chain of poly(TCDA). The further increase of pH causes abrupt decrease

of the negative zeta potential. This is attributed to the effect of Na^+ counterion, reducing the overall negative surface charge. However, the poly(TCDA)/ZnO nanocomposite changes color at pH~13. In the system of poly(HDDA)/ZnO nanocomposite, the highest negative charge is detected at pH~10.5. At this pH, the color of this nanocomposite suspension slightly changes. This suggests that the repulsive force between carboxylate groups slightly perturbs the conformation of the poly(HDDA) backbone. The extent of color transition systematically increases and reaches maximum at pH~13. The negative zeta potential, on the other hand, drops to lowest value at this condition. This observation indicates that the mechanism of the color transition hardly relate with change of surface charge. It is likely to occur at the inner region of the nanocomposites. Our result also suggests that specific sodium cation binding to carboxylate groups promotes for the colorimetric blue-red transition[24]. This hypothesis is supported by the results in the following section.

5.1.5.3. Dissolution of ZnO nanoparticles

It has been known that the dissolution of ZnO nanoparticles can occur in acidic or basic conditions[86-88]. It is possible that this property is one of the main reasons responsible for the color transition of PDA/ZnO nanocomposites upon variation of pH. Therefore, this section investigates the dissolution behaviors of ZnO nanoparticles used in this study. We titrate 5 mL of 0.01 wt.% ZnO aqueous suspension with HCl or NaOH solutions and then follow the reaction by utilizing UV-vis absorption spectroscopy. The results are shown in Fig. 5.23. Absorption spectrum of the original ZnO aqueous suspension at pH = 7.81 exhibits a sharp peak at 375 nm. The addition of small quantity of 0.1 M HCl solution causes the decrease of pH to 6.91 and slight drop of the absorbance (see Fig. 5.23a). In this condition, acidic protons react with ZnO surface, resulting in the dissolution[86]. The decrease of absorbance indicates the disappearance of ZnO nanoparticles in the suspension. Further addition of the HCl solution causes continuous decrease of the absorbance while the pH remains roughly the same at about 6.8 (see inset of Fig. 5.23a). It requires relatively large amount of HCl solution to

decrease the pH to 4. The absorbance drastically drops at this condition. Our result indicates that the dissolution process of bare ZnO nanoparticles takes place at pH~6.8.

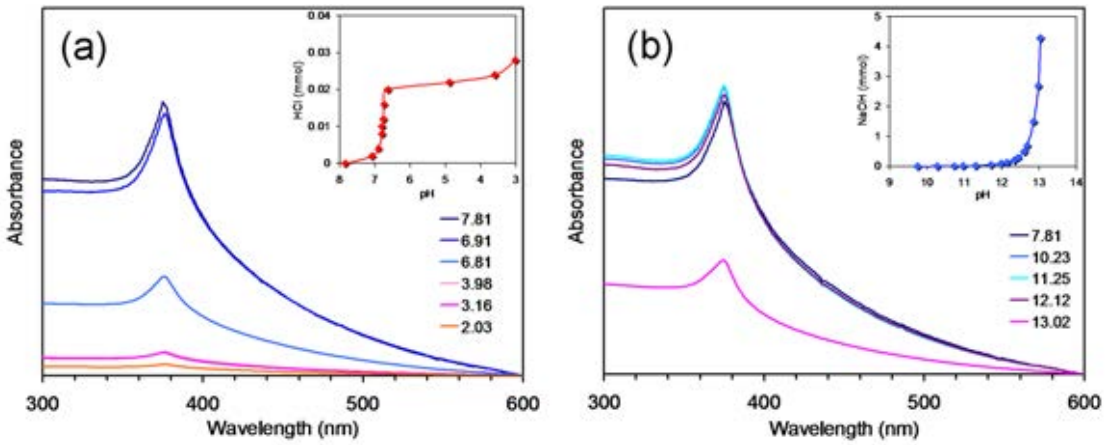

Fig. 5.23 Absorption spectra of ZnO nanoparticle suspension measured upon (a) decreasing pH and (b) increasing pH. The insets show titration curve of ZnO nanoparticle suspension with HCl and NaOH solution.

In the nanocomposite systems, the color transition of poly(PCDA)/ZnO, poly(TCDA)/ZnO and poly(HDDA)/ZnO nanocomposites is detected at pH~2, ~3.5 and ~5, respectively (see Fig. 5.19). The dissolution of bare ZnO nanoparticles, however, occurs at much higher pH value. This discrepancy probably arises from architecture of the nanocomposites, constituting ZnO nanoparticles at the core region. The coating of PDA layers on ZnO surface prohibits the dissolution process. However, some small areas of the ZnO surface may remain uncoated, allowing the reaction with acidic protons. The dissolution of ZnO surface through the uncoated areas inevitably destroys interfacial interactions with the carboxylate head groups of the PDAs. In addition, the repulsive interaction between free carboxylate head groups causes the segmental rearrangement of PDAs. To induce the color transition, the repulsive interaction needs to overcome attractive interactions within the PDA layer. The difference of dispersive interaction within the PDA layers causes the color transition to occur at different pH regions. The alkyl chain length of PDA increases from poly(HDDA), poly(TCDA) and

poly(PCDA), respectively, corresponding to systematic increase of dispersive interaction. Therefore, it requires the lowest concentration of acidic protons to induce the color transition of poly(HDDA)/ZnO composite. The color transition of poly(TCDA)/ZnO and poly(PCDA)/ZnO nanocomposites takes place at higher concentrations of acidic protons, respectively. This result is consistent with their thermochromic behaviors where the color transition temperature increases with increasing alkyl chain length of the constituent PDAs. The further decrease of pH leads to the protonation at the carboxylate head group transforming them into the carboxylic one as shown in previous sections by IR and zeta potential studies.

At high pH region, the increase of pH to 12 hardly affects the absorption spectrum of ZnO nanoparticles (see Fig. 5.23b). The dissolution process is observed at pH~13, indicated by drastic drop of the absorbance. Although 10 M NaOH solution is continuously added, the pH of the suspension remains at ~13. At this condition, the ZnO nanoparticles decompose to form zincates such as $[Zn(OH)_3]^-$ and $[Zn(OH)_4]^{2-}$ [86]. The color transition of poly(PCDA)/ZnO and poly(TCDA)/ZnO nanocomposites is observed at this pH. Similar to the behavior in acidic pH, the dissolution of ZnO nanoparticles frees the carboxylate head groups, leading to the color transition. For the system of poly(HDDA)/ZnO nanocomposite, the color transition occurs at pH~10 where the dissolution of ZnO nanoparticles does not occur. This observation suggests that the color transition of this system is induced by different mechanism. As shown in previous section, the negative surface charge of poly(HDDA)/ZnO nanocomposite reaches maximum at pH~10. We suggest that the increase of repulsive force between carboxylate head groups can overcome interfacial interaction and other attractive interactions within this system, causing segmental rearrangement of some poly(HDDA) chains. This behavior is facilitated by relatively weak dispersive interaction within the system due to the presence of short alkyl chains. At pH~13, the suspension turns completely red caused by the dissolution of ZnO nanoparticles. The IR study observes the presence of free carboxylate groups at this condition.

5.1.5.4. Proposed mechanism

We propose mechanism for color transition of poly(HDDA)/ZnO nanocomposite upon variation of pH in Fig. 5.24. In the low pH region, the ZnO nanoparticles decompose, which in turn breaks the attractive ionic interaction between carboxylate head groups and positive species at ZnO surface. The repulsive ionic interaction between free carbxylate head groups causes segmental rearrangement, resulting in the color transition. The excess protons transform the carboxylate head group into the carboxylic one. In the systems of poly(PCDA)/ZnO and poly(TCDA)/ZnO nanocomposites, it requires larger fraction of the carboxylate head groups to overcome the stronger attractive interaction within the PDA layers. Therefore, the color transition takes place at lower pH values.

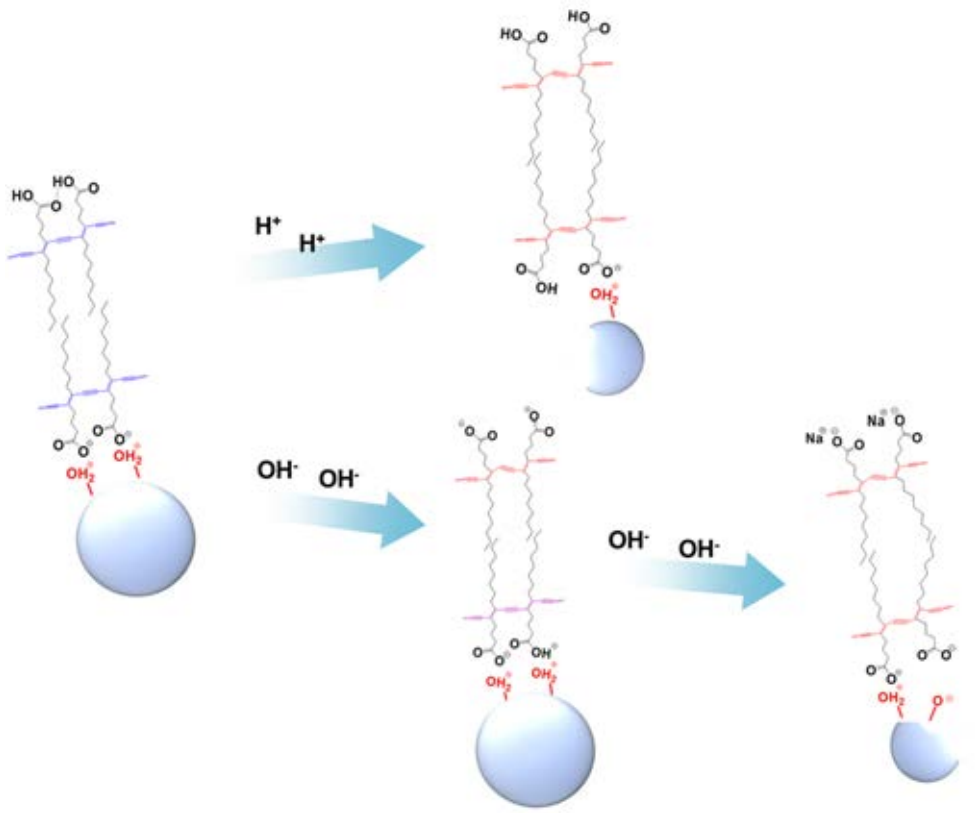

Fig. 5.24 Proposed mechanism for color transition of poly(HDDA)/ZnO nanocomposite upon variation of pH

In high pH region, the added OH- ions abstract protons of the carboxylic head groups causing a systematic increase of the negatively charged carboxylate. In other words, the magnitude of repulsive force between the head groups increases with increasing the pH. In the system of poly(HDDA)/ZnO nanocomposite, the dispersive force within the PDA layer is relatively weak because of its short constituent alkyl segments. Therefore, the repulsive force can induce the segmental rearrangement of some poly(HDDA), resulting in partial color transition. This is not the case for the systems of poly(PCDA)/ZnO and poly(TCDA)/ZnO nanocomposites where the constituent alkyl segments are much longer. The further increase of pH to ~13 causes the dissolution of ZnO nanoparticles, leading to the color transition of all systems. We note that the investigation of size distribution and morphologies do not observe the collapse of the structure at the low and high pH regions (see supporting in formation).

5.1.6. Colorimetric response to alcohols

5.1.6.1. Addition of ethanol

In the previous work[67], it was found that the colorimetric behaviors of poly(PCDA)/ZnO nanocomposite was clearly different compared to that of pure poly(PCDA) vesicles. The addition of alcohols and some solvents did not induce the color transition of this nanocomposite. This is due to strong ionic interaction at ZnO surface which strengthens layered structure of the poly(PCDA). In addition, the dispersion interaction between alkyl side chains of the inner and outer layers also restrain the distortion of conjugated backbone. In this continuation study, we used the nanocomposites prepared from TCDA and HDDA to investigate the chromatic transition upon addition of alcohols. Firstly, the color transition of poly(TCDA) vesicles upon addition of ethanol was observed. From absorption spectra illustrated in Fig. 5.25a, a new peak at ~540 nm is detected when the concentration of ethanol is 28.6 vol%. Further increasing concentration of ethanol, this peak continuously grows. A drastic

change takes place when concentration is about 44.4 vol%. The suspension completely changes to red color at the concentration of 54.5 vol%. In the system of poly(TCDA)/ZnO nanocomposite which has slightly shorter alkyl tail (compared to poly(PCDA)), however, the addition of ethanol does not induce color transition in this nanocomposite. The spectra upon increasing ethanol concentration exhibit similar pattern (see Fig. 5.25b). The systematic decrease of absorbance is due to the dilution. This result exhibits that the dispersion interaction between alkyl side chains of this nanocomposite is still sufficient for resist the distortion of conjugated backbone upon addition of ethanol.

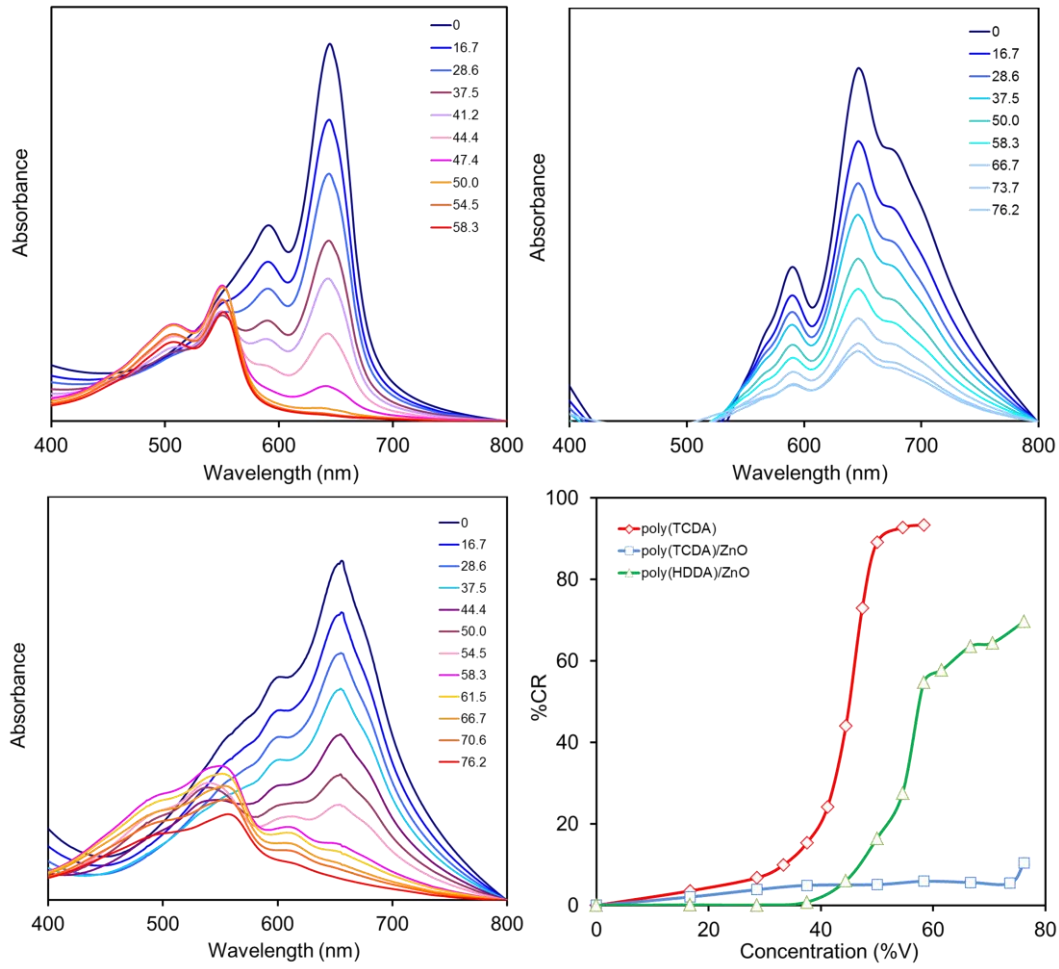

Fig. 5.25 Absortion spectra of (a) poly(TCDA), (b) poly(TCDA)/ZnO and (c) poly(HDDA)/ZnO nanocomposites upon addition of ethanol, (d) the plots of colorimetric response (%CR) during adding ethanol

Interestingly, the color transition upon addition of ethanol was observed in the system of poly(HDDA)/ZnO nanocomposite. From the absorption spectra shown in Fig. 5.25c, the decrease of λ_{max} clearly occurs when the concentration of ethanol is in a range of 50 to 54.5 %V. Further adding ethanol to about 70 vol%, the color of the suspension completely change to red. The rationalization for the chromatic transition of this nanocomposite is due to relatively short distance between the carboxylic head group and the conjugated backbone, causing the decrease of dispersion interaction, the molecule of ethanol can insert the outer layer and perturb the conformation of polymer backbone. The comparison of colorimetric response of pure poly(TCDA) vesicles, poly(TCDA)/ZnO and poly(HDDA)/ZnO nanocomposites are illustrated in Fig. 5.25d. The plots of %CR clearly demonstrates that the color transition of poly(TCDA)/ZnO nanocomposite does not occur upon addition of ethanol. The %CR values of this nanocomposite slightly increase although ethanol concentration is increased to 76 vol%. In contrast, the %CR value of poly(HDDA)/ZnO nanocomposite at ethanol concentration of 76 vol% is around 70%, corresponding to color change in the suspension.

5.1.6.2. Addition of 2-propanol

In addition, we also observed the color transition of poly(TCDA)/ZnO and poly(HDDA)/ZnO nanocomposites upon addition of 2-propanol. From previous literature[57], demonstrates that structure of alcohol such as alkyl tail length and position of –OH can affect the color transition of PDAs. The absorption spectra of poly(TCDA) shown in Fig. 5.26a exhibit the drop of absorbance at ~640 nm while a new peak of ~540 nm continuously grows when the concentration of 2-propanol is increased. The complete red phase takes place at ~41 vol%. From the plots of %CR illustrated in Fig. 5.26b, clearly show that the chromatic transition of poly(TCDA) vesicles upon addition of 2-propanol takes place faster than that of ethanol. This result exhibits that the addition of 2-propanol can induce faster color transition of poly(TCDA) than that of ethanol. In other word, the molecules of 2-propanol which penetrate into the layer of the PDA have more

affect the molecular conformation within the assemblies compared to ethanol molecules. Therefore, we used this type of alcohol to investigate the color transition of the nanocomposite.

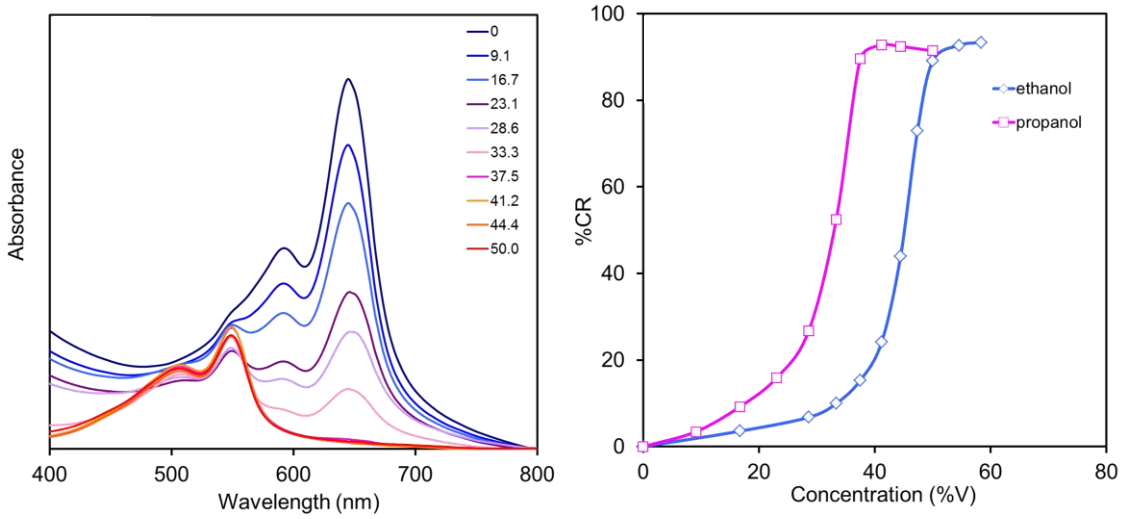

Fig 5.26 (a) Absorption spectra of poly(TCDA) vesicles upon addition of 2- propanol and (b) plots of %CR compared to that of the addition of ethanol

The absorption spectra of poly(TCDA)/ZnO nanocomposite upon addition of 2-propanol are illustrated in Fig. 5.27a. However, the color transition was still not observed. The spectrum of blue phase with the λ_{max}~643 nm is detected and has no different pattern when the concentration of 2-propanol is increased. The plots of %CR shown in Fig. 5.27c also exhibit slight increase of %CR value when the concentration of 2-propanol is increased to 76 vol%. Therefore the penetration of this alcohol can not disturb the electronic states of the polymer, corresponding to no change in color of the suspension.

In the system of poly(HDDA)/ZnO nanocomposite, the absorption spectra shown in Fig. 5.27b present the decrease of the absorbance at λ~660 nm upon the increase of 2-propanol concentration. When the concentration is 28.6 vol%, the drastic drop of λ_{max} to ~545 nm is observed and the color of the suspension change to purple. The suspension completely changes the color to red at the concentration of 54.5 vol% as the value of

%CR is about 65%. Fig 5.27d shows the plots compared the response of poly(HDDA)/ZnO nanocomposite upon addition of ethanol and 2-propanol. It show similar result as in the system of pure poly(TCDA). The color transition of poly(HDDA)/ZnO nanocomposite upon addition of 2-propanol is clearly faster than that of ethanol.

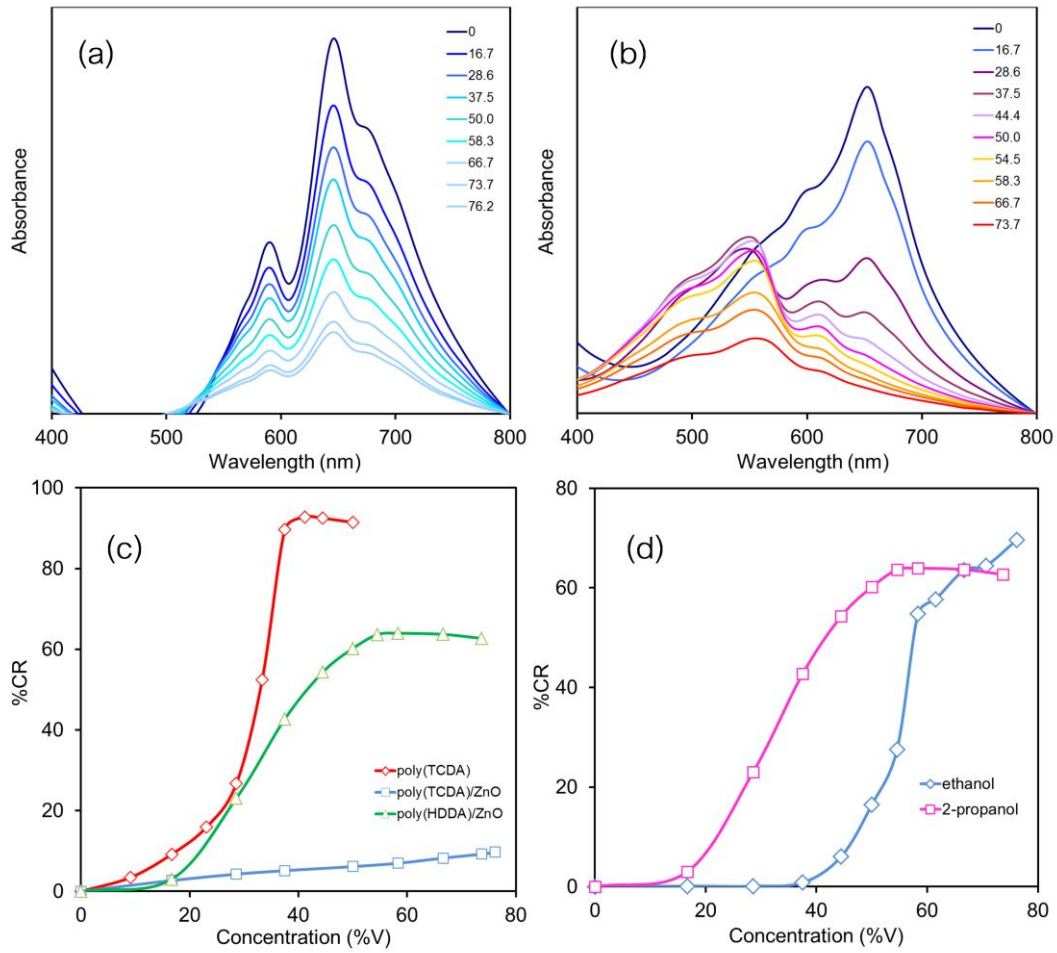

Fig. 5.27 Absorption spectra of (a) poly(TCDA)/ZnO and (b) poly(HDDA)/ZnO nanocomposites, (c) plots of %CR of poly(TCDA) and the nanocomposites upon addition of 2-propanol and (d) %CR of poly(HDDA)/ZnO nanocomposite during adding two types of alcohols

In this part, we demonstrate a simple method for improving colorimetric behaviors of PDA-based materials. The incorporation of ZnO nanoparticles into PDA assemblies promotes interfacial interactions within the system. The resultant PDA/ZnO nanocomposites exhibit reversible thermochromism and high thermal stability. Their color-transition temperatures can be systematically controlled by varying structure of the constituent polymers. The shortening of alkyl chain length, causing the decrease in dispersion interactions within the assemblies, leads to the decrease in color-transition temperature.

The colorimetric behaviors upon variation of pH of PDA/ZnO nanocomposites are significantly different from that of PDA vesicles. The color-transition of nanocomposite upon increasing pH takes place at much higher pH compared to that of pure PDA vesicles. The strong ionic interaction between carboxylate head groups and positive charge at the surface of ZnO nanoparticles can restrain the dynamic of alkyl side chain upon addition of OH- ions. The shortening of alkyl side chain also causes highly sensitive colorimetric response of the nanocomposites, which comparable to that of pure PDAs. Moreover, PDA/ZnO nanocomposite interestingly exhibits more sensitive colorimetric response upon decreasing pH compared to their PDA counterparts. In the system of poly(HDDA)/ZnO nanocomposite which constitutes relatively short alkyl chains show interesting color-transition in both low and high pH region. The addition of alcohols such as ethanol and 2-propanol cannot induce the color transition of poly(PCDA)/ZnO and poly(TCDA)/ZnO nanocomposites. However in the system of poly(HDDA)/ZnO nanocomposite, due to relatively short alkyl chain of this polymer, the addition of alcohols can induce the blue-red transition.

5.2. Effects of UV irradiation on colorimetric behaviors of PDA/ZnO nanocomposites

Polymerization time can affect the colorimetric behaviors of PDA-based materials; however, it is rarely reported. In the previous study of our research group, the effects of polymerization time on colorimetric behavior of poly(PCDA)/ZnO nanocomposites were investigated[67]. The results clearly showed that increasing the polymerization time decreased the color transition temperature of poly(PCDA)/ZnO nanocomposites. In this study, the effects are further investigated in the system of poly(TCDA)/ZnO and poly(HDDA)/ZnO nanocomposites with shorteralkyl side chain length compared to poly(PCDA)/ZnO nanocomposites.

5.2.1. Optical properties

Absorption spectra of poly(TCDA)/ZnO nanocomposites subjected to different UV irradiation times are illustrated in Fig. 5.28a. The spectrum of the nanocomposite obtained by UV irradiating for 1 min shows typical peaks at 640 nm with vibronic shoulder at 590 nm. The aqueous solution exhibits light blue color. With increasing UV irradiation time to 20 min, it can be clearly observed the increase of the low energy band ~673 nm, corresponding to the increase of conjugation length in the polymer. At UV irradiation time of 30 min, the peak of vibronic shoulder shifts from 590 nm to ~563 nm. The λ_{max} values slightly decrease as a function of irradiation time in the range of 1-40 min as shown in Fig. 5.28c. At UV irradiation time of 60 min, the λ_{max} significantly decreases to 616 nm with vibronic shoulder ~563 nm. The color of the solution changes to purplish blue. The spectra continue in similar pattern when increasing UV irradiating to 120 min. The decrease of λ_{max} is hardly observed.

In the system of poly(HDDA)/ZnO nanocomposite, polymerization time exhibits more effect on the molecular conformation than in the system of poly(TCDA)/ZnO nanocomposite. The spectra of poly(HDDA)/ZnO nanocomposites derived from different polymerization times are shown in Fig. 5.28b. The aqueous solution of the

nanocomposite obtained from 15s-UV irradiating time exhibits deep blue color with a peak at ~660 nm and vibronic shoulder at 600 nm. The slight decrease of λ_{max} is observed at UV irradiating time of only 4 min. With increasing UV irradiating time to 10 min, a peak at ~614 nm is detected. The λ_{max} significantly drops to ~614 nm when the nanocomposite is irradiated for 30 min as illustrated in Fig. 5.28c. Further increasing in UV irradiating time causes insignificant changes in the spectra. We can conclude from the results that the increase of UV irradiation time affects the conformation of the polymer backbone. The decrease of λ_{max} attributes to the increase of side chain dynamics, which causes partial twisting of π-orbitals. The energy band gap is wider and electrons need higher energy to move to the conduction band. Therefore, the PDA absorbs relatively higher energy.

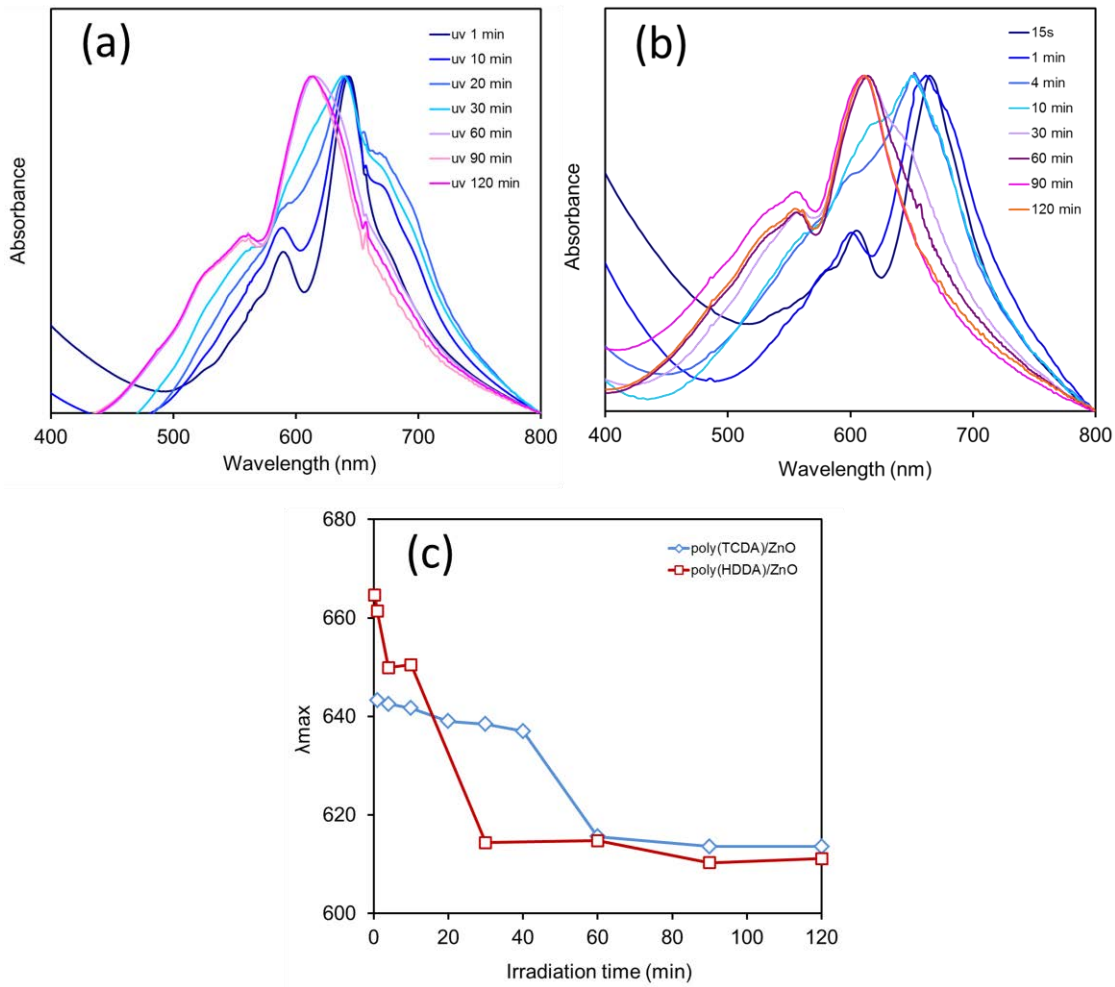

Fig. 5.28 Absorption spectra of (a) poly(TCDA)/ZnO and (b) poly(HDDA)/ZnO nanocomposites upon increasing polymerization time, and (c) λ_{max} of these nanocomposites with increasing polymerization time.

5.2.2. Interactions in the nanocomposites

The interactions in the nanocomposites upon increasing UV irradiation time are investigated by using infrared (IR) spectroscopy. It was shown in the system of poly(PCDA)/ZnO nanocomposites that the spectrum of blue phase nanocomposite irradiated for 60 min exhibits no difference compared to that of the nanocomposite irradiated for 4 min[67]. The similar results are exhibited for the system of poly(TCDA)/ZnO

nanocomposites in this study. The differences among the spectrum pattern of the nanocomposite irradiated for various time are not observed.

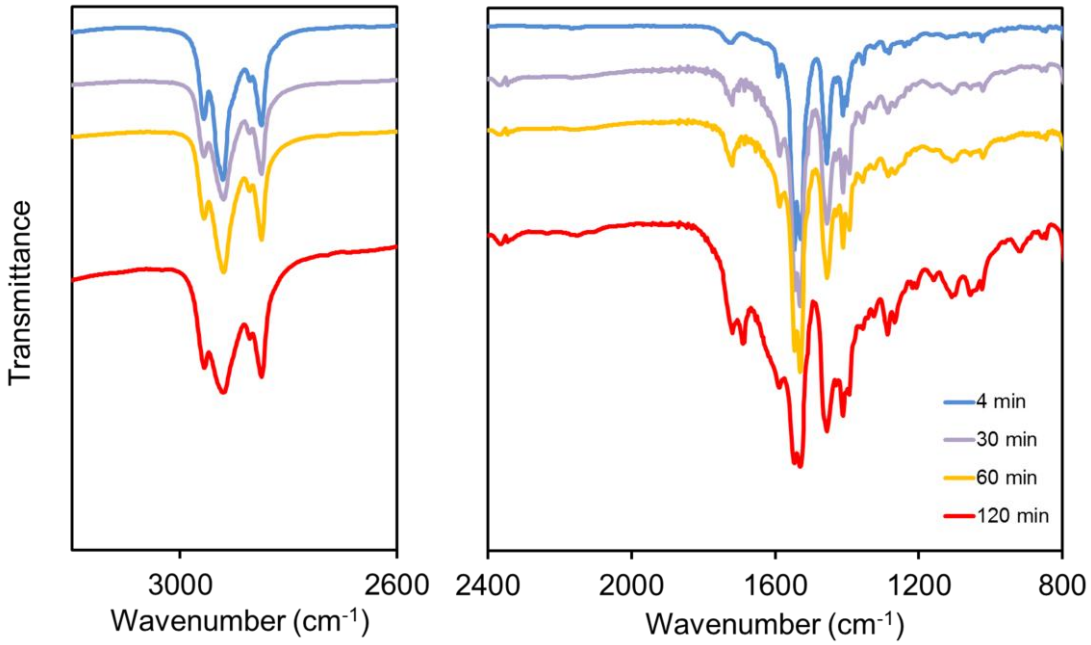

Fig. 5.29 FTIR spectra of poly(HDDA)/ZnO nanocomposites prepared with various polymerization times.

However, in the system of poly(HDDA)/ZnO nanocompositewith relatively short alkyl chain, the effects of UV irradiation time on the conformation of the electronic backbone are more obvious. As shown in Fig. 5.28c that λ_{max} decreases from 664 to 616 nm within 30 min of UV irradiation time, and the suspension clearly changes its color to purple. In addition, the decrease of λ_{max} upon increasing UV irradiation time of poly(HDDA)/ZnO nanocomposite is more than in the system of poly(PCDA)/ZnO or poly(TCDA)/ZnO nanocomposites. The results are quite different from the nanocomposites subjected to heat, in which the decreases of λ_{max} upon increasing temperature in poly(PCDA)/ZnO or poly(TCDA)/ZnO nanocomposites are more than in the system of poly(HDDA)/ZnO nanocomposite (refer to topic 5.1.3.). Therefore, it can be imagined that the UV light could directly affect the backbone conformation of this polymer. However, this assumption should be further investigated in the future.

The FTIR spectrum of the blue-phase poly(HDDA)/ZnO nanocomposite shows the peaks at 2848, 2918, and 2954 cm^{-1} correspond to $\nu_s(CH_2)$, $\nu_{as}(CH_2)$, and $\nu_{as}(CH_3)$, respectively (Fig. 5.29). After increasing polymerization time to 120 min, all of these peaks are at the same position, indicating no changes in conformation of the alkyl side chains. Independent of UV irradiation time, the peaks at around 1540 and 1410 cm^{-1}, corresponding to the stretching vibrations, i.e., $\nu_{as}(COO)$ and $\nu_s(COO)$, of carboxylate anion split into multiple peaks in all samples. This suggests the non-homogeneous interactions between poly(HDDA) carboxylate head groups and Zn-OH_2^+ groups at ZnO surface, which still occur upon increasing UV irradiation time to 120 min. However, a slight difference can be observed in the IR pattern of poly(HDDA)/ZnO nanocomposite irradiated for 120 min. The peak of carboxylate anion slightly shifts to ~1600 cm^{-1}, indicating that the interaction with ZnO surface is in a different manner. In addition, a new peak at 1685 cm^{-1} is clearly observed. This result suggests partial rearrangement of the interactions inside the nanocomposite during increasing irradiation time.

5.2.3. Morphologies

Morphologies of PDA/ZnO nanocomposites obtained from various UV irradiation times are investigated by SEM as shown in Fig. 5.30. The samples of the nanocomposites were prepared without filtration. The results show that polyTCDA)/ZnO nanocomposites obtained from irradiating for 30 and 120 min (see Fig. 5.30a and b) exhibit spherical and ellipsoidal shapes, which is similar to poly(TCDA)/ZnO nanocomposites irradiated for 1 min. In the system of poly(HDDA)/ZnO nanocomposite, the long irradiated samples in Fig. 5.30 c,d exhibit ellipsoidal and irregular shapes, which are similar to the poly(HDDA)/ZnO nanocomposite irradiated for 15s (see Fig. 5.2f). Therefore, it can be concluded that although the increase of polymerization time can change the optical properties, it does not affect the morphologies of the nanocomposites.

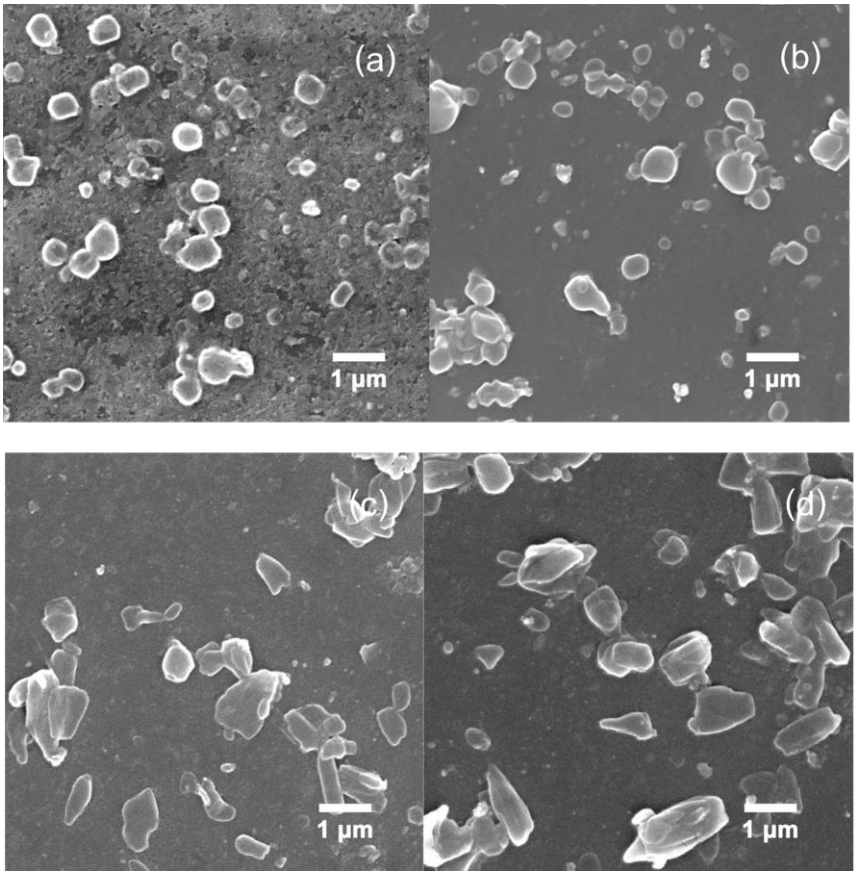

Fig. 5.30 SEM images of the nanocomposites obtained from various irradiation times: (a) poly(TCDA)/ZnO irradiated for 30 min, (b) poly(TCDA)/ZnO irradiated for 120 min, (c) poly(HDDA)/ZnO irradiated for 30 min and (d) poly(HDDA)/ZnO irradiated for 60 min.

5.2.4. Colorimetric response to temperature

5.2.4.1. Poly(TCDA)/ZnO nanocomposites

The colorimetric response to temperature of poly(TCDA)/ZnO nanocomposites prepared with various UV irradiation times is shown in Fig. 5.31. The result exhibits that polymerization time clearly affects the thermochromic behaviors of this nanocomposite. The nanocomposite prepared with irradiating UV for 4 min displays slight color transition in the range of 30-60 ^{o}C. The drastic drop of λ_{max} to ~590 nm is observed when increasing temperature to 70 ^{o}C, corresponding to blue-purple transition (see Fig. 5.32a). In the system of the nanocomposites irradiated for 30 min, the sudden decrease

of the λ_{max} to ~617 nm occurs at only 40°C. This result demonstrates that the increase of polymerization time causes partial rearrangement of the polymer conformation. This results in the decrease of attractive interaction such as hydrogen bonding, dispersion interaction or ionic interaction in the nanocomposites. Therefore, the color transition of the nanocomposite prepared with longer UV irradiation time takes place at lower temperature region.

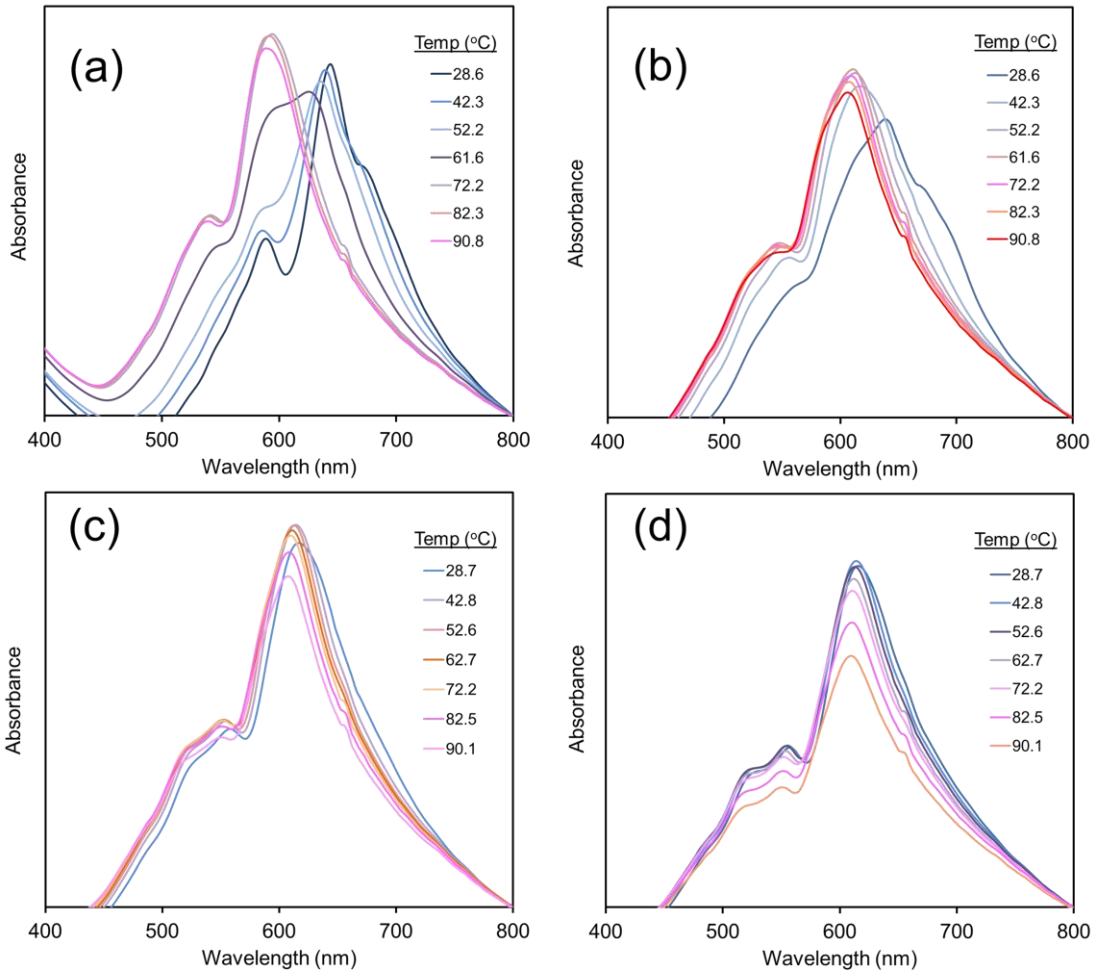

Fig. 5.31 Absorption spectra upon increasing temperature of poly(TCDA)/ZnO nanocomposites obtained by irradiating for (a) 4 min, (b) 30 min, (c) 60 min and (d) 120 min

For the system of poly(TCDA)/ZnO nanocomposites obtained by irradiating for 60 min and 120 min, the initial λ_{max} are 617 nm and 615 nm, respectively. Upon increasing

temperature, the λ_{max} slightly decrease and the drastic drop of λ_{max} cannot be detected. The λ_{max} of the nanocomposite obtained by irradiating for 60 and 120 min decreases to 608 nm and 609 nm, respectively, when temperature increases to 90 °C. This result indicates that the segmental rearrangement of the polymer in this nanocomposite slightly takes place although it is heated up to 90°C.

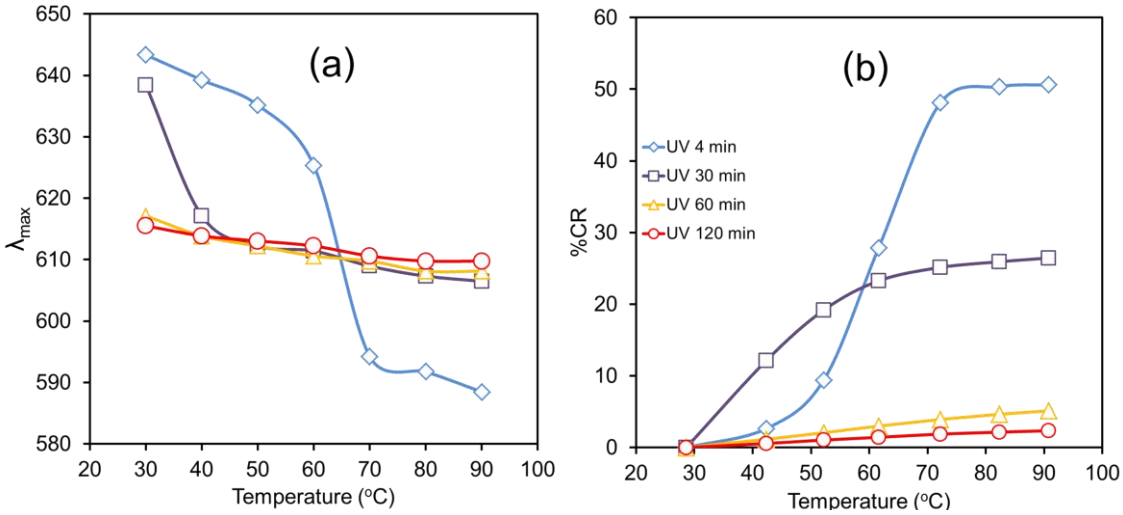

Fig. 5.32 The plots of colorimetric response (%CR) and λ_{max} of poly(TCDA)/ZnO nanocomposites prepared with various polymerization times

From the plot of %CR (Fig. 5.32b), it is clearly observed the lower values of %CR for the nanocomposites with longer UV irradiation time when temperature is in a range of 70-90 °C. For example, at 90 °C, %CR of the nanocomposite obtained by irradiating UV for 4 min is around 55% while the nanocomposite irradiated for 60 min exhibit %CR of 18%. This result demonstrates that, at high temperature region, poly(TCDA)/ZnO nanocomposite with longer UV irradiation time exhibits lower degree of color change than the nanocomposite prepared with shorter period of irradiation. It can be possibly believed that increasing UV irradiation time promotes the release of mechanical strain in the side chain of PDA. This causes the reduction of the planarity of π-orbital arrangement along the conjugated backbone. Therefore, poly(TCDA)/ZnO nanocomposite prepared with long UV irradiation is purplish blue and under less strain than the deep blue nanocomposite irradiated for short time (Fig. 5.33). When subjected

to heat, the release of strain upon thermal stimulation in nanocomposite irradiated for long time is less than in the one irradiated for short time. The segmental rearrangement is less occurred, resulting in the lower degree of color changing in the nanocomposites with long period of irradiation.

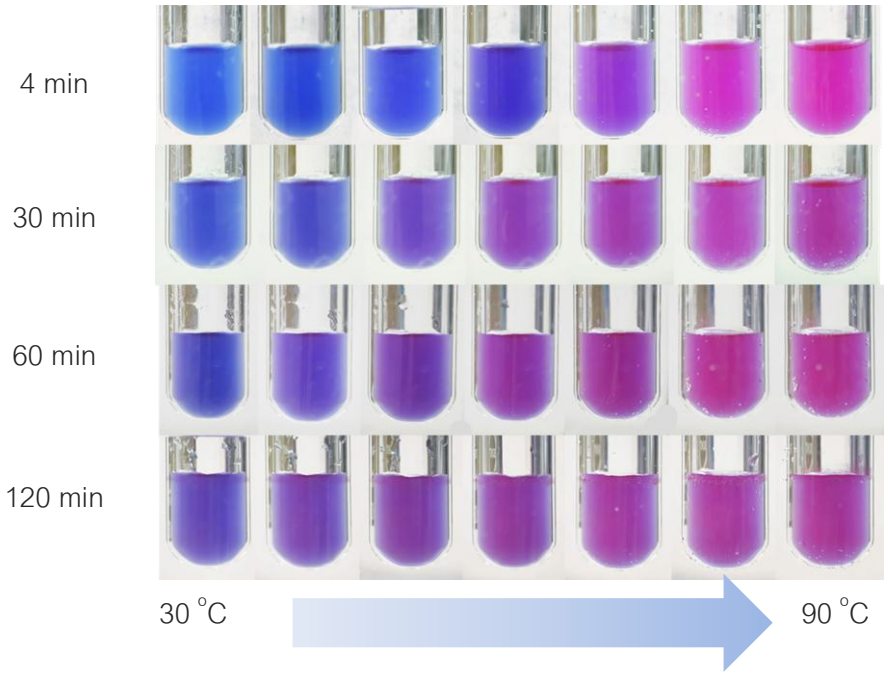

Fig. 5.33 Color photograph of poly(TCDA)/ZnO nanocomposites with various polymerization times upon increasing temperature.

The color photograph of poly(TCDA)/ZnO nanocomposite prepared with various polymerization times upon increasing temperature are illustrated in Fig. 5.33. It can be clearly seen that the increase of UV irradiation time causes the chromic transition of nanocomposite suspension to take place at lower temperature. For example, the nanocomposite suspension obtained by irradiating for 4 min is still in blue color at 50 °C while the color of the suspensions irradiated for longer time exhibits violet color. In addition, the degree of color changing in high temperature region of the nanocomposite with longer UV irradiation time is less than that of the nanocomposite obtained by shorter period of irradiation.

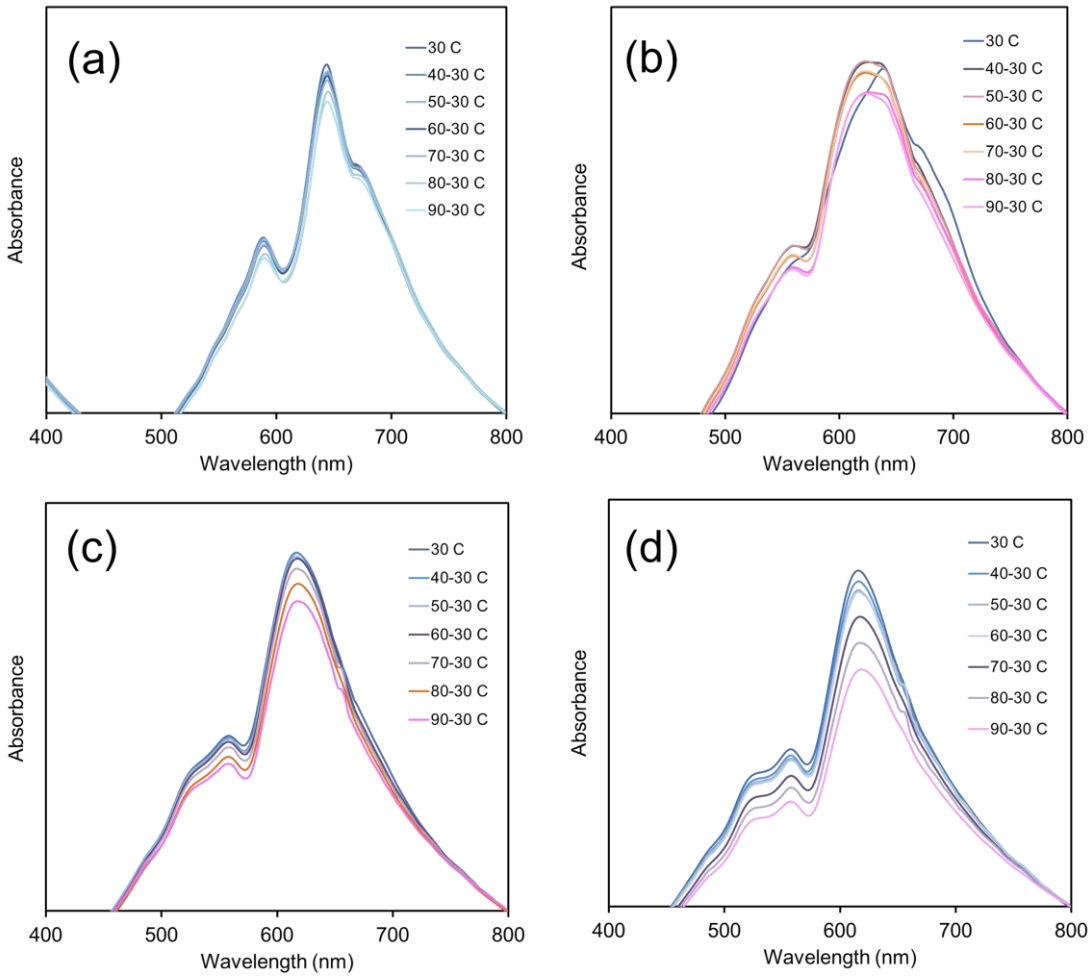

Fig. 5.34 Absorption spectra of poly(TCDA)/ZnO nanocomposites obtained by irradiating for (a) 4 min, (b) 30 min, (c) 60 min and (d) 120 min upon cooling from designate temperatures.

The colorimetric behaviors upon cooling to room temperature of poly(TCDA)/ZnO nanocomposite obtained by various polymerization times are investigated. Fig. 5.34 shows the absorption spectra when the suspensions are cooled from desired temperatures (e.g. 60-30 ^{o}C is the spectrum of the suspension cooled to 30 ^{o}C from 60 ^{o}C). It can be observed that the nanocomposite irradiated for 4 min exhibits complete thermochromic reversibility although the suspension is cooled from 90 ^{o}C (see Fig. 5.34a). In contrast, in the system of nanocomposite irradiated for 30 min, the color of the

suspension cannot completely return to the initial blue after cooling from 40 °C. This is due to the weakening of overall interactions in the nanocomposite upon increasing UV irradiation time. However, this color is stable over the next higher temperature as the spectra are in similar pattern after cooling to 30 °C (see Fig. 5.34b). In the system of the nanocomposite obtained by irradiating for 60 min and 120 min shown in Fig. 5.34c and d, the spectra after cooling to room temperature are similar to the initial spectrum, indicating the complete reversibility. The rationalization for this behavior is as follows. The nanocomposites irradiated for 60 and 120 min at the initial stage exhibit relatively weak overall interactions including the ionic interaction at the ZnO surface. Increasing temperature cause the segmental rearrangement of the polymer to occur only slightly. Therefore, the conformation can change back to the initial stage when cooling to room temperature.

Thermal stability of poly(TCDA)/ZnO nanocomposite derived from various polymerization times is also investigated. The aqueous suspensions are subjected to multiple heating/cooling cycles, switching between 30 and 90 °C. Poly(TCDA)/ZnO nanocomposite irradiating for 4 min exhibits completely color reversibility. Its purple color at elevated temperature fully reverses to the initial blue color upon cooling. The color reversibility can be repeated for more than 10 heating/cooling cycles as illustrated in the plot of %CR value (see Fig. 5.35a). In the case of poly(TCDA)/ZnO nanocomposite prepared with irradiation time of 30 min, the color does not return to the original one after the first heating/cooling cycle as the value of %CR is around 10% after cooling to room temperature. However, this color is stable over the next nine heating/cooling cycles as shown in Fig. 5.35b.

Thermal stability of poly(TCDA)/ZnO nanocomposite derived from irradiating for 60 min is shown in Fig. 5.35c. Although the attractive interactions within the nanocomposites are weaker, the complete thermochromic reversibility is clearly observed for more than 10 heating/cooling cycles.

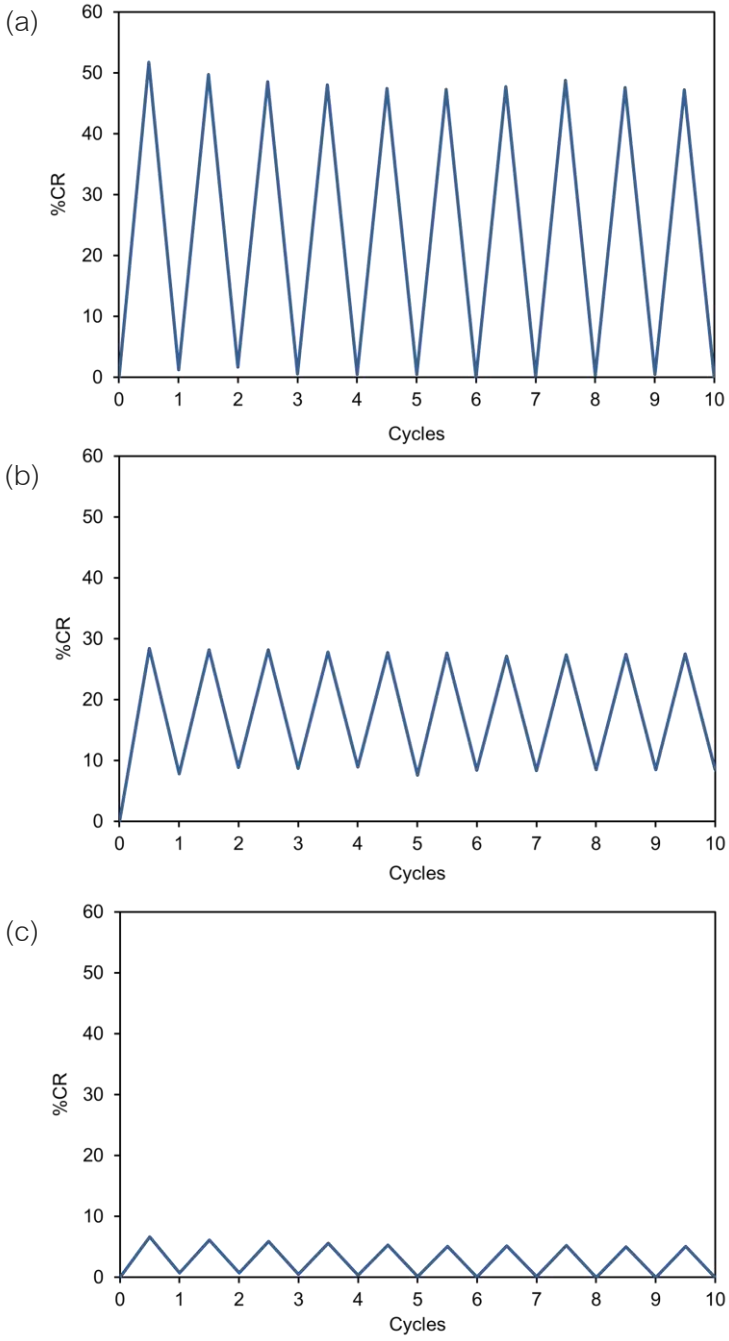

Fig. 5.35 Changes of %CR during 10 heating/cooling cycles, switching between 25 °C and 90 °C, of poly(TCDA)/ZnO nanocomposites prepared with various polymerization times; (a) 4 min, (b) 30 min and (c) 60 min

5.2.4.2. poly(HDDA)/ZnO nanocomposites

Absorption spectra of poly(HDDA)/ZnO nanocomposites obtained by different irradiation time ranging from 4min to 60 min upon heating are illustrated in Fig. 5.36. The results also exhibit in similar trend compared to the system of poly(TCDA)/ZnO nanocomposite. The color transition of the nanocomposite prepared with longer period of UV irradiation takes place at lower temperature compared to the shorter one. The spectra of the nanocomposite irradiated UV for 4 min displays a drastic change of λ_{max} when increasing temperature to around 50 ^{o}C and the color of the suspension changes to purple. The complete blue-purple transition takes place at about 60 ^{o}C. The drop of absorbance is due to the precipitation of the nanocomposite. In the system of the nanocomposite obtained by irradiating for 10 min, an abrupt change of absorption pattern is detected at around 40 ^{o}C and the suspension completely change to purple color at about 50 ^{o}C. For poly(HDDA)/ZnO nanocomposites irradiated for 30 min, the λ_{max} is at ~620 nm and there is a peak at around 650 nm, which completely disappear at ~40 ^{o}C. Further heating up to ~90^{o}C, the absorption pattern slightly changes and the λ_{max} is at 614 nm. In the case of poly(HDDA)/ZnO nanocomposite obtained by irradiating for 60 min, The spectra upon increasing temperature exhibit in a similar pattern. We cannot observe the abrupt change upon increasing temperature. The plots of %CR representing to the chromatic transition upon heating of poly(HDDA)/ZnO nanocomposites prepared with various irradiation time are summarized in Fig. 5.37a. It clearly reveals that the magnitude of color change upon heating significantly decreases with the increasing UV irradiation time.

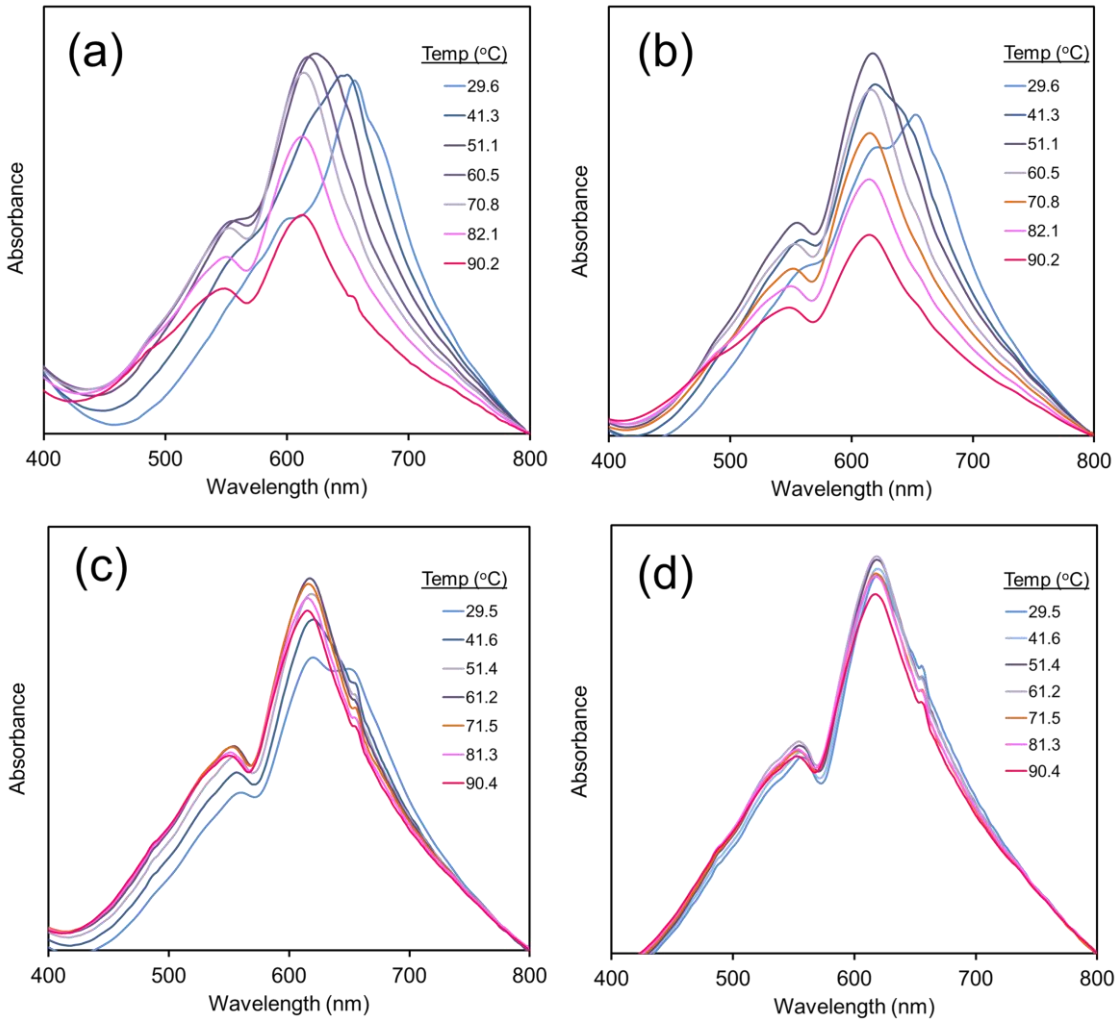

Fig. 5.36 Absorption spectra upon increasing temperature of poly(HDDA)/ZnO nanocomposites prepared with various UV irradiation times: (a) 4 min, (b) 10 min, (c) 30 min and (d) 60 min.

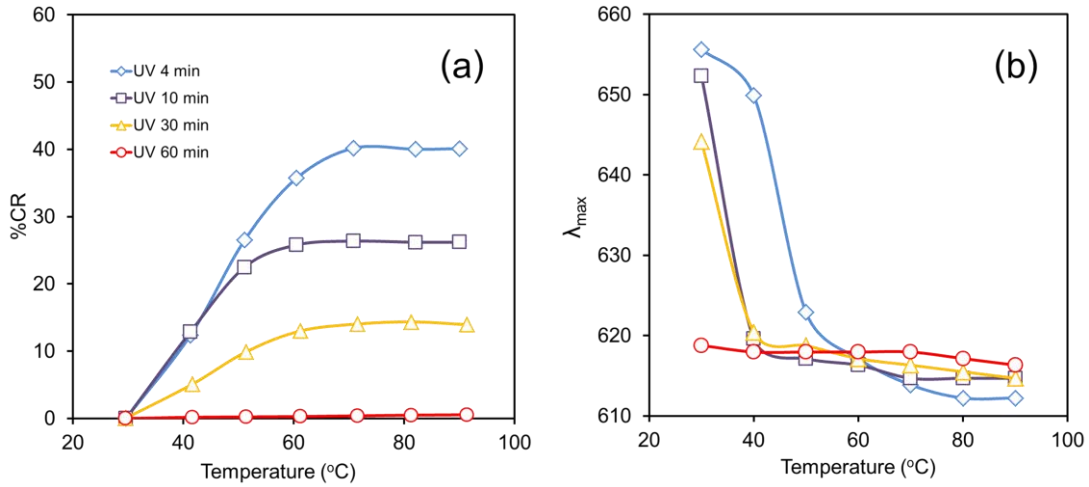

Fig. 5.37 (a) The plots of colorimetric response (%CR) and (b) λ_{max} upon increasing temperature of poly(HDDA)/ZnO nanocomposites prepared with various polymerization times

It can be observed from the plots of λ_{max} in Fig. 5.37b, upon increasing temperature, the drop of λ_{max} is significantly less for the nanocomposites irradiated with longer period. The decrease of λ_{max} in the system of poly(HDDA)/ZnO nanocomposite derived from irradiation time of 60 min is only around 2 nm when increasing the temperature to 90 °C. This result is also similar to the system of poly(TCDA)/ZnO nanocomposite presented in the previous section.

The color photograph at different temperatures of the aqueous suspensions of poly(HDDA)/ZnO nanocomposites derived from different polymerization times are illustrated in Fig. 5.38. The nanocomposites obtained by irradiating for less than 30 min are apparently show color transition. It can be clearly seen that the color transition of samples irradiated for longer period takes place at lower temperature. The nanocomposite suspension obtained by irradiating for 4 min changes to violet color at ~50 °C while this similar color is observed at 40 °C for nanocomposite irradiated for 10 min. The nanocomposite derived from irradiating for 30 min exhibits purplish-blue color at room temperature and change to reddish purple after heating to ~40 °C. On the other

hand, poly(HDDA)/ZnO nanocomposite obtained by irradiating for 60 min nearly exhibits color stability upon heating to 90 °C.

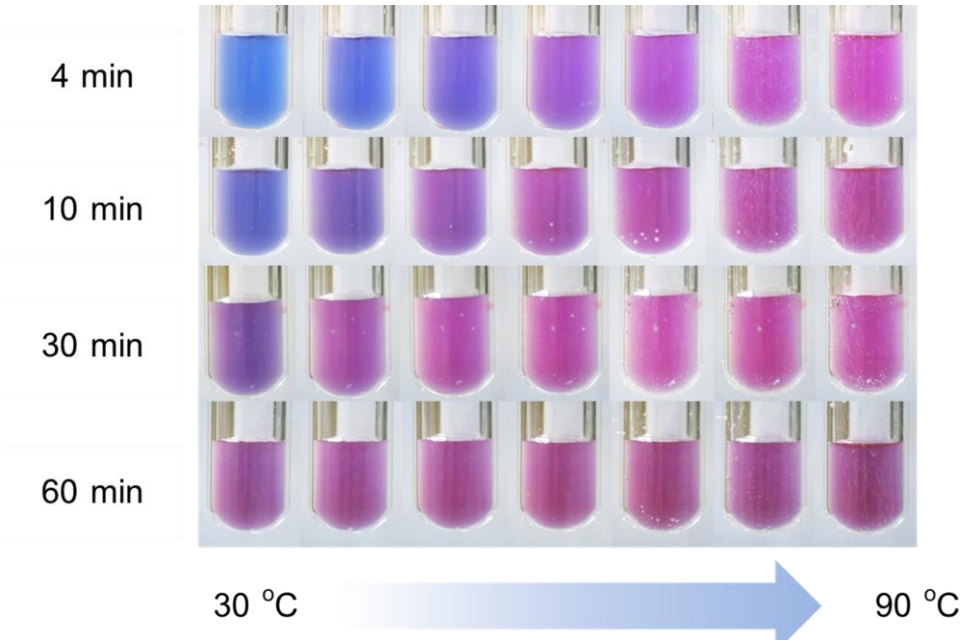

Fig. 5.38 Color photograph upon increasing temperature of poly(HDDA)/ZnO nanocomposites prepared with various polymerization times

The colorimetric behaviors upon cooling to room temperature of poly(HDDA)/ZnO nanocomposite obtained by various polymerization times are illustrated in Fig. 5.39. Poly(HDDA)/ZnO nanocomposite obtained by irradiating for 4 min can exhibit complete thermochromic reversibility when it is cooled from 70 °C to room temperature. However, the spectra after cooling from 80-90 °C show a peak around 540 nm, corresponding to the formation of a small fraction of red phase (see Fig. 5.39a). This result is also similar to poly(HDDA)/ZnO nanocomposite irradiated for 15s illustrated in previous chapter [topic 5.1.3.1.]. In the case of poly(HDDA)/ZnO nanocomposite obtained by irradiating for 10 min, the growth of a peak at about 540 nm is still observed when temperature is cooled from 90 °C. In contrast, poly(HDDA)/ZnO nanocomposite derived from irradiating for 30 min exhibit a nearly complete color reversibility. The spectrum of the suspension cooled from 90 °C to room temperature is similar to the spectrum of the initial phase as

illustrated in Fig. 5.39c. Moreover, the growth of red-phase peak is not observed. The rationalization for this behavior is also similar to the system of poly(TCDA)/ZnO nanocomposite explained in the previous section. The spectra of the nanocomposite obtained by irradiating for 60 min are shown in Fig. 5.39d. It can be observed that the spectra of suspension cooled to room temperature exhibit similar patterns compared to the original suspension. However, it is noted here that the color transition of this nanocomposite is hardly observed when temperature increases.

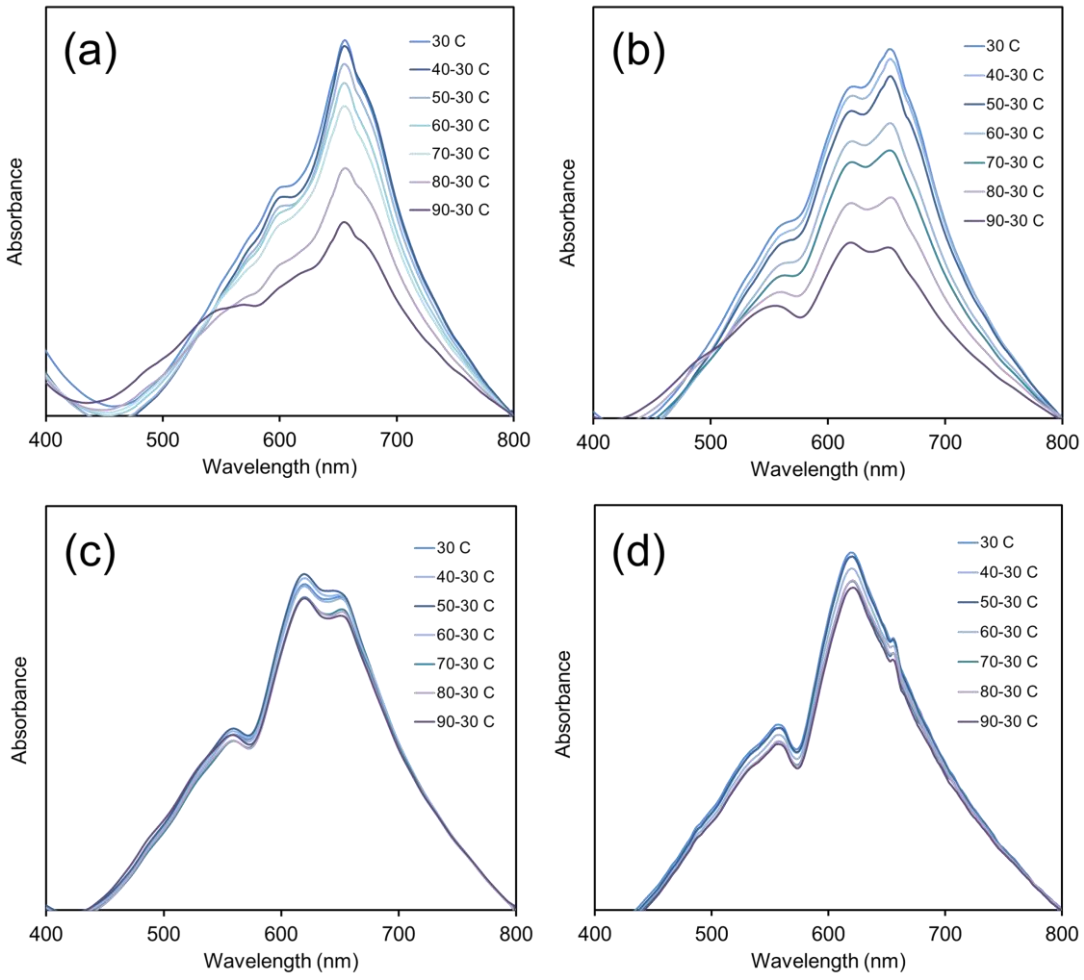

Fig. 5.39 Absorption spectra measured upon cooling from designate temperature of poly(HDDA)/ZnO nanocomposites with various polymerization times: (a) 4 min, (b) 10 min, (c) 30 min and (d) 60 min

Thermal stability of poly(HDDA)/ZnO nanocomposite obtained by irradiating UV for 4, 10 and 30 min is illustrated in Fig. 5.40a, b and c, respectively. Poly(HDDA)/ZnO nanocomposite obtained by irradiating for 4 and 10 min cannot exhibit completely color reversibility after the first heating/cooling cycle. The value of %CR after cooling to room temperature is around 8% and 4% for the nanocomposites irradiated for 4 and 10 min, respectively. However, these colors of the 1^{st} cycle are stable over the next nine heating/cooling cycles. This result is quite similar to poly(HDDA)/ZnO nanocomposites obtained by irradiating for 15s shown in topic 5.1.3.1. In the system of poly(HDDA)/ZnO nanocomposite derived from irradiating for 30 min, the plots of %CR of heating/cooling nearly exhibit complete color reversibility which can be repeated for more than 10 heating/cooling cycles. The purple color of this nanocomposite at ~90 ^{o}C nearly reverses to the initial color after cooling to room temperature. The slight increase of %CR of cooling (~2%) possibly takes place from the slight difference in cooling temperature.

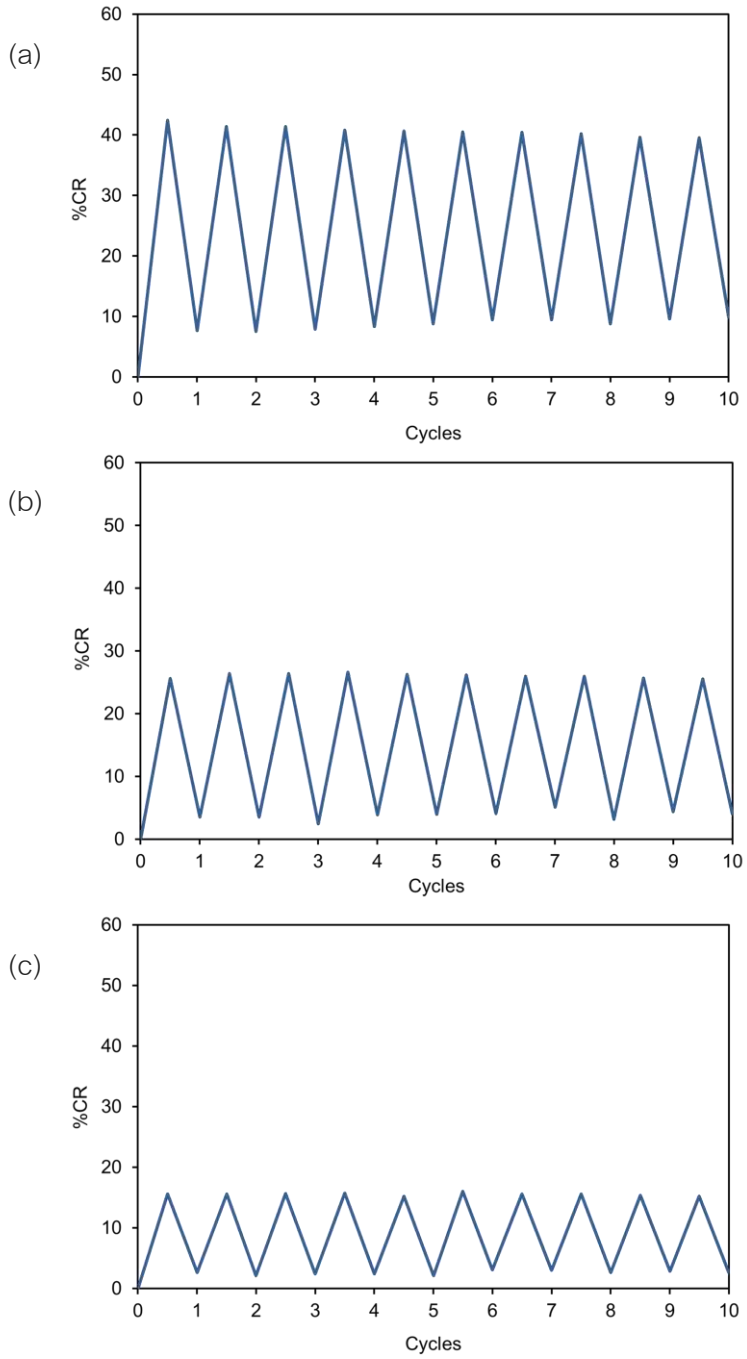

Fig. 5.40 Change of CR during 10 heating/cooling cycles switching between 25 °C and 90 °C of poly(HDDA)/ZnO nanocomposites prepared with various polymerization times; (a) 4 min, (b) 10 min and (c) 30 min

5.2.5. Colorimetric response to pH

Absorption spectra of poly(TCDA)/ZnO nanocomposites prepared with various polymerization time measured upon the decrease of pH are illustrated in Fig. 5.41. It can be observed that the addition of H^+ ions significantly affects the color of the nanocomposite suspensions. In the system of poly(TCDA)/ZnO nanocomposites irradiated for 1-10 min, a new peak at 550 nm is detected when pH is decreased to around 3.5 and the peak continuously grows upon further adding H^+ ions. The complete blue-red transition is observed at pH ~0.5. In contrast, the complete color transition is not observed in the system of nanocomposites obtained by irradiating UV for longer than 10 min. Large fraction of the blue phase (λ~640 nm) is still remain although pH is decreased to 0.5. From the plot of %CR shown in Fig. 5.43a, it can be observed that the degree of color transition upon decreasing pH is lower for the nanocomposites irradiated with longer period. The magnitude of color change significantly decreases when irradiation time increases (e.g. when the pH is decreased to ~1, %CR of the nanocomposite irradiated for 1 min is 67% while the nanocomposite irradiated for 120 min is only 23 %.). The result suggests that the nanocomposite subjected to long polymerization time slightly change conformation of the conjugated backbone when response to stimuli.

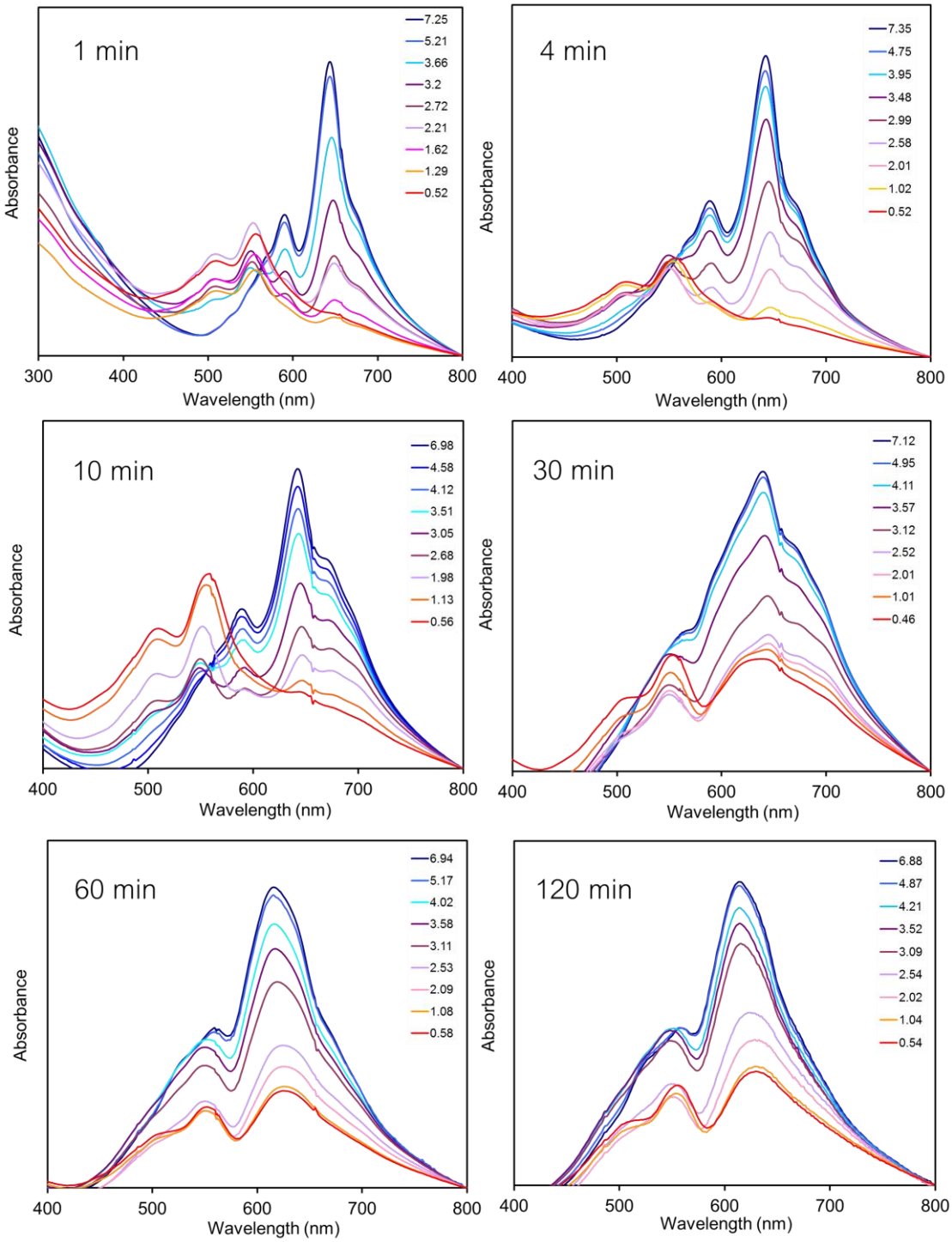

Fig. 5.41 Absorption spectra upon decreasing pH of poly(TCDA)/ZnO nanocomposites prepared with various polymerization times

Absorption spectra upon increasing pH of poly(TCDA)/ZnO nanocomposite suspensions derived from different UV irradiation times are exhibited in Fig 5.42. It can be observed that the absorption patterns of all nanocomposites after adjusting pH from 7 to 12 are not different. At pH~13, the minor peak at ~546 nm is observed, corresponding to the formation of the red phase. The plots of %CR shown in Fig 5.43b indicate that the color transition of all nanocomposites does not take place at pH lower than 12. The %CR value of the nanocomposites irradiated for 1 to 30 min slightly increases at pH~12.5, while the value of %CR of the nanocomposite irradiated for 60 and 120 min slightly increases at pH~13. Further increasing pH to higher than 13, a peak at 546 nm continuously grows but a large fraction of their initial phase is still observed. At this condition, the color of the suspensions changes to purple.

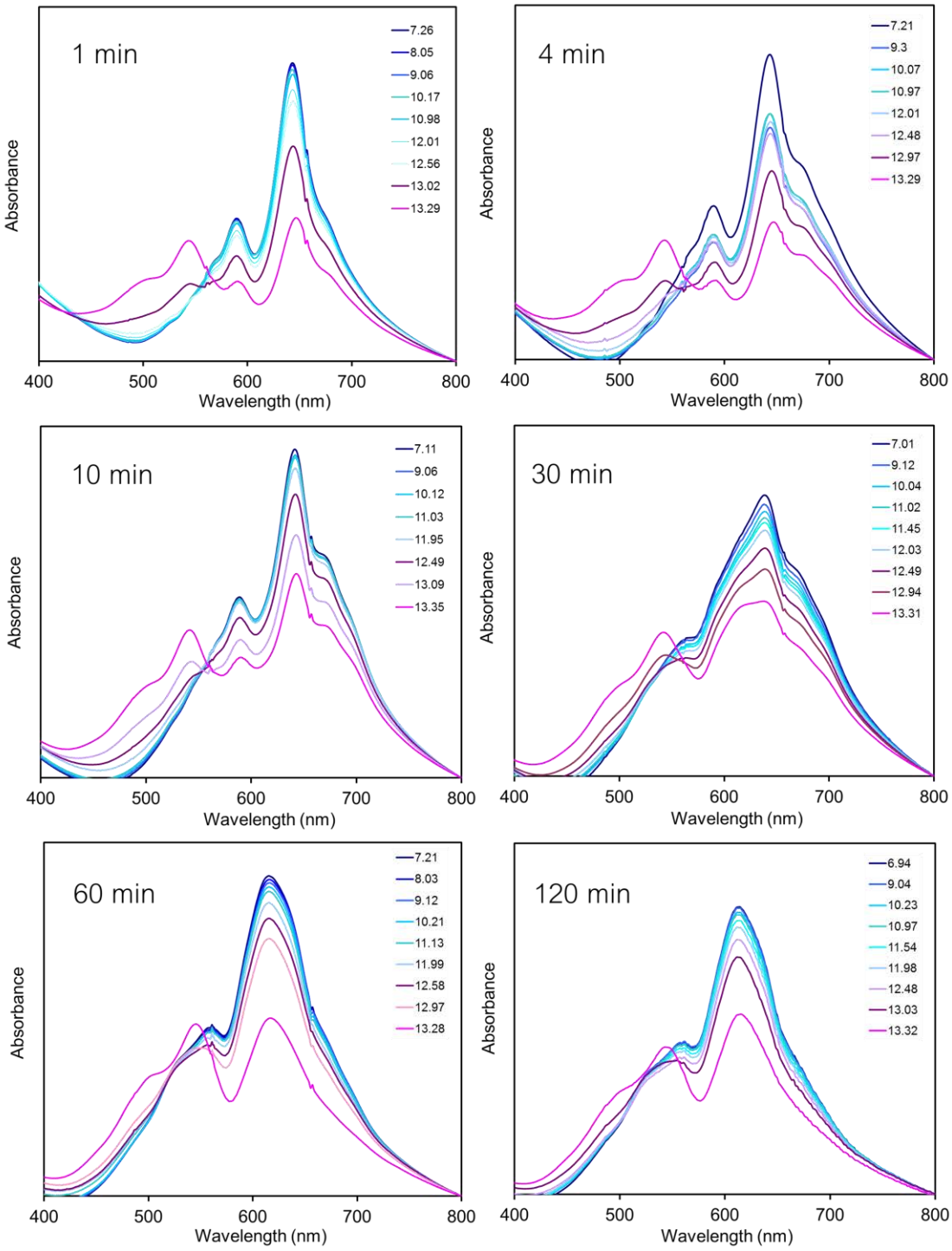

Fig. 5.42 Absorption spectra upon increasing pH of poly(TCDA)/ZnO nanocomposites prepared with various polymerization times

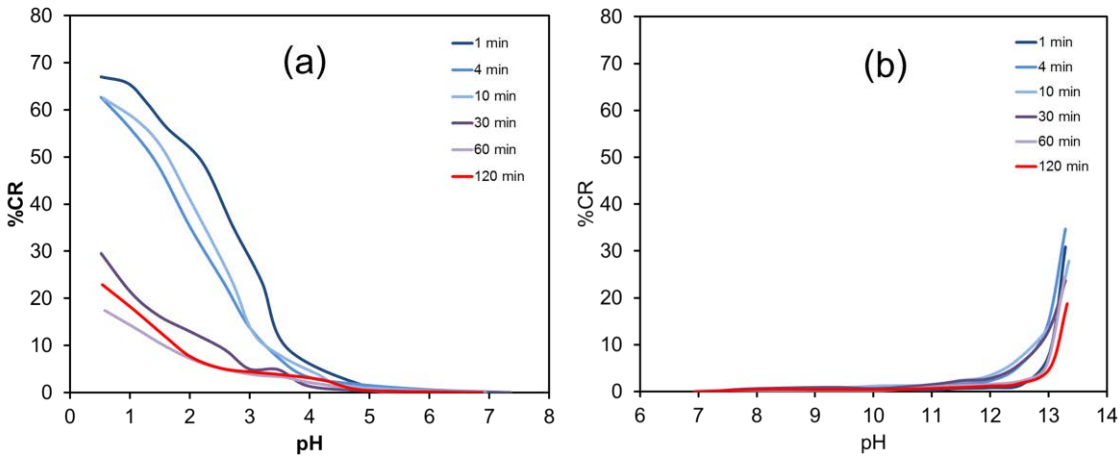

Fig. 5.43 Colorimetric response of poly(TCDA)/ZnO nanocomposites prepared with various polymerization times upon variation of pH; (a) in acidic and (b) basic condition

Absorption spectra upon the decrease pH of poly(HDDA)/ZnO nanocomposites obtained by various polymerization times measured are illustrated in Fig. 5.44. The color transition upon addition of H^+ ions is clearly observed in all nanocomposites. A new peak at 550 nm is detected when pH is decreased to around 5 and the peak continuously grows upon further adding H^+ ions. The spectra of poly(HDDA)/ZnO nanocomposites irradiated for 1-10 min completely exhibit the blue-red transition at pH ~3.5. In the case of poly(HDDA)/ZnO nanocomposites obtained by longer period of irradiation (30-60 min), the complete blue-red transition is not observed although the pH is decreased to ~1. A peak with λ_{max} ~612 nm is still detected, corresponding to the fraction of their initial phase. The plot of colorimetric response as a function of pH illustrated in Fig. 5.46a shows that the color transition is firstly observed at pH ~5 in these nanocomposites. However, similar to the system of poly(TCDA)/ZnO nanocomposites, the magnitude of color change upon decreasing pH is reduced for the nanocomposites obtained by longer period of irradiation. For example, the %CR value of the nanocomposite irradiated for 4 min is around 65% at pH 3.5 while the nanocomposite obtained by irradiating for 60 min is only 24 %.

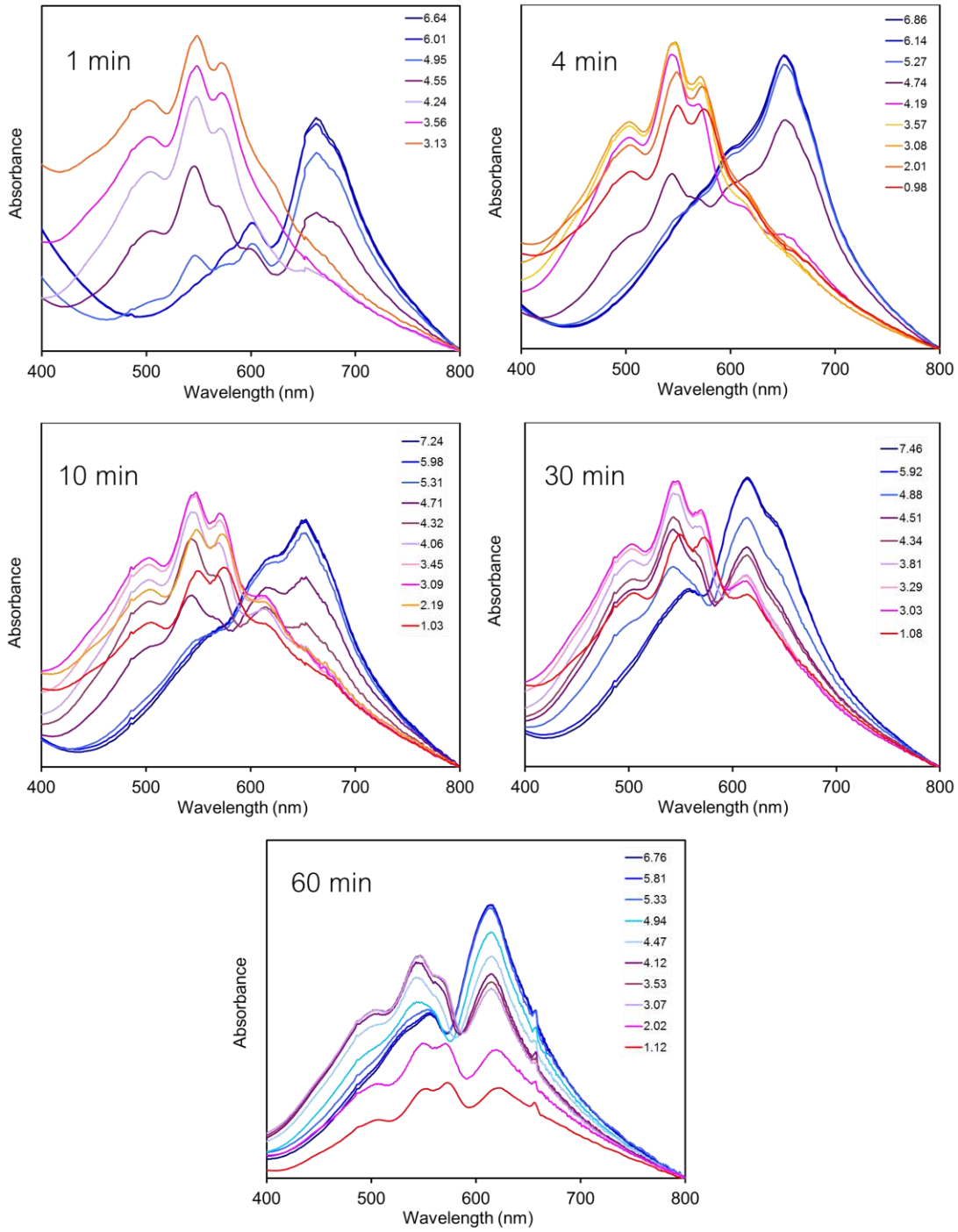

Fig. 5.44 Absorption spectra upon decreasing pH of poly(HDDA)/ZnO nanocomposites prepared with various polymerization times

Fig. 5.45 shows the absorption spectra upon increasing pH of poly(HDDA)/ZnO nanocomposite suspensions with different polymerization times. The blue-red transition upon adding OH^- ions is clearly observed in all nanocomposites. A small peak at around 546 nm is detected at pH ~11 and the peak continuously grows upon further increasing pH while the absorbance of the initial phase continuously drops. Poly(HDDA)/ZnO nanocomposite with polymerization time of 1 min can exhibit complete blue-red transition when the pH is increased to more than 13. For the nanocomposites derived from longer period of irradiation, the complete red phase is not observed although the pH is increased more than 13. The small peak at around 612 nm is still observed, indicating to the fraction of the initial phase. The plots of %CR shown in Fig. 5.46b indicate that the color transition of all nanocomposites takes place at pH ~11. The magnitude of color change is decreased when the nanocomposite is prepared by longer period of irradiation. Poly(HDDA)/ZnO nanocomposites obtained by irradiating for 1 min exhibit complete blue-red transition at pH ~13 with the %CR value of around 70% whereas the %CR value of the nanocomposite irradiated for 60 min is only 30%.

The rationalization for this behavior can be explained as follows. The increase UV irradiation time causes the increase of length of the conjugated backbone. Since the monomers assemble into vesicles around the ZnO nanoparticle, the increase in length of the conjugated backbone may cause an increase in distance between head groups. When OH- ions are added to produce the repulsive force between negative carboxylate head groups, this force only slightly affects the conformation of the side chains, and thus, that of the conjugated backbone. Therefore, the degree of color changing in the nanocomposite irradiated for longer time is less.

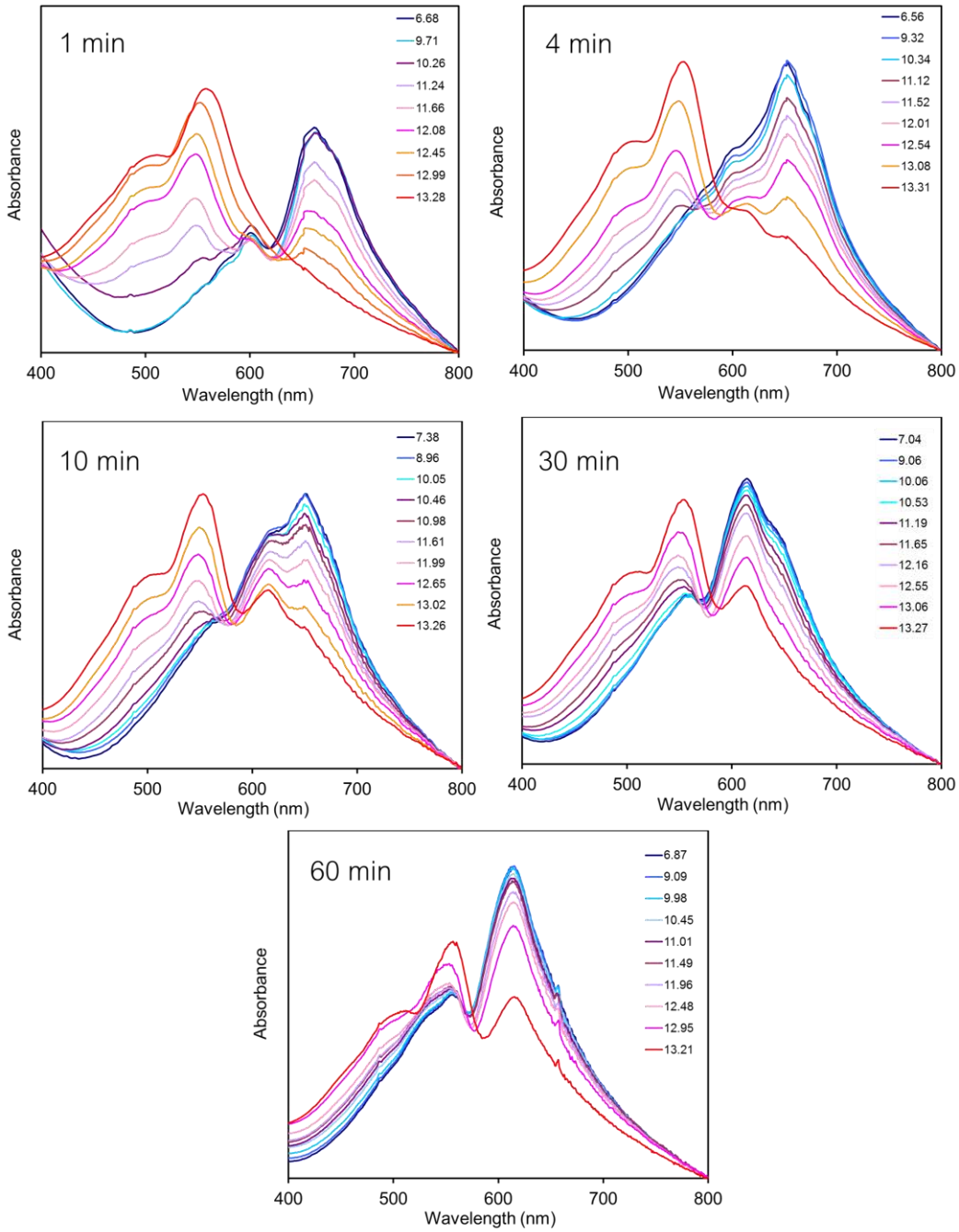

Fig. 5.45 Absorption spectra upon increasing pH of poly(HDDA)/ZnO nanocomposites obtained by various polymerization times

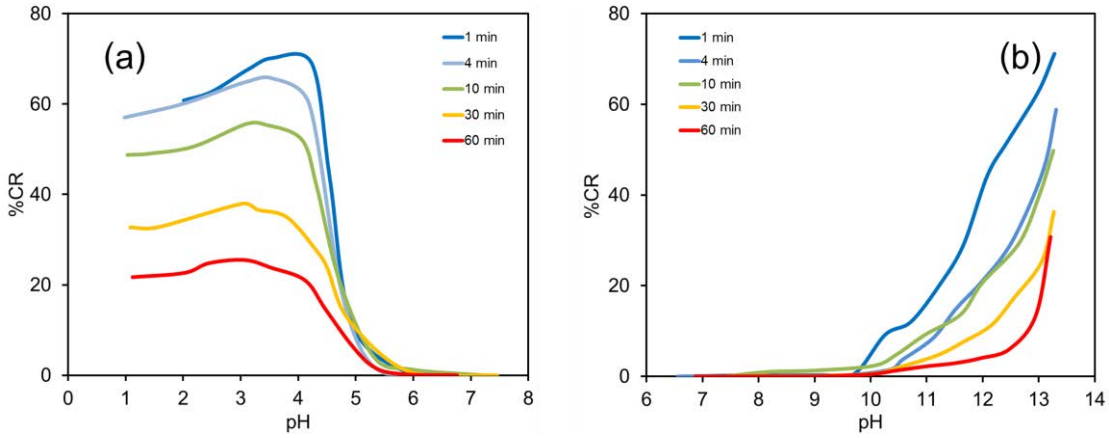

Fig. 5.46 The plots of colorimetric response upon variation of pH of poly(HDDA)/ZnO nanocomposites prepared with various polymerization times

The color photograph upon variation of pH of poly(HDDA)/ZnO nanocomposites obtained by various polymerization times are illustrated in Fig.5.47. The chromatic transition upon variation of pH is apparently observed. It can be seen that the color transition of samples irradiated for 4 min is clearly observed in both acidic and basic condition. The sample exhibits red color after decreasing pH to 3 or increasing pH to 13. In the case of the nanocomposites obtained by longer period of irradiation, the color transition is observed at the same pH but the magnitude of color change decreases significantly, e.g. the nanocomposite obtained by irradiating for 10 min exhibit only purplish-red color at pH ~3. In the system of poly(HDDA)/ZnO nanocomposite obtained by irradiating for 60 min, it can be observed only slight chromatic transition although the pH is decreased to ~1 or increased to higher than 13.

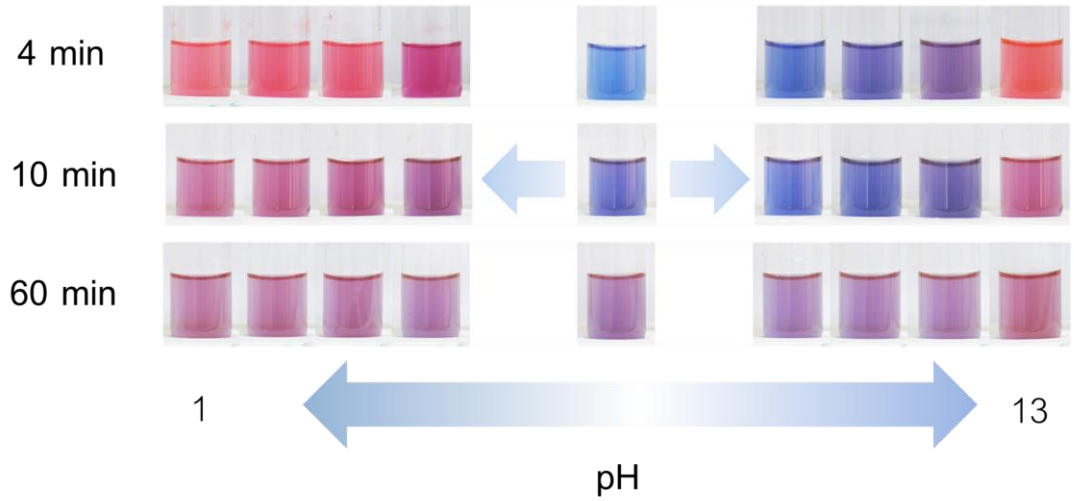

Fig. 5.47 Color photograph upon variation of pH of poly(HDDA)/ZnO nanocomposites prepared with various polymerization times

5.2.6. Colorimetric response to alcohols

The increase of polymerization time results in the decrease of overall interaction in the nanocomposites, which could affect the colorimetric behaviors upon addition of alcohols. From the previous result [see topic 5.1.6.], the addition of ethanol does not induce color transition in the system of poly(TCDA)/ZnO nanocomposite derived from irradiating for 1 min. In this study, we investigate the response to ethanol of poly(TCDA)/ZnO nanocomposite obtained from longer period of irradiation as shown in Fig. 5.48. We found that the color transition is still not observed. The spectra upon increasing ethanol concentration of poly(TCDA)/ZnO nanocomposites obtained by irradiating for 4 min and 60 min exhibit similar patterns compared to their initial phase. The color of the suspension is similar to the original although the concentration of ethanol is around 76.2 vol%. The systematic decrease of absorbance is due to the dilution by ethanol. From the plots of %CR shown in Fig. 5.48c, the value of %CR of poly(TCDA)/ZnO nanocomposite irradiated for 4 min slightly increases to about 10% when the concentration of ethanol is increased to 76%. However, it is difficult to observe the color change of the suspension. In the case of poly(TCDA)/ZnO nanocomposite

irradiated for 60 min, the value of %CR is nearly unchanged at ethanol concentration of 76 vol%.

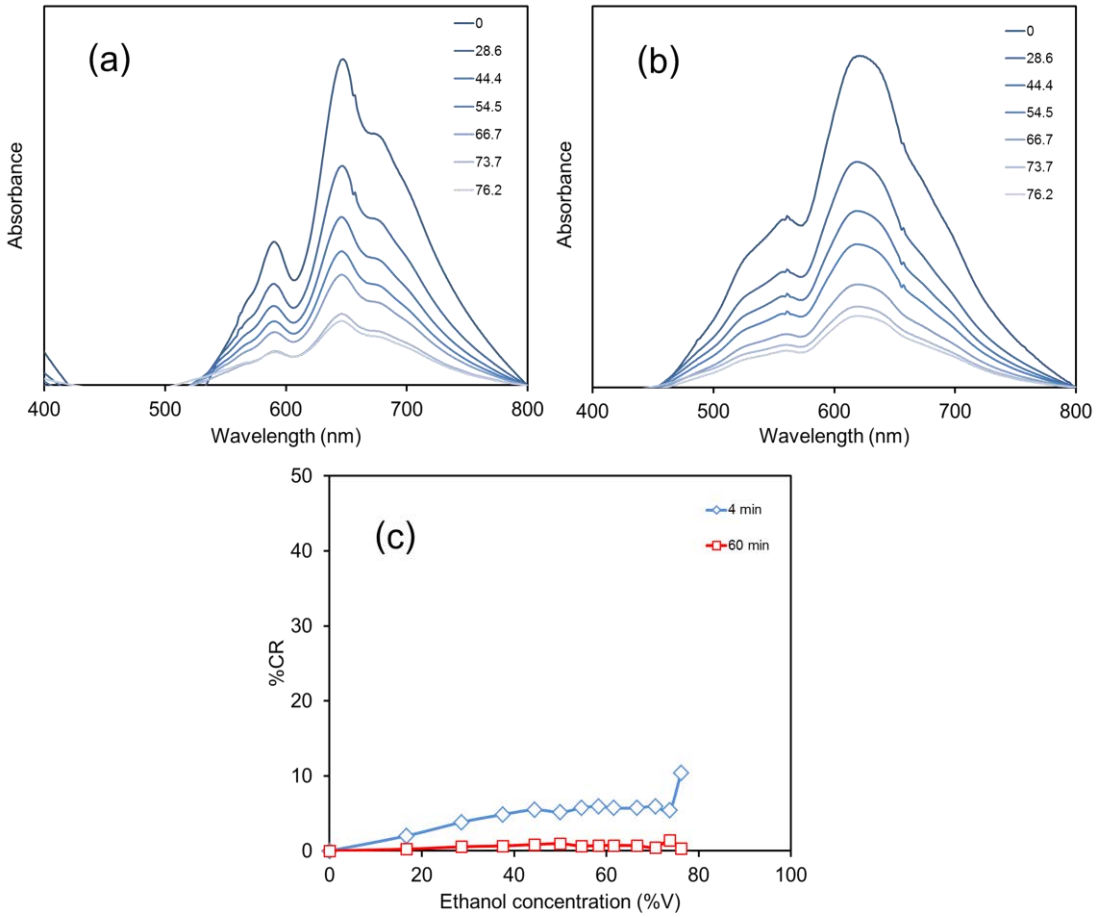

Fig. 5.48 Absorption spectra upon addition of ethanol of poly(TCDA)/ZnO nanocomposites obtained by irradiating for (a) 4 min and (b) 60 min, (c) the plots of %CR as a function of ethanol concentration

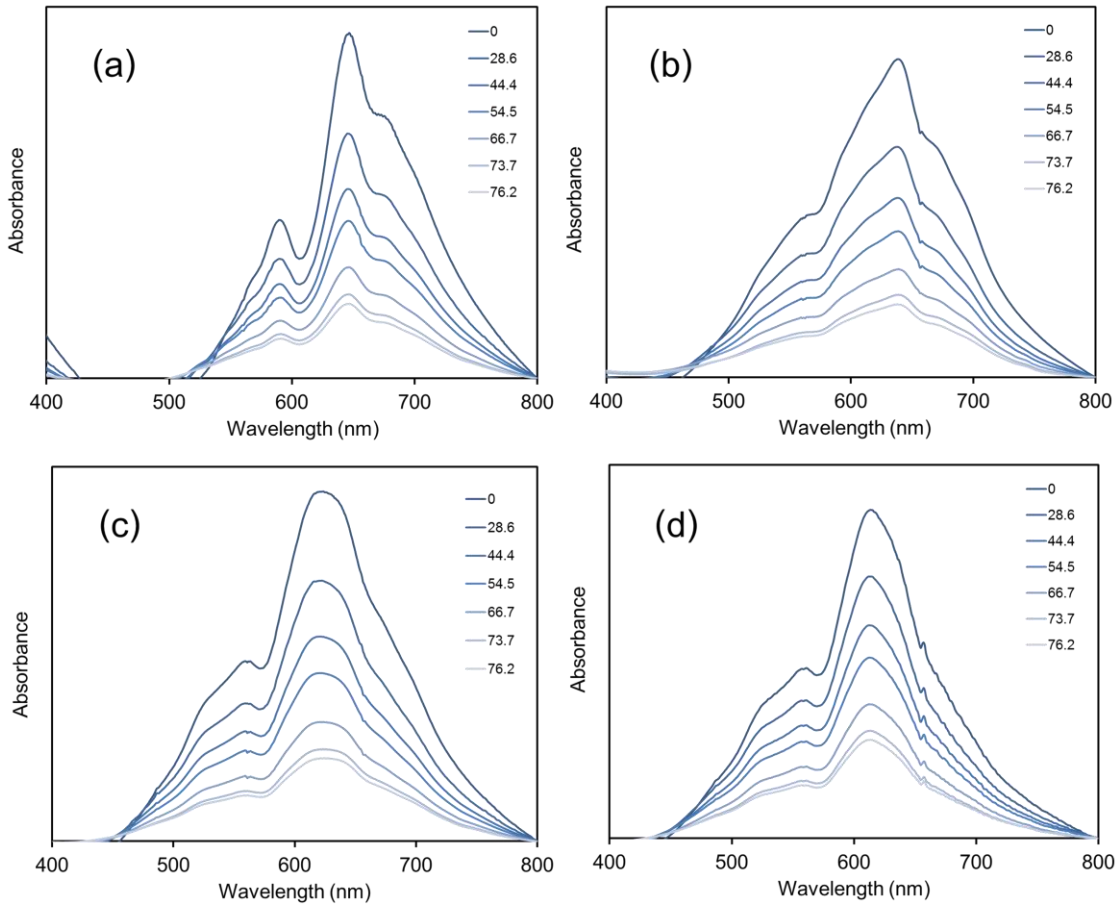

Fig. 5.49 Absorption spectra of poly(TCDA)/ZnO nanocomposites obtained by irradiating for (a) 4 min, (b) 30 min, (c) 60 min and (d) 120 min upon addition of 2-propanol

In addition, we also study the effect of 2-propanol on the colorimetric behaviors of poly(TCDA)/ZnO nanocomposites derived from various polymerization times. The addition of 2-propanol causes higher color transition in the polydiacetylene system as demonstrated in previous chapter. The absorption spectra upon addition of 2-propanol of the nanocomposites irradiated for various times are illustrated in Fig. 5.49. It is still found that the addition of 2-propanol into aqueous suspensions of poly(TCDA)/ZnO nanocomposites hardly affects their absorption spectra. The spectra of all nanocomposites exhibit similar patterns compared to their initial phase. The plots of %CR shown in Fig. 5.50 exhibit slight increase of %CR value to around 10% at 76 vol% 2-propanol in the case of poly(TCDA)/ZnO nanocomposite irradiated for 4 min. However, the observed color of the suspension of this nanocomposite is still light blue. For

poly(TCDA)/ZnO nanocomposites obtained by irradiating for 30, 60 and 120 min, the value of %CR at 76 vol% of 2-propanol is around 5%, 3% and 1%, respectively, indicating high color stability upon exposure to 2-propanol.

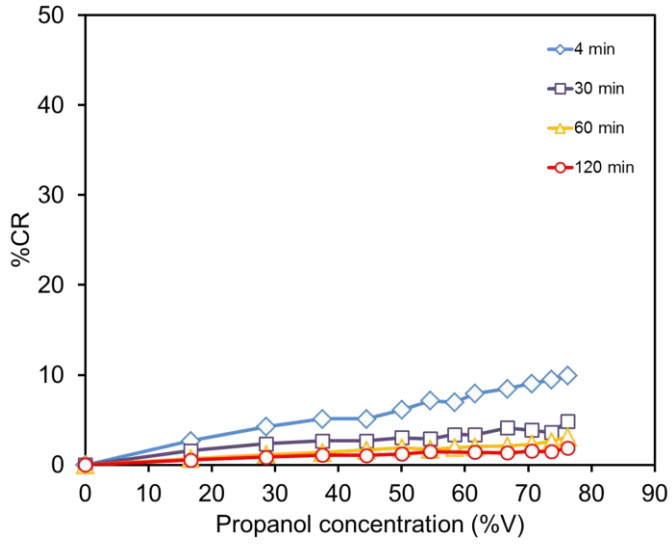

Fig. 5.50 The plots of colorimetric response upon addition of 2-propanol of poly(TCDA)/ZnO nanocomposites with various polymerization times

For poly(HDDA)/ZnO nanocomposite, blue-red transition upon addition of alcohols is clearly observed [see topic 5.1.6.]. Therefore, effects of variation in polymerization time are further investigated. Absorption spectra upon addition of 2-propanol of poly(HDDA)/ZnO nanocomposites obtained by various polymerization times are illustrated in Fig. 5.51. The spectra of poly(HDDA)/ZnO nanocomposite obtained by irradiating for 4 min clearly exhibit the decrease of λ_{max} to ~550 nm at 30 vol% 2-propanol and this peak continuously grows with further addition of 2-propanol. The color of the suspension completely changes to red at ~76 vol% 2-propanol. In the case of poly(HDDA)/ZnO nanocomposite derived from irradiating for 10 min, the spectrum of the initial phase constitutes of three peaks at around 650 nm, 618 nm and 556 nm (see Fig. 5.51b). The addition of 2-propanol causes the drop of a peak at ~650 nm while a peak at 556 nm continuously grows. When the concentration of 2-propanol is up to 76 vol%, the peak at 650 nm is completely disappeared. A peak at 618 nm however, still remains

as in the initial condition. The spectra pattern upon addition of 2-propanol of poly(HDDA)/ZnO nanocomposite obtained by irradiating for 30 min exhibit in similar trend. A peak at around 650 nm continuously drops until it is disappeared when the concentration of 2-propanol is increased to 74 vol%. In the system of poly(HDDA)/ZnO nanocomposites obtained by very long period of irradiation (60 min), the initial phase shows the shift of λ_{max} to ~618 nm. Upon addition of 2-propanol, the color transition is slightly observed.

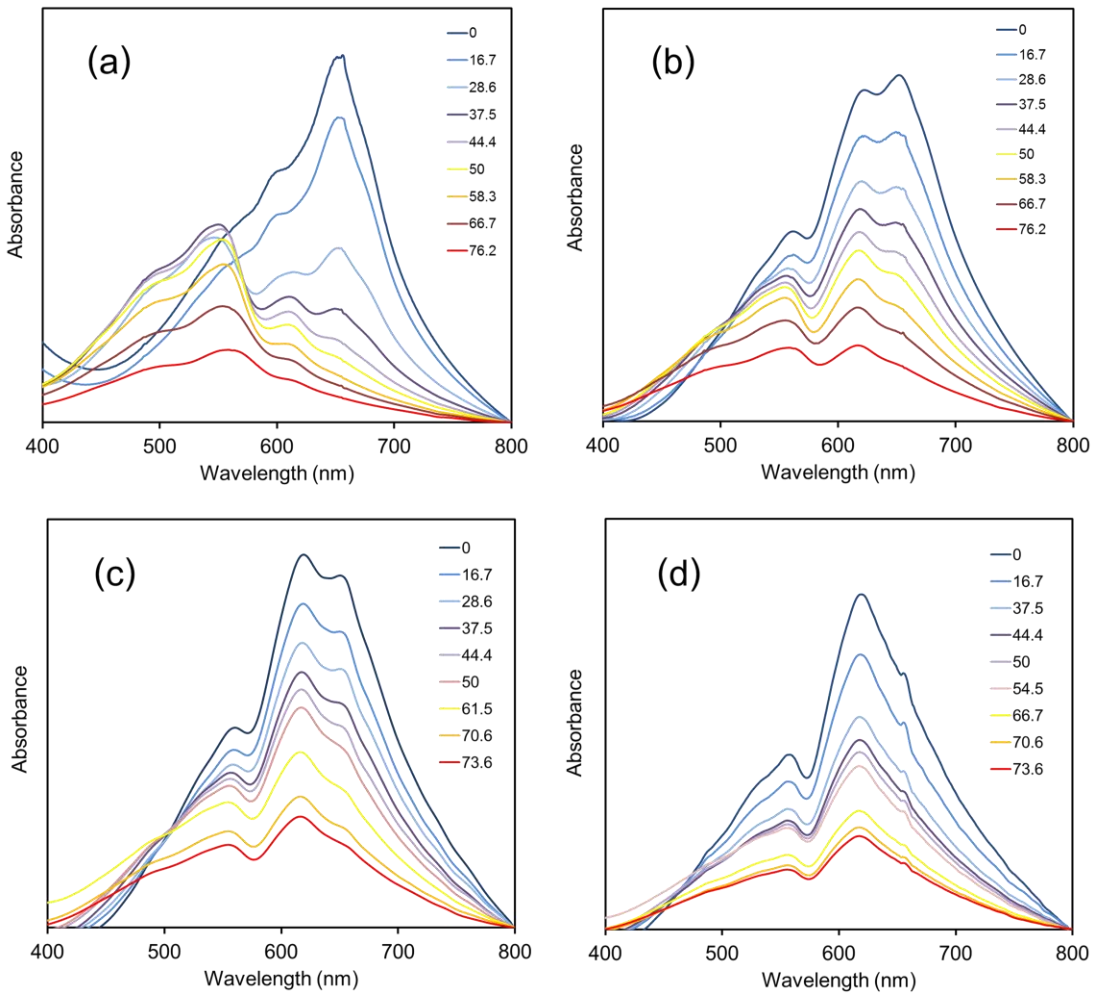

Fig. 5.51 Absorption spectra upon addition of 2-propanol of poly(HDDA)/ZnO nanocomposites obtained by irradiating for (a) 4 min, (b) 10 min, (c) 30 min and (d) 60 min

The plots of %CR as a function of 2-propanol concentration are illustrated in Fig 5.52. The color transition can be clearly observed in poly(HDDA)/ZnO nanocomposite irradiated for 4 min, in which the value of %CR increases to about 65% at 76 vol%. With increasing polymerization time, the magnitude of color change of the nanocomposites decrease significantly. The %CR value of poly(HDDA)/ZnO nanocomposite derived from 60 min irradiation is only 8% at 76 vol% 2-propanol, corresponding to a slight chromatic transition in this nanocomposite.

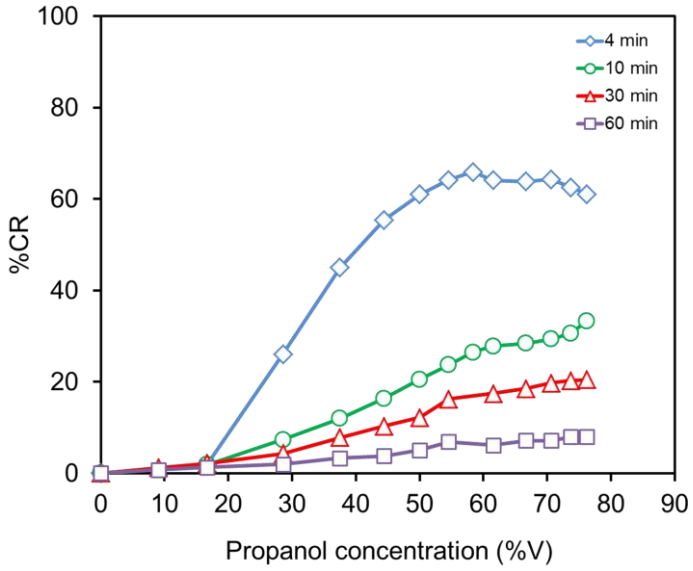

Fig. 5.52 The plots of colorimetric response of poly(HDDA)/ZnO nanocomposites obtained by different polymerization times upon addition of 2-propanol

In this part, we demonstrate that the polymerization time can affect the colorimetric behaviors of PDA/ZnO nanocomposite upon exposure to external stimuli. The color transition of nanocomposites irradiated for longer period of irradiation takes place at lower temperature compared to that of the nanocomposite with shorter irradiation time. This is due to the weakening of the overall interactions in the nanocomposites upon UV irradiation. Poly(TCDA)/ZnO nanocomposite derived from irradiating for 4 min can exhibits complete thermochromic reversibility while the reversibility decreases in nanocomposites polymerized for 30 min. However, the complete color reversibility can be observed in poly(TCDA)/ZnO nanocomposite irradiated for 60 min. In the system of

poly(HDDA)/ZnO nanocomposites, the nearly complete thermochromic reversibility is observed in the nanocomposite polymerized for 30 min. The complete reversibility detected in the nanocomposites with relatively long UV irradiation could be due to the slight change in the molecular orientation upon increasing temperature. The strong ionic interactions can then induce the conformation to return to their initial stage when cooling to room temperature.

Poly(TCDA)/ZnO nanocomposite derived from short period of irradiation can exhibit a complete blue-red transition in acidic condition, which cannot be observed in the nanocomposite obtained by long period of irradiation. In high pH region of all poly(TCDA)/ZnO nanocomposites obtained by different irradiation times exhibit similar color transition at pH higher than 13. For poly(HDDA)/ZnO nanocomposite, the color transition occurs in both acidic and basic condition. The increase of polymerization time causes the decrease of the magnitude of color changing upon variation of pH.

In the case of colorimetric response to alcohols, all poly(TCDA)/ZnO nanocomposites prepared from different UV irradiation times exhibit color stability upon exposure to ethanol or 2-propanol. In poly(HDDA)/ZnO nanocomposite system, the complete blue-red color transition is observed in the nanocomposite irradiated for short period upon exposure to ethanol or 2-propanol. The increase of polymerization time causes the decrease of the magnitude of color changing upon addition of 2-propanol. It can be observed that poly(HDDA)/ZnO nanocomposite derived from irradiating for 60 min nearly exhibits color stability upon exposure to 2-propanol.

5.3. Effect of types of nanoparticles on colorimetric behaviors of PDA/inorganic oxide nanocomposites

In this study, we investigated the effects of types of nanoparticles on colorimetric response to external stimuli of PDA/inorganic oxide nanocomposites. Inorganic oxide nanoparticles selected for this work exhibit different surface property when they are dispersed in water. Therefore, the difference of interfacial interactions between the head groups of diacetylene monomer and nanoparticles of various types is expected, which, in turn, alters dynamics of the side chains upon subjecting to external stimuli. Table 5.1 shows theoretical isoelectric point (IEP) of metal compound.

Table 5.1 Common isoelectric point (IEP) for super clean surfaces of inorganic oxides[73]

Compound	pH at IEP
SiO_2	2
TiO_2	6
Al_2O_3	9
ZnO	10
CaO	-
MgO	12

Zeta potential values of all inorganic oxide nanoparticles dispersed in deionized water are measured without adjusting pH. The value of zeta potential of all nanoparticles and pH of the suspensions are summarized in table 5.2

Table 5.2 Zeta potentials and pH of the nanoparticle in aqueous suspension

Compound	pH	Zeta potential (mV)
ZnO	7.84	18.29
SiO_2	6.21	-34.16
TiO_2	7.87	-20.71
Al_2O_3	6.87	27.39
CaO	11.41	14.30
MgO	10.61	11.34

5.3.1. Optical properties and interfacial interactions

The method for preparing nanocomposites with other types of inorganic oxide nanoparticles is similar to the preparation of PDA/ZnO nanocomposites. After polymerization by irradiating with UV light, the absorption spectra of the suspensions are illustrated in Fig. 5.53. In the system of poly(PCDA)/SiO_2, poly(PCDA)/TiO_2 and poly(PCDA)/Al_2O_3 nanocomposites, the suspensions exhibit deep blue color with λ_{max} of 637.22 nm, 639.66 nm and 640.48 nm, respectively and vibronic shoulder at ~580 nm, which are not significantly different from the spectrum of poly(PCDA)/ZnO nanocomposite (λ_{max} ~642 nm). However, it cannot be observed peak at ~675 nm in these nanocomposites. In contrast, the suspensions of nanocomposites prepared from CaO and MgO nanoparticles are purple after UV irradiation and agglomerates occur. The spectrum of poly(PCDA)/MgO nanocomposite shows the λ_{max} at ~630 nm with vibronic shoulder at 580 nm. In addition a peak at ~ 540 nm is observed, corresponding to the fraction of red phase. The spectrum of poly(PCDA)/CaO nanocomposite exhibits two main peaks. The peak corresponding to the blue phase is detected at about 650 nm and the peak of red phase is clearly observed at 540 nm. Moreover, the absorbance of these two nanocomposites is very low. It should be noted that pH of aqueous

suspensions before adding the monomer of MgO and CaO nanoparticles are 10.61 and 11.41, respectively. These pHs are very high that could be unfavorable for vesicle formation. In addition, the vesicles that could be formed are in reddish purple phase due to the high pH.

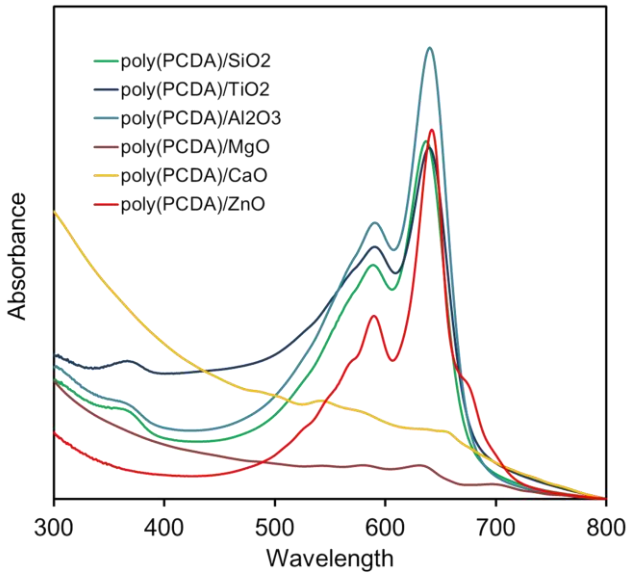

Fig. 5.53 Absorption spectra of PDA/inorganic oxide nanocomposites after irradiating by UV light

The interaction within the nanocomposites is explored by utilizing infrared (IR) spectroscopy as illustrated in Fig. 5.54. All nanocomposites are in the blue phase. The IR spectra of poly(PCDA)/SiO_2, poly(PCDA)/TiO_2 and poly(PCDA)/Al_2O_3 nanocomposites similarly show $\nu_s(CH_2)$, $\nu_{as}(CH_2)$ and $\nu_{as}(CH_3)$ at 2848, 2918 and 2954 cm^{-1}, respectively. The bands around 1690 cm^{-1} and 1465 cm^{-1} are clearly detected in these three nanocomposites, assigning to hydrogen-bonded carbonyl stretching of –COOH head group and methylene scissoring $\delta(CH_2)$ of side chain, respectively. The pattern of the spectra of these nanocomposites is hardly different compared to that of the pure poly(PCDA). Considering the IEP of nanoparticles shown in Table 5.1, the surface of SiO_2 particle is acidic with IEP at pH 2. At nearly neutral pH, the SiO_2 surface is mostly populated by negative species with the value of zeta potential of -34.16 mV (from Table 5.2). Therefore the carboxylate head groups cannot assemble onto this surface by ionic

interaction. Although Y-L. Su reported that SiO_2 nanoparticles could be used as a template to induce ordered arrangement of PCDA monomers, the driving force comes from the interactions of the polar groups of PCDA monomers and hydroxyl groups of silica nanoparticle, as well as the interactions among the PCDA monomers (van de Waals force, hydrogen bond, etc.)[62]. This is quite similar to the system of poly(PCDA)/TiO_2 nanocomposite. The value of zeta potential of TiO_2 in aqueous suspension is -20.71 mV. Therefore, carboxylate head groups of the monomer cannot interact with TiO_2 by ionic interaction. However, in the system of poly(PCDA)/Al_2O_3 nanocomposites, a small peak around 1570 cm^{-1} is observed. This can be assigned to a type of C=O stretching vibration of the ionic carboxyl group ($–COO^-$). This possibly causes from the positive species on surface of Al_2O_3 nanoparticles at pH ~7, which can form ionic interaction with the carboxylate head groups in different manner.

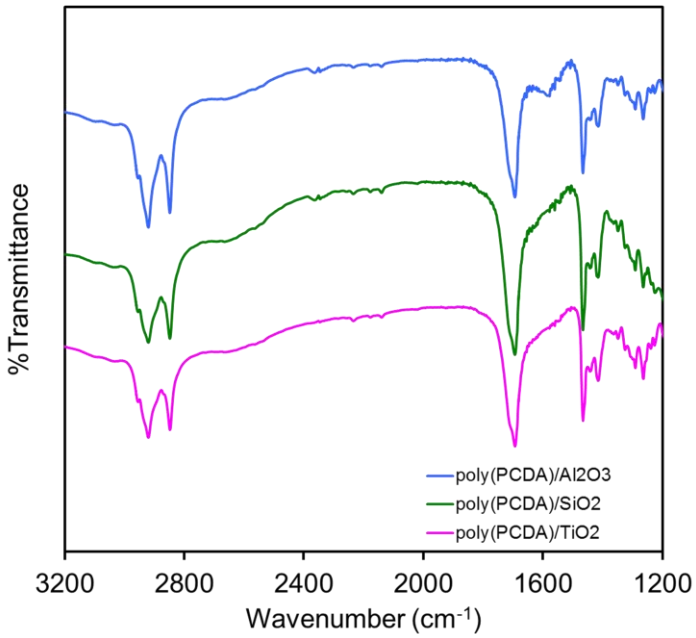

Fig. 5.54 FT-IR spectra of the blue-phase poly(PCDA)/SiO_2, poly(PCDA)/TiO_2 and poly(PCDA)/Al_2O_3 nanocomposites

5.3.2. Morphologies

Morphology of the nanocomposites prepared with various types of inorganic oxide nanoparticles is investigated by SEM as shown in Fig. 5.55. The SEM samples are prepared from suspensions without filtration. The images show that the blue-phase poly(PCDA)/SiO_2, poly(PCDA)/TiO_2 poly(PCDA)/Al_2O_3 and poly(PCDA)/CaO nanocomposites similarly exhibit spherical, ellipsoidal and some irregular shapes. In the case of poly(PCDA)/MgO nanocomposite, planar and platelet-like particles are clearly observed. This possibly causes by high pH of the suspension in preparing the nanocomposite. This result is unexpected because this nanocomposite was prepared at high pH as same as in the system of poly(PCDA)/MgO nanocomposite.

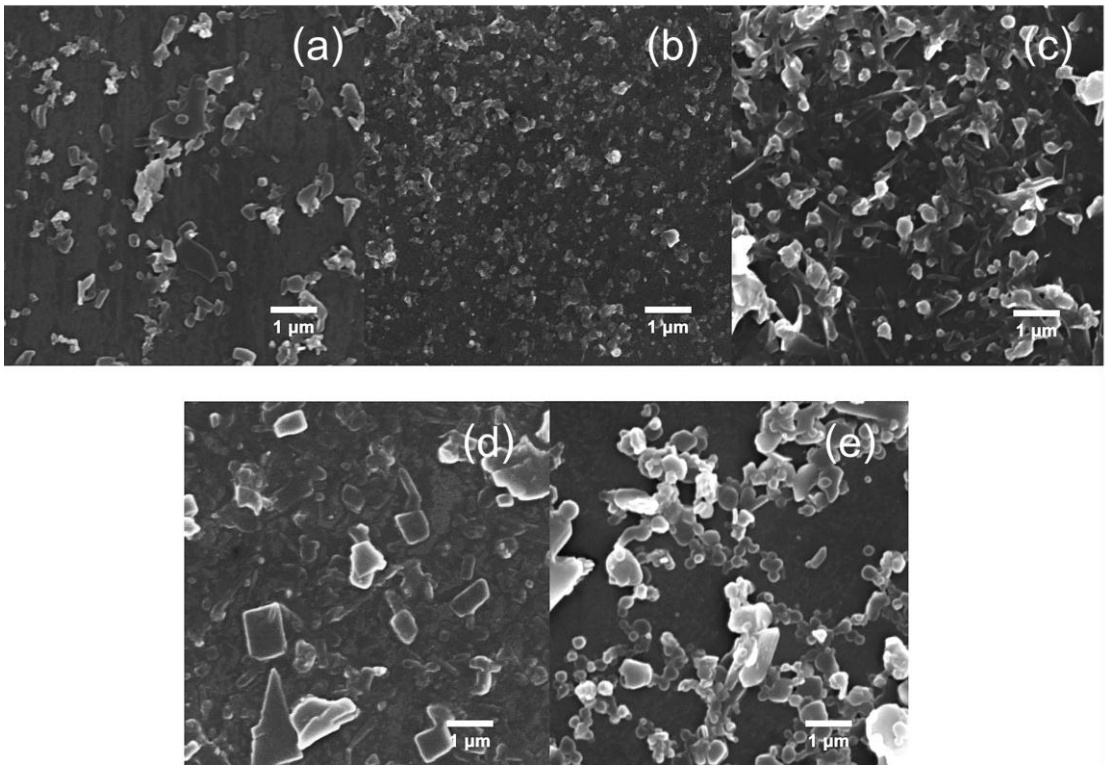

Fig. 5.55 SEM images of (a) poly(PCDA)/SiO_2, (b) poly(PCDA)/TiO_2, (c) poly(PCDA)/Al_2O_3, (d) poly(PCDA)/MgO and (e) poly(PCDA)/CaO nanocomposites

5.3.3. Thermochromism

The absorption spectra of the nanocomposites upon heating compared to the system of pure poly(PCDA) vesicles are shown in Fig 5.56. The results show that the irreversible color transition upon heating is observed in all nanocomposites, which is similar to the pure poly(PCDA) vesicles. At the first stage, the increase of temperature causes a gradual blue-shift with a slight drop of absorbance while the spectrum pattern is hardly affected. The abrupt change of the absorption spectra is observed when the temperature is increased above 65 ^{o}C. The blue-shift of λ_{max} from 620 nm to 543 nm corresponds to the color transition of both poly(PCDA) and the nanocomposites. A complete transition to the red phase takes place at around 70-75 ^{o}C, in which the interfacial interaction between carboxylic head groups and the species at the surface of these inorganic oxide nanoparticles cannot restrain the side chain dynamic. In the system of poly(PCDA)/Al_2O_3 nanocomposite, the IR spectrum exhibits a small peak of carboxylate group at around 1570 cm^{-1} ,which possibly arise from the ionic interaction at the surface of this nanoparticle but the band of hydrogen-bonded carbonyl stretching of –COOH head group is mostly observed. Therefore it can be concluded that the main attractive interaction at the surface of Al_2O_3 nanoparticle is hydrogen bond which cannot restrict the side chain dynamic upon heating.

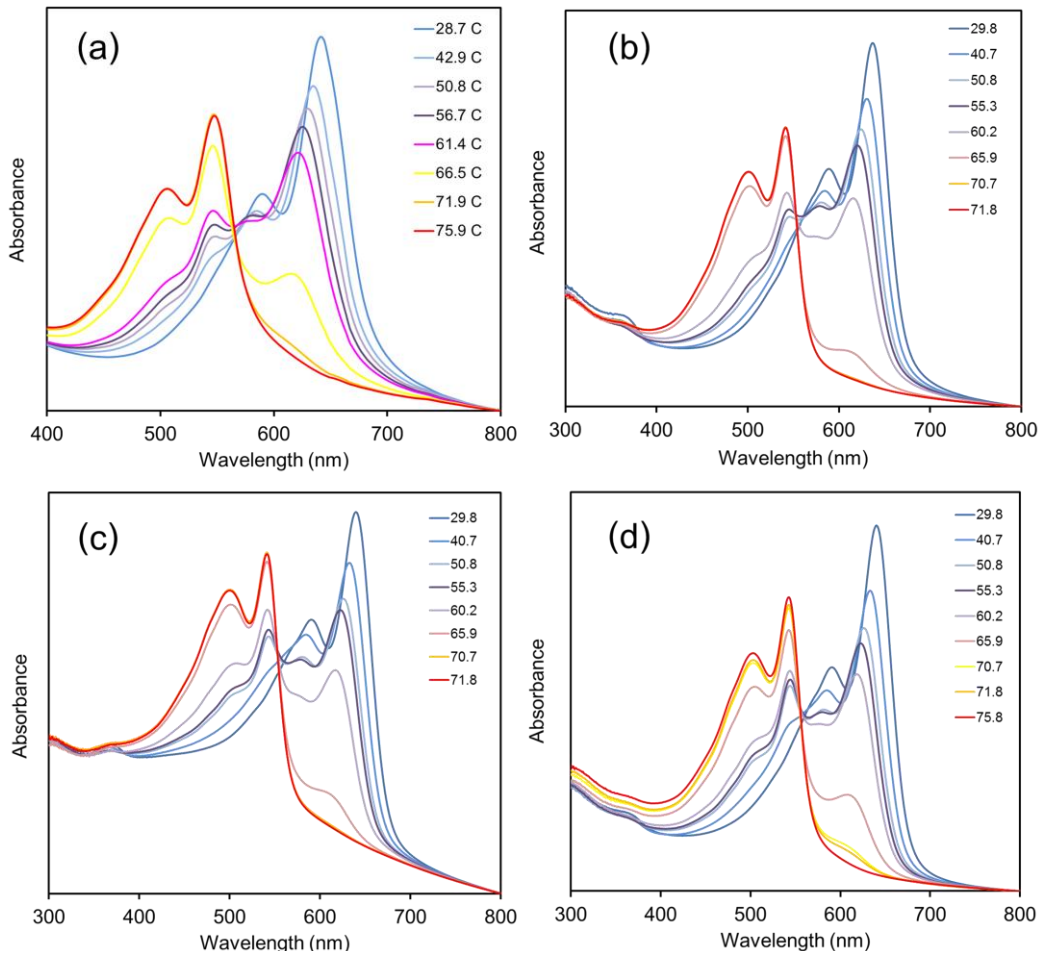

Fig. 5.56 Absorption spectra of (a) poly(PCDA) vesicles, (b) poly(PCDA)/SiO_2, (c) poly(PCDA)/TiO_2 and poly(PCDA)/Al_2O_3 nanocomposites upon increasing temperature

The plots of colorimetric response of the pure poly(PCDA) vesicles and the nanocomposites as a function of temperature are illustrated in Fig. 5.57. It can be observed that the degree of color change of the nanocomposites is hardly different from that of the pure poly(PCDA) vesicles. The sharp increase of %CR value takes place at temperature above 65 ^{o}C and the complete red phase is observed around 70 ^{o}C in all nanocomposites.

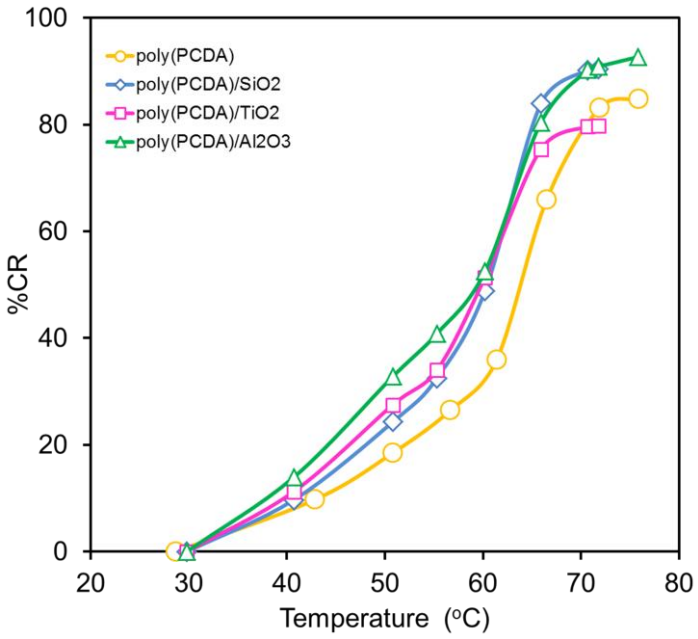

Fig. 5.57 The plots of colorimetric response (%CR) of the nanocomposites upon heating

5.3.4. Colorimetric response to pH

In the system of PDA/ZnO nanocomposites, the chromatic transition can be clearly observed in acidic condition. This is possibly due to the dissolution of ZnO nanoparticles as suggested in the previous section. In the basic condition, the color transition of this nanocomposite takes place at much higher pH compared to pure PDA. The nanocomposites prepared from other types of inorganic oxide nanoparticles, however, exhibit similar colorimetric behaviors to the pure poly(PCDA) as shown in Fig. 5.58.The blue-shift is not detected when H^+ ions is continuously added. After adjusting pH to ~1, a minor peak ~ 550 nm occurs, indicating the slight change of the solution color. The significant drop of the absorbance results from the agglomeration of the nanocomposites. The plots of %CR illustrated in Fig. 5.60a clearly show that the value of %CR of the nanocomposites prepared from SiO_2, TiO_2 and Al_2O_3 nanoparticles slightly increases to only around 4% when pH of the suspension is lower than 1 whereas %CR of poly(PCDA)/ZnO nanocomposite increases to around 60%.

The absorption spectra of poly(PCDA)/SiO_2, poly(PCDA)/TiO_2 and poly(PCDA)/Al_2O_3 nanocomposites upon increasing pH are illustrated in Fig. 5.59b-d. Again, we also observed the irreversible blue-red transition of these three nanocomposites, which is similar to the system of pure poly(PCDA) vesicles. In all nanocomposites, a peak at ~546 nm presents at pH ~8 and continuously grows when increasing OH^- ion concentration. This indicates that the interfacial interaction at the surface of these nanoparticles cannot restrict the side chain dynamic occurred by the repulsive force of negative head groups. The abrupt change of absorption spectra is observed at pH ~11 for poly(PCDA)/SiO_2 and poly(PCDA)/Al_2O_3 nanocomposites and at pH ~10 for poly(PCDA)/TiO_2 nanocomposites.. The complete red phase of all nanocomposites takes place at pH ~13. Although we can observe the small fraction of the blue phase at around 640 nm in the system of poly(PCDA)/SiO_2 and poly(PCDA)/TiO_2 nanocomposites, the peak is too small to distinguish the difference in chromatic transition from the pure poly(PCDA) system.

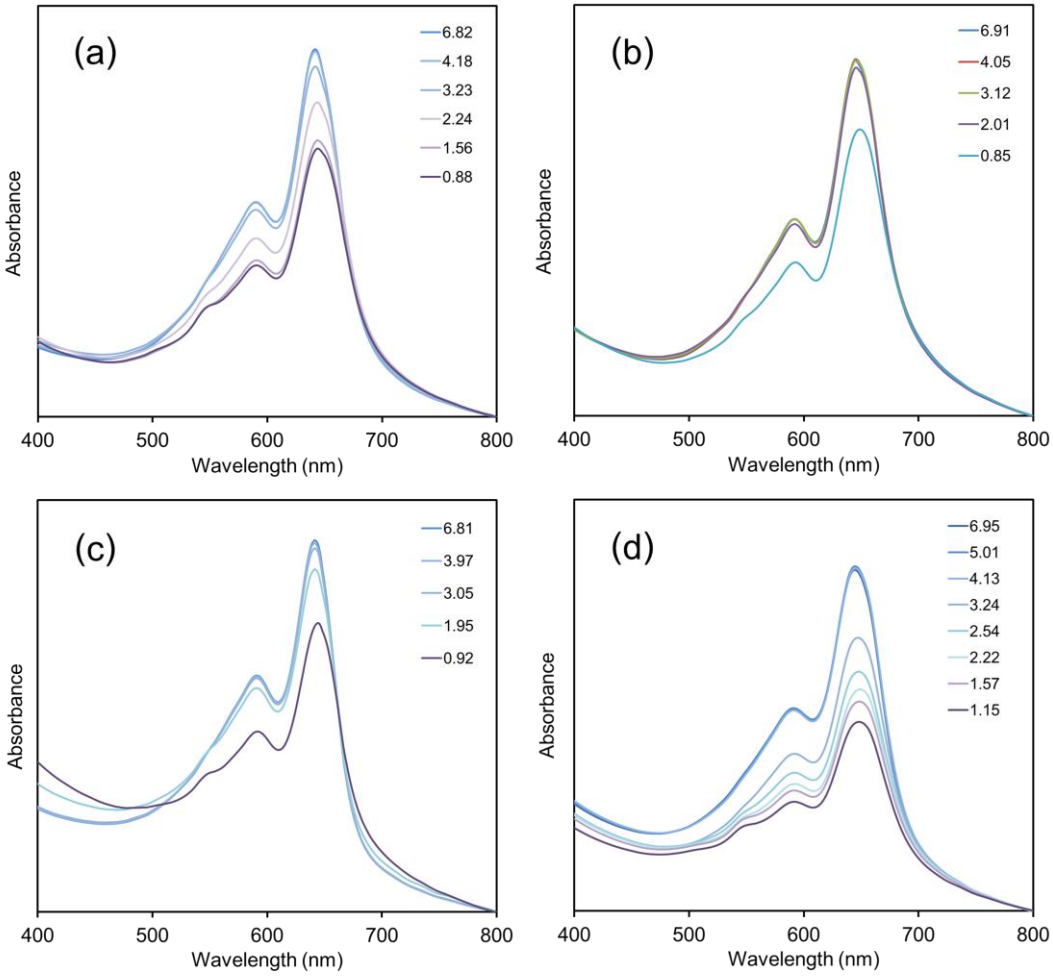

Fig. 5.58 Absorption spectra of (a) poly(PCDA) vesicles, (b) poly(PCDA)/SiO_2, (c) poly(PCDA)/TiO_2 and poly(PCDA)/Al_2O_3 nanocomposites upon decreasing pH

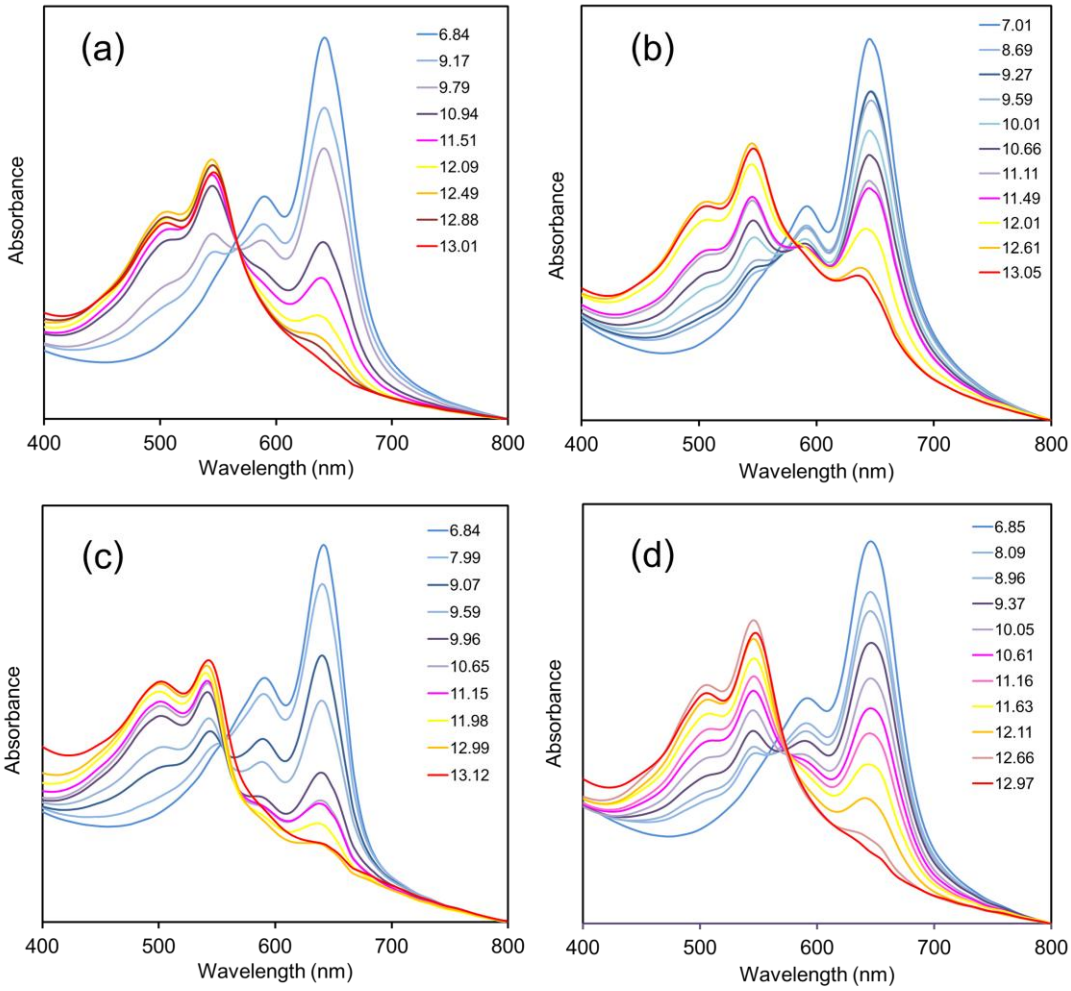

Fig. 5.59 Absorption spectra of (a) poly(PCDA) vesicles, (b) poly(PCDA)/SiO_2, (c) poly(PCDA)/TiO_2 and poly(PCDA)/Al_2O_3 nanocomposites upon increasing pH

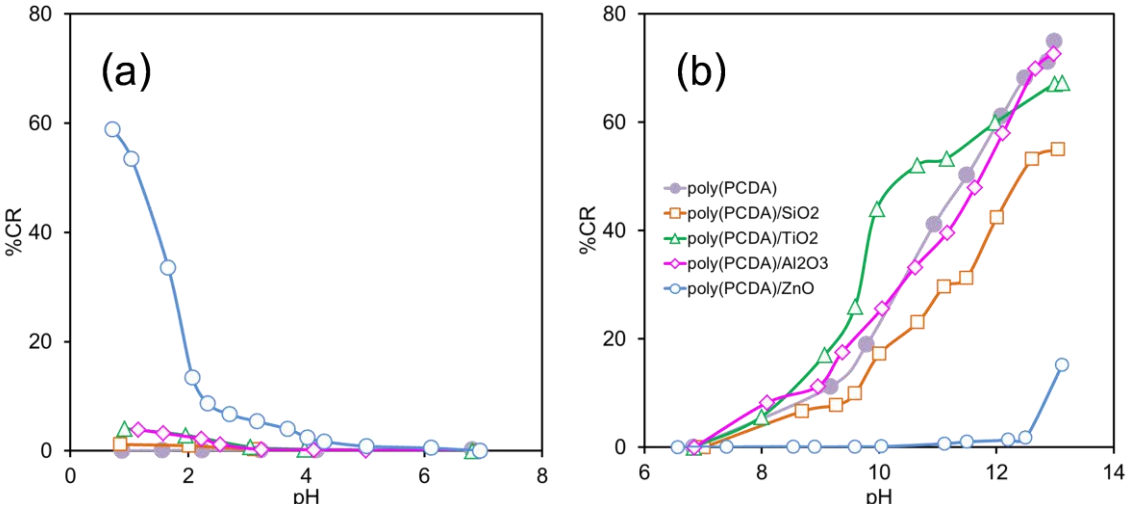

Fig. 5.60 The plot of colorimetric response as a function of pH of poly(PCDA) and poly(PCDA)/inorganic oxide nanocomposites ;(a) in acidic condition and (b) in basic condition

The plots of %CR of poly(PCDA) vesicles and the nanocomposites upon increasing pH are shown in Fig. 5.60b. At pH ranging from 8 to 11, it can be observed that the degree of color transition of poly(PCDA)/TiO_2 is slightly higher than that of the other nanocomposites and the pure poly(PCDA) vesicles. For poly(PCDA)/SiO_2 nanocomposite the degree of color transition is slightly lower than that of the pure poly(PCDA). However, the difference in color transition among these three nanocomposites and the pure poly(PCDA) is not significant when compares to the poly(PCDA)/ZnO nanocomposites. The cause of the observed color transition behaviors must be further investigated.

5.3.5. Colorimetric response to ethanol

Lastly, we observed the colorimetric response to ethanol of these nanocomposites. The absorption spectra of poly(PCDA)/SiO_2, poly(PCDA)/TiO_2 and poly(PCDA)/Al_2O_3 nanocomposites upon addition of ethanol are illustrated in Fig. 5.61. Similar to the system of pure poly(PCDA) vesicles, the color transition of all nanocomposite suspension is clearly observed. A new peak at ~540 nm is detected when the concentration of ethanol is 16.7 vol%. Further increasing the concentration of ethanol, this peak continuously grows. The abrupt change of λ_{max} takes place when the concentration of ethanol is about 44.4-50.0 vol%. All nanocomposite suspensions completely change to red color at the concentration of 58.3 vol%. The plots of colorimetric response as a function of ethanol concentration are shown in Fig. 5.61d. The result exhibits that the color transition of all nanocomposite takes place at slightly lower degree than that of pure poly(PCDA). In addition, the degree of color change of the nanocomposites prepared from SiO_2 nanoparticles is slightly greater than that of the nanocomposites prepared from TiO_2 and Al_2O_3 nanoparticles. However, similar to the colorimetric response to temperature and pH, the difference in chromatic transition among these three nanocomposites and the pure poly(PCDA) is very small. The observed color transition behaviors must be further investigated to verify the cause.

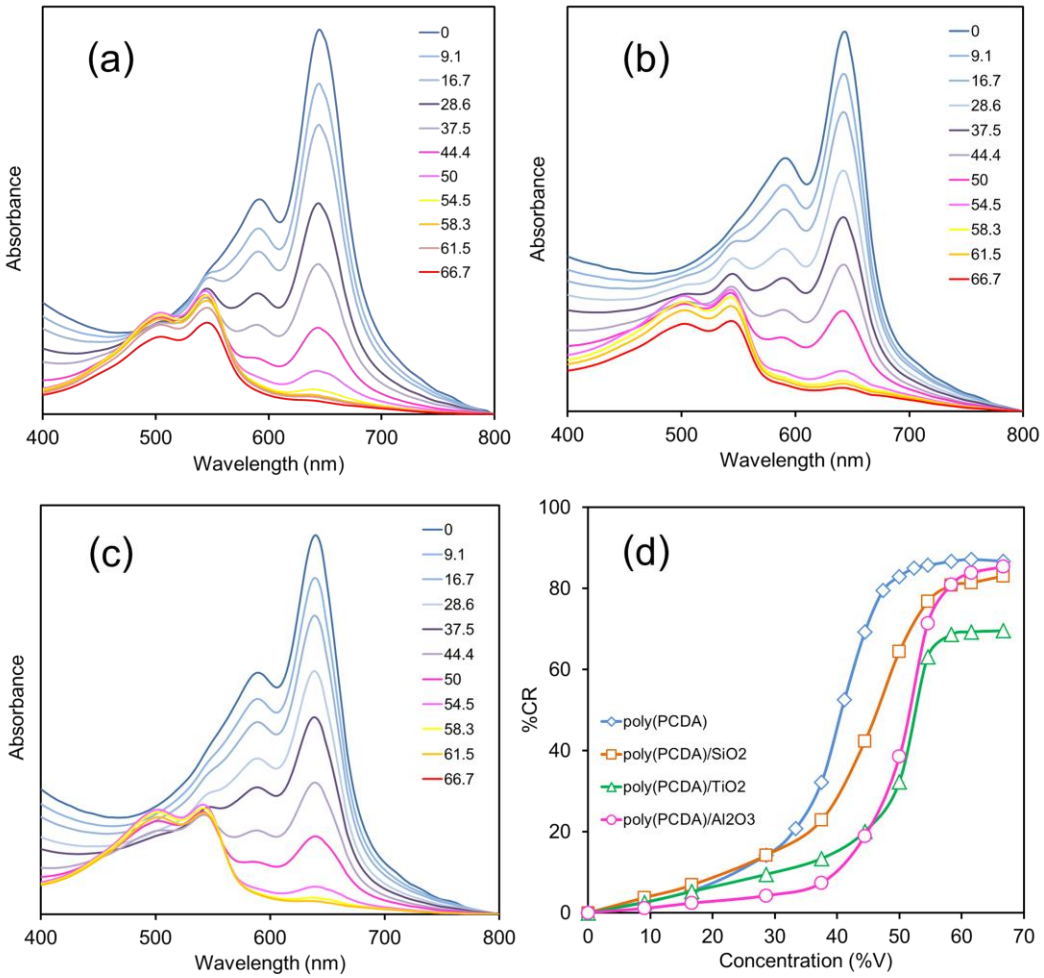

Fig. 5.61 Absorption spectra of (a) poly(PCDA)/SiO_2, (b) poly(PCDA)/TiO_2 and (c) poly(PCDA)/Al_2O_3 nanocomposites upon addition of ethanol

In this part, we explore the nanocomposites prepared with inorganic oxide nanoparticles other than ZnO. SiO_2, TiO_2, Al_2O_3, CaO and MgO nanoparticles are used in this study. It is found that the blue phase of poly(PCDA)/CaO and poly(PCDA)/MgO nanocomposites cannot be prepared. This is possibly due to the very high pH of the nanoparticle suspensions. The nanocomposites prepared from SiO_2, TiO_2 and Al_2O_3 exhibit the blue phase. However, unlike poly(PCDA)/ZnO, the chromatic transition of poly(PCDA)/SiO_2, poly(PCDA)/TiO_2 and poly(PCDA)/Al_2O_3 when subjects to external stimuli is not significantly different from the system of pure poly(PCDA) vesicles.

CHAPTER VI

CONCLUSIONS AND RECOMMENDATIONS

6.1 Conclusions

In previous study, our research group presented a simple method for controlling colorimetric behaviors of PDA by addition of ZnO nanoparticles as a nano-substrate. The nanocomposite was prepared by using 10,12-pentacosadiynoic acid as a monomer. This PDA-based material clearly exhibited different colorimetric behaviors when subjects to external stimuli. The color transition occurred at higher temperature compared to that of the pure PDA and the nanocomposite interestingly showed reversible thermochromism. In addition, the chromatic transition of this nanocomposite occured at higher pH and it exhibited color stability upon exposure to ethanol.

This research is a continuation study. Effects of alkyl side chain length and periods of UV irradiation on colorimetric responseof PDA/ZnO nanocomposites upon exposure to external stimuli are investigated. In addition, the PDA-based nanocomposite prepared from other types of metal oxide nanoparticles is examined. The results can be concluded as follows;

6.1.1. Effects of alkyl side chain length on colorimetric responses of polydiacetylene/ZnO nanocomposites

The color-transition behaviors of PDA/ZnO nanocomposites can be systematically controlled by varying structure of the constituent polymers. The shortening of alkyl chain length causes the decrease in dispersion interactions within the assemblies, leading to the decrease in color-transition temperature. The decrease in alkyl chain length also promotes the backbone rigidity, which in turn influences the interfacial interactions and the color-transition behaviors. In the system of poly(HDDA)/ZnO nanocomposite with relatively short alkyl chain, the heterogeneity of interfacial interactions is detected. Its color transition is less pronounced, and color stability is also lower compared to the other nanocomposites.

The colorimetric behaviors upon variation of pH of the PDA/ZnO nanocomposites are significantly different from that of the PDA vesicles. The color transition of the nanocomposite upon increasing pH takes place at a much higher pH compared to that of the pure PDA vesicles. The shortening of alkyl side chain leads to highly sensitive colorimetric response of the nanocomposites, which comparable to that of the pure PDAs. Upon decreasing pH, however, the PDA/ZnO nanocomposite interestingly exhibits more sensitive colorimetric response compared to their PDA counterparts. The results could be explained based on dissolution of ZnO nanoparticles in low pH region and high pH region. The addition of alcohols such as ethanol and 2-propanol cannot induce the color transition of poly(PCDA)/ZnO and poly(TCDA)/ZnO nanocomposites. However, in the system of poly(HDDA)/ZnO nanocomposite with relatively short alkyl chain, the addition of alcohols can induce the blue-red transition.

6.1.2. Effects of UV irradiation on colorimetric behaviors of PDA/ZnO nanocomposites

The polymerization time can affect the colorimetric behaviors of PDA/ZnO nanocomposite upon exposure to external stimuli. The color transition of nanocomposites obtained by longer period of irradiation takes place at lower temperature compared to that of the nanocomposite with shorter irradiation time. This is due to the weakening of the overall interactions in the nanocomposites upon UV irradiation. Poly(TCDA)/ZnO nanocomposite derived from irradiating for 4 min can exhibits complete thermochromic reversibility while the reversibility decreases in nanocomposites polymerized for 30 min. However, the complete color reversibility can be observed in poly(TCDA)/ZnO nanocomposite irradiated for 60 min. In the system of poly(HDDA)/ZnO nanocomposites, the nearly complete thermochromic reversibility is observed in the nanocomposite polymerized for 30 min. The complete reversibility detected in the nanocomposites with relatively long UV irradiation could be due to the slight change in the molecular orientation upon increasing temperature. The strong ionic interactions can then induce the conformation to return to their initial stage when cooling to room temperature.

Poly(TCDA)/ZnO nanocomposite derived from short period of irradiation can exhibit complete irreversible blue-red transition in acidic condition whereas the nanocomposite irradiated for longer time cannot be observed. In high pH region, the color transition of these nanocomposites obtained by different irradiation times is similarly detected at pH higher than 13. In the system of poly(HDDA)/ZnO nanocomposite, color transition clearly occurs in both acidic and basic condition. The magnitude of color transition decreases with increasing polymerization time.

In the case of colorimetric response to ethanol and 2-propanol, all poly(TCDA)/ZnO nanocomposites prepared from different UV irradiation times exhibit color stability. The poly(HDDA)/ZnO nanocomposite obtained by short period of irradiation exhibits a complete blue-red color transition upon addition of these alcohols. The magnitude of color transition decreases with increasing polymerization time.

6.1.3. Effects of types of nanoparticles on colorimetric behaviors of PDA/inorganic oxide nanocomposites

In addition to ZnO, PDA-based nanocomposites are prepared using SiO_2, TiO_2, Al_2O_3, CaO and MgO nanoparticles. The SiO_2, TiO_2 and Al_2O_3 nanoparticles provide the nanocomposites with blue color. However, the nanocomposites prepared from CaO and MgO nanoparticles exhibit purple color. Since the pHs of CaO and MgO nanoparticle suspensions before adding the monomer are very high, formation of vesicles could be unfavorable. In addition, the vesicles that could be formed are in reddish purple phase due to the high pH. The chromatic transition when subjected to external stimuli of poly(PCDA)/ SiO_2, poly(PCDA)/TiO_2 and poly(PCDA)/Al_2O_3 nanocomposites in blue phase is similar to the system of the pure poly(PCDA) vesicles.

6.2 Recommendations

- In this study, three monomers with different alkyl chain length are used for preparing PDA/ZnO nanocomposites. The results clearly demonstrate the difference in chromatic transition in these nanocomposites. Therefore, diacetylene monomers with systematic variation in alkyl tail length or/and length between head groups and diacetylene unit could be considered to improve the knowledge onthe role of monomer structure on the colorimetric behaviors of the nanocomposites.
- The PDA/ZnO nanocomposites interestingly response to both acidic and basic pH, especially in the system of poly(HDDA)/ZnO nanocomposite. Therefore, the colorimetric response to organic acid and base should be further studied.
- Further study on the effects of polymerization time is recommended to complete the series of PDA/ZnO nanocomposites for sensing applications. Further investigation on the effects of types of nanoparticles should be done to gain more understanding in the interfacial interactions between the head groups of diacetylene monomer and nanoparticles.

REFERENCES

[1] Yoon, J., Jung, Y.-S. and Kim, J.-M. A Combinatorial Approach for Colorimetric Differentiation of Organic Solvents Based on Conjugated Polymer-Embedded Electrospun Fibers. Advanced Functional Materials 19 (2009): 209-214

[2] Yoon, J., Chae, S.K. and Kim J.-M. Colorimetric Sensors for Volatile Organic Compounds (VOCs) Based on Conjugated Polymer-Embedded Electrospun Fibers. Journal of the American Chemical Society 129 (2007): 3038-3039

[3] Champaiboon, T., Tumcharern, G., Potisatityuenyong, A., Wacharasindhu, S. and Sukwattanasinitt, M. A polydiacetylene multilayer film for naked eye detection of aromatic compounds. Sensors and Actuators B 139 (2009): 532–537

[4] Pumtang, S., Siripornnoppakhun, W., Sukwattanasinitt, M. and Ajavakom, A. Solvent colorimetric paper-based polydiacetylene sensors from diacetylene lipids. Journal of Colloid and Interface Science 364 (2011): 366–372

[5] Jaworski, J., Yokoyama, K., Zueger, C., Chung, W.-J., Lee, S.W. and Majumdar, A. Polydiacetylene Incorporated with Peptide Receptors for the Detection of Trinitrotoluene Explosives. Langmuir 27 (2011) 3180-3187

[6] Pires, A.C.S., Soares, N.F.F., Silva, L.H.M., Silveira, M.C.H., Mageste, A.B., Soares, R.F., Teixeira, A.V.N.C. and Andrade, N.J. Thermodynamic Study of Colorimetric Transitions in Polydiacetylene Vesicles Induced by the Solvent Effect. The Journal of Physical Chemistry B 114 (2010): 13365-13371

[7] Charoenthai, N., Pattanatornchai, T., Wacharasindhu, S., Sukwattanasinitt, M. and Traiphol, R. Roles of head group architecture and side chain length on colorimetric response of polydiacetylene vesicles to temperature, ethanol and pH. Journal of Colloid and Interface Science 360 (2011): 565–573

[8] Eaidkong, T., Mungkarndee, R., Phollookin, C., Tumcharern, G., Sukwattanasinitt, M. and Wacharasindhu, S. Polydiacetylene paper-based colorimetric sensor array for vapor phase detection and identification of volatile organic compounds. Journal of Materials Chemistry 22 (2012): 5970-5977

[9] Wu, S., Shi, F., Zhang, Q. and Bubeck, C. Stable Hydrogen-Bonding Complexes of Poly(4-vinylpyridine) and Polydiacetylenes for Photolithography and Sensing. Macromolecules 42 (2009): 4110-4117

[10] Ahn, D.J., Lee, S. and Kim, J.-M. Rational Design of Conjugated Polymer Supramolecules with Tunable Colorimetric Responses. Advanced Functional Materials 19 (2009): 1483-1496

[11] Yoon, B., Lee, S. and Kim, J.-M. Recent conceptual and technological advances in polydiacetylene-based supramolecular chemosensors. Chemical Society Reviews 38 (2009): 1958-1968

[12] Yu, L. and Hsu, S.L., A Spectroscopic Analysis of the Role of Side Chains in Controlling Thermochromic Transitions in Polydiacetylenes. Macromolecules 45 (2012): 420-429

[13] Pang, J., Yang, L., McCaughey, B.F., Peng, H., Ashbaugh, H.S., Brinker, C.J. and Lu, Y. Thermochromatism and Structural Evolution of Metastable Polydiacetylenic Crystals. The Journal of Physical Chemistry B. 110 (2006): 7221-7225

[14] Wacharasindhu, S., Montha, S., Boonyiseng, J., Potisatityuenyong, A., Phollookin, C., Tumcharern, G. and Sukwattanasinitt, M. Tuning of Thermochromic Properties of Polydiacetylene toward Universal Temperature Sensing Materials through Amido Hydrogen Bonding. Macromolecules 43 (2010): 716-724

[15] Phollookin, C., Wacharasindhu, S., Ajavakom, A., Tumcharern, G., Ampornpun, S., Eaidkong, T. and Sukwattanasinitt M. Tuning Down of Color Transition Temperature of Thermochromically Reversible Bisdiynamide Polydiacetylenes. Macromolecules 43 (2010): 7540-7548

[16] Gu, Y., Cao, W., Zhu, L., Chen, D. and Jiang, M. Polymer Mortar Assisted Self-Assembly of Nanocrystalline Polydiacetylene Bricks Showing Reversible Thermochromism. Macromolecules 41 (2008): 2299-2303

[17] Gou, M., Guo, G., Zhang, J., Men, K., Song, J., Luo, F., Zhao, X., Qian, Z. and Wei Y. Time–temperature chromatic sensor based on polydiacetylene (PDA)

vesicle and amphiphilic copolymer. Sensors and Actuators B, 150 (2010): 406–411

[18] Wu, S., Niu, L., Shen, J., Zhang, Q. and Bubeck, C. Aggregation-Induced Reversible Thermochromism of Novel Azo Chromophore-Functionalized Polydiacetylene Cylindrical Micelles. Macromolecules 42 (2009): 362-367

[19] Itoh, T., Shichi, T., Yui, T., Takahashi, H., Inui, Y. and Takagi, K., Reversible Color Changes in Lamella Hybrids of Poly(diacetylenecarboxylates) Incorporated in Layered Double Hydroxide Nanosheets. The Journal of Physical Chemistry B 109 (2005): 3199-3206

[20] Park, H., Lee, J.-S., Choi, H., Ahn, D.J. and Kim, J.-M. Rational Design of Supramolecular Conjugated Polymers Displaying Unusual Colorimetric Stability upon Thermal Stress. Advanced Functional Materials 17 (2007): 3447-3455

[21] Traiphol, N., Rungruangviriya, N., Potai, R. and Traiphol, R. Stable polydiacetylene/ZnO nanocomposites with two-steps reversible and irreversible thermochromism: The influence of strong surface anchoring. Journal of Colloid and Interface Science 356 (2011): 481–489

[22] Cheng, Q. and Stevens, R.C. Charge-Induced Chromatic Transition of Amino Acid-Derivatized Polydiacetylene Liposomes. Langmuir 14 (1998): 1974-1976

[23] Song, J., Cheng, Q., Kopta, S. and Stevens, R.C. Modulating Artificial Membrane Morphology: pH-Induced Chromatic Transition and Nanostructural Transformation of a Bolaamphiphilic Conjugated Polymer from Blue Helical Ribbons to Red Nanofibers. Journal of The American Chemical Society 123 (2001): 3205-3213

[24] Kew, S.J. and Hall, E.A.H., pH Response of Carboxy-Terminated Colorimetric Polydiacetylene Vesicles. Analytical Chemistry 78 (2006): 2231-2238

[25] Potisatityuenyong, A., Tumcharern, G., Dubas, S.T. and Sukwattanasinitt, M. Layer-by-layer assembly of intact polydiacetylene vesicles with retained chromic properties Journal of Colloid and Interface Science 304 (2006): 45-51

[26] Potisatityuenyong, A., Rojanathanes, R., Tumcharern, G. and Sukwattanasinitt, M. Electronic Absorption Spectroscopy Probed Side-Chain Movement in Chromic Transitions of Polydiacetylene Vesicles. Langmuir 24 (2008) 4461-4463

[27] Yuan, Z. and Hanks, T.W. A reversible colorimetric and fluorescent polydiacetylene vesicle sensor platform. Polymer 49 (2008): 5023-5026

[28] Seo, D. and Kim, J. Effect of the Molecular Size of Analytes on Polydiacetylene Chromism. Advanced Functional Materials 20 (2010): 1397-1403

[29] Lee J., Kim H.-J., Kim J., Polydiacetylene Liposome Arrays for Selective Potassium Detection, Journal of The American Chemical Society, 130 (2008): 5010-5011

[30] Lee, J., Jun, H. and Kim J., Polydiacetylene–Liposome Microarrays for Selective and Sensitive Mercury(II) Detection. Advanced Materials 21 (2009): 3674-3677

[31] Kolusheva, S., Shahal, T. and Jelinek, R. Cation-Selective Color Sensors Composed of Ionophore-Phospholipid-Polydiacetylene Mixed Vesicles. Journal of The American Chemical Society 122 (2000): 776-780

[32] Jang, Y.S., Yoon, B. and Kim, J.-M., Colorimetric detection of aluminium ion based on conjugated polydiacetylene supramolecules. Macromolecular Research 19 (2011): 97-99

[33] Narkwiboonwong, P., Tumcharern, G., Potisatityuenyong, A., Wacharasindhu, S. and Sukwattanasinitt, M. Aqueous sols of oligo(ethylene glycol) surface decorated polydiacetylene, vesicles for colorimetric detection of Pb^{2+}. Talanta 83 (2011): 872–878

[34] Jung, Y.K., Park, H.G. and Kim, J.-M. Polydiacetylene (PDA)-based colorimetric detection of biotin–streptavidin interactions. Biosensors and Bioelectronics 21 (2006): 1536–154

[35] Kolusheva, S., Kafri, R., Katz, M. and Jelinek, R. Rapid Colorimetric Detection of Antibody-Epitope Recognition at a Biomimetic Membrane Interface. Journal of The American Chemical Society 123 (2001): 417-422

[36] Guo, C.X., Boullanger, P., Liu, T. and Jiang, L. Size Effect of Polydiacetylene Vesicles Functionalized with Glycolipids on Their Colorimetric Detection Ability. The Journal of Physical Chemistry B 109 (2005): 18765-18771

[37] Reppy, M.A. and Pindzola, B.A. Biosensing with polydiacetylene materials: structures, optical properties and applications. Chemical Communications 42 (2007): 4317-4338

[38] Scindia, Y., Silbert, L., Volinsky, R., Kolusheva, S. and Jelinek, R. Colorimetric Detection and Fingerprinting of Bacteria by Glass-Supported Lipid/Polydiacetylene Films. Langmuir 23 (2007): 4682-4687

[39] Kim, K.-W., Choi, H., Lee, G.S., Ahn, D.J. and Oh, M.-K. Effect of phospholipid insertion on arrayed polydiacetylene biosensors. Colloids and Surfaces B: Biointerfaces 66 (2008): 213–217

[40] Deng, J., Sheng, Z., Zhou, K., Duan, M., Yu, C. and Jiang, L. Construction of Effective Receptor for Recognition of Avian Influenza H5N1 Protein HA1 by Assembly of Monohead Glycolipids on Polydiacetylene Vesicle Surface. Bioconjugate Chemistry 20 (2009): 533-537

[41] Kim, J.-M., Lee, Y.B., Yang, D.H., Lee, J.-S., Lee, G.S. and Ahn, D.J. A Polydiacetylene-Based Fluorescent Sensor Chip. Journal of The American Chemical Society 127 (2005): 17580-17581

[42] Gill, I. and Ballesteros, A. Immunoglobulin–Polydiacetylene Sol–Gel Nanocomposites as Solid-State Chromatic Biosensors. Angewandte Chemie 115 (2003): 3386-3389

[43] Chen, X., Kang, S., Kim, M.J., Kim, J., Kim, Y.S., Kim, H., Chi, B., Kim, S.-J., Lee, J.Y. and Yoon, J. Thin-Film Formation of Imidazolium-Based Conjugated Polydiacetylenes and Their Application for Sensing Anionic Surfactants. Angewandte Chemie 49 (2010): 1422-1425

[44] Su, Y.-L., Li, J.-R. and Jiang, L. Effect of amphiphilic molecules upon chromatic transitions of polydiacetylene vesicles in aqueous solutions. Colloids and Surfaces B: Biointerfaces 39 (2004): 113–118

[45] Carpick, R.W., Sasaki, D.Y., Marcus, M.S., Eriksson, M.A. and Burns, A.R. Polydiacetylene films: a review of recent investigations into chromogenic transitions and nanomechanical properties. Journal of Physics: Condensed Matter 16 (2004): R679

[46] Lifshitz, Y., Golan, Y., Konovalov, O. and Berman, A. Structural Transitions in Polydiacetylene Langmuir Films Langmuir 25 (2009): 4469-4477

[47] Huang, X., Jiang, S. and Liu, M. Metal Ion Modulated Organization and Function of the Langmuir-Blodgett Films of Amphiphilic Diacetylene: Photopolymerization, Thermochromism, and Supramolecular Chirality. The Journal of Physical Chemistry B 109 (2005): 114-119

[48] Wang, X., Whitten, J.E. and Sandman, D.J. Ultraviolet photoelectron spectroscopy study of the thermochromic phase transition in urethane-substituted polydiacetylenes. Journal of Chemical Physics 126 (2007): 184905-184909

[49] Lee, D., Sahoo, S.K., Cholli, A.L. and Sandman, D.J. Structural Aspects of the Thermochromic Transition in Urethane-Substituted Polydiacetylenes. Macromolecules 35 (2002): 4347-4355

[50] Kim, J.-M., Lee, J.-S., Choi, H., Sohn, D. and Ahn, D.J. Rational Design and in-Situ FTIR Analyses of Colorimetrically Reversibe Polydiacetylene Supramolecules. Macromolecules 38 (2005): 9366-9376

[51] Erbil, H.Y. Surface Chemistry of Solid and Liquid Interfaces, Blackwell Publishing Ltd, 2006

[52] Chemical Interactions [online]. Available from: www.chm.bris.ac.uk/~chdms/Teaching/Chemical_Interactions/page_06.htm

[53] Chapter 5 - Membrane Structure and Function[online]. Available from: www.biologycorner.com/APbiology/cellular/notes_cell_membrane.html

[54] Vesicle (biology and chemistry) [online]. Available from: http://commons.wikimedia.org/wiki/File:Liposome_scheme-en.svg

[55] Ji, E.-K., Ahn, D. J. and Kim, J.-M. The Fluorescent Polydiacetylene Liposome. Bulletin of the Korean Chemical Society 24 (2003): 667-670

[56] Jiang, H., Wang, Y., Ye, Q., Zou, G., Su, W. and Zhang Q. Polydiacetylene-based colorimetric sensor microarray for volatile organic compounds Sensors and Actuators B 143 (2010): 789–794

[57] Pattanatornchai, T., Charoenthai, N., Wacharasindhu, S., Sukwattanasinitt, M. and Traiphol, R. Control over the color transition behavior of polydiacetylene vesicles using different alcohols. Journal of Colloid and Interface Science 391 (2013): 45–53

[58] Chen, X. and Yoon, J. A thermally reversible temperature sensor based on polydiacetylene: Synthesis and thermochromic properties Dyes and Pigments (2010): 1-5

[59] Jonas, U., Shah, K., Norvez, S. and Charych, D. H. Reversible Color Switching and Unusual Solution Polymerization of Hydrazide-Modified Diacetylene Lipids. Journal of The American Chemical Society 121 (1999): 4580-4588

[60] Yuan, Z. and Hanks, T. W. A reversible colorimetric and fluorescent polydiacetylene vesicle sensor platform. Polymer 49 (2008): 5023–5026

[61] Yokoyama, T., Masuhara, A., Onodera, T., Kasai, H. and Oikawa, H. Development of fabrication process for Ag/polydiacetylene (core/shell) hybridized nanocrystals. Synthetic Metals 159 (2009): 897–899

[62] Su, Y.-L., Preparation of polydiacetylene/silica nanocomposite for use as a chemosensor. Reactive & Functional Polymers 66 (2006): 967–973

[63] Chen, X., Li, L., Sun, X., Liu, Y., Luo, B., Wang, C., Bao, Y., Xu, H. and Peng, H. Magnetochromatic Polydiacetylene by Incorporation of Fe_3O_4 Nanoparticles. Angewandte Chemie 50 (2011): 5486 –5489

[64] Yoon, J., Azizan, K.A.B., Yoo, H.O., Okada, S. and Kim, J-M. Unusual Photopolymerization Behavior of Amino Acid-Derived Polydiacetylene Supramolecules. Macromolecular Rapid Communications 30 (2009): 981–985

[65] Huo, Q., Russell, K. C. and Leblanc, R. M. Chromatic Studies of a Polymerizable Diacetylene Hydrogen Bonding Self-Assembly: A “Self-Folding” Process To Explain the Chromatic Changes of Polydiacetylenes. Langmuir 15 (1999): 3972-3980

[66] Rungruangviriya, N. and Traiphol, N. Versatile Route for Preparation of Polydiacetylene/ZnO Nanocomposites and Their Colorimetric Response to pH and Ethanol. Journal of Metals, Materials and Minerals 20 (2010): 35-41

[67] Faisaicha K., Effects of polymerization time and ZnO particle size on colorimetric response of polydiacetylene vesicles/ZnO, Master's thesis, Materials Science, Science, Chulalongkorn University, 2012

[68] หัสวิภา หมายมั่น. Scaning Electron Microscope : SEM [ออนไลน์]. 2012. แหล่งที่มา: http://www.mfu.ac.th/center/stic/index.php/micro-analysis-instrument-menu/item/96-scaning-electron-microscrope.html

[69] Electron-matter interactions [online]. Available from: http://www.ammrf.org.au/myscope/sem/background/concepts/interactions.php

[70] Zetasizer Nano Series User Manual, Malvern Instruments Ltd., 2004

[71] Dynamic Light Scattering: An Introduction in 30 Minutes, Malvern Instruments Ltd.

[72] Zeta Potential: An Introduction in 30 Minutes, Malvern Instruments Ltd.

[73] Instruction Manual for Using the BI-ZTU, The Autotitrator for Use With Brookhaven's Zeta Potential and Particle Sizing Instruments, Brookhaven Instruments Corporation, 2005

[74] Owen T. Fundamentals of modern UV-visible spectroscopy, Agilent Technologies 2000

[75] Introduction to Fourier Transform Infrared Spectrometry [online]. Available from: http://mmrc.caltech.edu/FTIR/FTIRintro.pdf

[76] อินฟราเรด สเปคโตรสโคปี (Infrared Spectroscopy) [Online]. Available from: http://e-book.ram.edu/e-book/c/CM328/CM328-10.pdf

[77] Marcelli, A., Cricenti, A., Kwiatek, W. M., Petibois, C. Biological applications of synchrotron radiation infrared spectromicroscopy. Biotechnology Advances 30 (2012): 1390–1404

[78] Nagarajan, R. Molecular Packing Parameter and Surfactant Self-Assembly: The Neglected Role of the Surfactant Tail. Langmuir 18 (2002): 31-38

[79] Mino, N., Tamura, H. and Ogawa, K. Analysis of color transitions and changes on Langmuir-Blodgett films of a polydiacetylene derivative. Langmuir 7 (1991): 2336-2341

[80] Sadagopan, K., Sawant, S.N., Kulshreshtha, S.K. and Jarori, G.K. Physical and chemical characterization of enolase immobilized polydiacetylene Langmuir–Blodgett film. Sensors and Actuators B 115 (2006): 526–533

[81] Tachibana, H., Hosaka, N. and Tokura, Y. Effect of alkyl chain length on thermochromic phase transition in urethane-substituted polydiacetylene crystals. Polymer 42 (2001): 8311-8314

[82] Grohens, Y., Hamon, L., Reiter, G., Soldera, A. and Holl, Y. Some relevant parameters affecting the glass transition of supported ultra-thin polymer films. European Physical Journal E 8 (2002): 217-224

[83] Lenhart, J.L. and Wu, W.-L., Deviations in the Thermal Properties of Ultrathin Polymer Network Films. Macromolecules 35 (2002): 5145-5152

[84] Kim, J-M., Lee, Y.B., Chae, S.K. and Ahn, D.J. Patterned Color and Fluorescent Images with Polydiacetylene Supramolecules Embedded in Poly(vinyl alcohol) Films. Advanced Functional Materials 16 (2006): 2103-2109

[85] Oliveira, C. P.D., Soares, N. D. F. F., Fontes, E. A. F., Oliveira, T. V. D. and Filho, A. M. M. Behaviour of polydiacetylene vesicles under different conditions of temperature, pH and chemical components of milk. Food Chemistry 135 (2012): 1052–1056

[86] Degen, A. and Kosec, M. Effect of pH and impurities on the surface charge of zinc oxide in aqueous solution. Journal of the European Ceramic Society 20 (2000): 667-673

[87] Han, J., Qiu, W. and Gao, W. Potential dissolution and photo-dissolution of ZnO thin films. Journal of Hazardous Materials 178 (2010): 115–122

[88] Bian, S-W, Mudunkotuwa, I. A., Rupasinghe, T., Grassian, V. H., Aggregation and Dissolution of 4 nm ZnO Nanoparticles in Aqueous Environments: Influence of pH, Ionic Strength, Size, and Adsorption of Humic Acid. Langmuir 27 (2011): 6059-606

BIOGRAPHY

Mr. Amornsak Chanakul was born in Singburi on March 8th, 1981. In 2003, he finished his Bachelor's Degree in Chemical Engineering from faculty of Engineering, Chulalongkorn University. Then, he studied for Master's Degree at the same department and graduated in 2005. His research topic was effects of types of anions and cosurfactants on ZnS nanoparticles synthesis in microemulsion. After that, He worked as a research assistant at NANOTEC and then Center of Excellence in Particle Technology. He continued his education at Department of Materials Science, Faculty of Science, Chulalongkorn University and earned Ph.D. in Materials Science in 2013.

Publications

- **Chanakul, A.**, Traiphol, N. and Traiphol, R. Controlling the reversible thermochromism of polydiacetylene/zinc oxide nanocomposites by varying alkyl chain length. Journal of Colloid and Interface Science 389 (2013): 106-114
- **Chanakul, A.**, Traiphol, N., Faisadchaa, K. and Traiphol, R., Dual colorimetric response of polydiacetylene/ZnO nanocomposites to low and high pH, submitted

Academic Conference Presentation

- **Amornsak Chanakul**, Nisanart Traiphol, Kunruethai Faisadcha, Rakchart Traiphol. Colorimetric Response to pH of Polydiacetylene/ZnO Nanocomposites with Various Alkyl Chain. International Symposium in Science and Technology at Kansai University 2013. Kansai University, Osaka, Japan (August 21-23, 2013)